



UNIVERSIDADE FEDERAL DE SANTA CATARINA  
CENTRO TECNOLÓGICO  
PROGRAMA DE PÓS-GRADUAÇÃO EM ENGENHARIA DE ALIMENTOS

Ana Caroline Cichella Frabetti

**Study of adhesion of food suspensions on flexible supports during drying**

Florianópolis/Nantes

2021

Ana Caroline Frabetti

**ESTUDO DE ADESÃO DE SUSPENSÕES ALIMENTARES EM SUPORTES  
FLEXÍVEIS DURANTE A SECAGEM**

Tese submetida ao Programa de Pós Graduação em Engenharia de Alimentos da Universidade Federal de Santa Catarina e pela Escola de Doutorado de Ciências da Engenharia (SPI Oniris) em regime de cotutela para a obtenção do título de doutor em engenharia de processos da indústria de alimentos.

Orientadores: Prof. Dr. João Borges Laurindo (UFSC) e Prof. Dr. Lionel Boillereaux (Oniris)

Coorientador: Dr. Jaqueline Oliveira de Moraes (UFSC) e Prof. Vanessa Jury (Oniris)

Florianópolis/Nantes  
2021

Ana Caroline Cichella Frabetti

**STUDY OF ADHESION OF FOOD SUSPENSIONS  
ON FLEXIBLE SUPPORTS DURING DRYING**

Doctoral thesis submitted to the Graduate Program in Food Engineering of the Federal University of Santa Catarina and to the Engineering Sciences Doctoral School (SPI Oniris) as requirement to obtain a Doctorate degree in Food Engineering.

Advisors: Prof. João Borges Laurindo (UFSC) and Prof. Lionel Boillereaux (Oniris)

Coordinators: Dr. Jaqueline Oliveira de Moraes (UFSC) and Pr. Vanessa Jury (Oniris)

Florianópolis/Nantes  
2021

Ficha de identificação da obra elaborada pelo autor,  
através do Programa de Geração Automática da Biblioteca Universitária da UFSC.

Frabetti, Ana Caroline Cichella  
Study of adhesion of food suspensions on flexible  
supports during drying / Ana Caroline Cichella Frabetti ;  
orientador, João Borges Laurindo, orientador, Lionel  
Boillereaux, coorientadora, Jaqueline Oliveira de Moraes,  
coorientadora, Vanessa Jury, 2021.

177 p.

Tese (doutorado) - Universidade Federal de Santa  
Catarina, Centro Tecnológico, Programa de Pós-Graduação em  
Engenharia de Alimentos, Florianópolis, 2021.

Inclui referências.

Trabalho elaborado em regime de co-tutela.

1. Engenharia de Alimentos. 2. composição de açúcar. 3.  
rugosidade. 4. secagem de alimentos. 5. desprendimento. I.  
Borges Laurindo, João. II. Boillereaux, Lionel III.  
Oliveira de Moraes, Jaqueline. IV. Jury, Vanessa. V.  
Universidade Federal de Santa Catarina. Programa de Pós  
Graduação em Engenharia de Alimentos. VI. Título.

Ana Caroline Cichella Frabetti

**STUDY OF ADHESION OF FOOD SUSPENSIONSON FLEXIBLE SUPPORTS  
DURING DRYING**

O presente trabalho em nível de doutorado foi avaliado e aprovado por banca  
examinadora composta pelos seguintes membros:

Prof. Dr. João Borges Laurindo - Presidente UFSC (BRASIL)

Dra. Hélène Simonin - Membro externo AGROSUP DIJON (FRANÇA)

Prof. Dr. Francis Courtois - Membro externo UNIVERSITÉ DE MONTPELLIER  
(FRANÇA)

Prof. Dra. Ana Silvia Prata Soares - Membro externo UNICAMP (BRASIL)

Certificamos que esta é a **versão original e final** do trabalho de conclusão que foi  
julgado adequado para obtenção do título de doutora em Engenharia de Alimentos.

Profa. Dra. Sandra Regina Salvador Ferreira.

Coordenadora do Programa

Prof. Dr. João Borges Laurindo

Orientador

Florianópolis, 2021.



*Este trabalho é dedicado aos meus pais,  
Júnior e Tânia, pelo apoio e amor incondicionais.*

## ACKNOWLEDGEMENTS

First and foremost, I would like to thank my advisors and co-advisors, Professor João Borges Laurindo, Professor Lionel Boillereaux, Jaqueline Oliveira de Moraes and Vanessa Jury. Their experience and theoretical knowledge were essential to decide the methodologies and discuss the results. Thank you for the countless meetings and discussions, and for encouraging me to seek answers with a scientific basis, to raise my work to a higher level. I would like to express my sincere gratitude to Professor João Laurindo for helping me in the search for an international experience, and to Professor Lionel Boillereaux for having accepted to be my advisor and to receive me in France.

My gratitude extends to CAPES (Brazil) and Oniris (France) for the funding of this work and particularly to the PrInt program (Institutional Internationalization Program from CAPES – Brazil), for making it possible to carry out the dual degree PhD (cotutelle).

I would also like to thank the technicians and those responsible of the laboratories in Brazil (PROFI, Central de Análises, LATESC, LCP, LABMAT) and in France (GEPEA – Nantes and Saint Nazaire), for all the support with the experiments.

I would like to thank my co-workers and friends from Brazil and France. It was their friendship that have made my study and life for these past few years a grateful time. I also thank my boyfriend for his help in communicating in French, for his understanding and patience. Finally, I am deeply thankful to my parents. Without their encouragement it would be impossible for me to complete my study.



*“I do not know anyone who has got to the top without hard work. That is the recipe.  
It will not always get you to the top, but should get you pretty near.”*

*Margaret Thatcher.*

## RESUMO

Na secagem de suspensões de alimentos por Cast-tape drying (CTD) em regime contínuo, o produto é espalhado como uma fina camada sobre um material de suporte que está em contato direto com a água aquecida ou com o vapor. Este processo é uma alternativa aos processos tradicionais, como spray-drying, drum-drying e liofilização, permitindo maior transferência de calor entre o meio de aquecimento e o produto, principalmente se materiais de suporte de baixa energia de superfície forem utilizados. No entanto, o desprendimento do material seco é fundamental, pois sua adesão ao suporte de secagem acarreta perda de rendimento do produto e dificuldades na limpeza do equipamento. Vários fatores influenciam o fenômeno de adesão, dependendo das características do alimento, bem como das propriedades do material de suporte. Assim, o presente trabalho está dividido em dois estudos. Primeiramente, foi utilizado um CTD contínuo com uma esteira de fibra de vidro revestida com Teflon<sup>®</sup> para a secagem de polpa morango. Polpas de frutas com alto teor de açúcar, como polpas de morango, podem mostrar pegajosidade quando processadas, então o objetivo foi determinar quais propriedades poderiam estar relacionadas à sua adesão. Foi realizada a caracterização das suspensões de morango e *leathers*, e observou-se que a adição de agentes carreadores (maltodextrina, amido e pectina) à polpa de morango aumentou a temperatura de transição vítrea e reduziu a adesividade dos produtos à esteira de Teflon<sup>®</sup>, promovendo sua remoção completa. Posteriormente, no segundo estudo, suspensões de amido de mandioca foram preparadas com diferentes concentrações de glicose, sacarose e frutose, a fim de avaliar o impacto da composição de açúcares de baixa massa molar na adesão do material à superfície de secagem. Um CTD em pequena escala, que permitiu a utilização de suportes de Teflon<sup>®</sup>, Mylar<sup>®</sup> e Teflon<sup>®</sup> abrasionados com lixa, foi utilizado para a secagem das suspensões, para determinar também a importância do material de superfície e sua rugosidade no fenômeno de adesão. As suspensões e filmes à base de amido foram avaliados por meio de reologia, temperatura de transição vítrea, isotermas de sorção, entre outros. A presença de sacarose na suspensão de amido mostrou uma grande influência no aumento da força de adesão ao suporte de Teflon<sup>®</sup> original (sem abrasões). Para o suporte de Teflon<sup>®</sup> mais rugoso (denominado Teflon<sup>®</sup> R1), a presença de sacarose, assim como de frutose, aumentou a força de adesão. Portanto, concluiu-se que a presença de frutose tem mais influência na adesão quando o material de superfície apresenta uma rugosidade mais profunda, comportamento também observado durante a secagem dos morangos (fruta com maior quantidade de frutose). A molhabilidade dos suportes, avaliada pelos ângulos de contato, foi afetada tanto pelas características de rugosidade do suporte quanto pela composição de açúcar

da suspensão a ser espalhada. O uso de Mylar<sup>®</sup> ou do Teflon<sup>®</sup> com maior rugosidade proporcionou maior molhabilidade, a qual é relacionada à maior adesão. Em geral, a presença de açúcares afetou a molhabilidade dos suportes de forma distinta. Assim, a composição dos açúcares é importante na análise de molhabilidade e adesão, mas a interação química entre suspensões e suportes também deve ser considerada.

**Palavras-chave:** composição de açúcar, rugosidade, molhabilidade, Teflon<sup>®</sup>, secagem de alimentos, desprendimento.

## RESUMO EXPANDIDO

### INTRODUÇÃO

A secagem de suspensões de alimentos em suportes flexíveis é uma alternativa aos processos de secagem por *spray-drying*, *drum-drying* e liofilização. Na secagem em *cast-tape drying* (CTD) é necessário espalhar a solução/suspensão sobre um suporte (de poliéster ou fibra de vidro revestido com Teflon®), bem como seu desprendimento após o processo de secagem, que depende da adesão do material à superfície. Alguns trabalhos científicos utilizados como referência para o presente estudo foram: Relationship between the glass transition temperature and the detachment of the dry film of food pastes, using a drying chamber and suspensions of maltodextrin, gum Arabic, and sugar cane molasses (F. P. Collares et al., 2004); Use of model solutions to build state diagrams for fruits (Grajales-Lagunes et al., 2018); Study of starch suspensions for tape-casting film production on a rigid surface (De Moraes et al., 2013).

### OBJETIVOS

As hipóteses investigadas foram que a composição, o teor de umidade e as condições de processamento de uma suspensão alimentar influenciam na formação do material desidratado (filme ou flocos); a adesão do filme seco ao suporte de secagem depende da composição dos açúcares de baixa massa molar, da temperatura de transição vítrea do produto em uma determinada umidade relativa e da rugosidade do material de suporte.

Dentro desse contexto, o objetivo geral desta tese foi investigar a influência da composição da suspensão alimentar, sua umidade e atividade de água, bem como a rugosidade e molhabilidade do suporte, no desprendimento de filmes secos de suportes flexíveis. Os objetivos específicos foram: estudar a adição de hidrocoloides à polpa de frutas para verificar sua influência na pegajosidade do filme seco ao suporte após secagem em *cast-tape drying*; compreender a relevância da composição da suspensão alimentar (por meio da adição de açúcares de baixo peso molecular) e a sua temperatura, bem como a rugosidade do suporte, no desprendimento da película desidratada; utilizar os conhecimentos obtidos com a solução modelo para a futura secagem de outras polpas de frutas em *cast-tape drying*.

### METODOLOGIA

As etapas experimentais envolveram a secagem da polpa de frutas em CTD contínuo (morango), com adição de agentes carreadores, para investigar o desempenho desses aditivos nas características de adesão, bem como na remoção de materiais desidratados; identificação do fenômeno de adesão e determinação das variáveis que podem estar envolvidas durante a secagem em CTD; adição de diferentes concentrações de frutose, glicose e sacarose a uma suspensão à base de amido (suspensão de modelo alimentar) para melhor compreender a influência dos açúcares de baixa massa molar na adesão da suspensão; Determinação da temperatura de transição vítrea, molhabilidade e comportamento reológico das suspensões; Estudo da influência da rugosidade do suporte no destacamento de filmes secos. Diferentes rugosidades foram criadas (com lixa) e caracterizadas; Determinação da força de desprendimento necessária para a retirada de produtos secos aderidos aos suportes (Mylar® - original e Teflon® - original e com duas rugosidades diferentes).

### RESULTADOS E DISCUSSÃO

Os resultados obtidos para o desprendimento dos filmes à base de amido mostraram que, conforme previsto pelas hipóteses do presente trabalho, a composição dos açúcares afeta a adesão do material seco ao suporte. A sacarose está relacionada ao aumento da adesão ao suporte de Teflon® (com sua rugosidade original). Os experimentos utilizando Teflon® com

maior rugosidade evidenciaram que quando a rugosidade é aumentada, a presença de frutose impacta significativamente na adesão, juntamente com a sacarose. A temperatura da suspensão também deve ser considerada, pois influencia na sua molhabilidade, o que pode aumentar a adesão. A molhabilidade das suspensões à base de amido foi determinada à temperatura ambiente por meio de ângulos de contato, sendo que a suspensão contendo apenas sacarose (6S) apresentou menor molhabilidade no suporte original de Teflon<sup>®</sup>, o que indica menor adesão neste material. Porém, durante o processo de secagem, em que a temperatura da suspensão foi aumentada, provavelmente a molhabilidade dessa suspensão aumentou, aumentando a adesão. Com a diminuição da temperatura do sistema após a secagem, as forças de adesão aumentaram até a temperatura mais baixa testada (35 °C), na qual os filmes aderiram fortemente ao suporte de Teflon<sup>®</sup>, sendo removidos como flocos. A composição de açúcar do filme afetou esta análise pela diferença na força de adesão e nos produtos obtidos a cada temperatura de resfriamento, quando se utilizou a amostra com três açúcares (Filme 1,98 GSF) ou a amostra somente com sacarose (Filme 6S). A hipótese inicial do estudo de que a adesão depende da temperatura de transição vítrea do produto é comprovadamente correta. Embora não seja o principal fator de influência, visto que todas as amostras estavam acima da T<sub>g</sub>, algumas delas aderiram mais ao material sólido, dependendo da composição do açúcar e da rugosidade do suporte. A suposição de que o teor de umidade desempenha um papel na formação de filmes ou flocos também foi verificada por meio do armazenamento dos filmes na umidade relativa escolhida. De fato, a uma umidade relativa de 33%, as amostras foram removidas na forma de flocos. A umidade relativa intermediária (44% a 54%) facilitou a retirada do material seco como um todo, com um destacamento inicial com espátula. A alta umidade relativa do ar (68% e 84%) facilitou a retirada das amostras, pois os produtos eram muito úmidos, embora notavelmente pegajosos.

### **CONSIDERAÇÕES FINAIS**

Embora as hipóteses previstas no início do presente trabalho tenham sido avaliadas, o estudo da adesão durante a secagem ainda é um assunto cercado de muitas incógnitas. Algumas sugestões para estudos futuros incluem a adição de fibras às suspensões do modelo, para avaliar o comportamento de filmes mais resistentes durante a remoção dos suportes. Além disso, alguns outros parâmetros interessantes para estudar são a secagem de suspensões com maiores espessuras de espalhamento, e desenvolver uma metodologia sem variação do ângulo de desprendimento, permitindo assim a determinação de uma força de adesão que é diretamente comparável a outros estudos de adesão em alimentos.

**Palavras-chave:** composição de açúcar, rugosidade, molhabilidade, Teflon<sup>®</sup>, secagem de alimentos, desprendimento.

## ABSTRACT

In the drying of food suspensions by continuous Cast-tape drying (CTD), the product is spread as a thin layer over a support material that is in direct contact with the heated water or vapor. This process is an alternative to traditional processes such as spray-drying, drum-drying, and freeze-drying, allowing greater heat transfer between the heating medium and the product, especially if low surface energy support materials are used. Nevertheless, the detachment of the dry material is essential, since its adhesion to the drying support causes loss of product yield and difficulties in cleaning the equipment. Multiple factors influence the adhesion phenomenon, depending on the food characteristics as well as support material properties. Thus, the present work is divided into two studies. Firstly, a continuous CTD with a conveyor belt made of fiberglass coated with Teflon<sup>®</sup> was employed for strawberry pulp drying. Fruit pulps with high sugar content, such as strawberry pulps, can show a sticky character when processed, so the goal was to determine which properties could be related to their adhesion. The characterization of the strawberry suspensions and leathers was performed, and it was observed that the addition of carrier agents (maltodextrin, starch, and pectin) to the strawberry pulp increased the glass transition temperature and reduced the adhesiveness of the products to the Teflon<sup>®</sup> belt, promoting their complete removal. Subsequently, in the second study, suspensions of cassava starch were prepared with different concentrations of glucose, sucrose, and fructose, in order to assess the impact of the composition of low molar mass sugars on the material's adhesion to the drying surface. A small-scale CTD, which allowed the use of Teflon<sup>®</sup>, Mylar<sup>®</sup>, and Teflon<sup>®</sup> supports abraded with sandpaper, was used to the drying of the suspensions, to determine also the importance of the surface material and its roughness in the adhesion phenomenon. The starch-based suspensions and films were evaluated through rheology, glass transition temperature, sorption isotherms, among others. The presence of sucrose in the starch suspension showed a major influence in increasing the force of adhesion to the original Teflon<sup>®</sup> support (without abrasions). For the roughest Teflon<sup>®</sup> support (called Teflon<sup>®</sup> R1), the presence of sucrose, as well as fructose, increased in the force of adhesion. Therefore, it was concluded that the presence of fructose has more influence on adhesion when the surface material has a deeper roughness, a behavior also noticed during the drying of strawberries (a fruit with a higher amount of fructose). The wettability of the supports, evaluated by the contact angles, was affected both by the roughness characteristics of the support and by the sugar composition of the suspension to be spread. The use of Mylar<sup>®</sup> or Teflon<sup>®</sup> with increased roughness caused greater wettability, which is related to greater adhesion. In general, the presence of sugars

affected the wettability of the supports differently. Thus, the composition of sugars is important in the analysis of wettability and adhesion, but the chemical interaction between suspensions and supports must also be considered.

**Keywords:** sugar composition, roughness, wettability, Teflon<sup>®</sup>, food drying, detachment.

## RESUMÉ

Lors du séchage de suspensions alimentaires par *Cast-tape drying* (CTD) en régime continu, le produit est étalé en couche mince sur un matériau de support qui est en contact direct avec l'eau ou la vapeur chauffée. Ce procédé est une alternative aux procédés traditionnels, tels que le séchage par atomisation, le séchage au tambour et la lyophilisation, permettant un plus grand transfert de chaleur entre le milieu chauffant et le produit, en particulier si des matériaux de support à faible énergie de surface sont utilisés. Néanmoins, le détachement de la matière sèche est indispensable, car son adhérence au support de séchage entraîne une perte de rendement en produit et des difficultés de nettoyage de l'équipement. De multiples facteurs influencent le phénomène d'adhérence, en fonction des caractéristiques alimentaires ainsi que des propriétés du matériau de support. Ainsi, le présent travail est divisé en deux études. Tout d'abord, un CTD continu avec un tapis roulant en fibre de verre enduite de Teflon<sup>®</sup> a été utilisé pour le séchage de la pulpe de fraise. Les pulpes de fruits à haute teneur en sucre, comme les pulpes de fraise, peuvent montrer un caractère collant lorsqu'elles sont traitées. L'objectif était donc de déterminer quelles propriétés pouvaient être liées à leur adhérence. La caractérisation des suspensions et *leathers* de fraises a été réalisée, et il a été observé que l'ajout d'agents d'aide au séchage (maltodextrine, amidon et pectine) à la pulpe de fraise augmentait la température de transition vitreuse et réduisait l'adhésivité des produits au tapis en Teflon<sup>®</sup>, favorisant leur détachement complet. Par la suite, dans la deuxième étude, des suspensions d'amidon de manioc ont été préparées avec différentes concentrations de glucose, de saccharose et de fructose, afin d'évaluer l'impact de la composition des sucres de faible masse molaire sur l'adhérence du matériau à la surface de séchage. Un CTD à petite échelle, qui a permis l'utilisation de supports en Teflon<sup>®</sup>, Mylar<sup>®</sup> et Teflon<sup>®</sup> abrasés au papier de verre, a été utilisé pour le séchage des suspensions, pour déterminer également l'importance du matériau de surface et sa rugosité dans le phénomène d'adhérence. Les suspensions et films à base d'amidon ont été évalués par rhéologie, température de transition vitreuse, isothermes de sorption, entre autres. La présence de saccharose dans la suspension d'amidon a montré une influence majeure en augmentant la force d'adhésion au support en Teflon<sup>®</sup> original (sans abrasions). Pour le support Teflon<sup>®</sup> le plus rugueux (appelé Teflon<sup>®</sup> R1), la présence de saccharose, ainsi que de fructose, a augmenté la force d'adhérence. Par conséquent, il a été conclu que la présence de fructose a plus d'influence sur l'adhérence lorsque le matériau de surface a une rugosité plus profonde, ce qui a également été remarqué lors du séchage des fraises (un fruit avec une quantité plus élevée de fructose). La mouillabilité des supports, évaluée par les angles de contact, était affectée à la fois



par les caractéristiques de rugosité du support et par la composition en sucres de la suspension à étaler. L'utilisation de Mylar® ou de Teflon® avec une rugosité accrue a entraîné une plus grande mouillabilité, ce qui est lié à une plus grande adhérence. En général, la présence de sucres affecte différemment la mouillabilité des supports. Ainsi, la composition des sucres est importante dans l'analyse de la mouillabilité et de l'adhérence, mais l'interaction chimique entre suspensions et supports doit également être prise en compte.

**Mots clés :** composition des sucres, rugosité, mouillabilité, Teflon®, séchage des aliments, détachement.

## LIST OF FIGURES

Figure 1 - Typical drying curves as a function of time: (a) drying kinetics; (b) drying rate. ...	36
Figure 2 - Operation diagram of an RW dryer. ....	39
Figure 3 - Mango leather produced in CTD. ....	41
Figure 4 - Changes in the physical state of an amorphous material as a function of temperature and time. ....	47
Figure 5 - (a) Change in enthalpy or volume of a material with temperature (b) exothermic change corresponding to the change in thermal capacity ( $C_p$ ), in the glass transition region. ....	47
Figure 6 - Fluid rheological behaviors: (a) time-independent (b) time-dependent. ....	53
Figure 7 - Representation of the (a) Cassie-Baxter and (b) Wenzel states. ....	58
Figure 8 - Angles configuration for the peel test. ....	60
Figure 9 - Creation of the grooves in the support samples using sandpaper. ....	63
Figure 10 - Average roughness measurement ( $S_a$ ). ....	63
Figure 11 - Scheme of operation of the cast-tape drying equipment under a continuous regime. ....	66
Figure 12 - Image of the continuous CTD equipment used in the experiments. ....	66
Figure 13 - Doctor-blade spreader. ....	67
Figure 14 - Spreading of mango pulps with different °Brix on the continuous CTD support. ....	71
Figure 15 - (a) Small-scale experimental equipment for the drying of the starch-based suspensions; (b) Top view of the small-scale equipment; (c) View of the stainless-steel bath. ....	74
Figure 16 - Aluminum plate with water circulation for drying and cooling the starch-based samples. ....	74
Figure 17 - Aluminum plate heated by electrical resistances to perform the drying of the starch-based suspensions. ....	75
Figure 18 - Texturometer used for the starch's detachment experiments: (a) texturometer and CTD equipment, (b) spreading frame and a piece of Mylar <sup>®</sup> attached to the tensile grip. ....	79
Figure 19 - Aluminum plate employed to detachment tests with cooling. ....	80
Figure 20 - Topographic images of Teflon <sup>®</sup> support samples: (a) Teflon <sup>®</sup> - original; (b) Teflon <sup>®</sup> with fewer abrasions (R2); (c) Teflon <sup>®</sup> with more abrasions (R1). ....	83
Figure 21 - Viscosity curves of strawberry suspensions (all graphs also show shear rates up to $100 \text{ s}^{-1}$ , to highlight the decay of the curves): (a) Strawberry pulp; (b) Strawberry + 5% starch; (c) Strawberry + 5% maltodextrin; (d) Strawberry + 5% pectin. ....	87

Figure 22 - Strawberry drying curves in continuous CTD. ....	90
Figure 23 - Thermographic images of drying in continuous CTD of (a) pure strawberry pulp and (b) strawberry-starch suspension. ....	93
Figure 24 - Sorption isotherm of strawberry leathers produced by CTD. ....	96
Figure 25 - Visual assessment of the detachment of strawberry leathers. ....	100
Figure 26 - Viscosity curves of starch-based suspensions (all graphs also show shear rates up to $100 \text{ s}^{-1}$ , to highlight the decay of the curves): (a) Suspension of cassava starch 4%; (b) Suspension 6F (6 g fructose/100 g suspension); (c) Suspension 1.98GSF (1.98 g glucose + 1.98 g sucrose + 1.98 g fructose/100 g suspension); (d) Suspension 6S (6 g sucrose/100 g suspension). ....	103
Figure 27 - Response surface plots of surface tension as a function of the sugar composition of starch-based suspensions. ....	107
Figure 28 - Response surface plots of contact angle as a function of the sugar composition of the starch-based suspensions, when measured on the supports: (a) original Teflon <sup>®</sup> ; (b) Teflon <sup>®</sup> R1; (c) Teflon <sup>®</sup> R2; (d) Mylar <sup>®</sup> . ....	112
Figure 29 - Isotherms of starch-based films at $20 \text{ }^{\circ}\text{C}$ . ....	115
Figure 30 - DSC thermograms. ....	118
Figure 31 - Response surface plots of Tg as a function of the sugar composition of the starch-based films. ....	120
Figure 32 - Response surface plot of (a) thickness and (b) tensile strength as a function of the sugar composition of the starch-based films. ....	124
Figure 33 - Response surfaces for the maximum load, concerning sugar composition, to detach starch-based films from the supports after drying: (a) original Teflon <sup>®</sup> ; (b) Teflon <sup>®</sup> R1; (c) Teflon <sup>®</sup> R2; (d) Mylar <sup>®</sup> . ....	129
Figure 34 - Average tensile strength and adhesive forces of starch-based films. ....	135
Figure 35 - Average load to detach Film 1.98 GSF when subjected to cooling temperatures; description of the type of product obtained. ....	140
Figure 36 - Average load to detach Film 6S when subjected to cooling temperatures; description of the type of product obtained. ....	141
Figure 37 - Dehydrated starch-based films obtained at several cooling temperatures. ....	142
Figure 38 - Moisture content of the Films 1.98 GSF and 6F stored at a relative humidity of 33%, 44%, 54%, 68%, and 84%, concerning its appearance. ....	143
Figure 40 - Parameters of qualitative analysis of the starch-based films. ....	145
Figure 41 - Appearance of the starch-based films stored at 44% RH. ....	146

Figure 42 - Starch-based films formed over (a) Teflon<sup>®</sup>; (b) Teflon<sup>®</sup> R1; (c) Teflon<sup>®</sup> R2 and (d) Mylar<sup>®</sup> ..... 147

Appendix A 1 - Shear stresses versus shear rates of strawberry suspensions: (a) Pure strawberry; (b) Strawberry + 5% starch; (c) Strawberry + 5% maltodextrin; (d) Strawberry + 5% pectin..... 171

Appendix A 2 - Viscosity curves of starch formulations: (a) Suspension 3G3F (3 g of glucose + 3 g of fructose / 100 g suspension); (b) Suspension 3G3S (3 g glucose + 3 g sucrose / 100 g suspension); (c) Suspension 6G (6 g glucose / 100 g suspension); (d) Suspension 3S3F (3 g sucrose + 3 g fructose / 100 g suspension)..... 172

Appendix A 3 - Shear stresses versus shear rates of starch formulations: (a) Suspension of cassava starch 4%; (b) Suspension 6F (6 g fructose / 100 g suspension); (c) Suspension 1.98 GSF (1.98 g glucose + 1.98 g sucrose + 1.98g g fructose / 100 g suspension); (d) Suspension 6S (6 g sucrose / 100 g suspension). ..... 173

Appendix A 4 - Shear stresses versus shear rates of starch formulations: (a) Suspension 3G3F (3 g glucose + 3 g fructose / 100 g suspension); (b) Suspension 3G3S (3 g glucose + 3 g sucrose / 100 g suspension); (c) Suspension 6G (6 g glucose / 100 g suspension); (d) Suspension 3S3F (3 g sucrose + 3 g fructose / 100 g suspension). ..... 174

Appendix B 1 - Thermographs of the drying of the strawberry suspension with the addition of maltodextrin in continuous CTD..... 176

Appendix B 2 - Thermographs of the drying of the strawberry suspension with the addition of pectin in continuous CTD. .... 177

## LIST OF TABLES

Table 1 - Main dryers used in food and their characteristics.....	38
Table 2 - Molar masses and glass transition temperatures of anhydrous food materials. ....	49
Table 3 - Classification of Newtonian and non-Newtonian fluids.....	52
Table 4 - Surface tension of several solid materials.....	56
Table 5 - Surface tension of liquids.....	57
Table 6 - Water activities of airtight pots with saturated saline solutions.....	69
Table 7 – Three-factor simplex-centroid experimental design to define the sugar composition of the starch-based suspensions.....	72
Table 8 - Formulation of starch-based suspensions.....	73
Table 9 - Mean roughness values (Sa) of Teflon <sup>®</sup> samples and contact angles with water on Teflon <sup>®</sup> and Mylar <sup>®</sup> .....	82
Table 10 - Equilibrium contact angles and surface tensions of support materials at 20 °C.....	84
Table 11 – Parameters of the Ostwald model adjusted to the shear stress vs. shear rate curves of strawberry suspensions.....	88
Table 12 - Adjustment of shear stress vs. shear rate curves of strawberry suspensions to the Herschel-Bulkley model.....	89
Table 13 - Strawberry drying rates in continuous CTD.....	92
Table 14 - Initial and final moisture content and water activities of strawberry suspensions processed in continuous CTD.....	94
Table 15 - Estimated parameters of the GAB model for strawberry leathers.....	97
Table 16 - Tg of strawberry powder samples produced in continuous CTD.....	99
Table 17 - Adjustment of shear stress vs. shear rate curves of the starch-based suspensions to the Ostwald model.....	104
Table 18 - Adjustment of shear stress vs. shear rate curves of the starch-based suspensions to the Herschel-Bulkley model.....	105
Table 19 - Surface tension of starch-based suspensions without Tween and with 0.1% Tween 20.....	106
Table 20 - Equations fitted to quadratic models for the surface tension of the starch-based suspensions.....	108
Table 21 - Contact angles between starch-based suspensions on both Mylar <sup>®</sup> and Teflon <sup>®</sup> supports.....	109
Table 22 – Equations fitted to linear and quadratic models for the contact angles.....	113

Table 23 - Moisture content and water activities of starch-based suspensions and films processed in an aluminum plate with internal heating. ....	114
Table 24 - Glass transition temperatures of starch-based films. ....	118
Table 25 - Equation fitted to the quadratic model for the Tg of starch-based films with added sugar. ....	120
Table 26 – Thicknesses of the starch-based films, maximum and average load (N) during the tensile test, and tensile strength of the starch-based films. ....	122
Table 27 - Equation fitted to the linear model for the thickness and tensile strength of the starch-based films with added sugar. ....	124
Table 28- Maximum and average load (N) for the detachment of starch-based films from Teflon <sup>®</sup> support. ....	126
Table 29 - Moisture content and water activity of starch-based films produced by small-scale CTD with water circulation using Teflon <sup>®</sup> support. ....	126
Table 30 – Maximum and average load (N) for the detachment of starch-based films from Mylar <sup>®</sup> support. ....	127
Table 31 - Moisture content and water activity of starch-based films produced by small-scale CTD with water circulation using Mylar <sup>®</sup> support. ....	127
Table 32 - Equations fitted to quadratic models for the maximum load to detach starch-based films with added sugar from the supports after drying. ....	130
Table 33 – Maximum and average load (N) for the detachment of Film 1.98 GSF and Film 6S from original Teflon <sup>®</sup> support, for different cooling temperatures. ....	137
Table 34 - Moisture content and water activity of Film 1.98 GSF and Film 6S produced on aluminum plate and using different cooling temperatures. ....	137

## LIST OF SYMBOLS, ABBREVIATIONS AND UNITS

Average surface roughness	Sa
Carrier agent	CA
Cast-tape drying	CTD
Component acid from the Van Oss model	$\gamma_S^+$
Component acid from the Van Oss model	$\gamma_S^-$
Consistency index (Pa.s <sup>n</sup> )	K
Contact angle	$\theta$
Differential Scanning Calorimetry	DSC
Diiodomethane	DIM
Dry basis	d.b.
Dynamic Vapor Sorption	DVS
Equilibrium moisture content (g g <sup>-1</sup> , d.b.)	X
Flow index	<i>n</i>
Fructose	F
Glass transition temperature	Tg
Glucose	G
Gram of water per gram of dry solid	g g <sup>-1</sup> (d.b.)
Guggenheim - Anderson - de Boer	GAB
GAB constant	<i>k</i>
Guggenheim constant	C
Lifshitz–van der Waals component from the Van Oss model	$\gamma_S^{LW}$
Maximum load (N)	P <sub>MAX</sub>
Milli Newton per meter	mN m <sup>-1</sup>
Milli Pascal per second	mPa s <sup>-1</sup>
Moisture content in the monolayer (g g <sup>-1</sup> , d.b.)	X <sub>0</sub>
Newton	N
Original cross-sectional area (mm <sup>2</sup> )	A <sub>0</sub>
Refractance window	RW

Shear deformation rate	$\dot{\gamma}$
Shear stress	$\sigma$
Analysis of variance	ANOVA
Solid-liquid interfacial tension	$\gamma_{SL}$
Sucrose	S
Surface tension of the liquid	$\gamma_L$
Surface tension of the solid	$\gamma_S$
Tensile strength (MPa)	$\sigma_{MAX}$
Tensile strength	TS
Thickness	$e$
Relative humidity	RH
Revolution per minute	rpm
Viscosity (Pa s or mPa s)	$\eta$
Water activity	$a_w$
Weight/volume	W/V
Width	$\omega$



## CONTENTS

<b>1. INTRODUCTION</b> .....	31
<b>2. BIBLIOGRAPHICAL REVIEW</b> .....	34
2.1. DRYING.....	34
<b>2.1.1. Energy and mass transfer mechanisms</b> .....	35
<b>2.1.2. Drying kinetics</b> .....	35
2.2. TYPES OF DRYERS .....	37
2.3. CAST-TAPE DRYING .....	38
2.4. MODEL FOOD SOLUTIONS .....	41
<b>2.4.1. Strawberries</b> .....	42
<b>2.4.2. Hydrocolloids</b> .....	43
2.5. AMORPHOUS STATE AND GLASS TRANSITION.....	45
<b>2.5.1. Plasticization effect on amorphous solids</b> .....	47
<b>2.5.2. Effect of the molar mass of food polymers on amorphous solids</b> .....	49
2.6. FLUID RHEOLOGY .....	50
2.7. ADHESION IN SUPPORTS AND WETTABILITY .....	53
<b>3. MATERIAL AND METHODS</b> .....	62
3.1. CHARACTERIZATION OF FLEXIBLE SUPPORTS .....	62
<b>3.1.1. Surface roughness</b> .....	62
<b>3.1.2. Contact angle</b> .....	64
<b>3.1.3. Surface tension of support materials</b> .....	64
3.2. CASE STUDY OF CAST-TAPE DRYING OF STRAWBERRY PULP WITH ADDED HYDROCOLLOIDS.....	64
<b>3.2.1. Materials</b> .....	65
<b>3.2.2. Rheology</b> .....	65
<b>3.2.3. Cast-tape drying</b> .....	65

<b>3.2.4.</b>	<b>Experimental procedure</b> .....	67
<b>3.2.5.</b>	<b>Thermographs</b> .....	68
3.3.	<b>CHARACTERIZATION OF STRAWBERRY LEATHERS</b> .....	68
<b>3.3.1.</b>	<b>Moisture content and water activity</b> .....	68
<b>3.3.2.</b>	<b>Thickness</b> .....	69
<b>3.3.3.</b>	<b>Sorption isotherms</b> .....	69
<b>3.3.4.</b>	<b>Glass transition temperature</b> .....	70
<b>3.3.5.</b>	<b>Detachment of strawberry leathers</b> .....	70
3.4.	<b>STUDY OF ADDING LOW MOLAR MASS SUGARS IN STARCH-BASED SUSPENSION FOR CTD DRYING</b> .....	70
<b>3.4.1.</b>	<b>Materials</b> .....	71
<b>3.4.2.</b>	<b>Preparation of starch-based suspensions</b> .....	72
<b>3.4.3.</b>	<b>Small-scale batch CTD experimental apparatus</b> .....	73
<b>3.4.4.</b>	<b>Experimental drying procedure</b> .....	75
<b>3.4.5.</b>	<b>Contact angle</b> .....	75
<b>3.4.6.</b>	<b>Surface tension of starch-based suspensions</b> .....	76
<b>3.4.7.</b>	<b>Rheology</b> .....	76
<b>3.4.8.</b>	<b>Moisture content and water activity</b> .....	76
3.5.	<b>CHARACTERIZATION OF STARCH-BASED FILMS</b> .....	76
<b>3.5.1.</b>	<b>Thickness</b> .....	77
<b>3.5.2.</b>	<b>Water sorption isotherms</b> .....	77
<b>3.5.3.</b>	<b>Glass transition temperature</b> .....	77
<b>3.5.4.</b>	<b>Mechanical tests</b> .....	77
<b>3.5.5.</b>	<b>Evaluation of the detachment of starch-based films</b> .....	78
3.5.5.1.	Effect of temperature on the dry products detachment.....	79
3.5.5.2.	Effect of relative humidity (RH) on the dry products detachment .....	80
<b>3.5.6.</b>	<b>Visual analysis</b> .....	80

3.6.	STATISTICAL ANALYSIS .....	81
<b>4.</b>	<b>RESULTS AND DISCUSSION.....</b>	<b>82</b>
4.1.	CHARACTERIZATION OF FLEXIBLE SUPPORTS .....	82
4.1.1.	<b>Surface roughness and contact angle.....</b>	<b>82</b>
4.1.2.	<b>Surface tension of support materials .....</b>	<b>84</b>
4.2.	CASE STUDY OF THE DRYING OF STRAWBERRY PULP WITH ADDED HYDROCOLLOIDS BY CTD .....	86
4.2.1.	<b>Rheology of the strawberry suspensions .....</b>	<b>86</b>
4.2.2.	<b>Strawberries drying kinetics.....</b>	<b>89</b>
4.2.3.	<b>Thermographs.....</b>	<b>92</b>
4.2.4.	<b>Moisture content, water activity and leather thickness .....</b>	<b>94</b>
4.2.5.	<b>Water sorption isotherms .....</b>	<b>96</b>
4.2.6.	<b>Glass transition temperature.....</b>	<b>98</b>
4.2.7.	<b>Detachment of strawberries leathers .....</b>	<b>99</b>
4.3.	STUDY OF ADDING LOW MOLAR MASS SUGARS IN STARCH-BASED SUSPENSION FOR CTD DRYING .....	102
4.3.1.	<b>Rheology of the starch-based suspensions.....</b>	<b>102</b>
4.3.2.	<b>Surface tension of the starch-based suspensions .....</b>	<b>106</b>
4.3.3.	<b>Contact angle between suspension and flexible supports .....</b>	<b>108</b>
4.3.4.	<b>Moisture content and water activity of starch-based suspensions and dried materials.....</b>	<b>113</b>
4.3.5.	<b>Sorption isotherms.....</b>	<b>114</b>
4.3.6.	<b>Glass transition temperature.....</b>	<b>117</b>
4.3.7.	<b>Mechanical tests and thickness of the starch-based films.....</b>	<b>122</b>
4.3.8.	<b>Evaluation of the detachment of starch-based films .....</b>	<b>125</b>
4.3.8.1.	Effect of temperature on the dry products detachment .....	136
4.3.8.2.	Effect of relative humidity (RH) on the dry products detachment.....	143
4.3.9.	<b>Visual analysis.....</b>	<b>144</b>

<b>5. CONCLUSION</b> .....	148
<b>REFERENCES</b> .....	150
<b>APPENDIX A</b> .....	171
<b>APPENDIX B</b> .....	176

## CONCEPTUAL SCHEME

### What? Why?

- Drying of food suspensions on flexible supports is an alternative to spray-drying, drum-drying, and freeze-drying processes.
- When drying in cast-tape drying (CTD) it is necessary to spread the solution/suspension on a support (of polyester or fiberglass coated with Teflon<sup>®</sup>), as well as its detachment after the drying process, which depends on the adhesion of the material to the surface.

### State of the art:

- Relationship between the glass transition temperature and the detachment of the dry film of food pastes, using a drying chamber and suspensions of maltodextrin, gum Arabic, and sugar cane molasses (F. P. Collares et al., 2004);
- Use of model solutions to build state diagrams for fruits (Grajales-Lagunes et al., 2018);
- Study of starch suspensions for tape-casting film production on a rigid surface (De Moraes et al., 2013).

### Hypotheses:

- The composition, moisture content, and processing conditions of a food suspension influence the formation of the dehydrated material (film or flakes);
- The adhesion of the dry film to the drying support depends on the composition of the low molar mass sugars, the glass transition temperature of the product at a certain relative humidity, and the roughness of the support material.

### Experimental steps:

- Drying of fruit pulp in continuous CTD (strawberries), with the addition of carrier agents (CA), to investigate the performance of these additives in adhesion characteristics, as well as in the removal of dehydrated materials. Identification of the adhesion phenomenon and determination of the variables that may be involved during CTD drying;
- Addition of different concentrations of fructose, glucose, and sucrose to a starch-based suspension (food model suspension) to better understand the influence of low molar mass sugars on the adhesion of the suspension;
- Determination of glass transition temperature, wettability, and rheological behavior of suspensions;
- Study of the influence of the support roughness on the detachment of dry films. Different roughnesses are created (with sandpaper) and characterized;
- Determination of the detachment force necessary for the removal of dry products adhered to the supports (Mylar<sup>®</sup> - original and Teflon<sup>®</sup> -original and with two different roughness).

### Expected results:

Influence of the composition and moisture content of the food suspension, as well as the surface roughness, on the detachment's force necessary to remove the dehydrated film from the drying surface.

## **SCHÉMA CONCEPTUEL**

### **Quoi ? Pourquoi ?**

- Le séchage des suspensions alimentaires sur supports souples est une alternative aux procédés de séchage par atomisation, séchage au tambour et lyophilisation ;
- Lors du séchage en cast-tape drying (CTD), il est nécessaire d'étaler la solution / suspension sur un support (en polyester ou fibre de verre enduit de Téflon<sup>®</sup>), ainsi que son décollement après le processus, qui dépend de l'adhérence du matériel à la surface du support.

### **L'état de l'art :**

- Relation entre la température de transition vitreuse et le détachement du film sec de s purées alimentaires, à l'aide d'une chambre de séchage et de suspensions de maltodextrine, de gomme arabique et de mélasse de canne à sucre (F. P. Collares et al., 2004) ;
- Utilisation de solutions modèles pour construire des diagrammes d'état pour les fruits (Grajales-Lagunes et al., 2018) ;
- Etude de suspensions d'amidon pour la production de films en tape-casting sur une surface rigide (De Moraes et al., 2013).

### **Hypothèses :**

- La composition de la suspension alimentaire, sa teneur en eau et les caractéristiques du procédé influencent la formation de la matière déshydratée (film ou flocons) ;
- L'adhérence du film sec au support de séchage dépend de la composition de sucres de faible masse molaire, de la température de transition vitreuse du produit à une certaine humidité relative et de la rugosité du matériel de support.

### **Étapes expérimentales :**

- Séchage d'une pulpe de fruit en CTD continu (fraises), avec l'ajout d'agents d'aide au séchage, pour étudier les performances de ces additifs dans les caractéristiques d'adhésion, ainsi que dans le détachement des produits déshydratés. Identification du phénomène d'adhésion et détermination des variables pouvant être impliquées lors du séchage en CTD ;
- Ajout de différentes concentrations de fructose, glucose et saccharose à une suspension à base d'amidon (modèle de suspension alimentaire) pour mieux comprendre l'influence des sucres de faible masse molaire sur l'adhésion de la suspension ;
- Détermination de la température de transition vitreuse, de la mouillabilité et du comportement rhéologique des suspensions ;
- Etude de l'influence de la rugosité du support sur le détachement des films secs. Différentes rugosités sont créées (avec du papier de verre) et caractérisées ;
- Détermination de la force de décollement nécessaire pour le détachement des produits secs adhérant aux supports (Mylar<sup>®</sup> et Teflon<sup>®</sup> - original et avec deux rugosités différentes).

### **Résultats attendus :**

Influence de la composition et de la teneur en eau de la suspension alimentaire, ainsi que de la rugosité de surface, sur la force de détachement nécessaire pour retirer le film déshydraté de la surface de séchage.

## 1. INTRODUCTION

Drying is an ancient technology used in food preservation, being until today one of the most applied in the food industry. Dried products have lower weight, chemical and microbial stability at room temperature, and convenience for transportation and storage (B. Bhandari & Howes, 1999).

One of the main challenges of drying is to remove water from a product at fast rates, to optimize energy expenditure while preserving the nutritional quality and the structure of the dried and rehydrated material. Therefore, it is essential to know the phenomena involved during the processing and transformation of materials by drying. There are several dehydration techniques, among which the most commonly applied are hot air, vacuum drying and freeze-drying. Among the hot air drying (or convective drying) processes, the spray-drying has been extensively used for food solutions and suspensions (Aguilera et al., 2003; B. Bhandari & Howes, 1999).

Spray-drying is a well-established and widespread method for turning a variety of liquid foods into powders. However, during drying, some materials become sticky, which causes them to adhere to the equipment wall, causing lower product yields and operational problems. This phenomenon is common during the drying of fruits and vegetables pulps, because they have high sugar concentrations. The dryer design must be modified for these products by injecting cold air or scrapers to remove the material, for example. Another option is the addition of additives (carrier agents) before the drying process (B. R. Bhandari et al., 1997).

Also, the technological development of drying methods is still limited by equipment energy expenditure, chemical reactions, applicability to a wide range of foods, preservation of physical, chemical, and nutritional characteristics, besides difficulties in rehydration. Thus, new food processing methods are studied continuously in order to minimize these limitations and improve the quality of the final product (Fellows, 2000; Gava et al., 2009; Nindo, Tang, et al., 2007).

Within this context, Cast-Tape Drying (CTD) is an innovative and suitable process for the production of dehydrated foods since drying times are shorter than those typically observed in conventional dryers and freeze-dryers. In this technique, food suspension is spread on the upper face of flexible support (Mylar<sup>®</sup> polyester film or Teflon<sup>®</sup> coated fiberglass film), which is heated by a hot water or steam on its underside.

Most of reported studies use CTD to dry fruit and vegetable purees (Abonyi et al., 2002; Caparino et al., 2012; Durigon et al., 2016; Frabetti et al., 2018; Nindo, Powers, et al., 2007; Ortiz-Jerez & Ochoa-Martínez, 2015; Zotarelli et al., 2017). However, foods are complex systems with widely variable compositions, which can lead to discrepancies in the literature data concerning drying times and dried product characteristics. Still, a few scientific papers have reported food drying with CTD while working in a continuous regime, considering that the products must be removed in the form of an intact and malleable dehydrated film. For this reason, the adhesion of solutions to flexible supports and the influence of different sugar concentrations on the cohesive property of the material must be elucidated.

Among fruits, glucose, sucrose, fructose, and pectin are the main water-soluble components, representing most of the dry matter and considered the major vitrifying agents in these foods. Such compounds form amorphous structures when subjected to drying, as the rapid removal of water does not allow sufficient time for crystallization to occur. These structures are known to be cohesive, hygroscopic, and difficult to flow and to be dispersed. Also, sugars' concentration influence the physical state of the dry material and its storage conditions (B. Bhandari & Howes, 1999; Sánchez-Moreno et al., 2012).

To better understand the adhesion and cohesion phenomena, model solutions can be employed to simulate different systems. The proportions of the major components can be well controlled so that the thermal transitions and parameters involved in processing real foods are properly studied (RUIZ-CABRERA et al., 2016). Nevertheless, it is not common to use this approach for practical purposes, and there are not many studies that use glass transition temperature to improve the drying process and the product characteristics (Femenia et al., 1997; Grajales-Lagunes et al., 2018; Jayasundera et al., 2011; Nguyen et al., 2020; Saavedra-Leos et al., 2012; Shah & Schall, 2006).

If a food is dried at a higher temperature than its glass transition temperature (commonly referred to as  $T_g$ , the temperature range between the glassy and rubbery state), the product will remain in a sticky state, and upon contact with a solid surface of high energy, it will stick. Based on this, the study of  $T_g$  is of essential importance to define the process characteristics and to better understand the properties of dried food materials, enabling the development of new products and technologies (B. Bhandari & Howes, 2005; Rha, 1975).

Collares, Finzer e Kieckbusch (2004) studied the relationship between the composition of a food model solution and its detachment from a drying surface, relating it to the glass transition temperature. However, Bhandari and Howes (2005) explained the detachment by the tension between molecules resulted from the material shrinkage upon drying. The increased



stress on the material microstructure is caused by the cohesive force within the material. Thus, adhesion cannot be fully explained by glass transition temperature. Detachment is also influenced by surface energy and roughness of the support material.

Therefore, the general objective of this thesis was to investigate the influence of food suspension composition, its moisture and water activity, as well as roughness and wettability of the support, on the detachment of dry films from flexible supports.

The specific objectives were:

- To study the addition of hydrocolloids to a fruit pulp to verify their influence on the stickiness of the dried film to the support after cast-tape drying;
- To understand the relevance of the food suspension composition (by adding low molecular weight sugars) and its temperature, as well as the roughness of the support, in the detachment of the dehydrated film;
- To use the knowledge obtained with the model solution for the future drying of other fruit pulps by cast-tape drying.

## 2. BIBLIOGRAPHICAL REVIEW

### 2.1. DRYING

Food drying is a unit operation whose main objective is to reduce moisture content in food products to levels that ensure their preservation, inhibiting microbial and enzymatic activity and consequent deterioration. Also, decreasing dry product volume, which facilitates packaging, transport, and the preparation of powders, flakes, films, among others, are equally significant advantages (Ratti & Mujumdar, 2006; Sabarez, 2015).

According to Okos et al. (2007), studies about drying processes in the food industry involve:

- Economic considerations: to reduce costs and improve the capacity of drying equipment, allowing the development of stable processes that can be operated continuously;
- Environmental considerations: to minimize energy consumption during operation and reduce environmental impact by reducing waste disposal, for example;
- Product quality: precise control of food moisture content at the end of the drying process, controlling changes in material structure and texture. The purpose is to obtain good characteristics of color, specific mass, among others, as well as to develop an adjustable drying that can produce several products for various types of consumers.

In a system as complex as a food in the sense that many different reactions can occur, it is necessary that drying allows, in addition to water removal, that the desired reactions proceed faster than the unwanted ones. Some of the reactions that contribute to the reduction of product quality, such as nutrient degradation and growth of spoilage microorganisms, are undesirable and should be kept to a minimum. On the other hand, reactions responsible for maintaining quality, such as the inactivation of unwanted enzymes and microorganisms, should be encouraged (Rha, 1975).

Solar drying, spray-drying, freeze-drying, osmotic dehydration, drum-drying, microwave, extrusion, fluid bed drying, and pneumatic drying are commonly used drying processes for food products (Vega-Mercado et al., 2001).

Moisture removal needs a heat source to supply the water evaporation heat. A complete understanding of the product changes during dehydration is crucial to develop better processes. Efficient drying methods must result in good product quality and rational energy use (Brennan, 1994).

### **2.1.1. Energy and mass transfer mechanisms**

The physical mechanisms underlying heat and mass transfer must be understood, thus enabling the use of equations to predict the behavior of materials during drying as well as to quantify the energy transfer per unit of time (Incropera et al., 2007).

The heat conduction mechanism is the thermal energy transfer inside solids and between connected particles. Atomic and molecular agitations are responsible for this mode of heat transfer. Higher temperatures are associated with higher molecular energies, therefore, energy transfer by conduction occurs in the direction of the highest to lowest temperature. Similarly, diffusion causes mass transfer due to the difference in species concentrations at the microscopic level (Incropera et al., 2007; P. Singh, 2007)

Convection is the main mode of heat and mass transfer between the surface of solid material and the surrounding fluid due to the macroscopic movement of that fluid. This movement, in the presence of a temperature and/or concentration gradient, causes the heat and mass transfer. In the case of forced convection, fluid flow is artificially induced by blowing air with a fan. On the other hand, in free (or natural) convection, fluid flow occurs mainly by changes in density caused by differences in temperature (Incropera et al., 2007; P. Singh, 2007).

Thermal radiation is the energy emitted by matter that is at a temperature greater than zero Kelvin. Regardless of the shape of matter, emission is attributed to changes in the electron configurations of atoms or constituent molecules. The energy of the radiation field is carried by electromagnetic waves (or photons). While conduction or convection transfer requires the presence of a material medium, radiation does not. Actually, radiation transfer occurs more efficiently under vacuum (Incropera et al., 2007).

Food drying requires the supply of energy and generally involves more than one heat transfer mechanism (Rha, 1975).

### **2.1.2. Drying kinetics**

The drying curve, shown in Figure 1.a., is typically obtained by exposing a wet sample to a drying environment and relating mass loss to drying time. The shape of this curve is similar for many food products. After a short period of adaptation (line A-B), moisture decreases rapidly and almost linearly over time from points B to C. This drying period is followed by a much slower drying rate, while the moisture content of the material decreases from C to E. The

drying rate is determined by the slope of the drying curve, being expressed by the mass variation per unit of time (Brennan, 1994).

The drying rate data plotted against time is the drying rate curve (Figure 1.b.). This generic curve shows the presence of a thermal adaptation period (A - B), a constant rate period (B - C), and two falling rate periods (C - D and D - E). During the constant drying rate period, the water evaporation at the surface is balanced by the water transfer from the inner to the surface of the product. For a given solid, the duration of this phase is related to the temperature, relative humidity, and air velocity inside the dryer. In the constant drying rate period, the solid temperature is constant and is equivalent to the wet bulb temperature. The moisture content at point C, at which the constant rate becomes a decreasing rate, is called the critical moisture content and depends on the processing conditions and several specific factors of the product to be dried. In the falling rate period, the shape of the curve is influenced by the microstructure of the material, and the drying rate is controlled by the heat and mass transfer within the solid (Brennan, 1994).

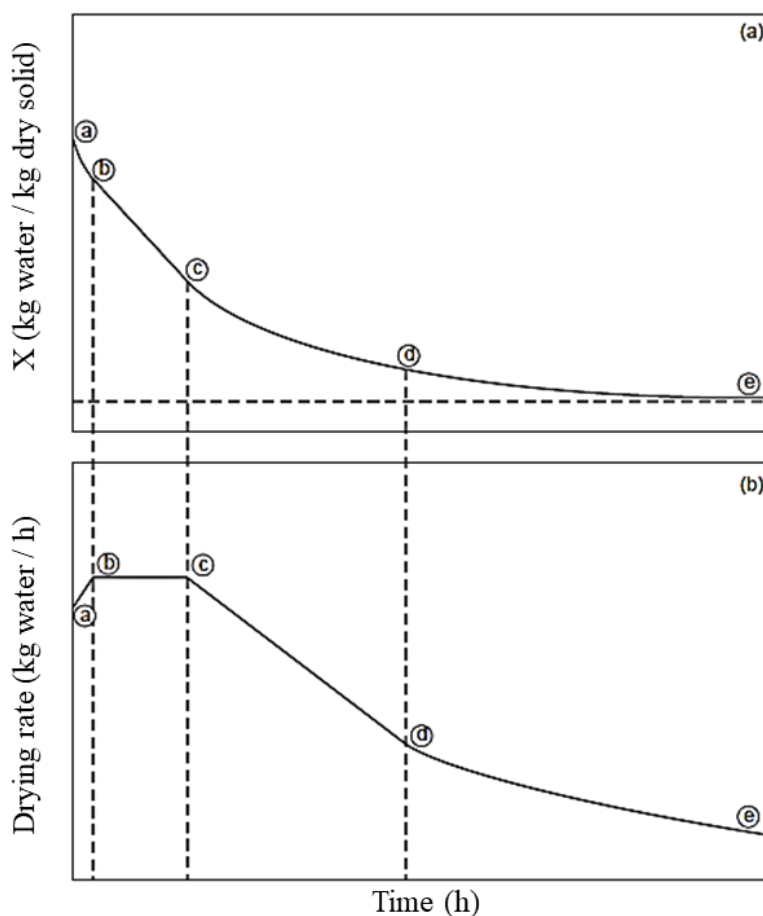


Figure 1 - Typical drying curves as a function of time: (a) drying kinetics; (b) drying rate.

Source: adapted from Araya-Farias & Ratti (2009).

## 2.2. TYPES OF DRYERS

There are several types of dryers, and many of them can be used for various food products. However, selecting a dryer should be based on the entire manufacturing process and properties of the dried product. Therefore, the characteristics of the raw material and final product need to be clearly defined, and in some cases, the pre-processing steps for partial water removal as well. The dryer selection should also include production capacity, moisture content of the initial product, particle size distribution, drying characteristics, maximum allowable product temperature, water sorption isotherms, and material physical data (Vega-Mercado et al., 2001).

Drying technologies can be divided into four groups or generations:

- First-generation: dryers involving hot air, which flows over a large area of the product to remove surface water. This technology is mainly employed for drying solid materials such as grains, fruits, and vegetables.
- Second-generation: Dryers dedicated to dehydrating pulps and purees, such as spray dryers and drum dryers. The resulting dehydrated products are powders and flakes.
- Third-generation: includes freeze-drying and osmotic dehydration. The former is designed to overcome structural damage and minimize losses of flavors and aromatic compounds, while the latter is primarily intended for processing fruits and vegetables by soaking in a hypertonic solution.
- Fourth-generation: involves high vacuum, fluidization, and use of microwaves, radiofrequency and refractance window (a special case of cast-tape drying). These technologies represent the latest advancement in the area of food drying. They have specific applications based on the characteristics of the raw materials to be processed and product' attributes. The design of a fourth-generation dryer considers the processing temperature, product residence times inside the dryer and whether the heating medium interacts with the material directly or indirectly (Nindo & Tang, 2007; Vega-Mercado et al., 2001).

Table 1 presents characteristics of the main types of dryers used for food drying.

Table 1 - Main dryers used in food and their characteristics.

<b>Dryer type</b>	<b>Process</b>	<b>Final product</b>	<b>Limitations</b>	<b>Examples of commercial use</b>
Spray dryer	Atomization; Flow of hot air; Lower cost compared to Freeze drying	High quality; Good rehydration	Product adhesion to the equipment; Use of large amounts of additives; Damage to high temperature sensitive foods; Agglomeration potential	Instant coffee, tea, milk
Freeze dryer	Absence of air; Low temperatures; High cost	High quality; Porous structure; Good rehydration	Operational cost; Long process times; Low product volume; Collapse of the material structure	Thermosensitive foods, biological samples, pharmaceutical products
Drum dryer	Viscous products; High energy efficiency; Easy to operate	Porous structure; Good rehydration; May show browning	High investment cost; Damage to temperature-sensitive products	Fruit and vegetable pulps, baby foods, dairy products
Vacuum dryer	Moisture removed at controlled temperatures; Lower cost compared to freeze-drying	Low oxidation; Storage stability; Good rehydration	Operational cost; Long process times; High energy expenditure.	Food additives, enzymes, pharmaceuticals

Source: adapted from Araya-Farias & Ratti (2009); Brennan (1994); Domínguez (2011).

### 2.3. CAST-TAPE DRYING

Refractance window (RW) drying denominates processes that use films transparent to infrared radiation (polyester films, e.g., Mylar®). The bottom face of the film is heated by hot water at temperatures near to 97-98 °C, as showed in Figure 2.

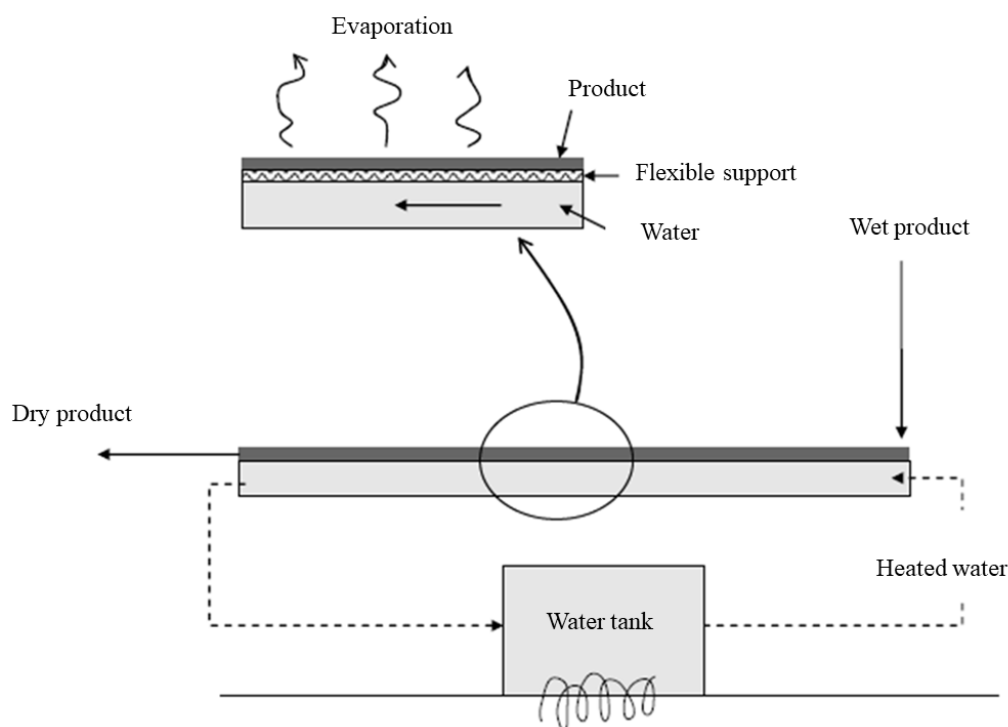


Figure 2 - Operation diagram of an RW dryer.

Source: adapted from Nindo, Powers, et al., (2007); Ratti (2009).

The food suspension (for instance, a fruit pulp) to be dried is spread on the upper face of the film, and the evaporated water is exhausted during drying (Nindo & Tang, 2007). In order to provide the evaporation heat during the drying process, the bottom of the polyester film must be wholly touched by the hot water. Nindo & Tang (2007) considered that both conductive and radiative heat transfers through the polymeric film are important. However, other authors showed that infrared radiation represents less than 3% of the total heat transfer and that RW is controlled by heat conduction (Ortiz-Jerez et al., 2015; Ortiz-Jerez & Ochoa-Martínez, 2015; Zotarelli et al., 2015). Therefore, Cast-tape drying (CTD) is assumed as a general denomination for dehydration processes in which liquid food is cast to be dried as a thin layer onto a flat belt (Durigon et al., 2017; Nindo, Powers, et al., 2007; Nindo & Tang, 2007).

Durigon et al. (2017) listed some powdered products obtained by CTD, as carrot, strawberry, pumpkin, tomato, acai berry, mango, pomegranate, and haskap berry. Tomato powder production by CTD was studied by Abul-Fadl & Ghanem (2011) by spreading tomato pulp over a flat glass plate, and by Castoldi et al. (2015) by drying tomato juice in a RW system. Abul-Fadl & Ghanem (2011) used hot water (60, 75, and 90 °C) under a glass plate to dry tomato pulp between 1.0 and 1.5 mm thick. Compared with convective hot-air drying, they reported shorter drying time, lower costs, higher rehydration rate and solubility, greater

lycopene content, ascorbic acid, and flavonoids. Castoldi et al. (2015) used hot water (65, 75, 85, and 95 °C) to dry 2- and 3-mm-thick pulp. The authors observed a relatively short dispersion time (below 9 s), solubility over 87%, and preserved luminosity values.

Cast-tape drying (or refractance window drying) can operate in batch or continuously. In continuous operation the wet product is spread on top of the flexible support (conveyor) by an automatic spreader; the conveyor moves while his bottom face in contact with the heating medium (hot water or vapor), resulting in very fast drying (Nindo & Tang, 2007). The dry product is removed from the flexible support as a film or by a blade when a film is not formed.

The product detaches from the support when it reaches low moisture contents, reducing its heating. Unlike direct dryers, cross-contamination is less probable to occur in indirect dryers such as CTD because the product does not come into contact with the heat transfer medium (G V Barbosa-Cánovas & Juliano, 2004; Nindo & Tang, 2007).

The mechanisms involved in the heat transfer to the product during CTD drying are convection between the hot water or vapor and the bottom of the support, conduction by the support in contact with the food suspension and convection between the carrying air that circulates over the food layer. Heat transfer by radiation occurs from the hot water to the product inferior surface if the conveyor is transparent to infrared radiation, as in the refractance window, which uses Mylar<sup>®</sup> as flexible support.

Within the scenario of food drying techniques and their limitations shown in Table 1, CTD is an alternative to mitigate some of the problems mentioned. An important advantage of CTD processing is that the temperature of the heated surface on which the product is spread is relatively lower (70-98 °C) when compared to the temperature of a drum dryer (above boiling point, reaching 120-150 °C). The use of milder temperatures results in dry products that exhibit excellent color, vitamin, and antioxidant retention compared to other drying methods (Abonyi et al., 2002; Caparino et al., 2012).

The versatility of CTD's application to produce a range of dehydrated foods, often without adding carrier agents, is an important advantage. Moreover, the adhesion of fruit pulps with high sugar content on equipment surfaces during drying (because of the high surface energy of metals) can be handled with the use of a low surface energy polymeric supports. The use of polyesters and conveyors coated with Teflon<sup>®</sup> plays a fundamental role in reducing the adhesion problem.

Thus, fruit and vegetable purees have been processed in CTD to obtain powders such as mango powder, tomato, acai, guava (de Souza, 2015; Durigon et al., 2016; Frabetti et al.,



2018; Zotarelli et al., 2017) as for obtaining fruit leathers, as seen in Figure 3 (da Silva Simão et al., 2019; Kaur et al., 2017; Tontul & Topuz, 2017).



Figure 3 - Mango leather produced in CTD.

Source: da Silva Simão (2018).

Nevertheless, no reports have been found in the literature on the adhesion of fruit and vegetable purees to different flexible supports used in cast-tape drying and refractance window drying.

As the processing parameters of these foods vary with their composition, food model solutions may be an alternative to understanding the influence of the suspension composition and drying conditions on the adhesion phenomena.

#### 2.4. MODEL FOOD SOLUTIONS

Model solutions are based on the formulation of real foods, being easily reproduced or modified to understand the influence of components' concentrations on the studied phenomena. It is not necessary to reproduce precisely the target (real) product because only its major components are essential to study most of the product properties. These formulations are useful to investigate the functionality of many food components, including starches, gums, and emulsifiers, as well as factors affecting the changes taking place during industrial processing (lipid oxidation, *Maillard* reaction, etc.). Therefore, model solutions provide a means of determining how the components of a product and processing can change the characteristics of

the final product. They are important to assess the sensitivity of food characteristics to the use of different ingredients and processing steps (Harper, 2009).

A typical fruit model solution can be formulated by adding sugars to a basic formulation. In these foods, the sugar content ranges from a nominal value (e.g., avocado) to more than 20% (e.g., ripe banana) by mass of wet matter. Sucrose, glucose, and fructose are the main sugars of most fruits. In general, fruits and vegetables contain more reducing sugars than sucrose (Brecht et al., 2008).

Some studies in the literature have employed model solutions for investigating state diagrams (Grajales-Lagunes et al., 2018; Y. Roos & Karel, 1991b; Ruiz-Cabrera et al., 2016), characterization of powders produced in spray drying (Jayasundera et al., 2011), glass transition temperature (Saavedra-Leos et al., 2012), among others.

Fruits and vegetables are largely dried by different processes, but their low molar sugar composition influences stickiness. Still, these foods undergo physiological transformations even after harvest, which interferes with the concentration of some components and results in different products and process parameters. Nevertheless, the use of model solutions to adhesion investigation is not common.

#### **2.4.1. Strawberries**

Strawberry (*Fragaria ananassa* Duch.) is a very popular pseudofruit originating from South America and known for its attractive appearance, unique flavor, and nutritional composition. It contains high levels of vitamin C and phenolic compounds, especially anthocyanins, which are responsible for their high antioxidant activity (Odrizola-Serrano et al., 2010). The currently cultivated strawberry (*Fragaria ananassa*) originated in Europe, from the hybridization between the American species *Fragaria chiloensis* Mill. and *Fragaria virginiana* Duch (Vaughan & Geissler, 1997). The hybridization between these two species did not occur in the Americas due to geographic isolation, but it took place in France, around 1750, as these species were cultivated side by side. The plants from these cross produced fruits of exceptional size, with a red pulp, different from the white pulp of *Fragaria chiloensis* (Jones, 1995).

According to FAO (2017), world strawberry production was over 9 million tons, with the United States being the largest fruit producer, accounting for almost 1.5 million tons. Brazil, with an area of 400 hectares for cultivation, produced 3,390 tons. The preference for fresh fruits is challenging due to their short shelf life and seasonality, limiting their availability. In this

sense, strawberries can be processed by methods like dehydration and consumed in other ways, such as juices, jams, among others (Cordenunsi et al., 2005; Mosquera et al., 2012).

100 g strawberry corresponds to 90.95 g water, 7.68 g carbohydrates (of which 0.47 g sucrose, 1.99 g glucose, and 2.44 g fructose), 2 g fiber, 0.67 g protein, 0.40 g ash, and 0.30 g lipid (USDA, 2015). The higher amount of fructose in the fruit, which is a highly hygroscopic sugar, may justify its sticky behavior on the walls of equipment, so the addition of drying aids is frequently required.

The concentration of sugars of low molar mass (sucrose, glucose, and fructose) in the composition of the strawberry, especially fructose, which is a highly hygroscopic sugar, explains its sticky behavior on the walls of the equipment and the need to add drying aids. Most scientific studies emphasize their objectives in drying the fruit to determine the physical-chemical properties and to preserve the nutritional value (Abonyi et al., 2002; Adak et al., 2017; de Bruijn & Bórquez, 2014; Maritza et al., 2012; Méndez-Lagunas et al., 2017; Nemzer et al., 2018).

#### **2.4.2. Hydrocolloids**

Hydrocolloids are high molar mass polysaccharides capable of forming a gel in water. They are used as thickeners because of their ability to bind to water, and are frequently used in the preparation of processed foods. Such additives are also known as texture modifiers as they provide appropriate flow properties when added to some liquid foods, increasing their viscosity, water retention, and firmness. Some polysaccharides, such as maltodextrin, increase powders' solubility and reduce adhesion to equipment (M. Sharma et al., 2017).

Besides its use to produce powders and flakes, hydrocolloids are added to fruit and vegetable pulps before drying by CTD, in order to produce food leathers. Some fruit pulps have low consistency to be dried by CTD, therefore, the addition of edible hydrocolloids as carrier agents improves the physical properties of the fruit pulp and dried films, i.e., the fruit leathers. In some cases, hydrocolloids are crucial to form a fruit pulp-based film that can be continuously detached from the drying surface as a film (fruit leather). The addition of such biomacromolecules increases the internal cohesion of the dehydrated material, surpassing the adhesion forces (Lorevice et al., 2012; McHugh & Senesi, 2000; Otoni et al., 2017; Park & Zhao, 2006). The literature reports that the chemical structures and molar masses of hydrocolloids influence the formation and properties of fruit leathers.

Hydrocolloids employed in film formulation can be extracted from plants (such as starch, pectin, and cellulose), animals (collagen, gelatin, and chitosan), microorganisms (e.g., bacterial cellulose), and algae (including alginate and carrageenan) (Otoni et al., 2017).

Starch is a predominant food reserve substance in plants and provides 70-80% of the calories consumed by humans. Starch-based or hydrolysis-based products constitute the bulk of digestible carbohydrates in the human diet. Also, the amount of starch used in food preparation far exceeds all other hydrocolloid foods. Commercial starches are obtained from cereal grain seeds, mainly corn, wheat, potatoes, and cassava (tapioca starch). Natural and modified starches have a vast range of applications, such as gelation, glazing, moisture retention, stabilization, texturing, thickening, film formation, foam reinforcement, and more (BeMiller & Huber, 2008).

Starch occurs in nature as water-insoluble granules. Its viscosity increases when hydrated and heated in water under agitation. Starch granules are composed of a mixture of two polymers, a linear polysaccharide called amylose ((1-4)  $\alpha$ -D-glucopyranosyl units) and a highly branched polysaccharide called amylopectin ((1-4)  $\alpha$ -D-glucopyranosyl units and (1-6)  $\alpha$ -D-glucopyranosyl units), which are structured as concentric rings forming semi-crystalline and amorphous layers (BeMiller & Huber, 2008; Copeland et al., 2009; Wani et al., 2012).

Maltodextrin is a hydrocolloid obtained from the incomplete hydrolysis of heat-treated starch dispersions by an acid or an enzyme. They are generally described by their equivalence to dextrose (or equivalent dextrose, DE) and are defined as products with measurable dextrose equivalent values, always less than 20. Lower DE maltodextrins is linked to higher average molar masses, being less hygroscopic, while higher DE maltodextrins are related to lower average molar masses and tend to be more hygroscopic. They are light, practically sweet, and used to give mass and consistency to food systems (BeMiller & Huber, 2008).

For cases where the presence of a single biopolymer is not sufficient, two or more of them can be combined (Otoni et al., 2017; X. Wang et al., 2011).

Pectin is the family of heteropolysaccharides found mainly in the primary cell walls of terrestrial plants and is the binder most commonly used in edible fruit and vegetable films. The pectic backbone is primarily a homopolymer of galacturonic acid bound by  $\alpha$ -1,4 glycosidic bonds, with varying degrees of esterified methyl carboxyl groups. Pectin must consist of at least 65% galacturonic acid (FAO, 2013).

The naturally occurring pectin present in plants has a high molar mass, while those obtained by industrial processing are usually modified to a low molar mass. Commercial pectin powder can be classified as high methoxylated (HM), with a percentage of esterified groupings

in the chain (esterification grade or DE) greater than 50% or low methoxylated (LM), with a DE less than 50% (BeMiller & Huber, 2008; Canteri et al., 2012; Naqash et al., 2017). Low methoxylated pectin has been shown to produce stronger and less extensible cranberry films than those produced with high methoxylated pectin (Park & Zhao, 2006).

## 2.5. AMORPHOUS STATE AND GLASS TRANSITION

Foods generally have a random, disordered molecular structure, that is, the position of any of the constituent molecules at any given time cannot be defined, known as the amorphous state, which is different from the highly organized crystalline state (Y. Roos, 2010).

Many foods and biological materials consist mostly of protein, carbohydrates, fat, and water; solids may be in an amorphous state, which is very sensitive to temperature and moisture variations. Sugars, along with starch and proteins, are the main components of the amorphous matrix that can be formed in various processes, such as baking, concentration, drum-drying, freeze-drying, spray-drying, and extrusion, which allow a sufficiently short time for water removal or cooling of concentrated solids (B. Bhandari & Howes, 1999; Y. Roos, 2010; Telis & Sobral, 2001; Zabetakis & Holden, 1997).

The transformation of an amorphous material from the vitreous state to a rubbery state is a second-order phase transition within a temperature range known as the glass transition temperature ( $T_g$ ), corresponding to an important physicochemical characteristic of material. The glass transition is reversible and is achieved by very quick cooling of a liquid to temperatures below the crystalline equilibrium ( $T_m$ ) fusion, which retains the molecular disorder and may allow the molecules to freeze at their random positions and form a high viscosity (vitrification) glass ( $10^{12}$ - $10^{14}$  Pa s<sup>-1</sup>), disorganized and non-crystalline. The vitreous state is a thermodynamic non-equilibrium state whose properties are time-dependent (Y. Roos, 2010).

Food products containing low molar mass compounds are generally difficult to dehydrate and exhibit poor stability when dehydrated or frozen above  $T_g$ . Typical changes in amorphous foods that occur above the glass transition include viscosity, collapse, and crystallization (Y. Roos, 1993b; Zabetakis & Holden, 1997).

Increased molecular mobility in the food matrix, which occurs at temperatures higher than glass transition, can affect the diffusion of components in the matrix and increase the rates of deteriorating reactions such as enzymatic and non-enzymatic browning oxidation. Changes

in food texture, such as crispness, may also be related to the water plasticization of amorphous components (Y. Roos, 1993b; Zabetakis & Holden, 1997).

Some food components that are present in smaller quantities, such as flavors, vitamins, enzymes, and microorganisms, are encapsulated in the amorphous matrix. Thus, maintaining the nutritional quality and stability of dehydrated foods, avoiding collapse and crystallization, is based on the control of the vitreous state during processing and storage. Likewise, knowledge of the differences between crystalline and amorphous food properties such as solubility, melting behavior, moisture absorption capacity, and flow characteristics of the dehydrated material is essential to optimize product shelf life (B. Bhandari & Howes, 1999; Y. Roos et al., 1996; Y. Wang & Truong, 2017).

Figure 4 shows the enthalpy or volume of materials in various states. The liquid and crystal states are equilibrium states, while the supercooled liquid may have an amorphous, disordered, liquid-like structure. Molecules of such materials may be cooled to form the glass structure below the glass transition region (Y. Roos, 2010).

Volume and enthalpy relaxations are typical of glass transition measurements, as they indicate translational mobility and the ability of the material to respond to temperature increases. Thus, an exothermic or endothermic peak with a corresponding volume change may occur, depending on the differences in thermodynamic properties between the vitreous state and the supercooled liquid in the glass transition region (Y. Roos, 2010).

As the temperature rises above  $T_g$ , the material increasingly behaves like rubber, and many of its physical properties suddenly change. The most important changes are increases in free molecular volume, thermal capacity ( $C_p$ ), thermal expansion coefficient ( $\alpha$ ), dielectric coefficient ( $\epsilon$ ), and changes in viscoelastic properties (Genin & René, 1995).

Some of the analytical methods for determining glass transition are differential scanning calorimetry (DSC), differential thermal analysis (DTA), and thermomechanical analysis (TMA). The first two methods detect changes in  $C_p$  (Figure 5), while the third one detects changes in elastic modulus (B. Bhandari & Howes, 1999).

The glass transition temperature is affected by three main factors: plasticizing material, molar mass, composition and crystallinity (F.P. Collares et al., 2002). In partially crystalline materials,  $T_g$  occurs in the amorphous fraction, as for example in gelatin and starch. Therefore, the  $T_g$  is also affected by the crystallinity of the material. The greater the crystallinity, the greater should be the  $T_g$ .

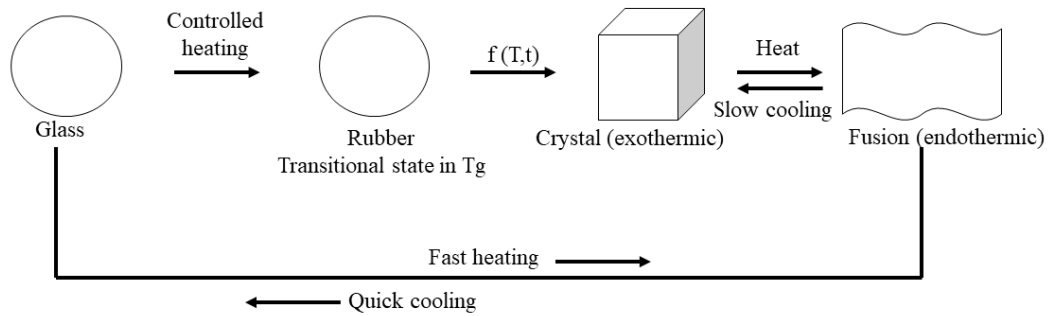


Figure 4 - Changes in the physical state of an amorphous material as a function of temperature and time.

Source: adapted from B. R. Bhandari et al., (1997).

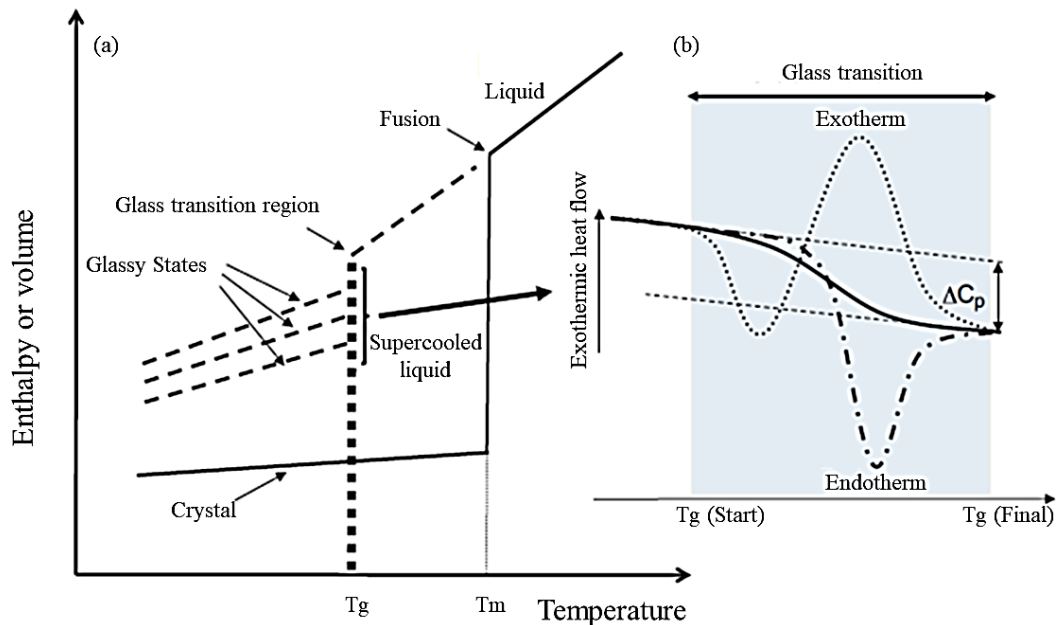


Figure 5 - (a) Change in enthalpy or volume of a material with temperature (b) exothermic change corresponding to the change in thermal capacity ( $C_p$ ), in the glass transition region.

Source: adapted from Y. Roos (2010).

### 2.5.1. Plasticization effect on amorphous solids

Water is recognized as a strong plasticizer of solid foods. In the field of polymer science, the classic definition of plasticizer is "a material incorporated into a polymer to facilitate its handling and increase its flexibility and extensibility." Thus, water is the main responsible for reducing the  $T_g$  of food products, making them soft, since it has a very low glass transition temperature ( $-135\text{ }^\circ\text{C}$ ). Since the  $T_g$  of biopolymers (proteins, carbohydrates) is considerably higher than that of water, the increase of water concentration will decrease the

glass transition temperature of the miscible mixture (Johari et al., 1987; Kumagai et al., 2002; Momany & Willett, 2002; Sears & Darby, 1982). Plasticization at a molecular level leads to an increase in intermolecular space or free volume, decreasing local viscosity and thus increasing mobility (Ferry & Myers, 1961).

Predicting the drop in glass transition temperature as a result of water plasticization helps to assess the effect of food composition on  $T_g$ ; it is well-known that changes related to this transition can affect the shelf life and quality of dehydrated products.

The values of glass transition temperatures can be further explained by the free volume theory (Fox & Flory, 1950). This theory explains the properties of a polymer as a function of its temperature (as specific volume, thermal expansion coefficients) and structure. In general, it can be stated that cyclic macromolecules which have no end groups (no free volume effect) present high glass transition temperatures. Sears & Darby (1982) resumed that the free volume comes from the motion of the chain; these motions would be increased by increasing the number of end groups (lower molecular weight solutes), increasing the number or length of side chains (internal plasticization). According to the authors, the addition of plasticizer molecules (water or other compounds) into a polymer structure implies the presence of molecules with  $T_g$  lower than the  $T_g$  of the polymer itself. Moreover, those relatively small plasticizer molecules add a great free volume to the system. In this way, the free volume theory helps to define the lowering of the glass transition temperature with the presence of the plasticizer (Marcilla & Beltrán, 2012).

An interesting phenomenon was discussed by Figueroa et al., (2016), who demonstrated that the addition of sucrose could alter cassava starch thermal properties at a low moisture content (less than 10%, in dry basis). The authors noticed that the water plasticization of starch-sugar-added samples (reducing the  $T_g$ ) occurred only at high moisture contents. In the low moisture content, sugar (4 to 6%) seemed to anti-plasticize samples, and  $T_g$  was higher than the  $T_g$  observed for neat cassava starch. When those authors added 8% of sucrose, the plasticization effect of water was obtained for the entire range of moisture content. The study's explanation for this anti-plasticizing effect was that, in low moisture contents, starch is interacting with sugar, as the sample is less hydrated. The water can interact with starch and sugar at higher moisture contents, and then plasticization occurs. Although, this phenomenon did not appear when authors increased sugar addition. The anti-plasticizing effect on the mechanical properties of films was also mentioned by Chang et al., (2000) while working with cassava starch, where a small addition of water promoted a more rigid structure with higher tensile strength. Perdomo et al., (2009) reported an anti-plasticizing behavior (an increase of



T<sub>g</sub> with the increase of moisture content) on cassava starch films at moisture contents lower than 11.4% (d.b.). Pérez et al., (2014) expressed that the addition of corn oil anti-plasticized cassava starch, with the blends exhibiting higher T<sub>g</sub> than the neat cassava starch. However, results obtained for García et al., (2012) for films of cassava starch with the addition of whey protein (WPC) did not show this effect in any range of moisture content evaluated (8 to 20%). Many authors cite the anti-plasticization effect affecting especially the mechanical properties of the films.

### 2.5.2. Effect of the molar mass of food polymers on amorphous solids

Low-molar mass polymers, such as sucrose, fructose and glucose, have in their pure form a low glass transition temperature, while larger chain molecules have higher glass transition temperatures, as can be seen from Table 2 (B. Bhandari & Howes, 1999).

Table 2 - Molar masses and glass transition temperatures of anhydrous food materials.

<b>Compounds</b>	<b>Molar mass (g mol<sup>-1</sup>)</b>	<b>T<sub>g</sub> (°C)</b>
Fructose	180	5
Glucose	180	31
Galactose	180	32
Sucrose	342	62
Maize starch	-	243
Maltose	342	87
Lactose	342	101
Maltodextrin		
DE 36	500	100
DE 25	720	121
DE 20	900	141

Source: adapted from B. Bhandari & Howes (1999).

The T<sub>g</sub> of very high molar mass food polymers, for instance, starches and proteins, is difficult to be determined experimentally as these materials have crystalline and amorphous structures and they can break down before reaching T<sub>g</sub>.

The addition of maltodextrins with different DE in a sucrose suspension proved that the higher the molar mass of this additive, and consequently, the lower dextrose-equivalent, the higher the glass transition temperature of the mixture (Y. Roos & Karel, 1991a). The authors Torreggiani et al., (1999) reported that increasing sucrose concentration in strawberry juices promoted a decrease in T<sub>g</sub>.

## 2.6. FLUID RHEOLOGY

By definition, rheology is the study of deformation and flow of matter. In terms of food, “rheology is the study of deformation and flow of raw materials, intermediate and final products of the food industry” (Bourne, 2002).

Processed foods can be viewed as edible structures that are created as a result of aqueous protein, polysaccharide, and lipid responses to different processing methods such as heat processing, homogenization, and other treatments. Most, if not all of these answers, are physical. Rheological responses are those at the macroscopic level; however, they are directly affected by changes and properties at the microscopic level. Therefore, it is useful to understand the role of food structure in its rheological behaviors (Rao, 2007a).

Rheology is important in many aspects of food production and consumption, involving the physical characteristics of semisolid fluids and foods, engineering and process design, new product development, and sensory properties (Gibson et al., 2018).

The rheological properties of foods are dependent on the temperature and composition, but they are also based on flow and strain responses when materials are subjected to normal and tangential stresses, being determined in relation to the stress applied to a material and subsequent strain as a function of time (G. V. Barbosa-Cánovas et al., 1996; Rao, 1977).

The main parameters involved in rheology are shear rate and stress measurements. The shear rate ( $\dot{\gamma}$ ), in  $s^{-1}$ , is the velocity gradient established in a fluid. Shear stress is the force per unit of measured area, and is determined by its direction on the surface, which can usually be an extension or compression. It is expressed in Pa or  $N\ m^{-2}$  and conventionally indicated by  $\sigma$  or  $\tau$  (Rao, 2007b).

Viscosity is the internal friction of a fluid, which means, a measure of its resistance to flow. It is represented by the symbol  $\eta$  in the case of Newtonian fluids whose viscosity does not depend on the shear rate or by  $\eta_a$  to show this dependence. Viscosity is defined as the ratio of applied shear stress ( $\sigma$ ) to shear strain rate ( $\dot{\gamma}$  or  $d\gamma/dt$ ), as shown in Equation 1 (Rao, 1977):

$$\eta = \frac{\sigma}{\dot{\gamma}} \quad (1)$$

where  $\eta$  is given in Pa s or mPa s,  $\sigma$  is given in Pa or N m<sup>-2</sup> and  $\dot{\gamma}$  is expressed in s<sup>-1</sup>.

Foods can be classified in different ways, including solids, gels, homogeneous liquids, solid suspensions in liquids, and emulsions. Liquid foods are those that do not retain their shape but take the form of their container, and their rheological behaviors are Newtonian, pseudoplastic, dilating, thixotropic, and viscoelastic (Rao, 2007b).

Newtonian liquids are independent of shear rate and are affected only by temperature and composition. Non-Newtonian liquids, such as fluids containing significant amounts of high molar mass dissolved compounds (polymers) and/or suspended solids, may be classified as time-independent or time-dependent (Rao, 1977).

In the case of time-independent non-Newtonian liquids at a constant temperature, viscosity depends only on the magnitude of the shear stress or the shear rate. If viscosity decreases as shear rate increases, fluid is pseudoplastic (shear thinning). In contrast, if the viscosity increases as the shear rate also increases, the fluid is called shear-thickening (Rao, 1977).

Non-Newtonian liquids with time-dependent properties are subdivided into two categories. Under constant temperature and shear rate, if viscosity decreases as a function of time, then the fluid is thixotropic; however, if viscosity increases over time, the fluid is rheopectic. Finally, some fluids have viscous and elastic properties; such fluids are called viscoelastic (Rao, 1977).

The typical equation to characterize pseudoplastic and dilating fluids is the power law (Equation 2) (G. V. Barbosa-Cánovas et al., 1996):

$$\sigma = K\dot{\gamma}^n \quad (2)$$

where  $K$  is the consistency index (Pa s<sup>n</sup>), and  $n$  is the flow behavior index.

If the flow behavior index is greater than unit ( $n > 1$ ), the shear stress graph by shear rate will be a downward curve representing the dilating fluid. When  $0 < n < 1$ , the graph will have an upward curvature, representing the pseudoplastic fluid, and for  $n = 1$ , the fluid will be Newtonian. The power law model is also known as the Ostwald de Waele model (Rao, 1977).

Some food materials exhibit a shear stress that can be defined as the minimum shear stress required to initiate flow (G. V. Barbosa-Cánovas et al., 1996).

The most common model for characterizing non-Newtonian fluids with this initial shear stress is the Herschel-Bulkley equation (Equation 3) (G. V. Barbosa-Cánovas et al., 1996):

$$\sigma = \sigma_0 + K\dot{\gamma}^n \quad (3)$$

where  $\sigma$  is the shear stress,  $\sigma_0$  is the initial shear stress,  $K$  is the consistency index,  $\dot{\gamma}$  is the shear rate and  $n$  is the flow behavior index.

Figure 6 illustrates the rheological behaviors of Newtonian and non-Newtonian fluids (time-dependent and independent), which are classified according to  $n$  and  $\sigma_0$  magnitudes (Table 3).

Table 3 - Classification of Newtonian and non-Newtonian fluids.

<b>Fluid</b>		<b><math>\sigma_0</math></b>	<b><math>n</math></b>	<b><math>K</math></b>
Newtonian		0	1	$K = n$
Non-Newtonian	Pseudoplastic (shear-thinning)	0	$0 < n < 1$	$> 0$
	Shear-thickening	0	$n > 1$	$> 0$
	Bingham	$> 0$	1	$> 0$
	Pseudoplastic with initial shear stress	$> 0$	$0 < n < 1$	$> 0$
	Shear-thickening with initial shear stress	$> 0$	$n > 1$	$> 0$

Source: adapted from G. V. Barbosa-Cánovas et al. (1996).

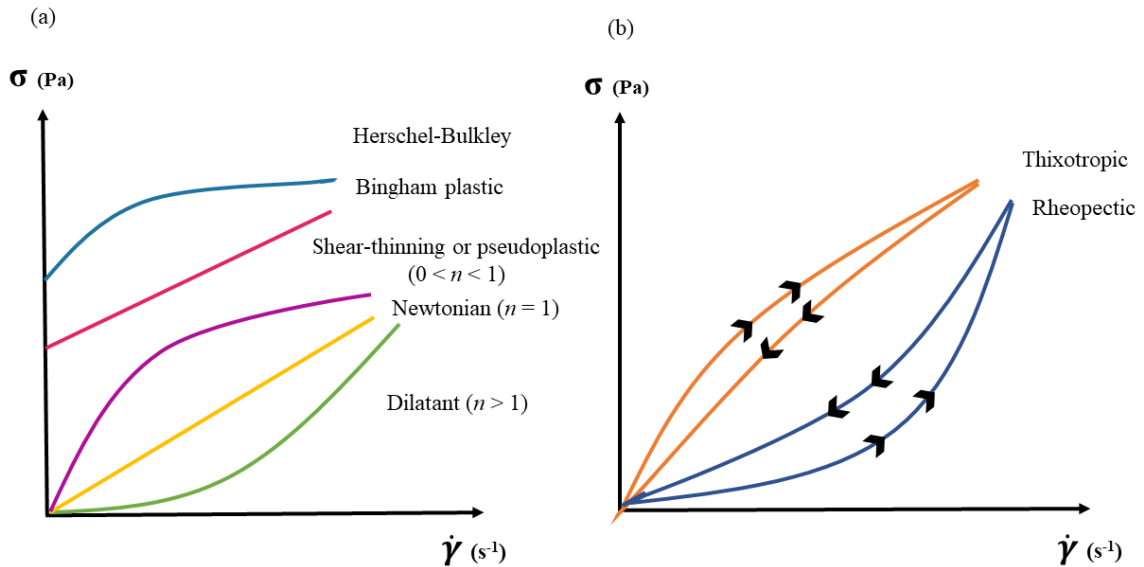


Figure 6 - Fluid rheological behaviors: (a) time-independent (b) time-dependent.

Source: adapted from Rao (2007a).

## 2.7. ADHESION IN SUPPORTS AND WETTABILITY

Adhesion is an interfacial property that is a measure of the forces that keep a substance or product adhered to the surface of a material. The product particles attach to the surface and this bond will only be broken by applying a force greater than the adhesive force. Cohesion, on the other hand, is an internal property of the material and is a measure of the forces holding particles together. Powder particles, for example, that come in contact with each other, come together in the form of a cluster, unless the bond between them is broken by applying forces greater than cohesive force (Papadakis & Bahu, 1992).

Studying the adhesion of fluids to solids is relevant for industrial applications. Stickiness, the strength of particle adhesion to surfaces, is a common problem in many unit operations and is often encountered during the production of dehydrated foods. The adhesion of materials on supports and walls of drying equipment causes low product yields, operational problems (e.g., dryer downtime for cleaning), and product handling difficulties. For heat-sensitive foods, this can also lead to overheating, resulting in unpleasant sensory characteristics and degradation (Papadakis & Bahu, 1992).

Multiple factors influence the adhesion phenomenon, depending on the food characteristics (composition, viscosity, porosity or presence of bubbles on the product, glass transition) as well as support material properties (surface tension, hydrophilicity, hydrophobicity, roughness, and stress states) (Liu et al., 2018; Noren et al., 2019). Different

theories have already explained the mechanisms of adhesion, which include mechanical adhesion (adhesion between surfaces by interlocking action), chemical adhesion, dispersive adhesion, electrostatic adhesion, and diffusive adhesion; however, there is no universal theory to predict this phenomenon (Nussinovitch, 2017). Most studies correlate surface roughness, adsorption thermodynamics, and rheological properties of food with stickiness (Adhikari et al., 2003; Bobe et al., 2007; Karbowski et al., 2006; Keijbets et al., 2009; Loibl et al., 2012; Pizzi & Mittal, 2003; Saikhwan et al., 2006).

It is essential to understand that adhesion can be discussed in theoretical and practical sense. Theoretical adhesion addresses the magnitude of interparticle forces which causes materials to adhere to one another, taking into account the mechanisms previously mentioned. Practical adhesion refers to determining the force of a bond, usually by stressing it to failure. The adhesion force between two materials depends on the mechanisms of adhesion and the surface area over which they are in contact (Pocius, 1986).

In relation to the influence of the product's viscosity and its adhesion to surfaces, most foods are viscoelastic as they exhibit a viscous component and an elastic component. Dehydrated liquid foods can present themselves in the form of amorphous glasses, that is, supercooled liquids in a metastable state below their glass-transition temperature ( $T_g$ ). The viscosity of the amorphous structure decreases with increasing difference between process temperature and glass transition temperature, as well as with increasing relative humidity. In general, the viscous properties of a material determine the adhesion through interfacial bonds and energy dissipation at a molecular level during its removal from a surface. Furthermore, the reduction in the material's viscosity greatly improves the molecular mobility of the system, assuming a more liquid character, which is related to adhesion. Caking of powders is also due to this liquid state (Adhikari et al., 2001; Downton et al., 1982; Guillemenet et al., 2002; M. L. Williams et al., 1955).

The wettability properties of a system are quantitatively characterized by the contact angle ( $\theta$ ) at the liquid-vapor interface and the solid surface. The contact angle is used to determine a liquid's wettability on a surface, which is an indirect measurement of adhesion. The wettability is related to the surface energy of the adhesive (liquid) and the adherent (solid material, also called substrate). When a liquid does not completely wet the solid, it forms a droplet on the surface, and two situations can occur: if the contact angle with the adherent is less than  $90^\circ$  and the liquid is water-based, the contact is called "hydrophilic", "wetting" or "lyophilic." On the contrary, if the surface of the solid has low energy, the contact angle is higher than  $90^\circ$  and is referred to as "hydrophobic", "nonwetting" or "lyophobic." In other

words, to achieve surface wettability, the surface tension of solid material must be greater than that of liquid (Berthier, 2013; Ramiasa et al., 2014).

In the case of liquids that wet solid surfaces, the work of adhesion can be described by Young-Dupré's equation (Equation 4) (Pocius, 1986):

$$W_A = \gamma_L (1 + \cos \theta_0) \quad (4)$$

Where  $W_A$  is the work of adhesion (in  $\text{J m}^{-2}$  or  $\text{N m}^{-1}$ ),  $\gamma_L$  is the surface tension of the liquid (in  $\text{mN m}^{-1}$ ), and  $\theta_0$  is the contact angle of the liquid coating on the substrate.

Therefore, the work of adhesion can be calculated by measuring the contact angle and the surface tension of the liquid (Ebnesajjad, 2011). The adhesion theory states that maximum adhesion is achieved when the adhesive comes into intimate contact with the adherent. Maximum adhesion will occur when the work of adhesion,  $W_A$ , is maximum (Pocius, 1986).

Many factors influence the wetting phenomenon at high temperatures; thus, the work of adhesion cannot be completely explained only by Young-Dupré's equation. Several processes may take place on the liquid-solid interface, as dissolution of the solid into the liquid, penetration/diffusion, or adsorption of the liquid components into the solid, among others. All these factors are strongly related to the movement of atoms, generating a time and temperature dependency (Passerone et al., 2013).

In this sense, the spreading solution's temperature is an important parameter to be considered in adhesion. Above the glass transition temperature of the product, the surface free energies of liquids decrease as the temperature rises. Therefore, the work of adhesion must decrease. As the temperature increases, the vibrational and translational energies of the monolayer adhered to the solid-liquid interface increase; as a consequence, the van der Waals' force of attraction will decrease. This means that the liquid suspension occupies a larger area of the surface, being "separated" from the first layer of the surface material, and that is why adhesion may be decreased (Padday, 1968). Nevertheless, with the temperature rising, thermal grooving at grain boundaries of the solid surface can occur, increasing wetting and adhesion and making it difficult to evaluate the correct roughness value of the material at the test temperature. Surface tension and wettability measurements at high temperatures and considering roughness are increasingly requested to characterize the behavior of systems of industrial interest. In this way, it is possible to more accurately predict the phenomenon of adhesion in processes above room temperature (such as drying) (Passerone et al., 2013).

Solid surfaces used as drying supports have different electrical and optical properties than those found in liquid suspensions, being characterized by roughness analysis at the atomic or molecular level. Surfaces are also energetically heterogeneous, i.e., although a wettability can be attributed to a solid material, this property is likely to be an average value of a distribution of surface regions with varying properties (McGuire, 2005). The surface tension of different solids is listed in Table 4. Similarly, the surface tension of some liquids is shown in Table 5.

Table 4 - Surface tension of several solid materials.

<b>Surface</b>	<b>Surface tension (mN m<sup>-1</sup>)</b>
Polytetrafluoroethylene (Teflon <sup>®</sup> )	18
Polymethylsiloxane (Silicone)	21
Polyethylene	31
Polystyrene	33
Polyvinyl Chloride (PVC)	39
Cured Epoxy Resin	43
Polyethylene Terephthalate (PET)	43
Nylon-6.6	46
Soda-lime glass	65
Stainless steel	71
Aluminum	90

Source: adapted from Pocius (2012a).



Table 5 - Surface tension of liquids.

<b>Liquid</b>	<b>Surface tension (mN m<sup>-1</sup>) at 25 ° C</b>
Water	72.0
Glycerol	63.0
Ethylene glycol	47.0
Nitrobenzene	43.9
Epoxy Resin	43.0
Benzene	28.9
n-hexane	18.0

Source: adapted from Pocius (2012a).

Metals are the most commonly used material in drying equipment manufacturing for their greater durability and ease of cleaning. Although, they have high surface tension, which favors adhesion. Otherwise, polymers usually employed as supports for refractance window and cast-tape dryers have low surface tension. Therefore food tends to adhere less to these surface materials and more to metal since liquids generally show greater wettability in metals than in polymers (B. R. Bhandari, 2007). Teflon<sup>®</sup> has low surface tension, so it has been increasingly used to produce food-grade surfaces. However, its durability must be evaluated because its surface roughness can be significantly altered by spreading and removing the product.

Another critical factor for adhesion is surface roughness because it is associated with surface wetting. Firstly, a liquid forming a contact angle of less than 90° with a solid surface may spread through fine pores, scratches, and other heterogeneities by capillary action, even though it will not spontaneously wet a planar surface. Also, it is recognized that the apparent contact angles are different from the predicted by Young-Dupré's equation (Equation 4), which assumes that the solid surface is smooth, homogeneous, rigid, as well as chemically and physically inert regardless of the liquids to be employed. Therefore, two models can explain this discrepancy. Increasing roughness on a hydrophobic surface can increase its hydrophobicity by incorporating air into the solid surface. Air pockets form within the surface grooves, leading to the combined presence of the liquid-air interface and the solid-liquid interface, resulting in a larger contact angle compared to the contact angle of a completely flat surface. This phenomenon is known as the Cassie-Baxter state of equilibrium contact angle. On the other hand, hydrophobic surfaces on which no air pockets form reveal a greater solid-liquid

interface, i.e., the liquid penetrates completely into the grooves of the rough surface, culminating in higher surface wettability due to the increase in contact area (Bormashenko et al., 2009; Buffa et al., 2001; Karim et al., 2018; Kinloch, 1987). Both wetting models are represented in Figure 7.

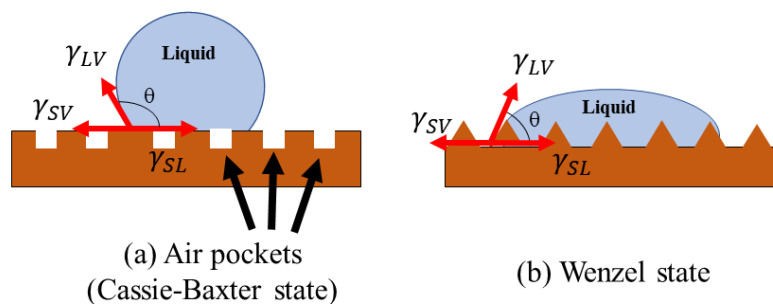


Figure 7 - Representation of the (a) Cassie-Baxter and (b) Wenzel states.

Source: author.

Determining the adhesion strength of a solid material to a substrate is a complex problem to be solved. An ideal adhesion test method measures only the adhesion of the material of interest, but in practice, all the known methods are influenced by other properties of the adhesive and the substrate or the interface; therefore, there are no standardized methods for this, and that makes comparisons hard. An adhesion test should ideally fulfill some requirements, such as the test pieces are real production parts (for instance, drills or other tools), it is nondestructive, viable for a wide range of geometries, easy to perform and interpret, and it should be fast in the same way (Valli, 1986).

The instrumental techniques most applied in foods are the peel tests and determination of plate separation force (probe tests). Some studies in the literature, for example, have evaluated droplet stickiness during drying using probes (Adhikari et al., 2003, 2007; Kilcast & Roberts, 1998; Valenzuela & Aguilera, 2015). Adhikari et al. (2003) measured stickiness during hot air drying of suspensions of fructose, honey, sucrose, maltodextrin, and a mixture of sucrose and maltodextrin. They reported that a favorable process condition is achieved when the cohesive strength of the system is greater than the adhesive strength at the drop-probe interface. Furthermore, the authors found that when the droplet's outer layer was transformed into a glassy matrix, in maltodextrin-containing suspensions, adhesion did not occur. The study suggested that stickiness may be alleviated if the sample viscosity is high enough to prevent failures within the droplet itself.

Regarding surface properties and stickiness, Adhikari et al. (2007) evaluated carbohydrate and protein suspensions with a probe and found that the surface tension of a material has a greater impact on adhesion than the viscosity of the suspension. In addition, the authors reported that cohesive failures occurred during the tests, indicating that the energy required to maintain the droplet cohesion was greater than the energy to obtain an adhesive failure at the probe-droplet interface. Keijbets et al. (2009) used Teflon<sup>®</sup>, polycarbonate, stainless steel, and quartz as chocolate molds, measuring adhesion with a probe to remove the chocolate after solidification. The authors found higher surface tension for quartz, stainless steel, and polycarbonate (of 54.36, 40.57, and 34.86 mN m<sup>-1</sup>, respectively), and the lower value was found for Teflon<sup>®</sup> (of 8.89 mN m<sup>-1</sup>). The chocolate presented a surface tension of 22.57 mN m<sup>-1</sup>, which means a lower value than the surface materials, with the exception of Teflon<sup>®</sup>. The experiments showed that the samples were completely separated from the probe when in contact with stainless steel, Teflon<sup>®</sup> and polycarbonate. The use of quartz, with highest surface tension, caused a cohesive failure, where the chocolate remained on the probe but separated from itself. These results evidence the effect of surface tension on the stickiness behavior; the material with the greatest difference in surface tension to the chocolate had the strongest adhesion causing the chocolate to behave as a sticky material, separating from itself instead of the probe.

The texture assessment procedure using a texturometer does not measure the stickiness itself. However, for sticky products, a force is produced between the adhesive and adherent material while the test probe moves away from the sample surface. The analysis proved to be useful in food development laboratories, although it is not always possible to differentiate the adhesive from the cohesive force (Ali et al., 2015; Hosoney & Smewing, 1999).

In addition to the classical and widespread use of probes, texturometers, and weighting methods for assessing adhesion, experimental configurations as the peel test, pull test, tape peel test, and scratch test can be applied and developed to study this phenomenon or to remove complex solutions from processing surfaces. These tests involve applying shear stress to the layer of material to be removed, monitoring the response. While rheological techniques can measure cohesive properties, the adhesive properties of foods are widely estimated through texturometer analysis (Ali et al., 2015; Hosoney & Smewing, 1999).

The peel test, specifically, is described in ASTM D1876 (ASTM, 2001), and is a commonly used technique to evaluate adhesives in general and particularly the stickiness of food to packaging materials. It is a cleavage test where at least one of the adherents is made from a flexible material, which is plastically deformed during the measurement. Two adherents

with the same thickness are bonded with an adhesive, and the “tabs” of the sample are placed in the jaws of a tensile testing machine and then separated at a chosen rate. The test can be carried out below and above room temperature (Kilcast & Roberts, 1998; Pocius, 2012b). During the peel test, the actual angle to pull is critical because it affects the amount of energy expended by the jaws of the tensile machine. In scientific studies of peel strength, the angle is usually controlled by manually holding the peel tab during the pull so that it maintains a 90° angle with the jaws (a “T” shape). Another possibility is to hold the sample horizontally so that it forms a 180° angle with the jaws (Morris, 2017). The two configurations are exhibited in Figure 8.

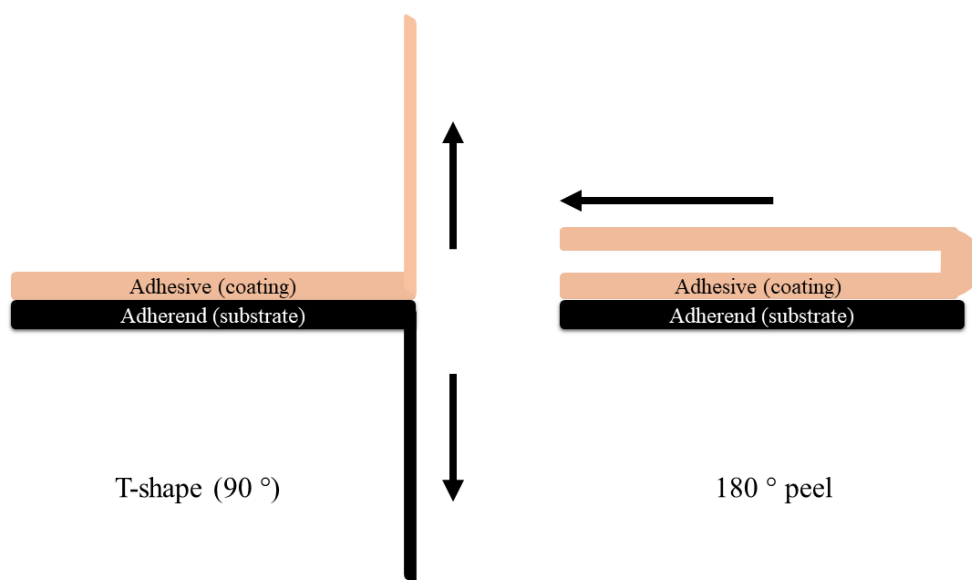


Figure 8 - Angles configuration for the peel test.

Source: author.

Thus, solving the problem of adhesion and stickiness in dryers has been a challenge, and alternatives that avoid or limit the sticky characteristics of a particular material are essential. Besides, adhesion and cohesion are phenomena partially determined by interfacial properties, and the effect of glass transition temperature ( $T_g$ ) of the adhesive material may be more important. An additive that reduces the  $T_g$  of a material below the test temperature, for example, causes an increase in cohesive strength and a decrease in adhesive strength (Krevelen & Nijenhuis, 2009; Papadakis & Bahu, 1992).

It is common to find works in the literature that reported the stickiness of fruits and vegetables during drying, usually relating to spray drying (B. R. Bhandari et al., 1997; Cano-Chauca et al., 2005; Fazaeli et al., 2012; Zotarelli et al., 2017). This behavior is attributed to

the presence of low-glass transition temperature sugars and organic acids. Alternatives for successful drying involve methods such as the addition of high-molar mass drying hydrocolloids to help increase the glass transition temperature, use of process conditions such as low humidity and temperature, scraping and/or cooling of dryer surfaces, among others (Muzaffar et al., 2015).

### 3. MATERIAL AND METHODS

This document was organized into different and complementary studies to facilitate the visualization of the experiments performed.

Strawberry has an important concentration of low molar mass sugars (glucose, fructose, and sucrose). Therefore, this fruit was adopted as a case study to be dried by CTD because it sticks to the low surface energy drying support (Teflon<sup>®</sup>). Therefore, it is an important technological problem to be understood. The adhesion phenomenon was identified in this study, as well as the main variables that could influence it, such as rheology, drying parameters, sorption, and glass transition temperature.

Afterward, formulations of starch-based suspensions with different concentrations of fructose, glucose, and sucrose were employed to better understand the influence of the composition, more specifically low molar mass sugars, on the adhesion of the product to flexible supports. The choice to work with starch suspensions as model solutions was motivated by the abundance of starch in foods, as in vegetables, and by not interacting strongly with added sugar.

#### 3.1. CHARACTERIZATION OF FLEXIBLE SUPPORTS

The surfaces usually employed in the CTD process (Mylar<sup>®</sup> and Teflon<sup>®</sup>) were characterized by roughness, contact angle with water and surface tension (using the contact angles with water, glycerol, and diiodomethane). The same was made for the surfaces with abrasions created by iron sandpaper, to simulate the aging of these support materials with constant use.

##### 3.1.1. Surface roughness

The flexible supports (Mylar<sup>®</sup> and Teflon<sup>®</sup>) employed in the drying were analyzed for their roughness. The influence of the support surface roughness on adhesion during drying was visually observed. This is important because the surfaces will change with continuous use. Therefore, artificial roughness was created on the support surfaces by abrasion with iron sandpapers. The flexible supports were glued to a metal sheet, and two types of iron sandpapers (3M, Brazil) with different grit (150 and 180) were fixed in an automatic spreader (doctor-blade). The spreader containing the sandpaper was slid 10 times over the surfaces, creating

grooves (Figure 9) to simulate the aging of the CTD belt. The Teflon<sup>®</sup> supports with fewer or more abrasions were called Teflon<sup>®</sup> R2 and Teflon<sup>®</sup> R1, respectively. Afterward, the supports were cut into specimens, and a white light optical interferometer (NV 7300, Zygo NewView 7300, USA) was used for non-contact surface topography measurements on the original materials (without abrasion) and on the supports subjected to scraping with sandpaper. The tests were performed at the Materials Laboratory (LABMAT) of the Department of Mechanical Engineering of the Federal University of Santa Catarina. Mean surface roughness (Sa) results, expressed in  $\mu\text{m}$ , were obtained after measurements in different regions of each sample area (Figure 10).

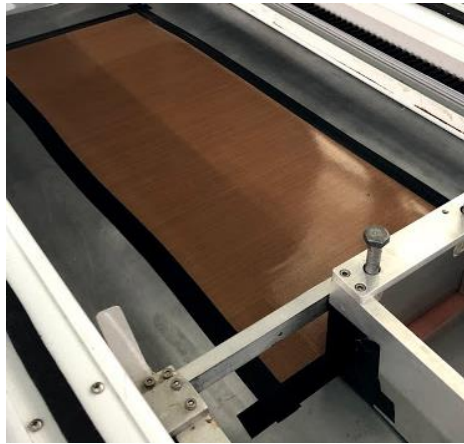


Figure 9 - Creation of the grooves in the support samples using sandpaper.

Source: author.

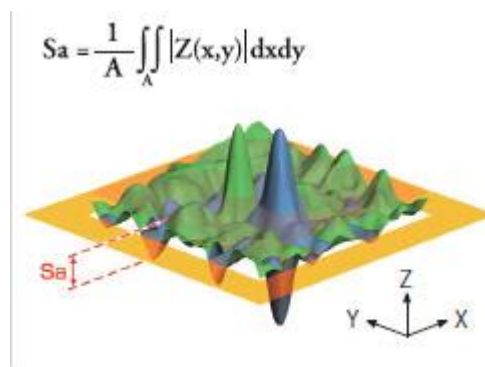


Figure 10 - Average roughness measurement (Sa).

Source: Olympus Corporation (2019).

### 3.1.2. Contact angle

Contact angle ( $\theta$ ) measurements were performed between water and flexible supports to relate them to different roughness. Measurements were performed on a Ramé-Hart goniometer (model 250, USA) using the sessile drop method at room temperature. The contact angle of a drop of distilled water was measured on the original Mylar<sup>®</sup> and Teflon<sup>®</sup> supports and on the materials modified by the sandpapers.

### 3.1.3. Surface tension of support materials

The contact angle of three pure liquids (water, glycerol, and diiodomethane) on the supports was measured with a Drop Shape Analyzer (DSA25, KRÜSS Scientific, Germany) according to Michalski et al. (1999). Measurements were performed at 20 °C, and an average of at least 5 measurements was taken. Ethanol was used to clean the solid materials for proper analysis. The thermodynamic work of adhesion,  $W_A$ , can be calculated using the Young-Dupré's equation (Equation 4), by measuring  $\gamma_L$  and  $\theta_0$ . The Young-Dupré's equation is applied for a range of standard liquids to calculate the solid surface tension ( $\gamma_S$ ). The Lifshitz–van der Waals ( $\gamma_S^{LW}$ ) and acid-base ( $\gamma_S^+$  and  $\gamma_S^-$ ) components are calculated from the Van Oss model, shown in Equation 5:

$$W_A = 2(\gamma_L^{LW}\gamma_S^{LW})^{1/2} + 2(\gamma_L^+\gamma_S^-)^{1/2} + 2(\gamma_L^-\gamma_S^+)^{1/2} \quad (5)$$

## 3.2. CASE STUDY OF CAST-TAPE DRYING OF STRAWBERRY PULP WITH ADDED HYDROCOLLOIDS

Continuous CTD using a Teflon<sup>®</sup> conveyor belt exhibits aging due to its frequent use. Therefore, the determination of material roughness after abrasion (item 3.1.1. of Material and Methods) was essential. CTD drying presents some challenges that have not yet been covered in the literature, such as drying fruit pulps that contain a high content of low molar mass sugars, and also the aging of the belt material due to use. As a case study, strawberry was selected for drying by CTD and product characterization. The incorporation of hydrocolloids in a real



suspension (strawberry pulp) during the drying process allowed investigating the performance of these additives in adhesion characteristics, as well as in the removal of dehydrated materials.

### 3.2.1. Materials

250 g strawberry trays were purchased locally, selecting the most reddish fruits with soluble solids concentration (determined in triplicate) between 5.8 and 7.5 °Brix, evaluated by portable refractometer (ATAGO, PAL-BX/RI model, Tokyo, Japan). Strawberries were sanitized in water with sodium hypochlorite for 10 min. They were then cut and homogenized in a blender (PHILCO, All in One 2 Citrus 800 W, China) for 1 min at minimum power, for subsequent freezing at -18 °C in laminated packaging until use.

After thawing the strawberry pulp, three formulations containing strawberry pulp as base and hydrocolloids at 5% (w/w) concentration were evaluated. The carrier agents (CA) adopted were maltodextrin GLOBE<sup>®</sup> 1915 (17 DE - equivalent dextrose) from Ingredion Ingredientes Industriais Ltda. (Mogi-Guaçu, Brazil), GENU<sup>®</sup> pectin type 106 BP from CP Kelco (Limeira, Brazil) or pregelatinized cassava starch from Horizonte Amidos (Mal. Cândido Rondon, Brazil). The suspensions were homogenized for 2 min in a mixer (OSTER, model FPSTHB2610R, Brazil).

### 3.2.2. Rheology

The flow properties of strawberry suspensions were determined using a Haake Mars rotary rheometer (Modular Advanced Rheometer System, Thermo Scientific<sup>®</sup>, Germany), with parallel plate geometry. A 35 mm diameter plate (PP35) and 1 mL suspension were applied.

Viscosity curves were obtained with a rotation ramp of 0.001 s<sup>-1</sup> to 600 s<sup>-1</sup> for 180 s, and the reverse path was also performed from 600 s<sup>-1</sup> to 0.001 s<sup>-1</sup> for 180 s.

During the experiment, the temperature was controlled by a water bath at 21 ± 2 °C.

The Ostwald (Equation 2) and Herschel-Bulkley (Equation 3) models were applied to the shear stress versus shear rate curves for all the samples.

### 3.2.3. Cast-tape drying

A diagram of the continuous CTD operation used for drying strawberry suspensions is shown in Figure 11. The equipment (303 cm long x 31.2 cm wide) operates with a heating zone

(200 cm) consisting of a stainless-steel tank filled with water, which is heated by electrical resistances and stirred with a pump, producing steam to heat the bottom surface of the support in contact with the product. Above this reservoir, a conveyor belt made of Teflon<sup>®</sup> moves continuously at an adjustable speed. The product is applied over one of its ends and removed after passing through a cooling zone (54 cm), with temperature-controlled water circulation. A four-fan cabin with adjustable speeds promotes air circulation and water vapor removal. Figure 12 shows a photograph of the equipment used for continuous-scale drying of strawberry.

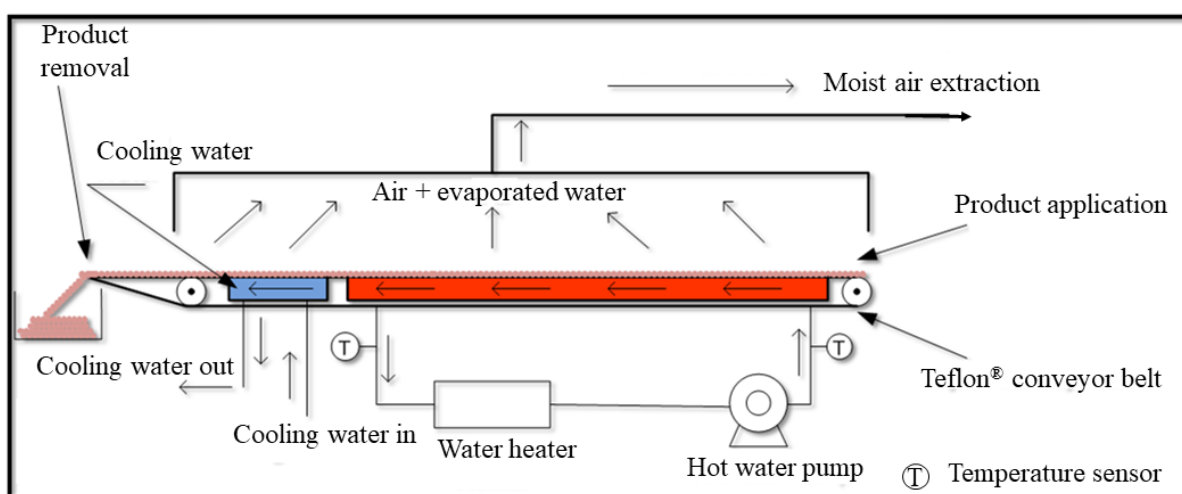


Figure 11 - Scheme of operation of the cast-tape drying equipment under a continuous regime.

Source: author.



Figure 12 - Image of the continuous CTD equipment used in the experiments.

Source: author.

The product application is performed by a doctor-blade spreader (Doctor Blade Assembly Tape Casting Warehouse, Morrisville, PA, USA), with a 27 cm wide x 17 cm long x 13 cm deep reservoir, shown in Figure 13. Suspension thickness can be altered by adjusting the micrometer screws.

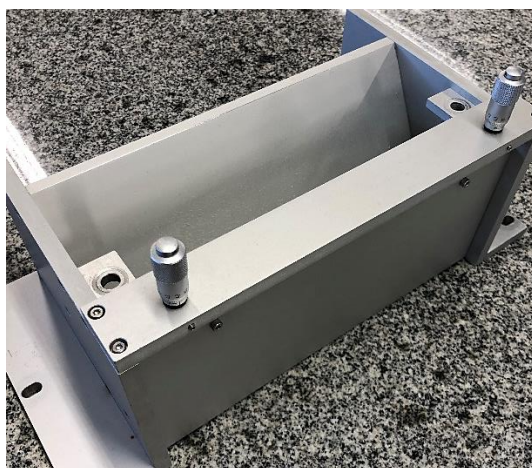


Figure 13 - Doctor-blade spreader.

Source: author.

#### 3.2.4. Experimental procedure

The configuration of the continuous CTD system to enable the best drying performance was defined according to studies published by authors of the same working group (Castoldi et al., 2015; da Silva Simão et al., 2019; Durigon et al., 2016, 2017; Frabetti et al., 2018; Zotarelli et al., 2015, 2017). Furthermore, previous experiments were carried out, testing several drying conditions until reaching the optimal setting.

In all the experiments, strawberry pulp samples (pure and with CA) were spread over the Teflon<sup>®</sup> with a thickness of 2 mm (pulp filling level within the spreader of 5 cm), while the temperature of the hot water was 98 °C and the belt velocity was 1.67 mm s<sup>-1</sup>. The average air velocity in the tunnel was measured with a compact thermal anemometer (Testo<sup>®</sup>, model 425, Lenzkirch, Germany) placed at 0.8 cm above the conveyor belt's surface, revealing an average of 0.83 ± 0.10 s<sup>-1</sup> (air temperature: 24.5 ± 1.0 °C; relative humidity (RH): 56.3 ± 7.1%). The cooling zone of the equipment was switched off because the low temperatures caused the film fragmentation during its removal.

The drying kinetics were determined by taking product samples from the Teflon<sup>®</sup> support at predetermined time intervals and in three pulp spreading regions. The moisture content ( $X$ ) of the pulp was determined by gravimetric vacuum method at 70 °C (TECNAL, model TE-395, Piracicaba, SP, Brazil), according to AOAC (2012). The curves were presented relating the dimensionless moisture content *vs.* drying time. The drying rates of each process were determined from the derivatives of the drying curves ( $\text{g g}^{-1}$ , dry basis).

### **3.2.5. Thermographs**

The temperatures during drying of strawberry suspensions in the continuous CTD process were recorded by a thermographic camera (FLIR, model T360, Täby, Sweden), which was positioned above the spreading. The emissivity ( $\epsilon$ ) of the samples was assumed to be 0.96, equal to that of its major component, water (Incropera et al., 2007). Thermographic images were captured after the product entered the heating zone and then every 2 minutes, and were analyzed using specific software (FLIR QuickReport 1.2 SP2, Täby, Sweden).

## **3.3. CHARACTERIZATION OF STRAWBERRY LEATHERS**

Preliminary tests (not shown) revealed a difficulty for the products' complete removal after passing through the cooling zone of the continuous CTD because they became brittle. Therefore, the dry samples were removed from the belt at the end of the heating zone, where they were malleable. Abonyi, Tang & Edwards (1999), who used a continuous refractance window to dry strawberries, removed the products in the same way.

The dehydrated leathers were kept in laminated packaging and inside a desiccator before the measurements.

### **3.3.1. Moisture content and water activity**

The initial and final moisture content ( $\text{g g}^{-1}$  in dry basis) of the strawberry suspensions and leathers, respectively, was determined in triplicate by the gravimetric method in a vacuum oven (TECNAL, model TE-395, Piracicaba, Brazil) at 70 °C (AOAC, 2012).

Water activity ( $a_w$ ) of the suspensions and dry products was measured using a digital hygrometer (Aqualab, Decagon Devices, USA) at room temperature ( $23 \pm 2^\circ\text{C}$ ). Analyzes were performed in triplicate.

### 3.3.2. Thickness

Thicknesses of strawberry leathers were assessed using a digital micrometer (Mitutoyo Co., USA) positioned in three different samples regions.

### 3.3.3. Sorption isotherms

The strawberry leathers were stored at room temperature in a desiccator with phosphorus pentoxide for 20 days to remove residual moisture. Then, samples of approximately 0.5 g were weighed (Shimadzu, model ATX224, Japan) and placed in two airtight pots containing solutions of salts, referring to relative humidity (RH) of 0%, 11%, 33%, 44%, 52%, 64%, 75%, 84% and 91% (Table 6). The containers were stored in an oven at 25 °C, and the mass of the samples was verified every two weeks until there was no significant change. Then, the moisture content of the samples was determined in a vacuum oven at 70 °C (TECNAL, model TE-395, Brazil).

Table 6 - Water activities of airtight pots with saturated saline solutions.

<b>Salt solutions</b>	<b>Water activity (Pot 1)</b>	<b>Water activity (Pot 2)</b>
Lithium chloride	0.112	0.113
Magnesium chloride	0.325	0.338
Potassium carbonate	0.437	0.439
Magnesium nitrate	0.536	0.539
Sodium nitrate	0.642	0.640
Sodium chloride	0.759	0.762
Potassium chloride	0.844	0.845
Barium Chloride	0.909	0.911

Source: author.

The GAB mathematical model (Guggenheim - Anderson - de Boer) was adjusted to the experimental data (Equation 6):

$$X_{eq} = \frac{X_0 k C a_w}{(1 - k a_w) (1 - k a_w + C k a_w)} \quad (6)$$

where  $X$  is the equilibrium moisture content ( $\text{g g}^{-1}$ , dry basis),  $X_0$  is the moisture content in the monolayer ( $\text{g g}^{-1}$ , dry basis),  $k$  is the GAB constant,  $C$  is the Guggenheim constant, and  $a_w$  is the water activity in which the sample was stored.

### 3.3.4. Glass transition temperature

Strawberry leathers were milled using a knife mill (TECNAL, TE 631/2, Brazil) at 19,500 rpm, and later classified into 20 and 25 mesh sieves. Powders were conditioned in 11% and 33% RH at 25 °C. As soon as the samples reached equilibrium with the inside of the humidity-controlled jars, the powders were placed in aluminum capsules ( $10 \pm 6$  mg), and the glass transition temperatures were determined by means of a DSC (Perkin-Elmer, Jade, Massachusetts, USA). A single trial was performed for each product. The equipment was previously calibrated with Indium and Zinc, and during the analysis, nitrogen was used as the carrier gas, with a flow rate of  $20 \text{ mL min}^{-1}$ . The materials' thermograms were obtained in a temperature range of -60 to 100 °C, with a heating speed of  $10 \text{ °C min}^{-1}$ . The results were analyzed using the Pyris DSC software.

### 3.3.5. Detachment of strawberry leathers

After strawberry suspensions drying in the continuous CTD, the leathers' detachment was studied by visual analysis at the end of the heating zone.

## 3.4. STUDY OF ADDING LOW MOLAR MASS SUGARS IN STARCH-BASED SUSPENSION FOR CTD DRYING

The components of foods are one of the factors that control the adhesion to surfaces during drying. During fruit ripening, low molar mass sugars increase, and it was noted that the

use of fruits in different ripening stages had an influence on spreading and adhesion to the CTD belt. Preliminary studies with several raw materials confirmed the influence of sugar concentration ( $^{\circ}\text{Brix}$ ) and fibers on the product spreading in the continuous CTD. In the drying of mango pulp the impact of the sugar concentration was evident (Figure 14), showing how the composition influenced the dehydration of fruits and vegetables.

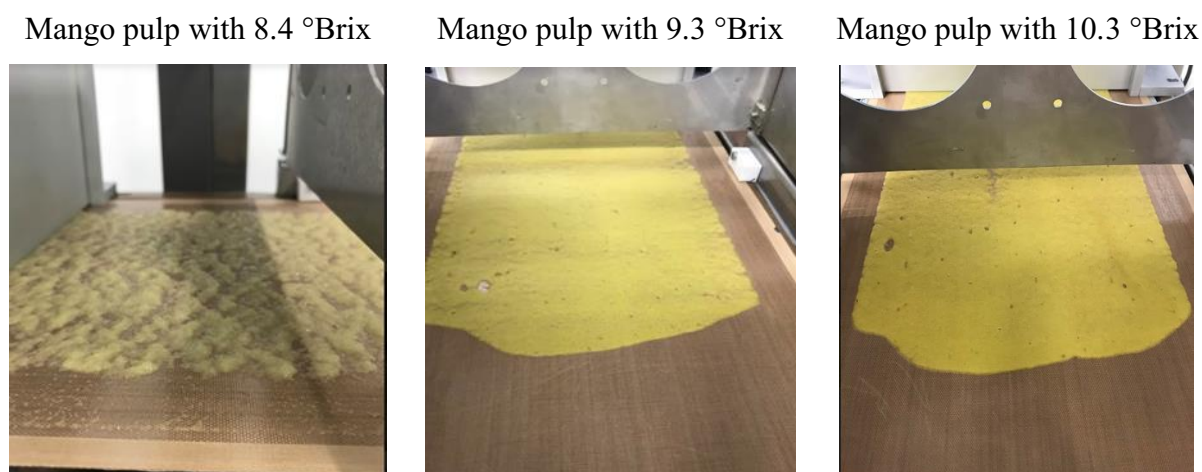


Figure 14 - Spreading of mango pulps with different  $^{\circ}\text{Brix}$  on the continuous CTD support.

Source: author.

In this study, suspensions of cassava starch were prepared with different concentrations of glucose, sucrose, and fructose in order to assess the impact of the presence of low molar mass sugars on the material's adhesion to the drying surface. A small-scale batch CTD equipment was employed to investigate the adhesion and detachment of products from flexible materials, with the possibility of applying Teflon<sup>®</sup> or Mylar<sup>®</sup> supports.

### 3.4.1. Materials

For the preparation of starch suspensions, cassava starch (Yoki Alimentos S.A.) was purchased from a commercial establishment.

D (-) Fructose PA 99.99% pure (molar mass  $180.16 \text{ g mol}^{-1}$ ), D (+) anhydrous glucose PA 99.50% pure (molar mass  $180.16 \text{ g mol}^{-1}$ ), and sucrose PA (molar mass  $342.30 \text{ g mol}^{-1}$ ) from NEON were used to evaluate how low molar mass carbohydrate composition affects adhesion on CTD drying support.

### 3.4.2. Preparation of starch-based suspensions

The cassava starch suspension was prepared at a concentration of 4 g per 100 g of water. Starch gelatinization was promoted under mechanical agitation (IKA RW20 digital, Germany) at 210 rpm and heating in an ultra-thermostatic water bath (MAXIM-LAB, Brazil) to 71 °C, maintaining this temperature for 5 min. Previous experiments were performed, and the spreading of starch suspensions was not possible in Teflon<sup>®</sup>. As a result, 0.1% (volume/mass of suspension) of surfactant *Tween 20* was added to allow spreading on the flexible supports (Mylar<sup>®</sup> and Teflon<sup>®</sup>). The amount of *Tween* was defined after preliminary testing to ascertain the minimum volume of reagent required to spread the starch suspension.

A three-factor simplex-centroid experimental design (DOE - mixture), shown in Table 7, was performed in Statistica 7.0 software (Statsoft Inc., Tulsa, USA) to evaluate the influence of low molar mass carbohydrate concentration (fructose, glucose, and sucrose). The sugars were added to 100 g of starch suspension at a temperature of about 65 °C, under constant stirring with a magnetic stirrer until the solutes were completely dissolved. The minimum and maximum amounts of each sugar were stipulated based on the amounts usually found in fruit composition (USDA, 2015). The formulations of starch and low molar mass sugars are presented in Table 8.

Table 7 – Three-factor simplex-centroid experimental design to define the sugar composition of the starch-based suspensions.

<b>Formulation of suspensions</b>	<b>Glucose</b>	<b>Sucrose</b>	<b>Fructose</b>
1	0.5	0.5	0.0
2	0.0	1.0	0.0
3	0.5	0.0	0.5
4	1.0	0.0	0.0
5	0.3	0.3	0.3
6	0.0	0.5	0.5
7	0.0	0.0	1.0

Source: author.



Table 8 - Formulation of starch-based suspensions.

<b>Suspensions</b>	<b>Glucose (g/100 g suspension)</b>	<b>Sucrose (g/100 g suspension)</b>	<b>Fructose (g/100 g suspension)</b>
Starch 4%	0	0	0
3G3F	3	0	3
6F	0	0	6
3G3S	3	3	0
6G	6	0	0
1.98GSF	1.98	1.98	1.98
3S3F	0	3	3
6S	0	6	0

F: Fructose; G: Glucose; S: Sucrose.

Source: author.

### 3.4.3. Small-scale batch CTD experimental apparatus

One of the equipment used in the drying operations to evaluate the detachment of starch-based films is exhibited in Figure 15, showing the elements of the apparatus and their measurements.

A stainless-steel bath (260 mm x 250 mm x 55 mm) covered with a 4.6 mm plate of the same material was coupled to an ultra-thermostatic bath (QUIMIS, Brazil) with water heated to 98 °C. Water circulation was promoted through two hoses, allowing its entry and exit. The flexible support (Teflon<sup>®</sup> or Mylar<sup>®</sup>) was fixed on the bath, and the detachment experiments of the dry films were conducted in this system.

An aluminum plate (Figure 16) with water circulation for cooling the product after drying was also employed to simulate the detachment of the dry products in the cooling zone of CTD.

Drying of starch-based suspensions were also performed on a thin aluminum plate, covered by original Teflon<sup>®</sup> (15 cm x 15 cm), heated by electrical resistances controlled by a PID, as seen in Figure 17. The resulting films were characterized for their mechanical and physical-chemical properties.

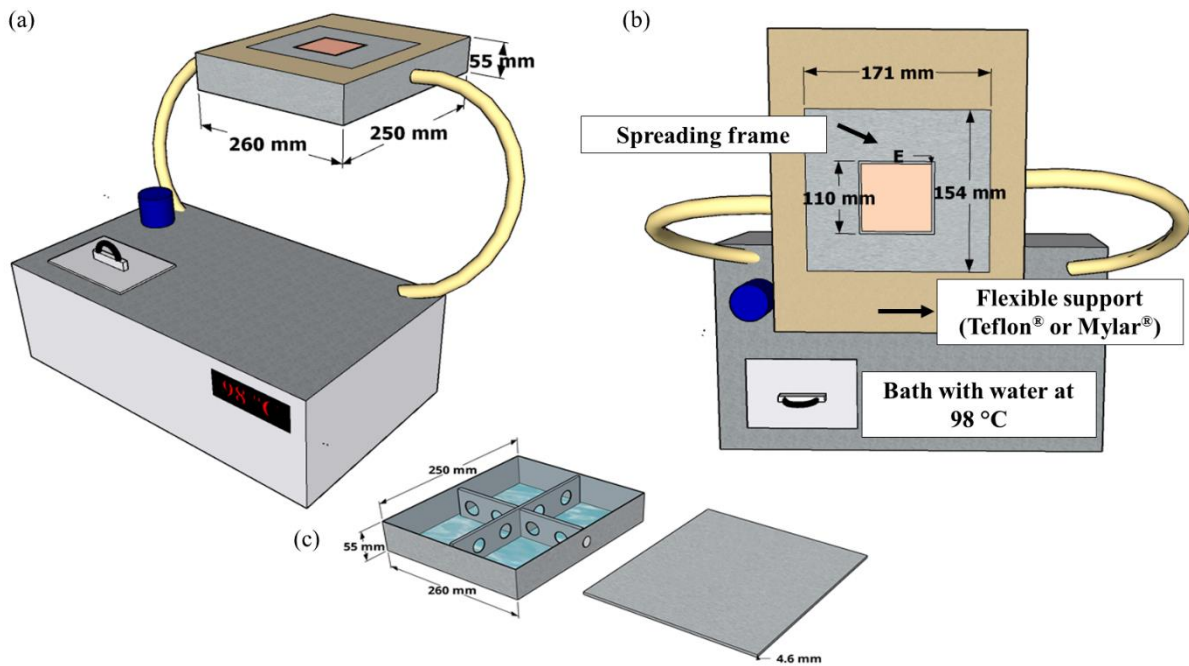


Figure 15 - (a) Small-scale experimental equipment for the drying of the starch-based suspensions; (b) Top view of the small-scale equipment; (c) View of the stainless-steel bath.

Source: author.

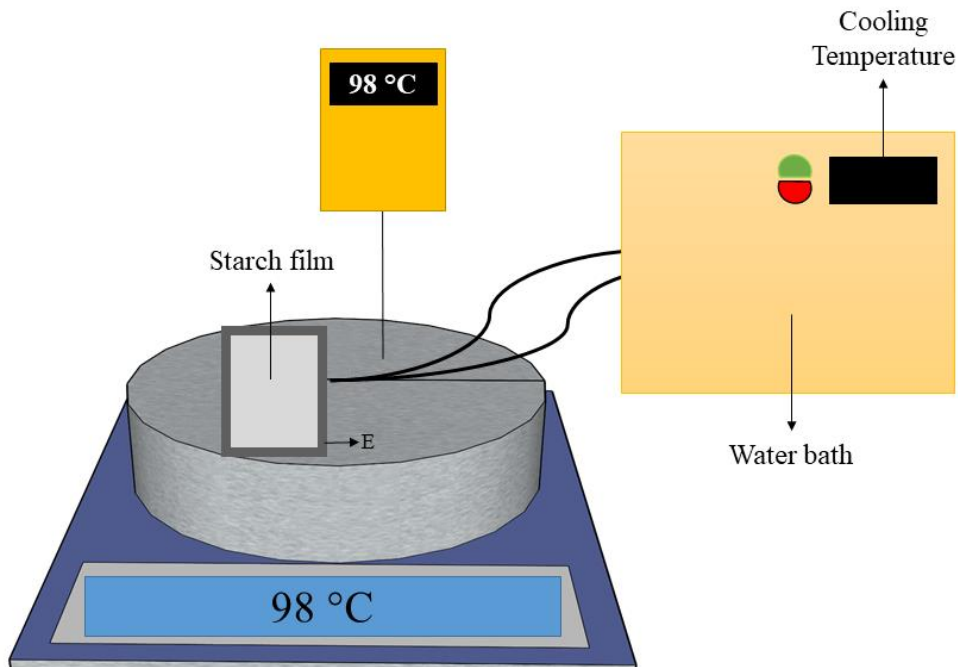


Figure 16 - Aluminum plate with water circulation for drying and cooling the starch-based samples.

Source: author.

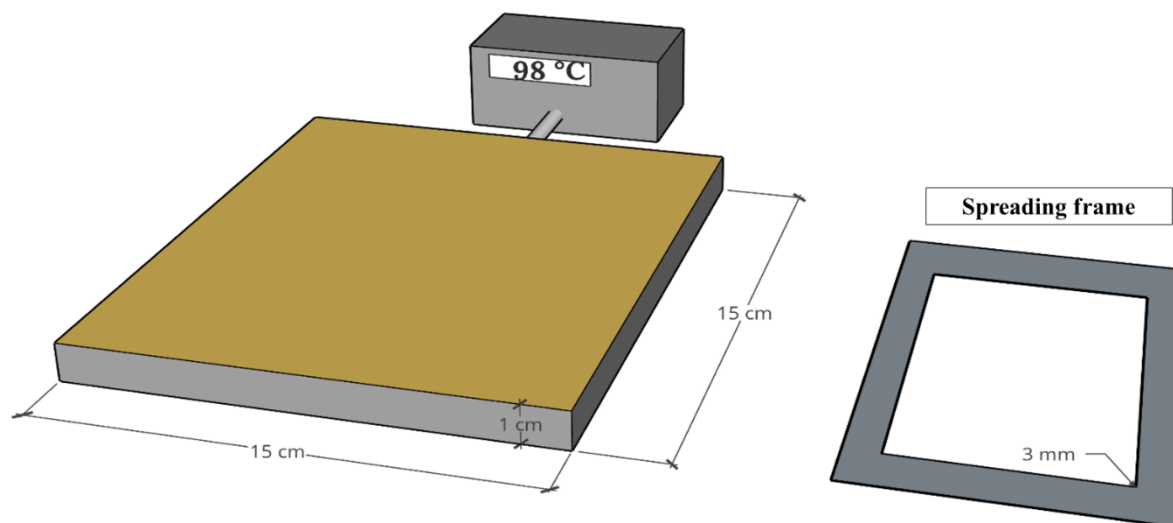


Figure 17 - Aluminum plate heated by electrical resistances to perform the drying of the starch-based suspensions.

Source: author.

#### 3.4.4. Experimental drying procedure

Drying experiments were carried out using one of the small-scale CTD apparatus, which was chosen according to the experiment to be performed and set to 98 °C.

The starch-based suspensions were prepared, and the spreading thickness was provided by a 3 mm thick rectangular frame (the spreading thickness was determined after preliminary tests carried out to optimize the process with shorter times and greater spreading homogeneity). The excess of suspension after spreading (on Teflon<sup>®</sup> or Mylar<sup>®</sup>) was removed with a polypropylene plate, and the drying lasted 40 - 50 min, depending on the CTD equipment.

Air temperature, of  $23.31 \pm 1.7$  °C, and relative humidity, of  $28.7 \pm 5.4\%$ , were controlled by a thermo-hygrometer (Rotronic<sup>®</sup> hygrolog, PST Group, Switzerland).

#### 3.4.5. Contact angle

The contact angle measurements of the starch-based suspensions were performed on a Ramé-Hart goniometer (model 250, USA) using the sessile drop method. A 5  $\mu$ L drop of each

solution was gauged in an automated micropipette and placed on the Mylar<sup>®</sup>, and Teflon<sup>®</sup> supports for a camera to assess contact angles.

#### **3.4.6. Surface tension of starch-based suspensions**

The surface tension of the starch-based suspensions without surfactants and with the addition of 0.1% (volume/mass of suspension) of *Tween 20* was measured using a tensiometer KRÜSS K12 (KRÜSS GmbH, Germany). Ten measurements were taken for each suspension, and the measurements were repeated at least twice. The surface tension (T) results were expressed in mN m<sup>-1</sup>.

#### **3.4.7. Rheology**

The rheological behavior of starch-based suspensions was determined as described in item 3.2.5. for the strawberry suspensions. A 60 mm diameter plate (PP60) and 3 mL of solution were used.

#### **3.4.8. Moisture content and water activity**

The moisture content (g g<sup>-1</sup>, d.b.) of the starch-based suspensions and films was obtained through a conventional oven at 105 °C (MEMMERT GmbH, Germany), where the samples remained for 24 h (AFNOR, 1995).

Water activity ( $a_w$ ) of the suspensions and dry products was measured using a digital hygrometer (Aqualab, Decagon Devices, USA). Analyzes were performed in triplicate.

### **3.5. CHARACTERIZATION OF STARCH-BASED FILMS**

The drying of the starch-based suspensions was performed using the aluminum plate heated by electrical resistances, shown in Figure 17. After 40 min of drying, the samples containing sugars were removed and stored at 44% RH and 20 °C, for characterization.

### 3.5.1. Thickness

The thicknesses of the starch-based films were determined using a digital micrometer (Mitutoyo Co., USA) positioned in different samples regions.

### 3.5.2. Water sorption isotherms

The changes in the mass of starch-based film samples under dynamic relative humidity were measured by dynamic vapor saturation (DVS Revolution, Surface Measurement Systems, UK). The test temperature was 20 °C, and the initial mass range was  $21.84 \pm 8.517$  mg.

### 3.5.3. Glass transition temperature

Samples of starch-based films were placed in aluminum capsules, weighed ( $12 \text{ mg} \pm 9 \text{ mg}$ ), and placed in a modulated DSC TA Instruments Q100 (New Castle, USA) to determine the glass transition temperatures. Nitrogen was used as the carrier gas, with a flow rate of  $50 \text{ mL min}^{-1}$ . The procedure consisted in equilibrating at 40 °C for 5 min, then cooling down to -60 °C with a speed of  $10 \text{ °C min}^{-1}$ . Afterward, the samples were heated to 90 °C, cooled down to -60 °C, and heated again to 150 °C and cooled down to -60 °C one last time. The glass transition temperature was determined from the midpoint of the heat capacity change observed on the second cycle to eliminate sample history. Three samples of each material were measured, and an average Tg was determined from the scans using the Universal Analyzer software (TA Instruments, New Castle, USA).

### 3.5.4. Mechanical tests

Tensile tests were performed in starch-based films with a texturometer TA-XT plus (Stable Micro Systems, UK) to estimate the cohesion of the samples. The samples had  $10.5 \pm 2$  cm in length and  $5 \pm 2$  cm in width. The maximum and average loads were determined using the procedure adapted from the method D 882-02 from the American Society for Testing and Materials (ASTM, 2002), with a test speed of  $0.80 \text{ mm s}^{-1}$  and distance of 30 mm. The tensile strength (TS) was calculated using Equation 7:

$$\sigma_{\text{MAX}} = \frac{P_{\text{MAX}}}{A_0} \quad (7)$$

where  $\sigma_{\text{MAX}}$  is the tensile strength (MPa),  $P_{\text{MAX}}$  is the maximum load (N) and  $A_0$  is the original cross-sectional area ( $\text{mm}^2$ ) (thickness x width;  $A_0 = e \omega$ ).

### 3.5.5. Evaluation of the detachment of starch-based films

Detachment tests were performed on starch-based films to better understand the magnitude of force required to remove the dry material adhered to the Teflon<sup>®</sup> and Mylar<sup>®</sup> supports. The system configuration was designed to simulate the release of a film by hand, starting at one end of the film and peeling it out. This methodology is an adaptation of the peel test widely employed to determine the peel resistance of adhesive bonds (ASTM, 2001). The objective was to observe the influence of the type of support, the abrasions made on the Teflon<sup>®</sup> (increased roughness), and the suspensions composition on the sample's detachment force.

In a first approach, the small-scale CTD with water circulation at 98 °C (shown in Figure 15) was adopted, replicating the continuous CTD used for strawberry drying. The detachment forces were obtained right after the end of drying, using a LLOYD LR5K texturometer and the Lloyd Nexygen software (AMETEK Inc, USA). Original Teflon<sup>®</sup>, Teflon<sup>®</sup> with two types of abrasions (made with sandpapers), as well as Mylar<sup>®</sup> were tested as supports. Starch-based suspensions were spread into a 3 mm thick rectangular frame, while a piece of thin Mylar<sup>®</sup> was positioned below the spreading. To start the test, once the drying was finished, the piece of Mylar<sup>®</sup> was attached to the tensile grip of the texturometer and then pulled up (Figure 18). When the piece of thin Mylar<sup>®</sup> was pulled up, it detached the starch film from the support at a constant peeling rate. The pre-load charge was 0.05 N, the initial distance between the grip and the spreading was 51 mm, and the test speed was 1.33  $\text{mm s}^{-1}$ , an adaptation of the standard adhesive peel strength test methodology (ASTM, 2001; Valenzuela & Aguilera, 2015).

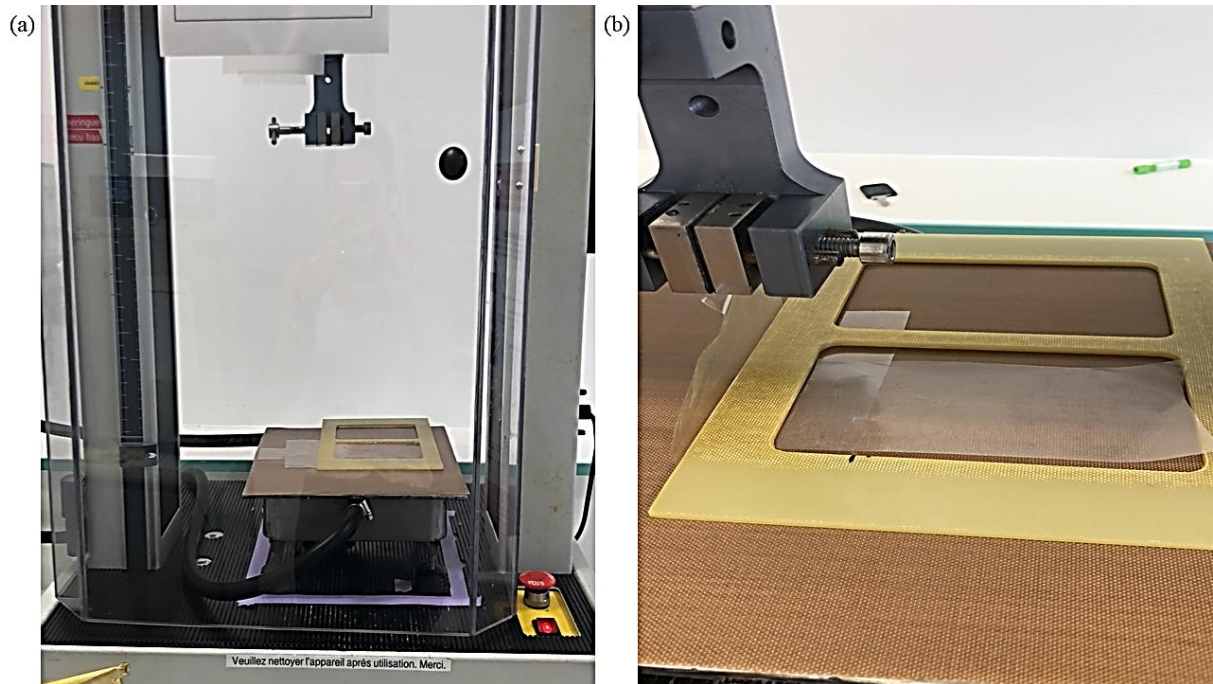


Figure 18 - Texturometer used for the starch's detachment experiments: (a) texturometer and CTD equipment, (b) spreading frame and a piece of Mylar<sup>®</sup> attached to the tensile grip.

Source: author.

### 3.5.5.1. *Effect of temperature on the dry products detachment*

The influence of the temperature on the sample removal was assessed from experiments with the aluminum plate with water circulation (Figure 16 and Figure 19). Two starch-based suspensions were chosen to be dried at a temperature of 98 °C, the suspension 1.98 GSF, and the suspension 6S. At the end of drying, the cooling was turned on (cooling rate of 10 °C min<sup>-1</sup>), and when the system has reached the established cooling temperature, the detachment test was carried out in the same manner as described above. Cooling temperatures of 35 °C, 45 °C, 55 °C, 65 °C, 80 °C, and 88 °C were applied.



Figure 19 - Aluminum plate employed to detachment tests with cooling.

Source: author.

#### 3.5.5.2. *Effect of relative humidity (RH) on the dry products detachment*

Two starch-based suspensions, 1.98GSF, and 6F, were chosen to be spread on original Teflon<sup>®</sup> strips and dried using the CTD system heated by electrical resistances shown in Figure 19. After 40 min of drying, the Teflon<sup>®</sup> strips containing the films were removed from the heated plate and stored in dissectors containing saturated salt solutions corresponding to 33%, 44%, 54%, 68%, and 84% RH. The dissectors were then placed in a temperature-controlled oven at 20 °C until equilibrium. The films were then removed from the Teflon<sup>®</sup> support, and their appearance and difficulty in removing from the support were observed. Also, the moisture content and water activity of the samples were evaluated.

#### 3.5.6. **Visual analysis**

The starch-based films were produced by CTD heated by electrical resistances (Figure 17). Soon after, a qualitative analysis of the films containing different concentrations of sugars was performed based on a study by Gontard (1991). The characteristics evaluated by the author were: malleability (ease of handling), uniformity (absence of insoluble particles, air bubbles, or areas of opacity), stickiness (adhesive character), and fragility (tendency to break). Each attribute received a score from 0 to 10, with the minimum value being the complete absence and the maximum value being the strong presence of a specific characteristic.



### 3.6. STATISTICAL ANALYSIS

The statistical analysis of the data was obtained using the software Statistica 7.0 (Statsoft Inc., Tulsa, USA), applying a simple analysis of variance (ANOVA). The multiple comparison of means was analyzed using the Tukey test at a 5% probability of error ( $p < 0.05$ ). Ternary graphs were plotted to examine the relationship between the sugar composition of the samples (suspensions and films) and the measured responses from the experiments. Quadratic or linear models were used to fit the data. The statistical significance of the equations was determined through the analysis of variance, at the 5% confidence level.

## 4. RESULTS AND DISCUSSION

### 4.1. CHARACTERIZATION OF FLEXIBLE SUPPORTS

The surface characteristics of the support materials, Teflon<sup>®</sup>, Teflon<sup>®</sup> with fewer abrasions (R2), Teflon<sup>®</sup> with more abrasions (R1) and Mylar<sup>®</sup>, were studied by means of surface roughness, contact angle and surface tension.

#### 4.1.1. Surface roughness and contact angle

The mean roughness values (Sa) obtained for the Teflon<sup>®</sup> support are shown in Table 9. Abrasions promoted by sandpaper with different grit led to roughness called R2 and R1. Furthermore, Table 9 displays the contact angles with water on Teflon<sup>®</sup> and Mylar<sup>®</sup>.

Table 9 - Mean roughness values (Sa) of Teflon<sup>®</sup> samples and contact angles with water on Teflon<sup>®</sup> and Mylar<sup>®</sup>.

Supports	Mean surface roughness ( $\mu\text{m}$ )	$\theta$ ( $^{\circ}$ )
Teflon <sup>®</sup> - original	$0.174 \pm 0.05^{\text{a}}$	$106.6 \pm 2.2^{\text{a}}$
Teflon <sup>®</sup> (R2)	$0.188 \pm 0.04^{\text{a}}$	$100.2 \pm 0.7^{\text{c}}$
Teflon <sup>®</sup> (R1)	$0.213 \pm 0.02^{\text{a}}$	$103.2 \pm 0.7^{\text{b}}$
Mylar <sup>®</sup> - original	-	$94.8 \pm 1.4^{\text{d}}$

\*a-c Means with the same superscript letters within a column indicate no significant differences ( $p < 0.05$ ).

Source: author.

It can be noticed that the supports that suffered abrasion resulted in a greater value of mean surface roughness, although there was no statistically significant difference between them. The grooves were created at specific points on the supports, and the “Sa” parameter expresses the average of absolute values in a measured area. Thus, the final roughness result is equivalent to the arithmetic mean of the region measured in the three-dimensional display diagram, and the influence of a single lesion on the measurement value becomes quite small, so stable results can be obtained (Olympus Corporation, 2019). The same response can be inferred from the topographic images shown in Figure 20. The sample of original Teflon<sup>®</sup>

showed regions with smaller values of roughness, and the supports submitted to sandpaper showed points with greater roughness on the evaluated surface.

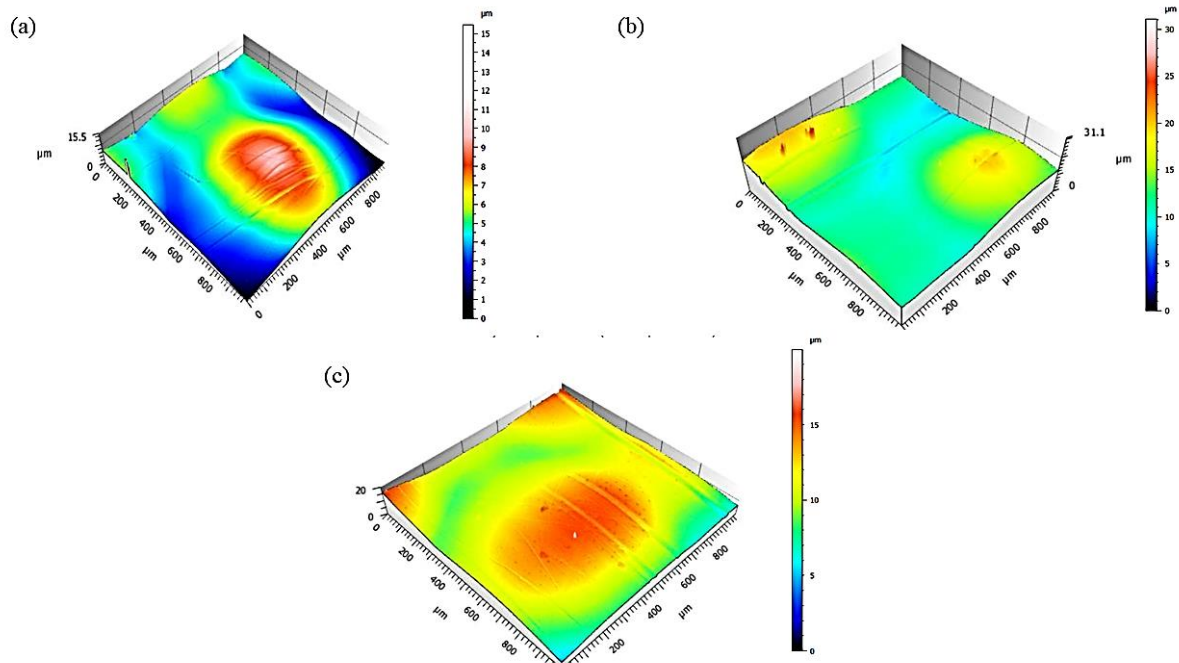


Figure 20 - Topographic images of Teflon® support samples: (a) Teflon® - original; (b) Teflon® with fewer abrasions (R2); (c) Teflon® with more abrasions (R1).

Source: author.

Fernanda Paula Collares, (2001) studied the detachment of food films from solid surfaces during drying. The author determined the roughness values of Nylon®, Teflon®, stainless steel, and ordinary glass surfaces and reported values of 0.088  $\mu\text{m}$ , 0.134  $\mu\text{m}$ , 0.180  $\mu\text{m}$  and 0.002  $\mu\text{m}$ , respectively. The work related the roughness of the tested materials to the respective detachment of the dehydrated film after drying; therefore, it was stated that the greater the roughness of the tested support, the lower the moisture content of the films should be so that the spontaneous detachment occurred. However, the influence of the chemical interaction between the surface and the product to be dried was also verified, since a dry maltodextrin film detached itself more easily from the Teflon® and the Nylon® materials, whose roughness was higher than that of ordinary glass. This work will be discussed in more detail on the topic of the removal of starch-based films (item 4.3.8).

Teflon® presented contact angles with water greater than 100°, which characterizes hydrophobic materials (Zisman, 1964). On the Mylar® surface, the result shows a less hydrophobic material, with smaller contact angles with water. Also, the abrasions caused a

decrease in the contact angle, while the original Teflon<sup>®</sup> support, without air pockets, resulted in a greater contact angle (explained by the Wenzel state). Karim, Rothstein & Kavehpour (2018) evaluated the spreading of polyethylene glycol (PEG) solutions on Teflon<sup>®</sup> plates with different roughness (305, 86 and 38  $\mu\text{m}$ ) and obtained equilibrium contact angles between 100° to 120°. The authors also noticed that the roughness of Teflon<sup>®</sup> surfaces had a significant effect in reducing contact angles.

During drying by CTD, the Teflon<sup>®</sup> surface aging implies a greater resistance of the dry material to be removed as a whole film. The improved wettability of the suspension on the support, caused by increased roughness through use and consequent decrease in the contact angle, may be responsible for the product adhesion. In addition, other factors can influence the increase in adhesion, such as spreading temperature and the material below the Teflon<sup>®</sup> layer, the fiberglass, which is less hydrophobic than Teflon<sup>®</sup>. If the Teflon<sup>®</sup> coating is partially scrapped off, for example, adhesion may increase.

In previous works that applied Mylar<sup>®</sup> support for processing in CTD (Durigon et al., 2017; Frabetti et al., 2018), it was shown difficulty in removing the dehydrated materials, which agrees with the results discussed above, in which Mylar<sup>®</sup> has smaller contact angle and consequently greater wettability and greater product adhesion.

#### 4.1.2. Surface tension of support materials

The contact angles and the surface tension components obtained for each support (original Teflon<sup>®</sup> and Mylar<sup>®</sup> and Teflon<sup>®</sup> with abrasions) are shown in Table 10.

Table 10 - Equilibrium contact angles and surface tensions of support materials at 20 °C.

Supports	Contact angle (°)			Surface tension components (mJ m <sup>-2</sup> )			
	DIM	Glycerol	Water	$\gamma_s$	$\gamma_s^{LW}$	$\gamma_s^+$	$\gamma_s^-$
Teflon <sup>®</sup> - original	92.7 ± 4.3 <sup>a</sup>	105.4 ± 2.5 <sup>a</sup>	124.0 ± 1.2 <sup>a</sup>	18.67	9.78	3.88	5.09
Teflon <sup>®</sup> (R2)	94.7 ± 3.8 <sup>a</sup>	102.2 ± 2.2 <sup>a</sup>	114.8 ± 2.8 <sup>a</sup>	31.95	7.54	7.65	19.46
Teflon <sup>®</sup> (R1)	89.5 ± 4.4 <sup>a</sup>	105.7 ± 1.8 <sup>a</sup>	113.8 ± 2.5 <sup>a</sup>	59.82	8.33	18.69	35.46
Mylar <sup>®</sup> - original	43.5 ± 2.0 <sup>b</sup>	75.4 ± 2.8 <sup>b</sup>	93.5 ± 1.3 <sup>b</sup>	132.05	26.60	40.07	69.38

Source: author.

To determine the  $\gamma_s$  of a solid, it is recommended to select three or more liquids from Table 3, with two of them being polar. In this work, water and glycerol were used as polar liquids and diiodomethane as the apolar one (completely dispersive).

Because of its inertness, Teflon<sup>®</sup> is expected to interact weakly and non-preferentially with liquids, which explains the greater contact angles with all tested liquids. The differences in contact angles with water, in comparison to the results showed in Table 9, are due to the fact that a different equipment was used to perform the measurements. Diiodomethane, an hydrophobic liquid with a chemical nature closer to Teflon<sup>®</sup>, interacted a bit more strongly with the support (Extrand, 2009). A surface with hydrophobic character is also characterized by lower  $\gamma_s^{LW}$ , with little (or zero) Lewis's acid or Lewis's base character. A surface may be hydrophilic on account of the presence of Lewis's base or acid groups, or of both. It is obvious that changes in the surface structure that increase, for example, the concentration of surface either groups, will increase the Lewis's base character of the surface, and hence its hydrophilicity, with little influence on the Lewis's acid character (Good, 1992).

As expected, original Teflon<sup>®</sup> showed lower surface tension, similar to the reported values in the literature (Dann, 1970; Zisman, 1964), which increased with the increase in the Teflon<sup>®</sup> roughness. For Mylar<sup>®</sup>, the smaller contact angle with water evidences the more hydrophilic character of this support.

To summarize this topic, it's interesting to be reminded that the objective of characterizing flexible supports, especially the Teflon<sup>®</sup> (this being the material used in the conveyor belt of the continuous), was to verify the surface properties and how they were affected by the presence of abrasions. In fact, with the increase in roughness the angle of contact with water has decreased and the surface tension has increased. Through the results shown above, the difference in surface properties between Teflon<sup>®</sup> and Mylar<sup>®</sup> (support used in the Refractance Window), is evident. One of the main advantages of using Teflon<sup>®</sup> is its low surface tension and its high contact angle, which suggests a low adhesion of food suspensions during processing.

## 4.2. CASE STUDY OF THE DRYING OF STRAWBERRY PULP WITH ADDED HYDROCOLLOIDS BY CTD

### 4.2.1. Rheology of the strawberry suspensions

The assessment of the rheological properties of strawberry pulps is essential for their processing by CTD. Figure 21 shows the viscosity curves for pure strawberry and strawberry-carrier agents (CA) suspensions. Shear stress curves *vs.* shear rates are shown in Appendix A.

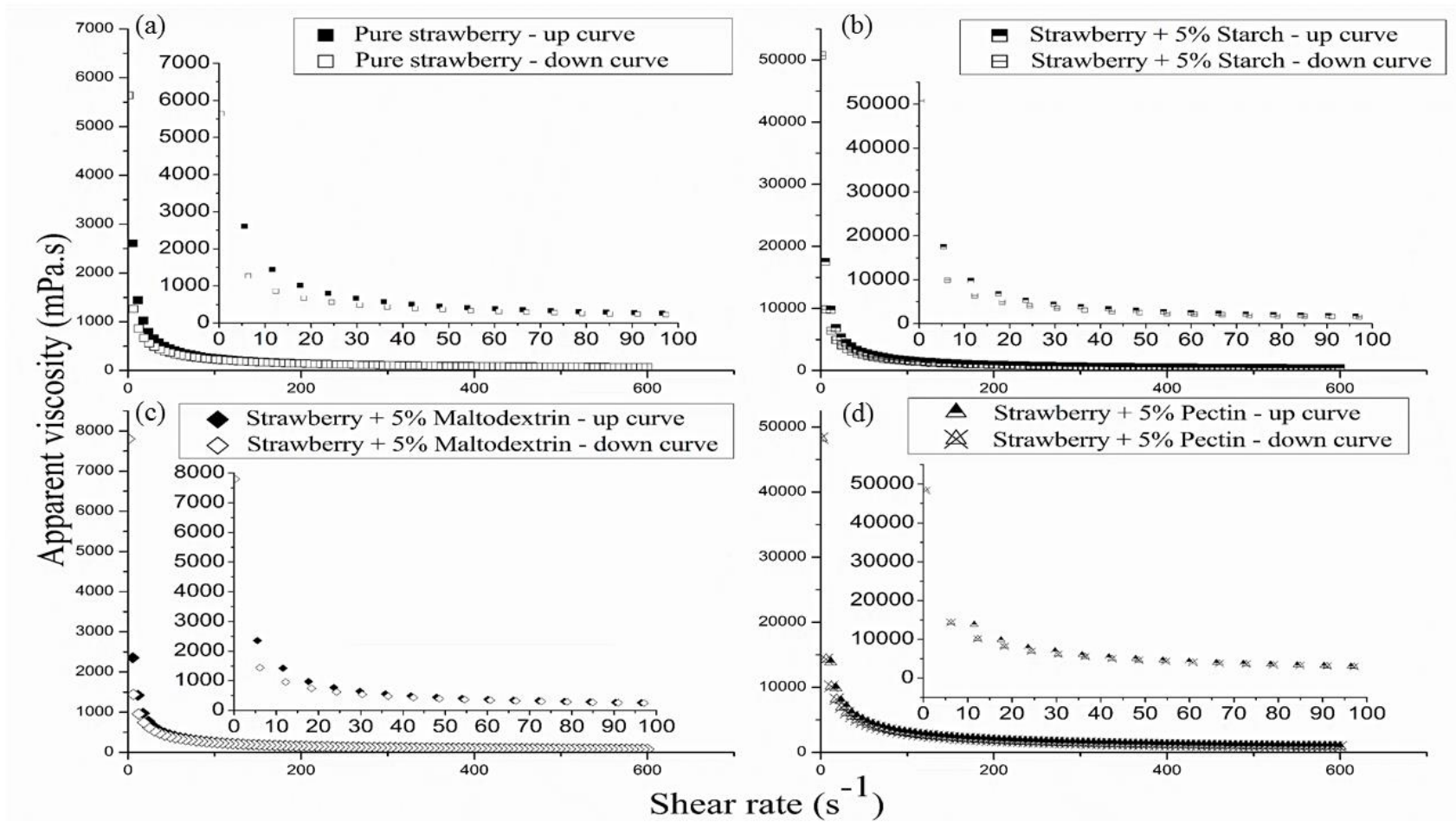


Figure 21 – Viscosity curves of strawberry suspensions (all graphs also show shear rates up to  $100\ s^{-1}$ , to highlight the decay of the curves): (a) Strawberry pulp; (b) Strawberry + 5% starch; (c) Strawberry + 5% maltodextrin; (d) Strawberry + 5% pectin.

Source: author.

The suspensions exhibited non-Newtonian fluid behavior. The viscosity curves show that the sample composition influenced the drop in apparent viscosity with increased shear rates. Among the hydrocolloids used in this study, the addition of maltodextrin had minimal influence on the flow curve of the suspension in relation to pure strawberry pulp. Strawberry-starch and strawberry-pectin suspensions reached apparent viscosities of approximately 50,000 mPa s (for shear rates close to zero), 10 times higher than the observed for the pure strawberry pulp. This result is explained by the higher molar masses of these CA. However, the strawberry-starch sample exhibited a greater drop in the apparent viscosity with the increasing shear rate compared to the strawberry-pectin mixture, which is related to a well-defined pseudoplastic behavior.

The addition of the CA starch, pectin, or maltodextrin to a fruit pulp increases its viscosity without substantially modifying other properties, such as its flavor. This higher viscosity is needed to fill the spreader (doctor-blade) and maintain a predetermined spreading thickness. The pulp's viscosity should allow it to flow through the spreader blade only by the action of hydrostatic pressure at the level of the moving belt (Gibson et al., 2018).

Table 11 and Table 12 exhibit the parameters for Ostwald and Herschel-Bulkley models, respectively.

Table 11 – Parameters of the Ostwald model adjusted to the shear stress vs. shear rate curves of strawberry suspensions.

<b>Ostwald model (Power Law)</b>	<b>K</b>	<b><i>n</i></b>	<b>R<sup>2</sup></b>
<b>Samples</b>	<b>[Pa. s<sup>n</sup>]</b>		
Pure strawberry	7.680 ± 1.032 <sup>c</sup>	0.190 ± 0.113 <sup>a</sup>	0.989
Strawberry + 5% Maltodextrin	6.463 ± 1.371 <sup>c</sup>	0.313 ± 0.045 <sup>a</sup>	0.987
Strawberry + 5% Pectin	92.45 ± 7.432 <sup>a</sup>	0.280 ± 0.021 <sup>a</sup>	1.000
Strawberry + 5% Starch	64.93 ± 8.828 <sup>b</sup>	0.190 ± 0.026 <sup>a</sup>	0.999

\*<sup>a-c</sup>Means with the same superscript letters within a column indicate no significant differences (p<0.05).

Source: author.



Table 12 - Adjustment of shear stress vs. shear rate curves of strawberry suspensions to the Herschel-Bulkley model.

<b>Herschel-Bulkley model</b>	$\sigma_0$ [Pa]	<b>K</b>	<b><i>n</i></b>	<b>R<sup>2</sup></b>
<b>Samples</b>				
Pure strawberry	11.81 ± 4.023 <sup>a</sup>	1.940 ± 0.552 <sup>c</sup>	0.445 ± 0.064 <sup>ab</sup>	0.997
Strawberry + 5% Maltodextrin	11.09 ± 1.348 <sup>a</sup>	1.767 ± 0.810 <sup>c</sup>	0.487 ± 0.093 <sup>a</sup>	0.997
Strawberry + 5% Pectin	0.000 ± 0.000 <sup>b</sup>	113.5 ± 25.06 <sup>a</sup>	0.260 ± 0.035 <sup>bc</sup>	1.000
Strawberry + 5% Starch	0.540 ± 0.471 <sup>b</sup>	68.24 ± 5.927 <sup>b</sup>	0.180 ± 0.032 <sup>c</sup>	0.999

\*a-c Means with the same superscript letters within a column indicate no significant differences (p<0.05).

Source: author.

Both models fitted well with the rheological experimental data ( $R^2 \geq 0.987$ ). For the strawberry-pectin suspension, the result of zero for the  $\sigma_0$  (initial shear stress) evidences that the Herschel-Bulkley model is not applicable to the data of this fluid. The same can be inferred in relation to the suspension containing starch. All the suspensions revealed pseudoplastic behavior (shear-thinning), with the parameter  $n$  between 0 and 1, and the consistency index (K) being greater than 1. The pseudoplastic (or shear-thinning) behavior is ideal for spreading the suspensions on the conveyor belt, which is crucial for the use of CTD (De Moraes et al., 2013; Gardini et al., 2010). The yield stress and shear-thinning characteristics influence the spreadability of a fluid; flow stops when the operational shear stress is less than the yield stress (Rao, 2007b). This means that the sample's viscosity must be high enough under static conditions to avoid particles sedimentation or inadequate flow and low at the shear rates applied while spreading, to enable appropriate flow conditions under the CTD blade. Other authors also reported similar shear-thinning results for strawberry pulp (Maceiras et al., 2007; Novotná et al., 2018; Yeow et al., 2002).

#### 4.2.2. Strawberries drying kinetics

Figure 22 shows the drying curves of strawberry suspensions in continuous CTD. The drying experiments were performed in duplicate. The graphs show the average moisture content in dry basis, in each drying time, together with the standard deviations, for both replicates.

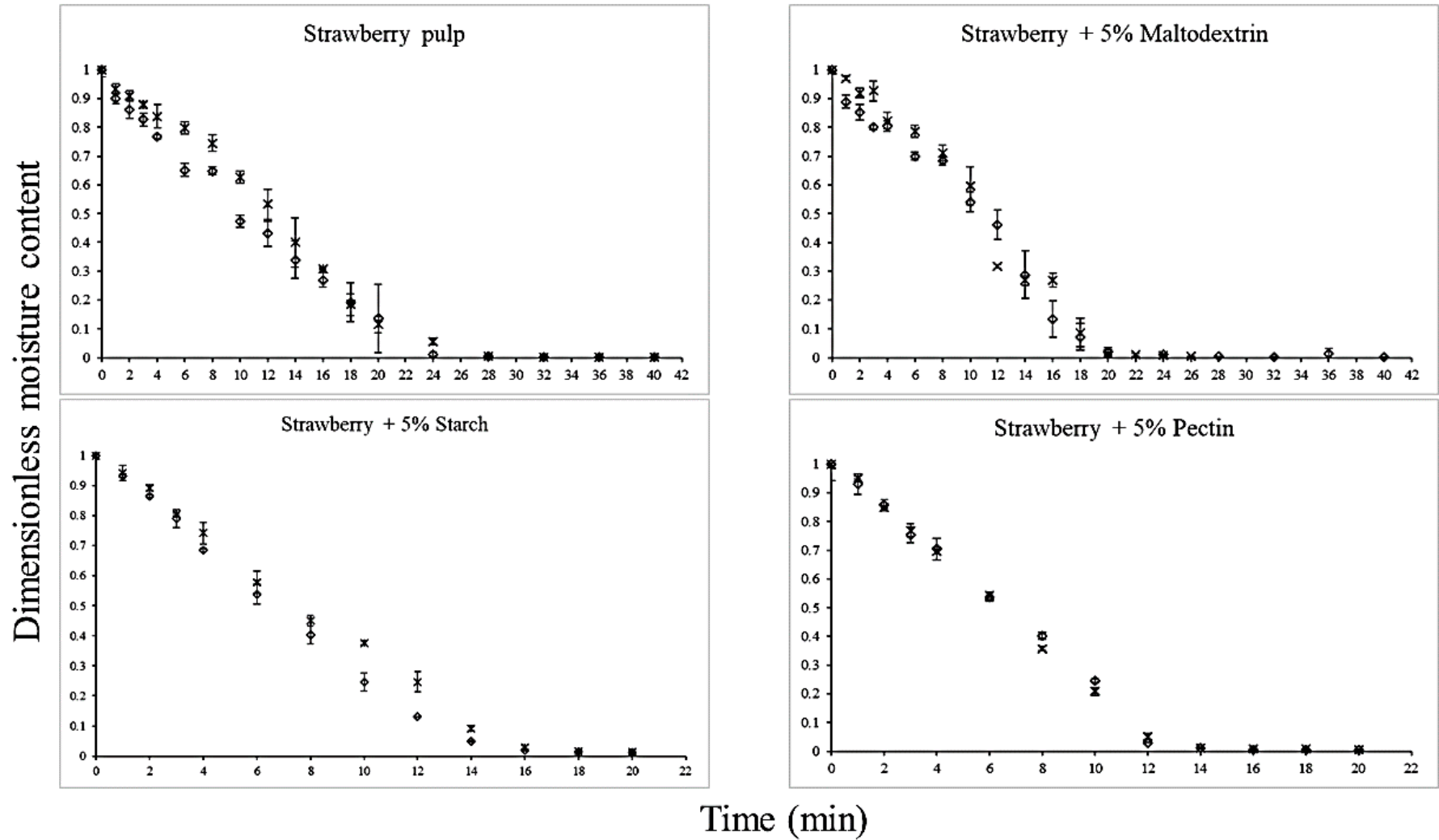


Figure 22 - Strawberry drying curves in continuous CTD.

Source: author.

The drying curves showed that the addition of pectin or starch influenced the drying time of the strawberry suspensions. Strawberry pulp without CA displayed moisture content lower than  $0.03 \text{ g g}^{-1}$  (d.b.) at 40 min of drying, similar to the observed for the pulp with maltodextrin. The addition of pectin and starch reduced the drying time by half (approximately 20 min), considering a final moisture content lower than  $0.10 \text{ g g}^{-1}$  (d.b.). As the speed of the conveyor belt remained unchanged and the viscosities of the strawberry suspensions were different, the product thickness after spreading was also different, which explains the longer drying times when the suspension was less viscous (this will be discussed again in the item 4.2.4, regarding the leathers thickness).

The drying curves showed an initial adaptation period (longer for the strawberry suspension and strawberry with addition of maltodextrin), followed by a period of constant drying rate, and a falling rate drying period at the end of the process. The drying curve of pure strawberry presented a constant rate period that lasted up to 24 min, causing most of the moisture evaporation (95%) and a falling rate period representing only 5% of the evaporated water. Abonyi, Tang & Edwards (1999) evaluated the drying of strawberries with and without the addition of maltodextrin in continuous refractance window, whose operation is identical to that of the continuous CTD equipment used in the present study; they reported the absence of a constant drying rate period. The authors justified this result from the thin layer of product (1 mm). Possible shrinkage and the formation of a hard layer on the material's surface can considerably increase mass transfer resistance and reduction of the drying rate (Geankoplis, 1998).

Table 13 shows the average rate values for each drying time interval in continuous CTD.

Table 13 - Strawberry drying rates in continuous CTD.

<b>Continuous CTD drying rates (g g<sup>-1</sup> min<sup>-1</sup>)</b>				
<b>Time interval</b>	<b>Pure strawberry</b>	<b>Strawberry + 5% Starch</b>	<b>Strawberry + 5% Maltodextrin</b>	<b>Strawberry + 5% Pectin</b>
0.5	0.902 ± 0.260	0.467 ± 0.023	0.526 ± 0.437	0.413 ± 0.066
1.5	0.328 ± 0.109	0.438 ± 0.075	0.325 ± 0.069	0.637 ± 0.203
2.5	0.367 ± 0.027	0.603 ± 0.108	0.392 ± 0.000	0.652 ± 0.056
3.5	0.531 ± 0.149	0.620 ± 0.188	0.754 ± 0.000	0.439 ± 0.155
5	0.422 ± 0.293	0.581 ± 0.077	0.266 ± 0.181	0.571 ± 0.025
7	0.156 ± 0.193	0.490 ± 0.004	0.165 ± 0.150	0.576 ± 0.175
9	0.787 ± 0.220	0.423 ± 0.196	0.483 ± 0.085	0.544 ± 0.034
11	0.369 ± 0.193	0.462 ± 0.063	0.658 ± 0.508	0.657 ± 0.086
13	0.604 ± 0.151	0.446 ± 0.213	0.415 ± 0.334	0.108 ± 0.061
15	0.438 ± 0.095	0.175 ± 0.100	0.355 ± 0.324	0.014 ± 0.002
17	0.541 ± 0.170	0.032 ± 0.020	0.387 ± 0.215	0.004 ± 0.005
19	0.341 ± 0.047	0.009 ± 0.001	0.233 ± 0.055	0.005 ± 0.007
22	0.247 ± 0.126	-	0.015 ± 0.000	-
26	0.079 ± 0.082	-	0.045 ± 0.045	-
30	0.007 ± 0.004	-	0.003 ± 0.000	-
34	0.001 ± 0.000	-	0.002 ± 0.000	-
38	0.000 ± 0.000	-	0.013 ± 0.014	-

Source: author.

Drying rates were higher in the initial time intervals, and this is because, at the beginning of the process, there is less resistance to heat and mass transfer. When the material reaches lower moisture content, more energy is required to evaporate water because of the sorption heat; at the falling rate period the drying rate is controlled by the diffusion mechanism. In general, the pulp without the addition of hydrocolloids exhibited drying at higher rates, due to the lower concentration of total solids in this sample.

#### 4.2.3. Thermographs

The temperature evolutions during strawberry drying are shown in Figure 23. Only the thermographic images of pure strawberry without CA (Figure 23.a.) and strawberry-starch (Figure 23.b.) suspension are presented. However, the drying behavior for the strawberry-maltodextrin and strawberry-pectin can be seen in Appendix B.

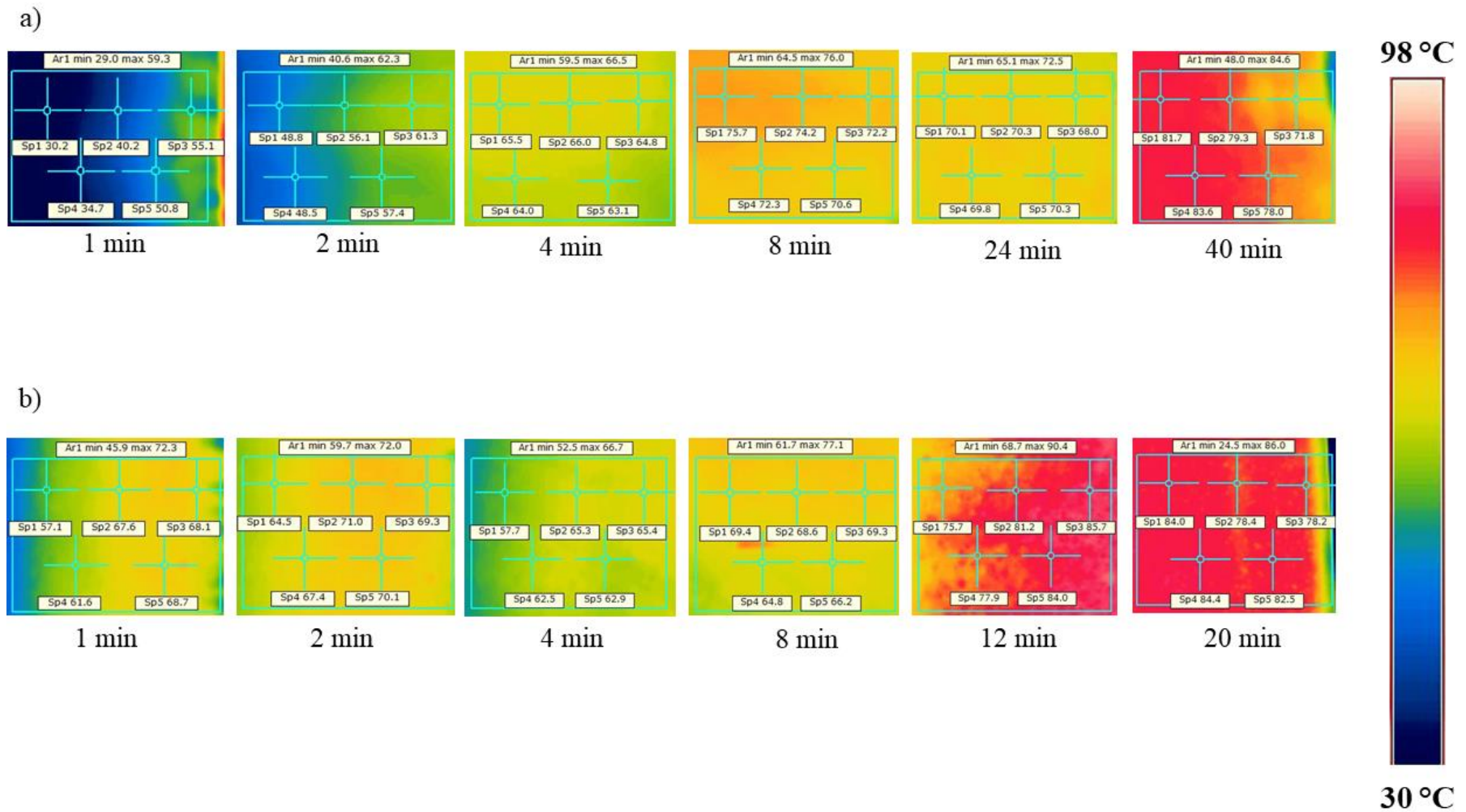


Figure 23 - Thermographic images of drying in continuous CTD of (a) pure strawberry pulp and (b) strawberry-starch suspension.

Source: author.

After spreading, the surface temperatures of the pure strawberry (Figure 23.a) increased from 40 to 70 °C in the first 24 min of drying. At the end of the drying process, in 40 min, temperatures increased to around 80 °C. For strawberry-starch suspension (Figure 23.b), the temperature reached 70 °C in the first 8 min, and at 20 min it was close to 80 °C. Studies in the literature described similar temperature behavior during the CTD process of different fruit pulps (da Silva Simão et al., 2019; Durigon et al., 2017; Frabetti et al., 2018).

Abonyi, Tang & Edwards (1999) performed drying of strawberries and carrots in continuous refractance window equipment and observed that the samples' temperature after spreading increased slightly with the drying time. In the authors' work, the temperature of the raw material during the process varied between 60 and 70 °C. In the present study, the slight increase in the strawberry temperature after spreading was observed between 2 and 4 min of drying in CTD, and then the temperature of the product increased further, remaining between 60 to 70 °C during the rest of the process.

#### 4.2.4. Moisture content, water activity and leather thickness

Table 14 shows the moisture content ( $\text{g g}^{-1}$ , d.b.) and water activity ( $a_w$ ) of the strawberry suspensions and leathers, as well as the thickness of the dehydrated samples.

Table 14 - Initial and final moisture content and water activities of strawberry suspensions processed in continuous CTD.

<b>Samples</b>	<b>Initial moisture content (<math>\text{g g}^{-1}</math> d.b.)</b>	<b>Final moisture content (<math>\text{g g}^{-1}</math> d.b.)</b>	<b>Initial <math>a_w</math></b>	<b>Final <math>a_w</math></b>	<b>Leather thickness (mm)</b>
Strawberry pulp	10.80 ± 0.197 <sup>a</sup>	0.011 ± 0.005 <sup>bc</sup>	0.995 ± 0.003 <sup>a</sup>	0.307 ± 0.064 <sup>b</sup>	0.390 ± 0.081 <sup>a</sup>
Strawberry + 5% Maltodextrin	7.437 ± 0.157 <sup>b</sup>	0.008 ± 0.004 <sup>c</sup>	0.996 ± 0.003 <sup>a</sup>	0.516 ± 0.048 <sup>a</sup>	0.415 ± 0.076 <sup>a</sup>
Strawberry + 5% Starch	7.463 ± 0.324 <sup>b</sup>	0.099 ± 0.021 <sup>a</sup>	0.998 ± 0.002 <sup>a</sup>	0.530 ± 0.031 <sup>a</sup>	0.225 ± 0.019 <sup>b</sup>
Strawberry + 5% Pectin	7.126 ± 0.580 <sup>b</sup>	0.029 ± 0.008 <sup>b</sup>	0.995 ± 0.002 <sup>a</sup>	0.366 ± 0.023 <sup>b</sup>	0.241 ± 0.023 <sup>b</sup>

\*<sup>a-c</sup>Means with the same superscript letters within a column indicate no significant differences ( $p < 0.05$ ).

Source: author.

The strawberry pulp without additives had a higher moisture content of 10.80  $\text{g g}^{-1}$  (d.b.). The addition of CA decreased the moisture content to values between 7.126 and 7.463  $\text{g g}^{-1}$  (d.b.). The pulps'  $a_w$  showed no statistical difference among them, and the values

were similar to those reported in the literature for strawberry pulp (Hammami & René, 1997; Moraga et al., 2004).

Strawberry leather without CA had moisture content lower than  $0.03 \text{ g g}^{-1}$  (d.b.) at 40 min of drying, similar to the observed for the leather with maltodextrin. The samples with addition of starch or pectin exhibited final moisture contents of approximately  $0.10 \text{ g g}^{-1}$  (d.b.) and  $0.03 \text{ g g}^{-1}$  (d.b.), respectively, at 20 min of drying.

All leathers were homogeneous, with thicknesses in the range of 0.2 to 0.4 mm. Concerning the differences in drying times and final product thicknesses (leathers), the rheology of the suspensions can explain this difference. All the samples were spread with a doctor-blade adjusted with a 2 mm gap; however, the pure strawberry pulp and the strawberry-maltodextrin suspension have low viscosity, so the effect of the gravity forces was more noticeable in these samples. As a larger amount of sample flows through the spreader gap, more time is required for complete drying, and this results in leathers with a greater thickness (as shown in Table 14). Additionally, pectin and starch increase the viscoelastic component (storage modulus  $G'$  much greater than the loss modulus  $G''$ ) of the strawberry pulp, ensuring spreading thickness (Rao, 2007a; P. A. Williams & Phillips, 2009).

The  $a_w$  of strawberry leathers was lower than 0.6. While  $a_w$  is lower than 0.6, most foods have stability regarding microbiological growth, and the products can be classified as dehydrated (Labuza, 1980). Nevertheless, the results show that the addition of hydrocolloids influenced the final moisture content and  $a_w$ . Mosquera, Moraga & Martínez-Navarrete, (2012), when drying strawberries by freeze-drying, also reported the same behavior regarding the addition of maltodextrin and gum Arabic. It can be assumed that the molecular structure of each of the additives that made up the suspensions influenced the way water was removed from the samples. Likewise, the interaction between these compounds and the components naturally present in the fruit (carbohydrates, proteins, fibers, etc.) is also related to moisture content variations and final  $a_w$  observed.

It can be seen that the strawberry-starch leather presented higher final moisture content of  $0.099 \text{ g g}^{-1}$  (d.b.) and final water activity of 0.530. Lund (1984) studied starch gelatinization at a temperature above that of gelatinization of starch. He reported that the water diffusion coefficient decreases with increasing temperature. As the starch gelatinizes, it retains additional water, decreasing the water diffusion coefficient with the increase of the moisture content. Thus, at higher temperatures, the reduced diffusion coefficient through the gelatinized layer tends to reduce the drying rate.

#### 4.2.5. Water sorption isotherms

Figure 24 shows the moisture sorption isotherms obtained for the dehydrated strawberry samples. Table 15 presents the parameters of the adjustment to the GAB model.

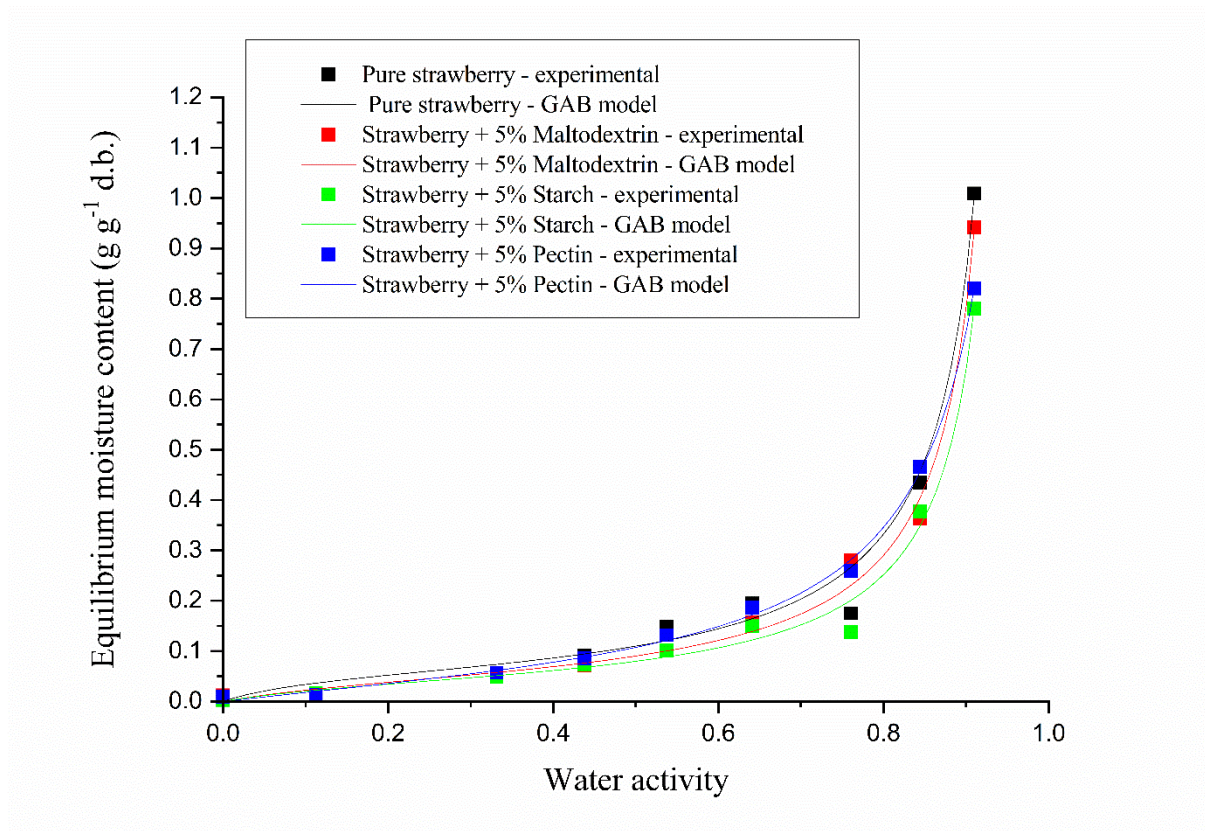


Figure 24 - Sorption isotherm of strawberry leathers produced by CTD.

Source: author.



Table 15 - Estimated parameters of the GAB model for strawberry leathers.

Leather Samples	GAB Parameters				
	$X_0$ (d.b.)	C	$k$	$R^2$	RSS
Pure strawberry	0.058	9.373	1.036	0.978	0.013
Strawberry + 5% Maltodextrin	0.050	5.678	1.040	0.991	0.005
Strawberry + 5% Starch	0.044	6.084	1.037	0.984	0.006
Strawberry + 5% Pectin	0.076	2.391	1.001	0.997	0.001

Source: author.

There were no great differences between the samples at water activities lower than 0.43. The leathers produced with pure strawberry adsorbed more water at  $a_w$  of 0.91, while the presence of hydrocolloids attenuated this behavior, being the strawberry-starch sample the less hygroscopic. The differences in chemical structure and the presence of hydrophilic/hydrophobic groups can explain this result. The molecule of maltodextrin has, for the most part, many ramifications and hydrophilic sites, and can easily adsorb water from the ambient air. This characteristic is also associated with their dextrose equivalency (DE), exhibiting higher hygroscopicity with increased DE (due to shorter chains and consequently more hydrophilic groups). On the other hand, starch is native and not hydrolyzed; thus, it has a lower hygroscopicity (Tonon et al., 2009).

The impact of adding hydrocolloids to sorption isotherms was also reported by several authors when working with fruits (Caparino et al., 2013; da Silva Simão et al., 2019; Mosquera et al., 2012; Telis & Martínez-Navarrete, 2009; Telis & Sobral, 2001; Valenzuela & Aguilera, 2015; Zotarelli et al., 2017).

Experimental data exhibited a typical behavior of sugar-rich foods: a slow increase in equilibrium moisture content in the low  $a_w$  range and a steeper increase in intermediate water activities (0.6) due to the predominant effect of solute-solvent interactions associated with sugar dissolution (Alhamdan & Hassan, 1999; Hubinger et al., 1992; Tsami et al., 1998).

The GAB model represented well the experimental data ( $R^2 \geq 0.978$  and  $RSS \leq 0.013$ ), and the parameters obtained by the model are shown in Table 15. The C value is normally close to 2 for type III isotherms, decreasing with the presence of hydrocolloids (M. S. Rahman, 2006). Higher C values indicate stronger bonds between water molecules and binding sites. The additives' influence on the C parameter can be attributed to the fact that these compounds are

less hygroscopic than the solutes of the strawberry pulp, thus promoting weaker bonds with water. Values of  $k$  close to 1 indicate that water in the monolayer tends to behave like liquid water (M. S. Rahman, 2006).

The  $X_0$  parameter represents the monolayer value and is the minimum moisture content strongly adsorbed on the hydrophilic sites of the product's surface. It is also a measure of the availability of these sites for water sorption in the material (McMinn & Magee, 1997; Quirijns et al., 2005; Rizvi, 2014). Through the evaluation of the  $X_0$  values provided by the GAB model, it can be noticed that CA incorporated into strawberry pulp tend to reduce water adsorption in the monolayer, except for pectin. Below  $X_0$ , there are minimal rates of deteriorative reactions (except oxidation). Thus, at a given temperature, the water activity for safe storage is that corresponding to  $X_0$  or lower. However, it is imperative to consider oxidation when storing a product with moisture content below  $X_0$  (Goula et al., 2008).

In the present study, in order to keep moisture content lower than  $X_0$ , a 33% RH is needed for the storage of pure strawberry, as well as for the starch and maltodextrin-added samples. The strawberry-pectin leather maintains its stability at RH lower than 44%. However, the difference between all the values is minimal due to the small amount of added CA. Leathers are generally marketed in intermediate  $a_w$  (0.31-0.71); thus, the CA reduced the hygroscopicity of the samples at higher RH, being starch and maltodextrin the greater water depressors.

Moraga et al. (2004), in strawberry freeze-drying with the addition of hydrocolloids, also adjusted the GAB model to their data and reported monolayer moisture content ( $X_0$ ) of 0.102 g g<sup>-1</sup> (d.b.) in the sample without additives, and 0.075 and 0.065 g g<sup>-1</sup> (d.b.) with the addition of 1 g g<sup>-1</sup> (w.b.) maltodextrin and gum Arabic, respectively. The  $k$  values of samples presented small variations, all close to 1. A monolayer value of 0.075 g g<sup>-1</sup> (d.b.) has been published for vacuum-microwave dried strawberries with a  $k$  value of 1.078 (de Bruijn & Bórquez, 2014). The results of these authors are close to those found in this study for the GAB model.

#### **4.2.6. Glass transition temperature**

The glass transition temperatures ( $T_g$ ) of the powdered strawberry samples were determined by DSC and the values are presented in Table 16.

Table 16 - T<sub>g</sub> of strawberry powder samples produced in continuous CTD.

RH	Strawberry powders	T <sub>g</sub> (°C)
11%	Strawberry pulp	-11.99
33%		-24.83
11%	Strawberry + 5% Maltodextrin	16.32
33%		-16.31
11%	Strawberry + 5% Starch	-4.32
33%		-13.82
11%	Strawberry + 5% Pectin	27.31
33%		-18.00

Source: author.

As  $a_w$  increased from 0.11 to 0.33, material's T<sub>g</sub> decreased due to the effect of water plasticization. Roos (1987) evaluated the T<sub>g</sub> of freeze-dried strawberries, also reporting that T<sub>g</sub> of humidified samples decreased with increasing moisture content.

T<sub>g</sub> was higher in samples containing additives, mainly pectin. Several authors reported T<sub>g</sub> changes in fruit pulps with hydrocolloids addition. This behavior was reported for strawberry and other fruits, which was explained by the increase of the mixture molecular weight with the presence of these compounds (Mosquera et al., 2012; Telis & Martínez-Navarrete, 2009; Telis & Sobral, 2001). Glass transition temperatures at  $a_w$  of 0.33 were low, and this could mean that strawberry samples were in a rubbery state when they were removed from the CTD process (with  $a_w$  close to 0.30), i.e., at a temperature above their glass transition. However, it was still possible to detach the leathers completely. This observation shows that the adhesion of fruits to drying supports may be related to T<sub>g</sub>, but it is not the only factor influencing this phenomenon, and characteristics such as surface roughness and product composition should also be considered.

#### 4.2.7. Detachment of strawberries leathers

The visual observation of the detachment of the strawberry leathers at the end of drying in continuous CTD can be seen in Figure 25.



Figure 25 - Visual assessment of the detachment of strawberry leathers.

Source: author.

The dry products were removed from the continuous CTD equipment at the end of the heating zone (according to the drying times determined in the kinetics). The temperatures of the samples in this region were close to 80 °C, as can be seen in the thermographs of Figure 25 and Appendix B. Previous tests (not shown) revealed greater difficulty for removal when the products passed through the cooling zone (due to the product's adhesion on the support), even when this zone was at room temperature. The cooling zone is located very close to the fans that promote air circulation during the process, which causes a drastic decrease in the temperature of the material and consequently leads to a brittle film that is strongly adhered to the support. That might occur due to multiple factors, such as the adhesion is higher than cohesion at this temperature or the temperature is approaching  $T_g$  (material tends to be more rigid). According to Adhikari et al. (2001), the physical state of a particular system can be related to its  $T_g$  (which influences stickiness), bulk temperature, and moisture content. Therefore, the strawberry leathers were removed from the continuous CTD equipment at the end of the heating zone, where they were malleable.

All the samples were obtained as films, removed after the initial detachment with the help of a spatula or using an initial withdrawal force with the hands. The removal of products through scraping causes abrasions, wearing out the surface with time and consequently

changing its roughness (item 4.1.1.). This alters the wettability properties of the surface, which may be related to the increase in the adhesion phenomenon.

The pure strawberry pulp film was difficult to remove from Teflon<sup>®</sup>, because it was fragile and with some regions firmly adhered to the support. Identical behavior was observed while removing strawberry-maltodextrin leathers. On the contrary, after the first part was detached, strawberry-starch and strawberry-pectin were removed from the conveyor belt as continuous films, without breaking. The addition of starch and pectin probably reduced the adhesion problem because it increased the film's cohesive force, which increased the tensile strength. High molar mass molecules increase the 3D network formed in the product structure, which results in greater cohesive forces. Consequently, the formed film resists better to the applied force for its removal, which must be greater than the adhesion force between the film and the drying surface (flexible support coated with Teflon<sup>®</sup>) (Otoni et al., 2017; Saha & Bhattacharya, 2010).

Continuous CTD proved to be an adequate drying technique to produce strawberry leathers and the carrier agents, such as starch and pectin, increased its viscosity; consequently, the use of the same spreader gap and same belt velocity led to shorter drying times compared to pure strawberry and strawberry-maltodextrin suspensions. Indeed, the force of gravity caused a larger amount of pure strawberry or strawberry-maltodextrin suspensions to flow through the gap of the spreader, thus increasing the time required for drying. The opposite behavior occurred with the suspensions containing starch or pectin, which due to the higher viscosity, presented a smaller spreading thickness and consequently shorter drying time. In addition, these CA reduced the stickiness of samples on the Teflon<sup>®</sup> belt, promoting the complete removal of the samples. Also, all leather samples presented homogeneous thickness, evidenced by the low standard deviation value between measurements, as well as low moisture content and water activity, indicating that it is an excellent value-added product. Strawberry-CA suspensions resulted in powders with higher glass transition temperatures for the two relative humidity investigated, which allows us to say that these additives collaborate to postpone materials change from brittle to the rubbery or sticky state.

### 4.3. STUDY OF ADDING LOW MOLAR MASS SUGARS IN STARCH-BASED SUSPENSION FOR CTD DRYING

The results of this study are divided into three main topics:

- The starch-based suspensions were characterized. The interaction between the suspensions and the flexible supports (Teflon<sup>®</sup> and Mylar<sup>®</sup>), by means of contact angles, was determined.
- The starch-based films, formed after drying, were characterized in terms of T<sub>g</sub>, thickness, tensile strength and water sorption isotherms, to explain part of the adhesion phenomena due to the formulation.
- Subsequently, the adhesion of the starch-based films was measured using an adaptation of the peel test. The impact of temperature and relative humidity on sample removal was evaluated.

#### 4.3.1. Rheology of the starch-based suspensions

Only the rheological behavior of suspensions with a single sugar in their composition are shown in Figure 26. In Appendix A, the other rheological curves can be evaluated, along with a table containing the shear stress and viscosity values for the shear rates of 11 s<sup>-1</sup>, 23 s<sup>-1</sup> and 101 s<sup>-1</sup>.

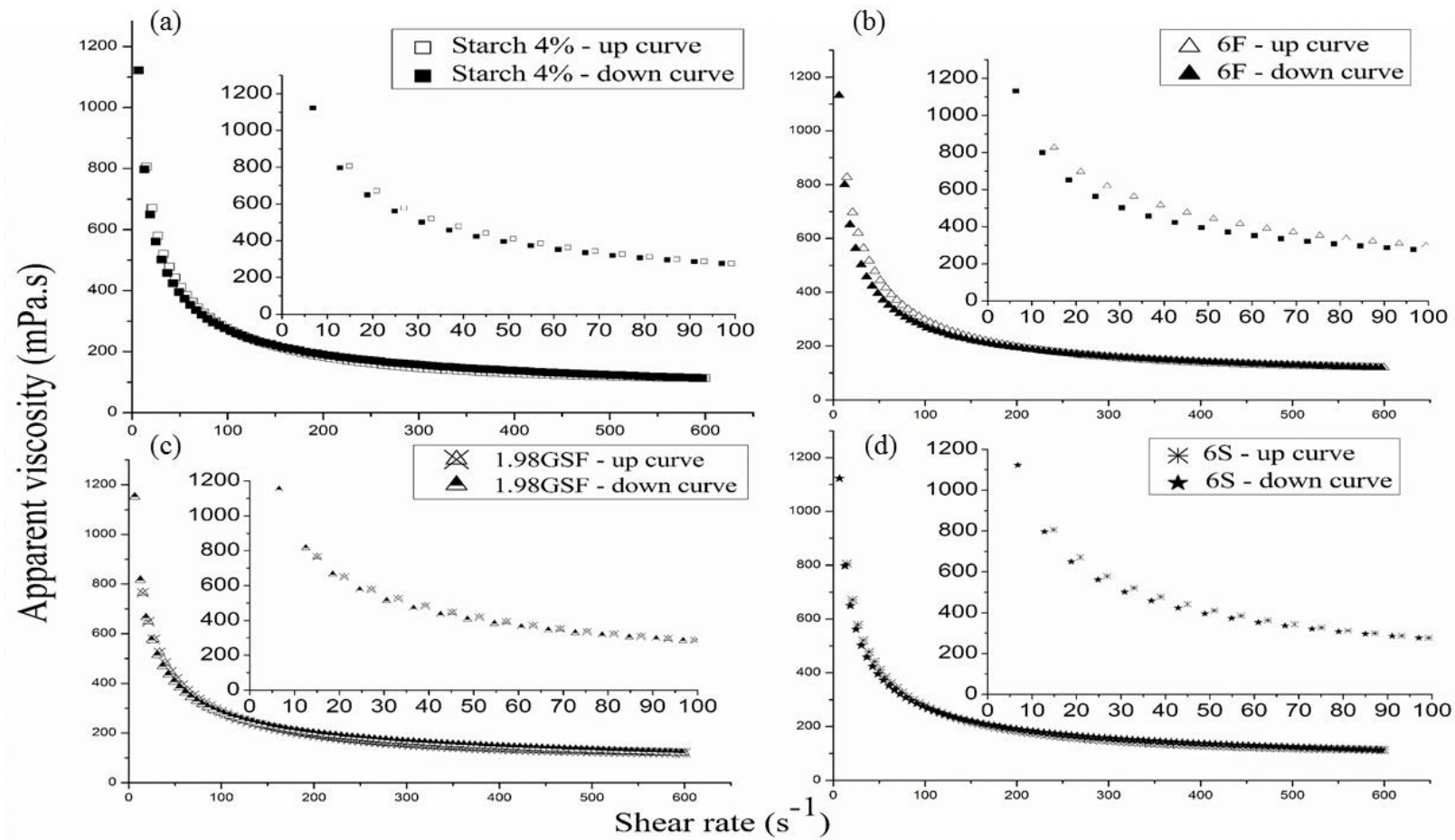


Figure 26 - Viscosity curves of starch-based suspensions (all graphs also show shear rates up to  $100 \text{ s}^{-1}$ , to highlight the decay of the curves): (a) Suspension of cassava starch 4%; (b) Suspension 6F (6 g fructose/100 g suspension); (c) Suspension 1.98GSF (1.98 g glucose + 1.98 g sucrose + 1.98 g fructose/100 g suspension); (d) Suspension 6S (6 g sucrose/100 g suspension).

F: Fructose; G: Glucose; S: Sucrose.

Source: author.

All starch-based suspensions showed non-Newtonian pseudoplastic behavior, as their apparent viscosities decreased with the increase in the shear rate, which is also reported by other authors when carrying out studies with starch suspensions (De Moraes et al., 2013; Peressini et al., 2003; Sajjan & Rao, 1987; A. Singh et al., 2017). The curves obtained were very similar to each other, exhibiting an identical decay, which cannot be attributed to the different compositions of the model solutions. As already mentioned, when discussing the rheology of strawberry suspensions, pseudoplastic behavior is required for CTD spreading.

Table 17 and Table 18 show the adjustment parameters of the shear stress *vs.* shear rate curves to the Ostwald and Herschel-Bulkley model, showing the flow index (*n*) values between 0 and 1 and  $K > 0$ , which confirms the pseudoplasticity of the solutions.

Table 17 - Adjustment of shear stress *vs.* shear rate curves of the starch-based suspensions to the Ostwald model.

<b>Ostwald model (Power Law) Suspensions</b>	<b>K [Pa. s<sup>n</sup>]</b>	<b><i>n</i></b>	<b>R<sup>2</sup></b>
Starch 4%	2.575 ± 0.361 <sup>a</sup>	0.515 ± 0.035 <sup>a</sup>	0.985
3G3F	2.520 ± 0.424 <sup>a</sup>	0.530 ± 0.028 <sup>a</sup>	0.986
6F	2.455 ± 0.460 <sup>a</sup>	0.535 ± 0.021 <sup>a</sup>	0.991
3G3S	2.200 ± 0.198 <sup>a</sup>	0.540 ± 0.014 <sup>a</sup>	0.994
6G	2.640 ± 0.269 <sup>a</sup>	0.525 ± 0.007 <sup>a</sup>	0.994
1.98GSF	2.095 ± 0.163 <sup>a</sup>	0.560 ± 0.014 <sup>a</sup>	0.990
3S3F	2.225 ± 0.049 <sup>a</sup>	0.530 ± 0.000 <sup>a</sup>	0.995
6S	2.470 ± 0.014 <sup>a</sup>	0.525 ± 0.007 <sup>a</sup>	0.989

F: Fructose; G: Glucose; S: Sucrose.

\*Means with the same superscript letters within a column indicate no significant differences ( $p < 0.05$ ).

Source: author.



Table 18 - Adjustment of shear stress vs. shear rate curves of the starch-based suspensions to the Herschel-Bulkley model.

<b>Herschel-Bulkley model Suspensions</b>	<b><math>\sigma_0</math> [Pa]</b>	<b>K</b>	<b><i>n</i></b>	<b>R<sup>2</sup></b>
Starch 4%	13.78 ± 1.181 <sup>ab</sup>	0.370 ± 0.113 <sup>cd</sup>	0.795 ± 0.064 <sup>ab</sup>	0.993
3G3F	14.61 ± 0.460 <sup>a</sup>	0.350 ± 0.127 <sup>d</sup>	0.815 ± 0.064 <sup>a</sup>	0.993
6F	11.95 ± 0.969 <sup>abc</sup>	0.520 ± 0.113 <sup>bcd</sup>	0.750 ± 0.028 <sup>ab</sup>	0.996
3G3S	9.125 ± 0.233 <sup>cd</sup>	0.680 ± 0.057 <sup>abc</sup>	0.710 ± 0.014 <sup>ab</sup>	0.997
6G	11.21 ± 1.280 <sup>bc</sup>	0.695 ± 0.007 <sup>ab</sup>	0.710 ± 0.000 <sup>ab</sup>	0.998
1.98GSF	12.69 ± 0.629 <sup>ab</sup>	0.365 ± 0.007 <sup>d</sup>	0.810 ± 0.000 <sup>a</sup>	0.996
3S3F	7.355 ± 0.233 <sup>d</sup>	0.865 ± 0.006 <sup>a</sup>	0.660 ± 0.014 <sup>b</sup>	0.998
6S	12.72 ± 0.693 <sup>ab</sup>	0.445 ± 0.035 <sup>bcd</sup>	0.770 ± 0.014 <sup>ab</sup>	0.996

F: Fructose; G: Glucose; S: Sucrose.

\*a-d Means with the same superscript letters within a column indicate no significant differences ( $p < 0.05$ ).

Source: author.

Both models fit well with the sample data, with high coefficients of determination ( $R^2$ ). The Herschel-Bulkley model, in particular, had an  $R^2$  greater than 0.99 for all solutions. The adjustment of the Herschel-Bulkley model to the experimental data showed that the suspensions presented an initial shear stress  $\sigma_0$  for the beginning of the flow (Table 18), which indicates the relationship with the samples' sugar composition. The initial shear stress  $\sigma_0$  was lower for suspension 3S3F and higher for suspension 3G3F, although the values are similar for all samples. In general, the addition of sugars increased the parameters of the Herschel-Bulkley model, increasing the consistency (K) and flow ( $n$ ) indexes. However, for  $n$ , there were no significant differences compared to the sample containing only starch. Other authors reported the increase in the initial shear stress  $\sigma_0$  and in the K value with the addition of sugars to starch suspensions (Zhang et al., 2013; Zhou et al., 2017). Abu-Jdayil, Mohameed & Eassa (2004) investigated the effect of sugars on the rheological properties of starch pastes and reported a pseudoplastic behavior for suspensions.

Other studies have attributed the most pronounced decay of the apparent viscosity vs. shear rate curve when adding solids to solutions, either by increasing the starch concentration or by adding hydrocolloids. The decrease in the flow index and the increase in the consistency index are also mentioned in the literature (De Moraes et al., 2013; Sajjan & Rao, 1987).

However, it is necessary to point out that the molar mass of hydrocolloids such as gum Arabic (around  $3.5 \cdot 10^5 \text{ g mol}^{-1}$ ), or the starch itself, is much greater than the molar mass of the sugars added to the model solutions, which significantly influences the rheological behavior of the suspensions. The rheology of the strawberry suspensions (item 4.2.1.) proves that the addition of solids of greater molar mass affects the rheological results more pronouncedly.

#### 4.3.2. Surface tension of the starch-based suspensions

Table 19 displays the surface tensions (T) of the starch-based suspensions without the addition of surfactants and with 0.1% of *Tween* 20.

Table 19 - Surface tension of starch-based suspensions without Tween and with 0.1% Tween 20.

Suspensions	T (mN m <sup>-1</sup> )	
	without <i>Tween</i>	with 0.1% <i>Tween</i> 20
Starch 4%	71.47 ± 1.908 <sup>aA</sup>	70.34 ± 2.738 <sup>aA</sup>
3G3F	69.67 ± 1.493 <sup>aA</sup>	64.72 ± 1.805 <sup>dB</sup>
6F	70.94 ± 1.269 <sup>aA</sup>	69.11 ± 2.087 <sup>abA</sup>
3G3S	70.55 ± 1.443 <sup>aA</sup>	67.78 ± 1.873 <sup>abcA</sup>
6G	66.19 ± 1.435 <sup>bA</sup>	65.92 ± 1.754 <sup>cdA</sup>
1.98GSF	66.68 ± 1.090 <sup>bA</sup>	65.29 ± 1.646 <sup>cdA</sup>
3S3F	65.64 ± 0.494 <sup>bB</sup>	67.76 ± 1.850 <sup>abcA</sup>
6S	65.85 ± 0.565 <sup>bA</sup>	67.20 ± 1.853 <sup>bcdA</sup>

F: Fructose; G: Glucose; S: Sucrose.

\* Means with different superscript capital letters on the line indicate that the values present a significant difference at a 95% confidence level by the Tukey test.

\*\* Means with different superscript lowercase letters in the column indicate that the values present a significant difference at a 95% confidence level by the Tukey test.

Source: author.

The surface tension of the suspension containing 4% starch, without sugars, resulted in a surface tension close to the water ( $72 \text{ mN m}^{-1}$ ). The results presented in Table 19 show that, for some of the suspensions containing sugars, there was a significant statistical difference by the Tukey test in relation to the 4% starch suspension.

For most suspensions, the surface tensions were similar to each other and with no significant statistical difference by the Tukey test, concerning the same sugar composition and the use or not of Tween. These results demonstrate that the addition of this surfactant did not strongly influence the surface tension of the starch-based suspensions, although a trend of lower values can be observed when *Tween* 20 was present (disregarding statistical analyses). *Tween* 20 was added to allow the surface to be wet during the spreading of the suspensions. However, the amount of surfactant added was small, which can explain why the results were not considerably impacted. Also, *Tween* has fast micellization in water, which may be the reason for its higher surface tension (close to the value of water) when present in small amounts in solutions (Kothekar et al., 2007). The presence of surfactants in suspensions can increase their wettability in certain materials, particularly surfaces that have undergone modifications (Fletcher & Nicholls, 2000; Lorentz et al., 2007).

The response surfaces to relate the sugar composition with the surface tension are shown in Figure 27. Table 20 show the adjustment to the quadratic models. The coefficients of the equations with significant influence are highlighted in red.

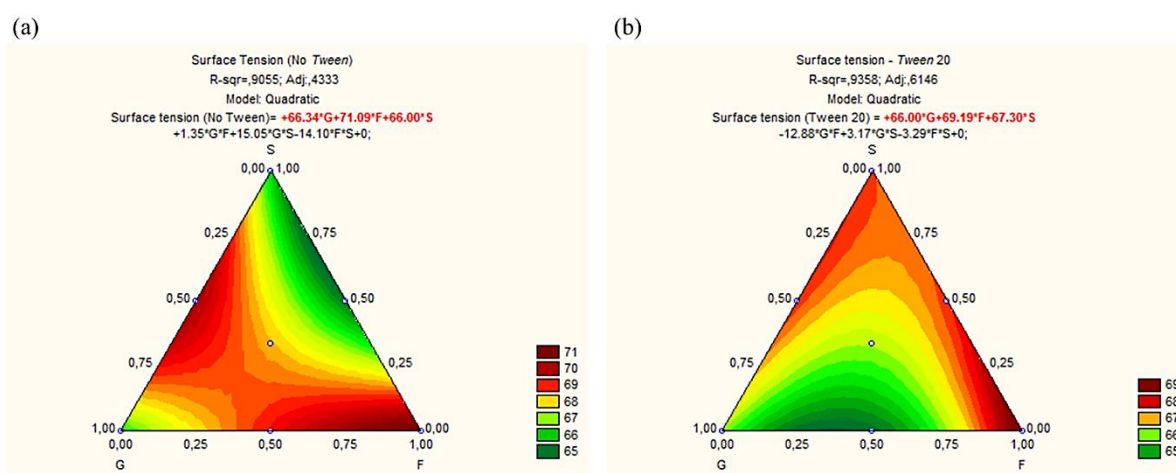


Figure 27 - Response surface plots of surface tension as a function of the sugar composition of starch-based suspensions.

Source: author.

Table 20 - Equations fitted to quadratic models for the surface tension of the starch-based suspensions.

<b>Response Surface tension</b>	<b>Equations fitted to models</b>	<b>R<sup>2</sup> R<sup>2</sup> -adj.</b>
Without <i>Tween</i>	T (No Tween) = $+66.34 \times G + 71.09 \times F + 66.00 \times S + 1.35 \times G \times F$ $+ 15.05 \times G \times S - 14.10 \times F \times S$	0.905; 0.433
<i>Tween</i> 20	T (Tween 20) = $+66.00 \times G + 69.19 \times F + 67.30 \times S - 12.88 \times G \times F$ $+ 3.17 \times G \times S - 3.29 \times F \times S$	0.936; 0.615

Source: author.

Regarding the suspensions containing sugars, the observation of the response surfaces in Figure 27 and the respective data fitted to the quadratic models (Table 20) allow us to say that glucose, fructose and sucrose as individual components had a significant influence in increasing the surface tension results, both without or with *Tween*. Fructose, in particular, showed the highest coefficient in the equations, evidencing the proximity to the surface tension of water due to the hygroscopicity of this sugar.

Oroian et al. (2015) evaluated the surface tension of sucrose, glucose and fructose solutions, using different temperatures and concentrations in water. The results showed that, at ambient temperature (25 °C), changes in concentration of sugar had little influence in the surface tension. For sugar's concentration varying from 0.01 to 0.10 mol L<sup>-1</sup>, values stayed around 37 and 39 mN m<sup>-1</sup>. It can therefore be concluded that the different concentrations of sugars, although a significant difference was found between sugars in the models adjusted to the data, do not have a strong impact on the results of the surface tension at the test temperature (20 °C).

#### 4.3.3. Contact angle between suspension and flexible supports

In order to fully understand the liquid-support interactions, contact angles were determined for the different formulations of starch-based suspensions, both in the original Teflon<sup>®</sup> and Mylar<sup>®</sup> supports and in the Teflon<sup>®</sup> supports with abrasions (R1 and R2). The results are shown in Table 21.

Table 21 - Contact angles between starch-based suspensions on Mylar<sup>®</sup> and Teflon<sup>®</sup> supports.

<b>Suspensions</b>	<b>Starch 4%</b>	<b>3G3F</b>	<b>6F</b>	<b>3G3S</b>	<b>6G</b>	<b>1.98 GSF</b>	<b>3S3F</b>	<b>6S</b>
<b>Supports</b>								
Mylar – original	92.6 ± 3.9 <sup>c,A</sup>	85.1 ± 4.7 <sup>c,CD</sup>	86.2 ± 3.2 <sup>d,BC</sup>	72.9 ± 6.3 <sup>e,G</sup>	80.0 ± 3.8 <sup>e,EF</sup>	79.2 ± 3.3 <sup>d,F</sup>	82.5 ± 6.5 <sup>d,D,E</sup>	88.7 ± 4.2 <sup>d,B</sup>
Teflon <sup>®</sup> - original	99.4 ± 4.1 <sup>b,CD</sup>	99.1 ± 3.7 <sup>a,D</sup>	99.1 ± 2.6 <sup>b,CD</sup>	100.4 ± 1.9 <sup>b,BC</sup>	100.0 ± 2.4 <sup>b,C,D</sup>	102.0 ± 2.2 <sup>a,A,B</sup>	99.5 ± 1.3 <sup>a,CD</sup>	102.9 ± 2.2 <sup>a,A</sup>
Teflon <sup>®</sup> - R1	99.5 ± 2.7 <sup>b,AB</sup>	96.3 ± 3.7 <sup>b,C</sup>	98.7 ± 2.8 <sup>b,B</sup>	101.1 ± 2.9 <sup>b,A</sup>	98.7 ± 1.5 <sup>c,B</sup>	93.3 ± 8.7 <sup>b,D</sup>	94.6 ± 3.7 <sup>b,c,CD</sup>	94.3 ± 1.8 <sup>c,CD</sup>
Teflon <sup>®</sup> – R2	99.6 ± 5.3 <sup>a,BCD</sup>	100.9 ± 4.0 <sup>a,ABC</sup>	98.2 ± 11.8 <sup>a,D</sup>	101.8 ± 3.0 <sup>a,AB</sup>	102.2 ± 1.8 <sup>a,A</sup>	99.7 ± 2.0 <sup>b,C,D</sup>	92.9 ± 2.9 <sup>c,F</sup>	99.9 ± 3.5 <sup>b,ABCD</sup>

F: Fructose; G: Glucose; S: Sucrose.

\* Means with different superscript capital letters on the line indicate that the values present a significant difference at a 95% confidence level by the Tukey test.

\*\* Means with different superscript lowercase letters in the column indicate that the values present a significant difference at a 95% confidence level by the Tukey test.

Source: author.

In general, all the suspensions exhibited greater contact angles when evaluated on Teflon<sup>®</sup> supports, compared to Mylar<sup>®</sup>, which is related to the lower surface energy of Teflon<sup>®</sup>. The literature refers to the greater wettability of a suspension on a certain surface as a determinant for the greater adhesion of the dry product to that surface (Bormashenko et al., 2009; Lam et al., 2002). Contact angle ranged from 72.9 to 92.6° between suspensions and Mylar<sup>®</sup>, evidencing the increase in the dependence of the formulation when liquid and surface have a higher interaction. For Teflon<sup>®</sup> without abrasion, the values were from 99.1 to 102.9°.

However, it is important to stress out that there are difficulties in accurately determining the contact angle between real solutions and surfaces. As explained by Michalski et al. (1999), in real systems, the advancing contact angle (during surface wetting) may be different from the receding contact angle (after the surface is wetted). A general approach may be the rapid measurement of the contact angle of a pure liquid (often water) on a solid surface when the drop is advancing, providing a good estimate of the differences between the surface properties of different solids, especially their hydrophilicity. The same approach was employed for the starch-based suspensions since they mainly consist of water.

When evaluating the wettability of the different suspensions in Teflon<sup>®</sup> without and with abrasions (R1 and R2), it was noted that the support without grooves, with its original roughness and consequently without air pockets (as discussed in item 4.1.1. concerning surface roughness), presented greater contact angles for most suspensions, in comparison to surfaces with higher roughness. These results agree with discussions already available in the literature, which state that the wettability of a solution can be adjusted by changing the roughness of the surface in contact (Dorrer & Rühle, 2009; Miller et al., 1996; Quéré, 2008; Ramiasa et al., 2014). The non-roughened Teflon<sup>®</sup> surface is composed of -CF<sub>2</sub>- bonds fragments forming an inert structure with low surface tension. Therefore, the contact angle of non-roughened Teflon<sup>®</sup> surfaces is above 100°. When the Teflon<sup>®</sup> surface is roughened, the -CF<sub>2</sub>- bonds are broken, and carbon-hydrogen and carbon-oxygen bonds are formed. So, the hydrophobic property of the non-roughened surface (-CF<sub>2</sub>-) becomes gradually more hydrophilic (-CH- or -C-O-), hence the resulting contact angle decrease (Tzeng et al., 1997).

In general, the contact angles were smaller for abraded Teflon<sup>®</sup> with higher roughness (R1). As the Teflon<sup>®</sup> material has a layer of this material adhered to its surface, the greater sandpaper granulometry, responsible for making the roughness R1, may have removed this layer by exposing the fiberglass and increasing the wettability of the samples. Moreover, the interaction between suspensions and supports must consider the sugar composition, as for some

of the starch-based suspensions the contact angles were smaller on Teflon<sup>®</sup> with lower roughness (R2).

The addition of emulsifiers in solutions for the production of films with low molar mass sugars and polysaccharides is common, to improve the stability of the suspension, promote the greater distribution of particles and disperse the material homogeneously for drying. Surfactants (such as *Tween*) added to food suspensions decrease the surface tension of the aqueous phase (reducing the contact angle) and enhance the interaction between the suspension and the support (Kothekar et al., 2007). However, in this work, *Tween* 20 did not significantly change the surface tension of the suspensions due to the small amount added (as discussed in the item 4.3.2.)

The results shown in Table 21 confirm the hypothesis that the wettability of the supports is affected both by the support's roughness and by the composition of the spread suspension. Michalski et al. (1999) studied the adhesive behavior of food emulsions in Teflon<sup>®</sup> and other surface materials. They stated that the surface roughness and fluid rheology and properties are the main factors influencing adhesion. The contact angles found for the suspensions with different sugar concentrations were different, with significant statistical analysis by the Tukey test for most of the compositions.

The response surfaces, to better visualize the influence of the sugar composition of the suspensions on the contact angle, are shown in Figure 28. The data were adjusted to the linear and quadratic models (shown in Table 22). The coefficients of the equations with significant influence are highlighted in red.

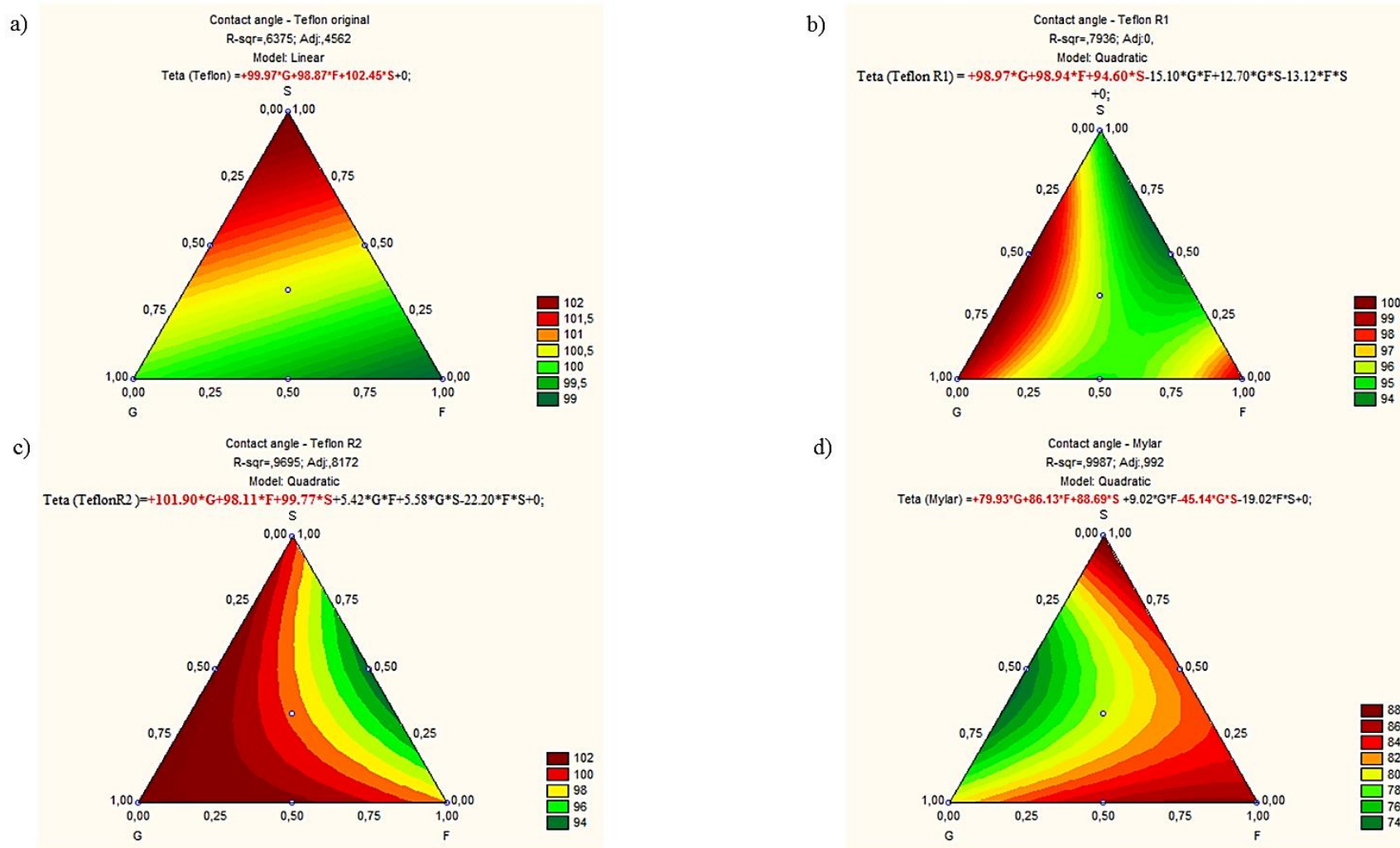


Figure 28 - Response surface plots of contact angle as a function of the sugar composition of the starch-based suspensions, when measured on the supports: (a) original Teflon<sup>®</sup>; (b) Teflon<sup>®</sup> R1; (c) Teflon<sup>®</sup> R2; (d) Mylar<sup>®</sup>.

Source: author.



Table 22 – Equations fitted to linear and quadratic models for the contact angles.

<b>Response Contact angle</b>	<b>Equations fitted to models</b>	<b>R<sup>2</sup> R<sup>2</sup>-adj.</b>
Teflon <sup>®</sup> – original	$\theta$ (Teflon) = <b><math>+100.0 \times G + 98.9 \times F + 102.4 \times S</math></b>	0.637; 0.456
Teflon <sup>®</sup> (R1)	$\theta$ (Teflon R1) = <b><math>+99.0 \times G + 98.9 \times F + 94.6 \times S</math></b> – 15.1 × G × F + 12.7 × G × S – 13.1 × F × S	0.794; 0.000
Teflon <sup>®</sup> (R2)	$\theta$ (TeflonR2) = <b><math>+101.9 \times G + 98.1 \times F + 99.8 \times S</math></b> + 5.4 × G × F + 5.6 × G × S – 22.2 × F × S	0.969; 0.817
Mylar <sup>®</sup>	$\theta$ (Mylar) = <b><math>+79.9 \times G + 86.1 \times F + 88.7 \times S</math></b> + 9.02 × G × F <b><math>- 45.1 \times G \times S - 19.0 \times F \times S</math></b>	0.999; 0.992

Source: author.

Figure 28 shows that the use of Teflon<sup>®</sup> or Mylar<sup>®</sup> was more important in contact angle results than formulation, presenting a distinct behavior with sugar composition. It can be seen through the graphs and the fitted equations that the presence of sugars as single components had a significant influence on the contact angles over all the supports. For the original Teflon<sup>®</sup>, sucrose exhibited a greater coefficient in the adjusted equation, meaning a greater influence of this sugar on the increase of the contact angle. The contact angles over the Teflon<sup>®</sup> R2 support was further increased by the presence of glucose, which is confirmed by the highest coefficient of the fitted equation and also seen in Figure 28.c. In Mylar<sup>®</sup>, Figure 28.d, both the individual sugars and the mixture of sucrose and glucose promoted a lower contact angle, implying greater wettability. Despite the importance of the sugar concentration of the suspensions on the contact angles and wettability, the interaction between the suspensions and the supports must always be carefully considered. The support's roughness implies greater wettability and, consequently, greater product adhesion. During the CTD process, the difficulty of removing dry products from the Teflon<sup>®</sup> support was observed with the natural aging due to its constant use.

#### 4.3.4. Moisture content and water activity of starch-based suspensions and dried materials

Starch-based suspensions and the respective dehydrated products were characterized in terms of moisture content and water activity. Table 23 shows the moisture content (g g<sup>-1</sup>, d.b.) and water activity (a<sub>w</sub>) of the starch-based suspensions and dehydrated films

produced using small-scale CTD heated by electrical resistances (Figure 17). The drying process lasted 40 min.

Table 23 - Moisture content and water activities of starch-based suspensions and films processed in an aluminum plate with internal heating.

Samples	Initial moisture content (g g <sup>-1</sup> , d.b.)	Final moisture content (g g <sup>-1</sup> , d.b.)	Initial a <sub>w</sub>	Final a <sub>w</sub>
Starch 4%	28.04 ± 0.393 <sup>a</sup>	0.103 ± 0.004 <sup>a</sup>	1.000 ± 0.005 <sup>a</sup>	0.440 ± 0.011 <sup>b</sup>
3G3F	10.33 ± 0.544 <sup>b</sup>	0.083 ± 0.001 <sup>c</sup>	0.999 ± 0.002 <sup>ab</sup>	0.381 ± 0.010 <sup>d</sup>
6F	10.65 ± 0.090 <sup>b</sup>	0.089 ± 0.001 <sup>ab</sup>	0.994 ± 0.003 <sup>b</sup>	0.363 ± 0.004 <sup>d</sup>
3G3S	10.22 ± 0.030 <sup>b</sup>	0.093 ± 0.016 <sup>ab</sup>	0.993 ± 0.002 <sup>b</sup>	0.424 ± 0.008 <sup>bc</sup>
6G	10.23 ± 0.077 <sup>b</sup>	0.086 ± 0.001 <sup>c</sup>	0.999 ± 0.006 <sup>ab</sup>	0.406 ± 0.004 <sup>c</sup>
1.98GSF	10.35 ± 0.025 <sup>b</sup>	0.098 ± 0.001 <sup>ab</sup>	0.998 ± 0.002 <sup>ab</sup>	0.434 ± 0.004 <sup>b</sup>
3S3F	10.29 ± 0.050 <sup>b</sup>	0.088 ± 0.003 <sup>ab</sup>	0.996 ± 0.000 <sup>ab</sup>	0.436 ± 0.006 <sup>b</sup>
6S	10.17 ± 0.039 <sup>b</sup>	0.093 ± 0.000 <sup>ab</sup>	0.998 ± 0.001 <sup>ab</sup>	0.485 ± 0.001 <sup>a</sup>

F: Fructose; G: Glucose; S: Sucrose.

\*<sup>a-d</sup>Means with the same superscript letters within a column indicate no significant differences (p<0.05).

Source: author.

Analogously to what was discussed concerning the strawberry suspensions, the starch suspension without added sugars (starch 4%) showed higher initial moisture content due to the lower concentration of total solids. All samples showed identical initial water activity and final water activity lower than 0.6.

All the dehydrated films showed moisture content lower than 0.103 g g<sup>-1</sup>, ensuring a dehydrated film. The incorporation of sugars decreased the final moisture content down to 0.083 g g<sup>-1</sup>, with significant statistical difference compared to the starch 4% film (without sugars). Food products containing sugars have little stability in the dehydrated state at a temperature above the glass transition and can easily absorb water (G. V. Barbosa-Cánovas et al., 2007; Y. Roos, 1993b). This will be seen above in the sorption isotherms results.

#### 4.3.5. Sorption isotherms

Sorption isotherms for the starch-based films are shown in Figure 29.

Temp: 20.2 °C

## DVS Isotherm plots for starch-based films

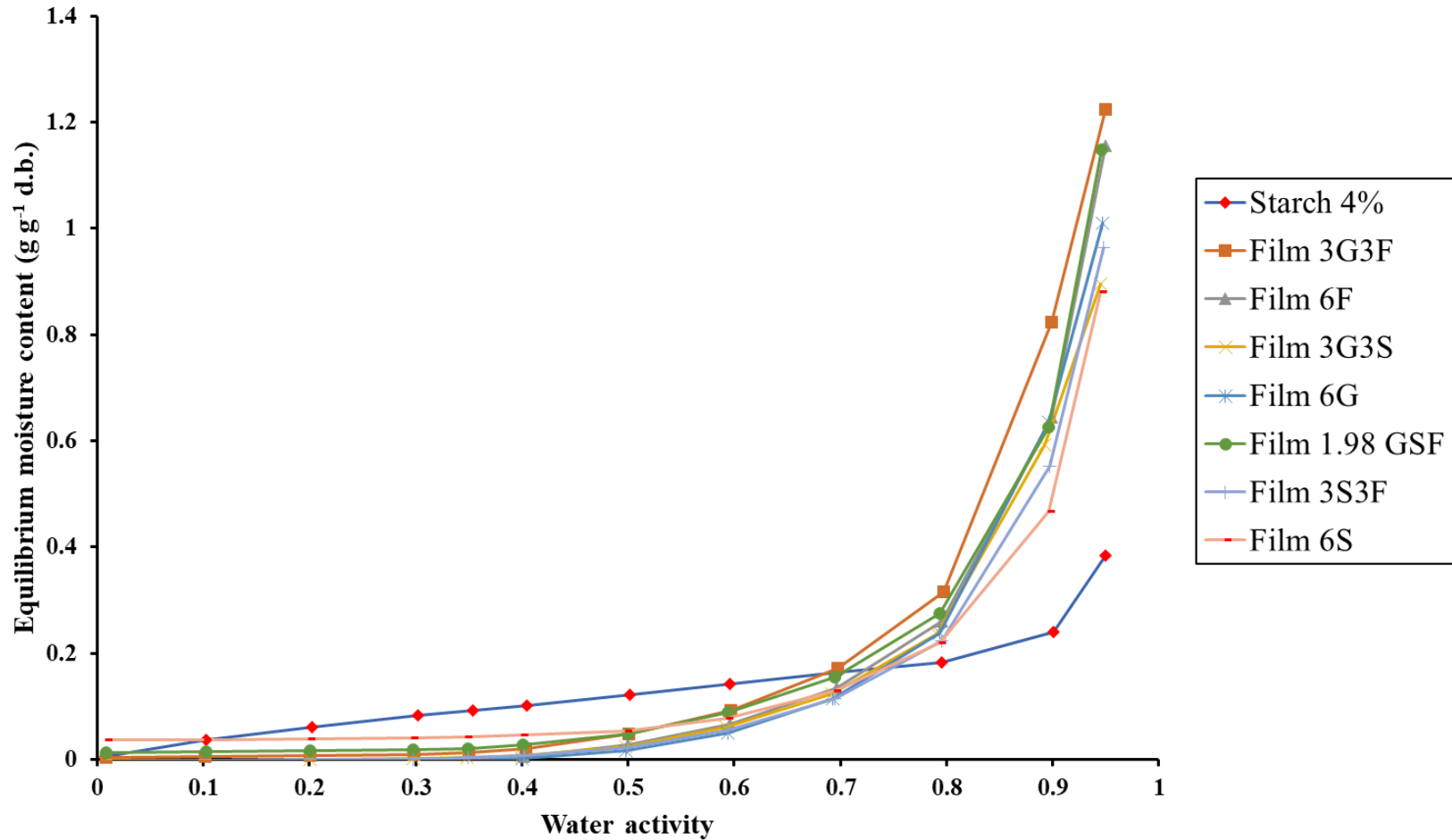


Figure 29 - Isotherms of starch-based films at 20 °C.

Source: author.

In the same way as seen for the strawberry leathers, water sorption by starch-based films with sugar addition was lower at low  $a_w$ , increasing rapidly at higher  $a_w$ . Other authors also reported this behavior while working with starch-solutes films (McMinn & Magee, 1997).

The shape of the moisture sorption isotherm for the starch sample without sugars (starch 4%) was sigmoidal and type II according to Brunauer's classification (Brunauer et al., 1940). Other authors also reported the same behavior for the isotherms of starchy products (Chang et al., 2000; Madrigal et al., 2011; Perdomo et al., 2009). For the most part, biological materials have been reported to present type II isotherms, as manifested by a non-linear, sigmoidal curve. However, the exception is foods rich in soluble components, such as sugars, which exhibit type III behavior, which means low moisture content in low water activities and a marked increase in humidity in high water activities (Saravacos & Stinchfield, 1965).

The starch-based films with different concentrations of sugars displayed type III isotherm characteristics, as previously reported for high-sugar systems (McMinn & Magee, 1997; Saravacos & Stinchfield, 1965), being influenced by the concentration and type of added sugar. Higher levels of plasticizer increased the film's moisture affinity due to the plasticizers' hydrophilicity, which presents hydroxyl groups capable of interacting with water by hydrogen bonds. Notably, low molar mass sugar molecules are small and hygroscopic, presenting a high capacity to interact with starch chains. This interaction can enhance the molecular mobility and increase free volume in the film matrix, which can lead to the higher water affinity of starch-based films with added sugar (Sothornvit & Krochta, 2001).

At low  $a_w$ , the relatively small quantity of sorbed moisture is indicative of the limited sorptive capacity of the sugar fraction. This may be attributed to the sugar present in a crystalline form. Moreover, the slight sigmoidal shape observed in the isotherm's initial section may reflect water sorption on the starch component. However, when approaching the region of high water activity, the sugar component may become a determining factor. This is demonstrated by the more rapid increase in moisture sorption. It can be taken into consideration the sugar-starch and solutes-water interactions existing within the suspensions (McMinn & Magee, 1997).

Saravacos and Stinchfield (1965) reported sigmoidal isotherms type II for high-starch systems. However, with the subsequent addition of glucose, sorption modifications were induced, and the isotherms approached a type III behavior. As explained by these authors, soluble solids (sugars, acids, minerals) adsorb very little water at low water activities, and adsorption is mainly due to the polymeric material (proteins, starch, pectin). As the ambient vapor pressure is increased above the saturated solution's vapor pressure (with specific soluble

solids), adsorption increases considerably, and a solution is formed. The maximum adsorption of foods between 10 °C and 30 °C may be due to a combination of dissolved soluble solids and the expected effect of temperature on the physical adsorption of water vapor by polymers.

Mazza (1982) evaluated the addition of glucose, sucrose, and lactose to freeze-dried potato slices and verified that these compounds caused equilibrium moisture content to decrease in the low and intermediate water activity ranges. With glucose and sucrose addition, the equilibrium moisture content increased significantly in the high relative humidity range, being the consequence of the dissolution of the sugars in the water. In the present work, the increase in equilibrium moisture content was significant in the higher  $a_w$  region, being more related to the presence of glucose and fructose. Moreover, the influence of glucose (film 6G) and sucrose (film 6S) is manifested at a relatively lower water activity, holding the samples moisture content lower to water activity close to 0.8. This may be related to the increased availability of hydroxyl binding sites and a reduction in the bond energies of the sugar structure. Even molecules with the same molecular weight, such as fructose and glucose, can display different moisture sorption curves. The arrangement of the molecules leading to water binding is essential to understand those differences (McMinn & Magee, 1997).

The GAB and BET models were not suitable for describing the sorption of the sugar-added samples, giving inconsistent results of monolayer value. Other models could describe the data; however, the GAB model would provide parameters to give a physical meaning to the results. When observing the curves in Figure 29, the difference in sorption between the films is clear, especially when compared to the sugar-free film (4% starch). The addition of sugars provides more active sites by exposing their hydrophilic hydroxyl groups on which water molecules can be adsorbed (Mali et al., 2005). This may be indicative of greater adhesion when sugars are present. An interesting observation to be pointed out is that the characterization of the suspensions was not strongly influenced by sugars, however, in the dehydrated products, the presence of sugars started to show a distinctly different behavior in relation to the film containing only starch.

#### **4.3.6. Glass transition temperature**

Table 24 shows the glass transition temperatures ( $T_g$ ) of the starch-based films stored at 44% RH, as well as the equilibrium moisture content ( $\text{g g}^{-1}$ , d.b.) of each sample evaluated. Figure 30 presents the DSC scans for the starch-based films with sugar addition. The  $T_g$  of the

starch film without sugars (starch 4%) could not be determined as it was not possible to detect a step in the baseline of the DSC scan.

Table 24 - Glass transition temperatures of starch-based films.

Film Samples	Moisture content (g g <sup>-1</sup> )	T <sub>g</sub> (°C)
3G3F	0.119 ± 0.007 <sup>ab</sup>	-25.84 ± 1.12 <sup>ab</sup>
6F	0.132 ± 0.006 <sup>a</sup>	-27.33 ± 2.52 <sup>a</sup>
3G3S	0.106 ± 0.016 <sup>bc</sup>	-18.09 ± 3.66 <sup>bc</sup>
6G	0.104 ± 0.003 <sup>bc</sup>	-26.34 ± 1.63 <sup>a</sup>
1.98GSF	0.102 ± 0.002 <sup>bc</sup>	-17.75 ± 3.33 <sup>c</sup>
3S3F	0.105 ± 0.007 <sup>bc</sup>	-15.92 ± 1.95 <sup>c</sup>
6S	0.086 ± 0.002 <sup>c</sup>	-19.87 ± 4.24 <sup>abc</sup>

F: Fructose; G: Glucose; S: Sucrose.

\*<sup>a-c</sup>Means with the same superscript letters within a column indicate no significant differences (p<0.05).

Source: author.

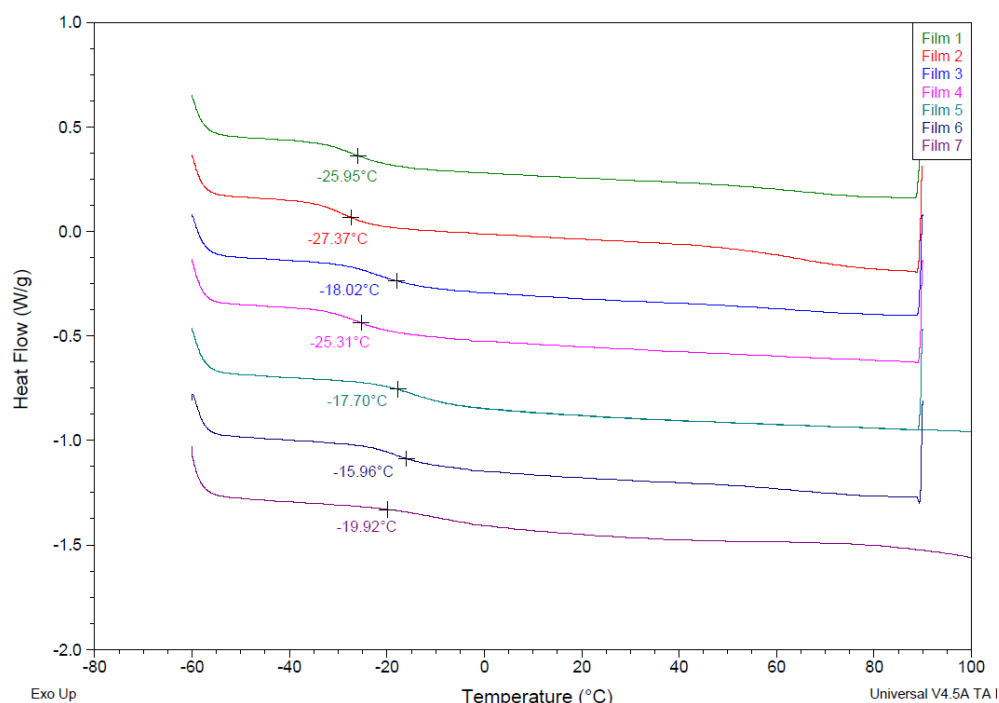


Figure 30 - DSC thermograms.

Film 1: 3G3F; Film 2: 6F; Film 3: 3G3S; Film 4: 6G; Film 5: 1.98GSF; Film 6: 3S3F; Film 7: 6S.

F: Fructose; G: Glucose; S: Sucrose.

Source: author.

As shown in Figure 30, the change of the heat flow that characterizes the T<sub>g</sub> was subtle, but the effect of plasticization by water and low molar mass sugars in reducing T<sub>g</sub> is easily perceived. Generally, the thermograms obtained by DSC show a typical second-order transition, the glass transition of amorphous materials in which a change in the heat flow occurs due to changes in the product's thermal capacity at the phase transition temperature (Goula et al., 2008). However, it is more difficult to determine the T<sub>g</sub> of a sample containing low molecular weight carbohydrates, such as mono and disaccharides, as it occurs over a wider temperature range (Kilburn et al., 2005; S. K. Sharma et al., 2011). Also, the synergistic effect of several components in a film results in broader transitions at T<sub>g</sub>, made this phenomenon more difficult to discern from the baseline (Arvanitoyannis et al., 1997).

The glass transition of thermoplastic starch depends on plasticizer concentration and type, as additives in general (including sugars), water, or polyols. The impact of plasticizers can be relatively complex since many of the substances used to plasticize starch are hydrophilic and may affect the availability and interaction of water with starch (Chaléat et al., 2014; Lourdin et al., 1997). In starch films with glycerol as a plasticizer, some authors could not detect a T<sub>g</sub> when samples were stored above 43% RH and had moisture content close to 0.10 (d.b.) (Anglès & Dufresne, 2000; Moraes, 2013). Chiumarelli and Hubinger (2014) affirmed that the glass transition temperature of cassava starch films with glycerol, carnauba wax, and stearic acid, could not be determined in the thermograms. The authors justified that the T<sub>g</sub> of carbohydrate films with plasticizer is challenging to be determined by DSC analysis because the change of heat capacity is very low in the glass transition (Chiumarelli & Hubinger, 2014; Ghanbarzadeh et al., 2010; Ghanbarzadeh & Almasi, 2011).

From data reported by the literature, the T<sub>g</sub> of cassava starch films can vary from 50 to 90 °C (moisture content between 0.10 to 0.23 g g<sup>-1</sup>, d.b.) (Chang et al., 2000; Perdomo et al., 2009). Aichayawanich et al. (2011) reported a T<sub>g</sub> of 144.70 °C for cassava starch at 0.086 g g<sup>-1</sup> (d.b.) moisture content and attributed the higher temperature to the different botanical origin of cassava. It is well known that plasticizers such as sugars and other low molar mass compounds have in their pure form a low glass transition temperature. Therefore, in general, the presence of these components tends to decrease the T<sub>g</sub> of the solution in which they are added. The lowest T<sub>g</sub> corresponds to the glass transition of a matrix formed by sugars and water (Telis & Sobral, 2002). Also, concerning the results obtained by this work and from the free volume theory, it can be stated that the plasticizers with lower T<sub>g</sub> are more efficient in promoting chain mobility and thus reducing the T<sub>g</sub> of the plasticized system.

Figure 31 shows the response surface for Tg, based on the fructose, glucose, and sucrose composition of the starch-based films. The quadratic equation fitted to the Tg values is displayed in Table 25, and the coefficients of the equations with significant influence are highlighted in red.

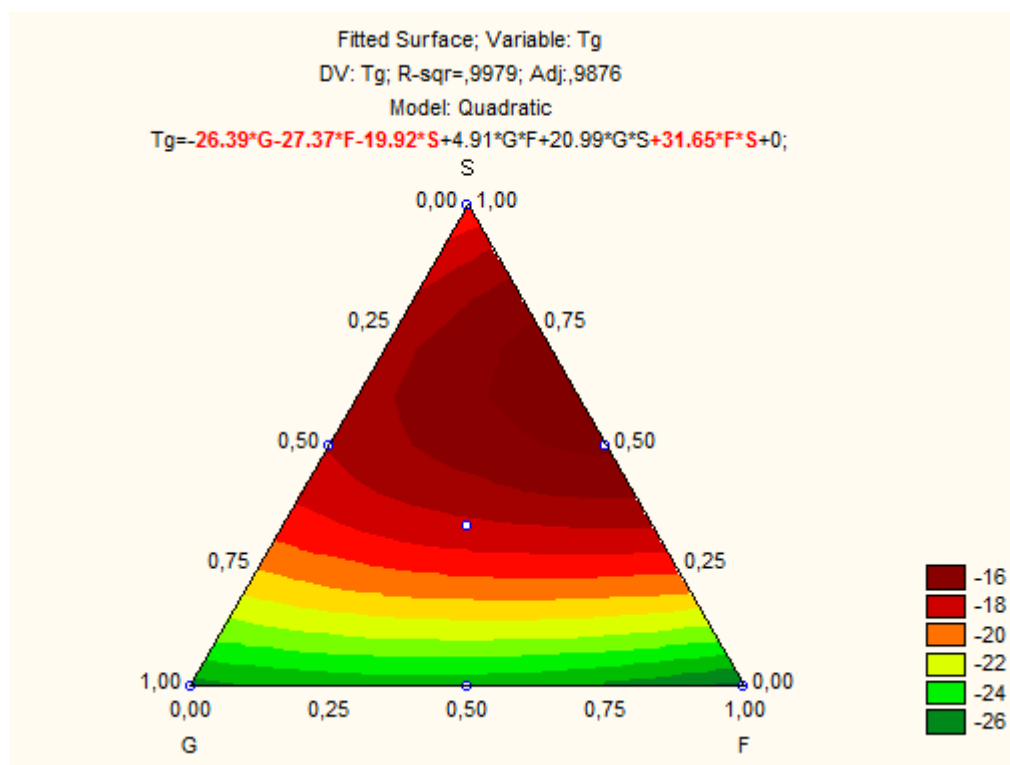


Figure 31 - Response surface plots of Tg as a function of the sugar composition of the starch-based films.

Source: author.

Table 25 - Equation fitted to the quadratic model for the Tg of starch-based films with added sugar.

Response Tg	Equations fitted to models	R <sup>2</sup> R <sup>2</sup> - adj.
	$Tg =$ $-26.39 \times G - 27.37 \times F - 19.92 \times S + 4.91 \times G \times F$ $+ 20.99 \times G \times S$	0.998; 0.988

Source: author.

As seen in the response surface plots and through the evaluation of the coefficients of the adjusted equation shown in Table 25, the presence of individual sugars had a plasticizing effect in decreasing the glass transition temperature, in comparison to the net cassava starch film (through the observation of the literature data).



The presence of sucrose affected less the decay of Tg. Indeed, the molar mass of the sucrose molecule ( $342.8 \text{ g mol}^{-1}$ ) is greater than that of glucose and fructose (similar molar masses,  $180 \text{ g mol}^{-1}$ ), which explains the higher Tg of the film with added sucrose, since the greater the molar mass of a compound, the greater its Tg. Fructose was the sugar that most impacted the lower value of Tg. Fructose is the most hygroscopic monosaccharide and absorbs more water than glucose, even though the two structures have similar molar masses. This is due to the organization of the fructose molecule, which allows greater availability of hydroxyl groups. Also, when pure, fructose has lower Tg, decreasing the final Tg of the mixture in which it is found, that is, of the film with its addition (BeMiller & Huber, 2008). The combination of fructose and sucrose also has a significant positive effect in increasing Tg (as evidenced by the positive coefficient of the adjusted equation, displayed in Table 25).

The decrease in Tg with the presence of sugars as plasticizers has been widely reported in the literature. Teixeira et al. (2007) performed DMTA measurements on mixtures of cassava starch/glycerol/sugars and observed that the starch system presented two main transitions. In a sample with 2% (wet basis, w.b.) of fructose (along with 50% of starch, 30% of glycerol, and 18% of water), a subtle transition temperature was seen in  $-22 \text{ }^{\circ}\text{C}$  (attributed to a fructose-rich phase) with Tg at  $8 \text{ }^{\circ}\text{C}$ . When glycerol was excluded from the composition and a mixture of cassava starch/sugar (50% of starch, 25% of water, and 8.3% of glucose, fructose, and sucrose) was evaluated, the transition dropped to  $-55 \text{ }^{\circ}\text{C}$  with Tg at  $35 \text{ }^{\circ}\text{C}$ . The authors explained these differences in temperature between the two transitions as a consequence of the lower degree of crystallinity of the samples, presenting a more heterogeneous structure due to sugar plasticization. Also applying DMTA, Nguyen Vu and Lumdubwong (2016) found two Tg values for a cassava starch film plasticized by glycerol (5% of starch and 33% of glycerol; moisture content of  $0.20 \text{ g g}^{-1}$ , d.b.); one value corresponding to the plasticizer rich-phase ( $-56.9 \text{ }^{\circ}\text{C}$ ) and the other to the starch rich-phase of ( $13.6 \text{ }^{\circ}\text{C}$ ).

Valenzuela and Aguilera (2015) worked with apple leathers and studied the addition of additives to increase (glucose) and to decrease (maltodextrin) the stickiness of the products. The authors found a Tg value of  $-22.06 \text{ }^{\circ}\text{C}$  for the pure apple leather, explained by its high amounts of monosaccharides, which exhibit low Tg values and sticky points. The sample containing 5% glucose and stored at 44% RH presented a Tg of  $-26.97 \text{ }^{\circ}\text{C}$ , due to glucose plasticization. When 10% maltodextrin was added, and the leathers were stored at 33% RH, the Tg was  $-11.87 \text{ }^{\circ}\text{C}$ , since Tg increases with molecular weight. A similar result was obtained in the present study, where the addition of maltodextrin in the strawberry leather increased considerably the Tg of the product.

The Tg of starch-based nanocomposite films (SNF) with low molecular mass sugars (fructose, glucose, and sucrose) and glycerol as co-plasticizers was determined for 10% and 20% sugar content. The glass transition values of the films with sugars were lower than that of the control film (SNF). For the films with 10% sugar, the Tg values ranged from  $-5.1$  °C for control to  $-11.6$  °C for the films with glucose addition. The increase of sugar content from 10% to 20% decreased the samples' Tg from  $-7.5$  °C to  $-8.0$  °C (sucrose),  $-8.4$  °C to  $-10.2$  °C (fructose), and  $-11.6$  °C to  $-14.2$  °C (glucose). As a consequence of the similarity of structure, starch has a preference for interacting with sugars, and the intermolecular hydrogen bond of starch is easily broken, resulting in lower Tg (Gao et al., 2019).

#### 4.3.7. Mechanical tests and thickness of the starch-based films

Table 26 displays the thickness and tensile strength results for the starch-based films produced by CTD heated with electrical resistances (Figure 17). The films were stored in a desiccator at 44% RH and presented average moisture content of 10% (moisture content of each film is display in Table 24).

Table 26 – Thicknesses and tensile strength of the starch-based films.

Film Samples	Thickness ( $\mu\text{m}$ )	Tensile strength at peak (MPa)
3G3F	$261 \pm 0.055^{\text{ab}}$	$0.045 \pm 0.020^{\text{c}}$
6F	$231 \pm 0.043^{\text{b}}$	$0.022 \pm 0.003^{\text{c}}$
3G3S	$259 \pm 0.060^{\text{ab}}$	$0.066 \pm 0.007^{\text{c}}$
6G	$353 \pm 0.143^{\text{a}}$	$0.028 \pm 0.007^{\text{c}}$
1.98GSF	$310 \pm 0.096^{\text{ab}}$	$0.149 \pm 0.049^{\text{b}}$
3S3F	$291 \pm 0.056^{\text{ab}}$	$0.040 \pm 0.018^{\text{c}}$
6S	$298 \pm 0.096^{\text{ab}}$	$0.252 \pm 0.044^{\text{a}}$

F: Fructose; G: Glucose; S: Sucrose.

\*<sup>a-c</sup>Means with the same superscript letters within a column indicate no significant differences ( $p < 0.05$ ).

Source: author.

The thicknesses of the starch-based films varied from 231 to 353  $\mu\text{m}$ . The samples' moisture content when the measurements were made impacted the results, since starch and sugars are hygroscopic compounds that can easily absorb water, becoming thicker.

Gutiérrez et al., (2015) reported thickness of 160  $\mu\text{m}$  for cassava starch films (produced from a film-forming solution containing 2% w/v of starch and 1.9% w/v of glycerol). In general, the addition of molecules (as sugars, in this study) into suspensions before the film

formation produces starch granules with greater molar volume, increasing thickness (Basiak et al., 2017).

Although the starch-based suspensions were capable of forming films, some of them were more difficult to handle due to the sugar's amount in the formulation. The film 6G (starch-based film with 6% of glucose) presented a greater thickness when compared to other samples. It was opaque and brittle, making it difficult to measure the thickness uniformly, as it presented regions with heterogeneities. This heterogeneity can be attested by the most significant standard deviation in the thickness of this film. The greater the thickness, the more opaque the films appear (Basiak et al., 2017). The visual evaluation of the films will be discussed in more detail below (item 4.3.9.).

The addition of a plasticizer to a starch-based suspension increases the inter-chain spacing (greater free volume), reducing direct interactions between the starch chains. This promotes greater mobility of the starch chain, leading to a lower Tg and more malleable material, with consequent lower tensile strength (Chaléat et al., 2014). Moreover, plasticizers with lower molecular weight can produce more film plasticization due to higher molecular contents (Cuq et al., 1997).

All starch-sugar films broke by tearing, not showing a total and quick break. The increased presence of water and sugars can change the breaking mechanism from a rapid brittle fracture at low strains, to a slow plastic fracture (tearing) (Nicholls et al., 1995). This behavior is strongly dependent on thickness: for the same plasticizer concentration, very thin films appear more plasticized and stickier while thicker films appear brittle. Even with the difficulty of handling some of the films, the tensile tests could be performed on all samples. Other authors found higher values of the tensile strength (TS) for starch-based films (ranging between 1.5 to 10 MPa). However, the type of starch used in the formulation of the film-forming suspensions influence these results, as well as the addition of compounds (such as fibers) with the capacity of reinforcing the films (De Moraes et al., 2013; Funke et al., 1998; Gutiérrez et al., 2015; Müller et al., 2009; Torres et al., 2011). Travalini et al. (2019), for instance, showed an increase in tensile strength of cassava starch from 4.8 MPa to 6.6 MPa, when lignocellulose nanofibers were added to the films. The mechanical properties of films are dependent on the polymer chain (starch) and its interactions, thickness, moisture content at the storage RH, as plasticizers and additives content (Arvanitoyannis et al., 1997; Basiak et al., 2017; Cuq et al., 1996).

Figure 32 presents the response surfaces relating the composition of sugars to the thickness and tensile strength values, adjusted to the linear model. The equations are shown in Table 27. The coefficients of the equations with significant influence are highlighted in red.

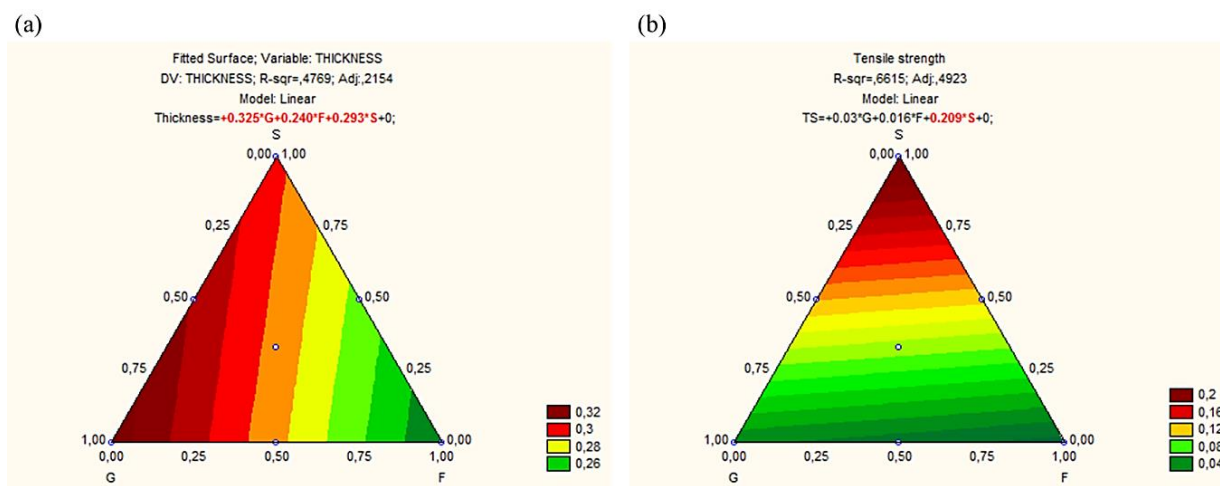


Figure 32 - Response surface plot of (a) thickness and (b) tensile strength as a function of the sugar composition of the starch-based films.

Source: author.

Table 27 - Equation fitted to the linear model for the thickness and tensile strength of the starch-based films with added sugar.

Response	Equations fitted to models	R <sup>2</sup> R <sup>2</sup> - adj.
Thickness	Thickness = <b><math>+0.325 \times G + 0.240 \times F + 0.293 \times S</math></b>	0.477; 0.215
Tensile Strength	TS= $+0.030 \times G + 0.016 \times F + 0.209 \times S$	0.661; 0.492

Source: author.

The response surfaces and the coefficients of the adjusted equations show that glucose, fructose and sucrose, individually, had an influence on the increase in thickness, with glucose being the sugar with the greatest impact on the greatest thickness. On the other hand, only sucrose had a significant influence on the increase in tensile strength. However, only the linear model showed significance when representing the data, and the R<sup>2</sup> and the R<sup>2</sup> - adj. were low.

Although all the starch-based films with added sugar presented low tension strength due to plasticization, the presence of sucrose helped to reinforce the films, compared to glucose and fructose, exhibiting a higher maximum load and consequently higher tensile strength. Likewise, when fructose, glucose, or sucrose were added to starch-based nanocomposite films (SNF), TS decreased in the order of control (without sugar) > film with sucrose > film with fructose > film with glucose. On the contrary, when glucose was added, the tensile strength

decreased up to 46%, from 3.23 MPa (control film) to 1.73 MPa (Gao et al., 2019). The authors' explained that the addition of sugars increased the competitive reactions between the starch granules and inhibited the formation of intercalated structures, leading to a decrease in the TS of the films. The reduction in the crystallinity indices should also be considered. The work stated that sugars had a good plasticization effect, and the addition of those compounds reduced the cohesive force of starch granules and enhanced the films' flexibility.

In glucose, fructose, and sucrose, hydroxyl groups are also present, explaining the low tensile strength values in films. In this manner, it can be concluded that the mechanical properties of films are largely associated with the distribution and density of intermolecular and intra-molecular interactions, depending on the arrangements and orientation of polymer chains in the network (Chambi & Grosso, 2006).

#### **4.3.8. Evaluation of the detachment of starch-based films**

Table 28 shows the maximum and average load (N) to detach the starch-based films from the Teflon<sup>®</sup> support and the Teflon<sup>®</sup> supports with abrasions, right after drying in small-scale CTD with water circulation (represented in Figure 15), at 98 °C for 50 min. The results represent the average of at least three repetitions. Table 29 presents the values of moisture content ( $\text{g g}^{-1}$ , d.b.) and water activity measured for the films produced after analysis using Teflon<sup>®</sup>.

Table 30 presents the maximum and average load (N) to detach the starch-based films from Mylar<sup>®</sup> support. In at least one of the repetitions, the film samples dried over Mylar<sup>®</sup> broke during the detachment essays, so the force result is the maximum force obtained before the break. Table 31 presents the values of moisture content ( $\text{g g}^{-1}$ , d.b.) and water activity of the films dried over Mylar<sup>®</sup>.

Table 28- Maximum and average load (N) for the detachment of starch-based films from Teflon® support.

Film Samples Support	Maximum load (N)			Average load (N)		
	Original Teflon®	Teflon® - abrasions R1	Teflon® - abrasions R2	Original Teflon®	Teflon® - abrasions R1	Teflon® - abrasions R2
3G3F	0.124 ± 0.019 <sup>bcB</sup>	0.193 ± 0.041 <sup>bcdA</sup>	0.130 ± 0.008 <sup>abAB</sup>	0.074 ± 0.021 <sup>abA</sup>	0.109 ± 0.032 <sup>bcdA</sup>	0.082 ± 0.001 <sup>aA</sup>
6F	0.082 ± 0.004 <sup>cB</sup>	0.149 ± 0.023 <sup>bcdA</sup>	0.076 ± 0.006 <sup>bB</sup>	0.060 ± 0.008 <sup>bAB</sup>	0.080 ± 0.016 <sup>bcdA</sup>	0.048 ± 0.009 <sup>bB</sup>
3G3S	0.126 ± 0.027 <sup>bcA</sup>	0.116 ± 0.017 <sup>dA</sup>	0.093 ± 0.017 <sup>abA</sup>	0.078 ± 0.013 <sup>abA</sup>	0.076 ± 0.010 <sup>dA</sup>	0.066 ± 0.017 <sup>abA</sup>
6G	0.122 ± 0.006 <sup>bcA</sup>	0.132 ± 0.027 <sup>cdA</sup>	0.103 ± 0.023 <sup>abA</sup>	0.072 ± 0.010 <sup>abA</sup>	0.079 ± 0.008 <sup>bcA</sup>	0.060 ± 0.004 <sup>abA</sup>
1.98GSF	0.092 ± 0.021 <sup>cB</sup>	0.220 ± 0.031 <sup>bcA</sup>	0.109 ± 0.017 <sup>abB</sup>	0.060 ± 0.004 <sup>bB</sup>	0.102 ± 0.023 <sup>bcA</sup>	0.073 ± 0.010 <sup>abAB</sup>
3S3F	0.278 ± 0.114 <sup>abAB</sup>	0.318 ± 0.041 <sup>aA</sup>	0.107 ± 0.027 <sup>abB</sup>	0.125 ± 0.042 <sup>abAB</sup>	0.162 ± 0.033 <sup>aA</sup>	0.063 ± 0.005 <sup>abB</sup>
6S	0.369 ± 0.119 <sup>aA</sup>	0.234 ± 0.039 <sup>abAB</sup>	0.137 ± 0.031 <sup>abB</sup>	0.137 ± 0.047 <sup>aA</sup>	0.110 ± 0.019 <sup>abA</sup>	0.067 ± 0.006 <sup>abA</sup>

F: Fructose; G: Glucose; S: Sucrose.

\* Means with different superscript capital letters on the line indicate that the values present a significant difference at a 95% confidence level by the Tukey test.

\*\* Means with different superscript lowercase letters in the column indicate that the values present a significant difference at a 95% confidence level by the Tukey test.

Source: author.

Table 29 - Moisture content and water activity of starch-based films produced by small-scale CTD with water circulation using Teflon® support.

Film Samples Support	Moisture content (g g <sup>-1</sup> d.b.)			a <sub>w</sub>		
	Original Teflon®	Teflon® - abrasions R1	Teflon® - abrasions R2	Original Teflon®	Teflon® - abrasions R1	Teflon® - abrasions R2
3G3F	0.165 ± 0.009 <sup>abcA</sup>	0.183 ± 0.047 <sup>bA</sup>	0.124 ± 0.026 <sup>bA</sup>	0.558 ± 0.002 <sup>aA</sup>	0.588 ± 0.081 <sup>aA</sup>	0.449 ± 0.047 <sup>bA</sup>
6F	0.109 ± 0.012 <sup>cA</sup>	0.168 ± 0.023 <sup>bA</sup>	0.146 ± 0.021 <sup>bA</sup>	0.358 ± 0.028 <sup>bA</sup>	0.531 ± 0.047 <sup>aA</sup>	0.449 ± 0.049 <sup>bA</sup>
3G3F	0.118 ± 0.008 <sup>bcA</sup>	0.164 ± 0.017 <sup>bA</sup>	0.122 ± 0.017 <sup>bA</sup>	0.507 ± 0.021 <sup>aA</sup>	0.607 ± 0.028 <sup>aA</sup>	0.515 ± 0.041 <sup>bA</sup>
6G	0.156 ± 0.020 <sup>bcA</sup>	0.186 ± 0.030 <sup>bA</sup>	0.191 ± 0.035 <sup>abA</sup>	0.617 ± 0.047 <sup>aA</sup>	0.591 ± 0.052 <sup>aA</sup>	0.598 ± 0.054 <sup>abA</sup>
1.98GSF	0.187 ± 0.039 <sup>abB</sup>	0.329 ± 0.012 <sup>aA</sup>	0.195 ± 0.016 <sup>abB</sup>	0.627 ± 0.053 <sup>aA</sup>	0.734 ± 0.022 <sup>aA</sup>	0.619 ± 0.042 <sup>abA</sup>
3S3F	0.128 ± 0.022 <sup>bcA</sup>	0.186 ± 0.034 <sup>bA</sup>	0.149 ± 0.010 <sup>bA</sup>	0.503 ± 0.052 <sup>abB</sup>	0.621 ± 0.065 <sup>aA</sup>	0.541 ± 0.023 <sup>abA</sup>
6S	0.231 ± 0.006 <sup>aA</sup>	0.277 ± 0.056 <sup>abA</sup>	0.269 ± 0.045 <sup>aA</sup>	0.570 ± 0.022 <sup>aA</sup>	0.722 ± 0.056 <sup>aA</sup>	0.697 ± 0.027 <sup>aA</sup>

F: Fructose; G: Glucose; S: Sucrose.

\* Means with different superscript capital letters on the line indicate that the values present a significant difference at a 95% confidence level by the Tukey test.

\*\* Means with different superscript lowercase letters in the column indicate that the values present a significant difference at a 95% confidence level by the Tukey test.

Source: author.

Table 30 – Maximum and average load (N) for the detachment of starch-based films from Mylar® support.

Film Samples	Support	Mylar®	
		Maximum load (N)	Average load (N)
3G3F		0.292 ± 0.080 <sup>cd</sup>	0.080 ± 0.102 <sup>cd</sup>
6F		0.234 ± 0.096 <sup>d</sup>	0.107 ± 0.036 <sup>d</sup>
3G3S		0.530 ± 0.097 <sup>bcd</sup>	0.209 ± 0.017 <sup>bcd</sup>
6G		0.462 ± 0.054 <sup>bcd</sup>	0.269 ± 0.029 <sup>bcd</sup>
1.98GSF		0.642 ± 0.116 <sup>abc</sup>	0.333 ± 0.115 <sup>abc</sup>
3S3F		0.756 ± 0.280 <sup>ab</sup>	0.471 ± 0.145 <sup>ab</sup>
6S		0.936 ± 0.024 <sup>a</sup>	0.213 ± 0.087 <sup>a</sup>

F: Fructose; G: Glucose; S: Sucrose.

\* Means with different superscript capital letters on the line indicate that the values present a significant difference at a 95% confidence level by the Tukey test.

\*\* Means with different superscript lowercase letters in the column indicate that the values present a significant difference at a 95% confidence level by the Tukey test.

Source: author.

Table 31 - Moisture content and water activity of starch-based films produced by small-scale CTD with water circulation using Mylar® support.

Film Samples	Support	Mylar®	
		Moisture content (g g <sup>-1</sup> d.b.)	a <sub>w</sub>
3G3F		0.114 ± 0.030 <sup>a</sup>	0.351 ± 0.004 <sup>b</sup>
6F		0.102 ± 0.021 <sup>a</sup>	0.331 ± 0.076 <sup>b</sup>
3G3F		0.214 ± 0.052 <sup>a</sup>	0.668 ± 0.056 <sup>a</sup>
6G		0.196 ± 0.065 <sup>a</sup>	0.604 ± 0.074 <sup>a</sup>
1.98GSF		0.174 ± 0.041 <sup>a</sup>	0.652 ± 0.040 <sup>a</sup>
3S3F		0.135 ± 0.005 <sup>a</sup>	0.558 ± 0.011 <sup>a</sup>
6S		0.189 ± 0.060 <sup>a</sup>	0.608 ± 0.049 <sup>a</sup>

F: Fructose; G: Glucose; S: Sucrose.

\* Means with different superscript capital letters on the line indicate that the values present a significant difference at a 95% confidence level by the Tukey test.

\*\* Means with different superscript lowercase letters in the column indicate that the values present a significant difference at a 95% confidence level by the Tukey test.

Source: author.

The test configuration is based on the 180° peel test that involves bonding a flexible adhesive to a rigid adherent. In the standard test, the flexible adherent is peeled away from the rigid adherent at a fixed rate so that the angle between the tab and the rigid adherent is kept 180°. Nevertheless, because of the organization of the drying equipment below the texturometer, it was impossible to detach the starch-based films at a constant angle. As the instruments' position was kept constant and all tests were done in the same way, the strength results are reproducible and comparable to each other. Modified peel-tests, including different configurations or using custom-made apparatus, were applied by other authors to measure food adhesion (Ben-Zion & Nussinovitch, 2002; Keijbets et al., 2009), but the results are hardly comparable, as they involve different arrangements for the detachment of the samples.

Valenzuela and Aguilera (2015) worked with apple leathers, evaluating four factors that could interfere with the samples' stickiness (ingredients, RH, surface rugosity of the apple leather, and compression time). The study performed the T-peel test, in which apple leathers were pulled out of low-density polyethylene (LDPE) strips. Adhesion force (N) was determined as the mean peel force. The adhesion force of leathers was maximum (1.35 N) when the samples contained 5% glucose and were conditioned at 44% of RH. Nevertheless, due to differences in definition, and the choice of methodology for the detachment tests, the comparison of data with literature is frequently difficult.

The maximum load, which can also be referred to as the detachment force or apparent adhesion, is defined as the peak separation force to detach the films from the drying support. The average load gives a dimension of the force throughout the release of the whole films, although the detachment is not homogeneous, and there are peaks of force during the test in the texturometer related to the areas of the sample that are more adhered to the support. For this reason, the results of adhesion tests are usually better evaluated by the maximum load, a decision also made by other authors (Guan & Seib, 1994; Hosney & Smewing, 1999; Keijbets et al., 2009).

In Table 28, it is noticed that there was a statistically significant difference between the maximum load values of each sample when they were detached from the original Teflon<sup>®</sup>. The films containing sucrose in the composition presented a higher maximum load, which means it required a greater force to remove the film from the support. The same result is attested by the response surfaces, shown in Figure 33, adjusted to the linear and quadratic models (equations shown in Table 32). The coefficients of the equations with significant influence are highlighted in red.



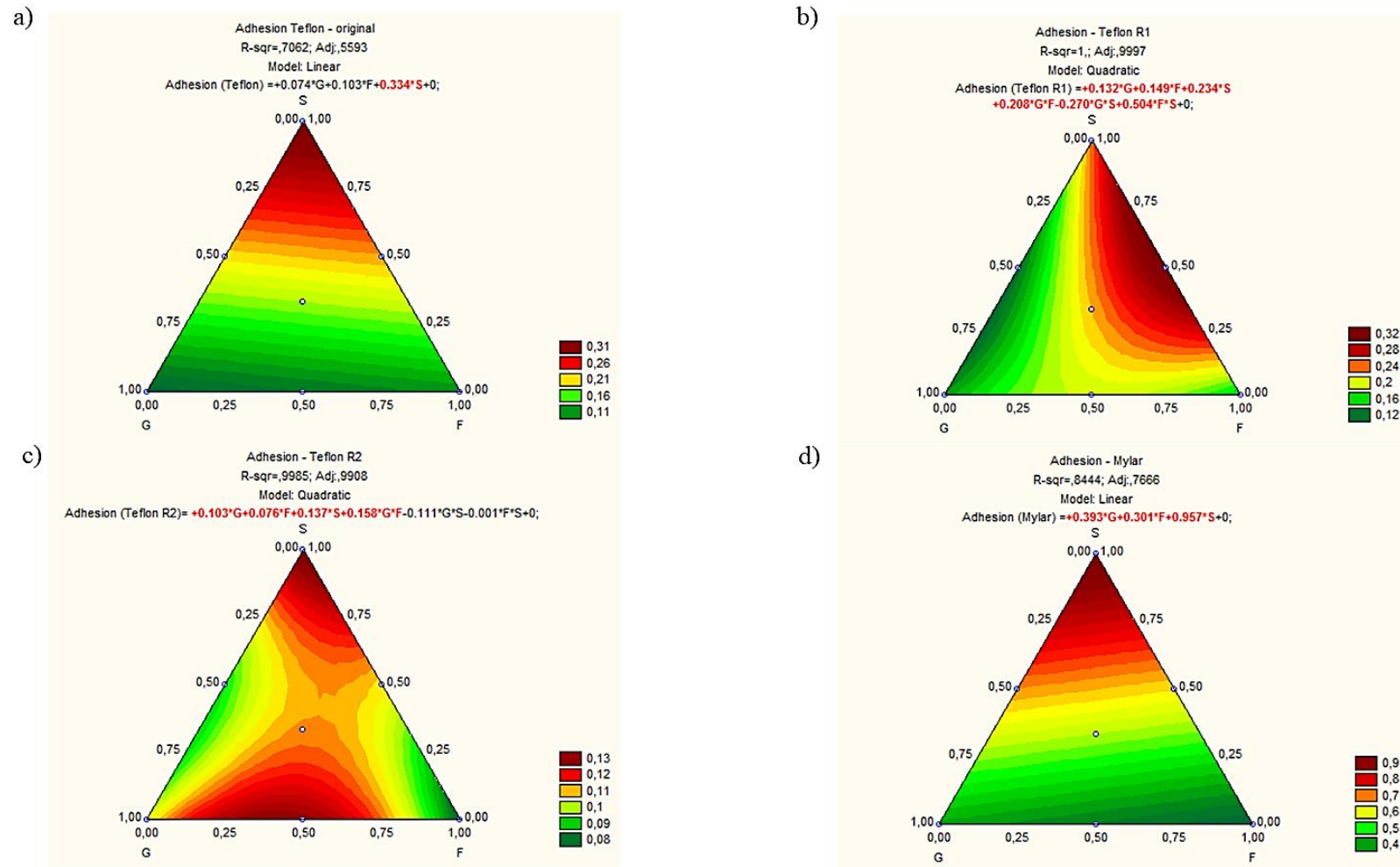


Figure 33 - Response surfaces for the maximum load, concerning sugar composition, to detach starch-based films from the supports after drying: (a) original Teflon<sup>®</sup>; (b) Teflon<sup>®</sup> R1; (c) Teflon<sup>®</sup> R2; (d) Mylar<sup>®</sup>.

Source: author.

Table 32 - Equations fitted to quadratic models for the maximum load to detach starch-based films with added sugar from the supports after drying.

<b>Response Adhesion</b>	<b>Models</b>	<b>R<sup>2</sup> R<sup>2</sup> - adj.</b>
Teflon <sup>®</sup> – original	Adhesion (Teflon) = $+0.074 \times G + 0.103 \times F + \mathbf{0.334 \times S}$	0.706; 0.559
Teflon <sup>®</sup> (R1)	Adhesion (Teflon R1) = $\mathbf{+0.132 \times G + 0.149 \times F}$ $\mathbf{+0.234 \times S + 0.208 \times G \times F - 0.270 \times G \times S}$ $\mathbf{+0.504 \times F \times S}$	1.000; 1.000
Teflon <sup>®</sup> (R2)	Adhesion (Teflon R2) = $\mathbf{+0.103 \times G + 0.076 \times F + 0.137 \times S + 0.158 \times G \times F}$ $\mathbf{- 0.111 \times G \times S}$	0.998; 0.991
Mylar <sup>®</sup>	Adhesion (Mylar) = $\mathbf{+0.393 \times G + 0.301 \times F + 0.957 \times S}$	0.844; 0.767

Source: author.

Figure 33.a. and the fitted model show that sucrose had a major influence on increasing adhesion in original Teflon<sup>®</sup>, especially for the film containing only sucrose (Film 6S), which exhibited a maximum load of 0.369 N. For mixtures of two sugars, when sucrose was present (Film 3G3S and 3S3F), the peaks were not as high, but even so, they were higher than when sucrose was not present in the composition, or it was present in smaller amounts (in Film 1.98 GSF). These results contradict the observed in the measurements of contact angles, in which the presence of sucrose increased the contact angles over the original Teflon<sup>®</sup>, implying lower wettability, a property related to adhesion. The chemical interaction between the support and the suspension may have been increased when the system was subjected to high temperature, providing greater adhesion. Padday (1968) showed that the work of adhesion of water advancing on paraffin wax increased slightly with the increase in temperature, and the author explained that the water structure at the liquid-air interface is different from the liquid-solid one, which can cause changes in the contact angle increasing wettability. As the starch-based suspensions contain mainly water, this may explain the increase in wettability with increasing temperature. The wettability of suspensions is related to adhesion in the literature. However, as the starch-based suspensions and films are different products and wettability is a property of liquids, a direct relationship with the adhesion of a dehydrated product cannot be proven but can be inferred.

In Teflon<sup>®</sup> with higher roughness (R1), the difference between the results evidenced that the increase in maximum load can be attributed to the presence of sucrose (as for original Teflon<sup>®</sup>) but also of fructose, with the mixture of both sugars (Film 3S3F) showing the highest

maximum load (of 0.318 N) and statistical significance in relation to the other samples. Sample containing glucose and sucrose (Film 3G3S) presented the smallest force to detach, as for the film with added glucose (Film 6G), so the presence of glucose may be linked to the decrease in the detachment force on this modified support. The coefficients of the equation adjusted to the data (Table 32) shows that both the individual sugars and the mixtures had an influence on the increase in adhesion (except for the mixture of glucose and sucrose). The mixture of sucrose and fructose presented the highest coefficient to the fitted equation, showing its greatest effect in increasing adhesion.

In the experiments performed over the altered Teflon<sup>®</sup> surface with intermediate roughness (R2), the sugars present individually also influenced the increase in adhesion, but the coefficients of the adjusted equation (Table 32) were lower (that is, less pronounced effect). Of the sugars as single component, sucrose's addition increased more the force necessary for the detachment. However, there was no statistically significant difference in the Tukey test, between most samples. The increase in adhesion to this support seem to have a relation to the mixture of glucose and fructose as well. Therefore, for this support in particular, the results were not sufficiently different for a conclusion to be drawn concerning the sugar composition and the detachment force of the films.

A relationship between real surfaces, with possible inhomogeneities, and the wetting phenomenon (as explained by the equilibrium states of Cassie-Baxter or Wenzel) can be applied to explain the differences in adhesion. The Cassie-Baxter state assumes that air can be trapped into the asperities of a rigid material, forming a solid-liquid-air contact on the surface's interface. Thus, the wettability would be low due to the presence of air, making adhesion to be lower as well. Contrarily, hydrophobic surfaces with no trapped air display a greater solid-liquid interface (Wenzel state). If the surface has not been mechanically abraded (like the original Teflon<sup>®</sup>) this will cause the contact angles to increase even more, by increasing the contact with the hydrophobic surface (as seen in the contact angles using water or the starch-based suspensions). However, on the Teflon<sup>®</sup> surface with abrasions, the contact between the liquid and the surface is less hydrophobic, because part of the Teflon<sup>®</sup> layer was partially removed. Thus, the contact between the liquid and the inner surface of the Teflon<sup>®</sup> material can promote greater wettability, leading to lower contact angles, increasing adhesion. In this sense, it can be inferred that the Teflon<sup>®</sup> with intermediary roughness R2 (0.188  $\mu\text{m}$ ) promotes "superficial" asperities that favor air trapping into the material roughness. Rougher Teflon<sup>®</sup> (R1) (0.213  $\mu\text{m}$ ) was damaged more deeply inside, and in this way, it was more difficult to

imprison the air as well as exposing the layer below the Teflon<sup>®</sup> coating (glass fiber, which is less hydrophobic), so wettability was greater and adhesion may be greater as a consequence.

Evaluating the detachment peaks of the same film on the different supports (original Teflon<sup>®</sup>, Teflon<sup>®</sup> R1, and Teflon<sup>®</sup> R2), it can be seen that the films with fructose (3G3F, 6F, 1.98GSF, and 3S3F) exhibited the highest adhesion on Teflon<sup>®</sup> R1 (higher roughness). It seems that the presence of fructose has more influence on adhesion when the support has a deeper roughness. This is in agreement with what was observed after the drying of strawberries (item 3.3.5), which have a high fructose content. In continuous CTD, where it is difficult to replace the Teflon<sup>®</sup> belt with a new material constantly, the support shows aging and consequent changes in its roughness. This greatest roughness may be responsible for the strawberry's adhesion to the Teflon<sup>®</sup> belt, requiring the addition of carrier agents to minimize the phenomenon and enable processing.

Regardless of the sugar's composition, all the samples showed greater adhesion (represented by the higher value of maximum load) when detached from the support with greater roughness (R1). As previously mentioned, surface roughness heavily influences the adhesion forces for food samples subject to normal force application. This is based on the theory of adhesion, the mechanical interlocking, where the ability of the food to penetrate the cavities and flow around the asperities of the contact surface determines the adhesion strength, besides being an expression of the stickiness of the products in contact with surfaces (Bosc et al., 2008; Ebnesajjad, 2014). Film 6S and Film 3G3S exhibited higher adhesion on original Teflon<sup>®</sup>, but there was no statistical difference between values.

The maximum loads obtained for the starch-based films detached from Mylar<sup>®</sup>, shown in Table 30, highlight the difference from the detachment forces over Teflon<sup>®</sup>. The greatest peak value of 0.936 N, found for the film with only sucrose (6S), was almost 2.54 times higher than the greatest peak for the same film obtained for Teflon<sup>®</sup> (of 0.369 N for the Film 6S). The combination of fructose and sucrose (Film 3S3F) also led to a higher detachment force with no significant statistical difference compared to the film with sucrose (6S). Similar observations are inferred from average loads (Table 30). The higher adhesion when using Mylar<sup>®</sup> as the support, in relation to Teflon<sup>®</sup>, can be related to the greater wettability of the suspensions over Mylar<sup>®</sup> (as discussed for the contact angles, item 4.3.3.). Concerning the sugar compositions, as shown on the response surface (Figure 33) and in the fitted models (Table 32), sucrose had a major influence on increasing adhesion, both when present as a pure component, and when present in a mixture.

From the values of moisture content, shown in Table 29 for Teflon<sup>®</sup>, it can be noted that there are only statistical differences between the different films dried over the same Teflon<sup>®</sup> support. For most samples, no significant differences were observed for the same film on the Teflon<sup>®</sup> supports with abrasion (R1 and R2) or without abrasion (original Teflon<sup>®</sup>). There were no statistically significant differences in the moisture content of the films dried over Mylar<sup>®</sup> (Table 31). Water activity also did not show a statistically significant difference for most samples dried over each support.

Films containing only sucrose showed greater maximum load when removed from the original Teflon<sup>®</sup>, even presenting a higher moisture content. On the other hand, Film 3S3F presented lower moisture content than the other films with added sucrose, and showed a high adhesion peak. Thus, unlike product stickiness, the adhesion force cannot be related only to the sample moisture content and to T<sub>g</sub>, because this property is influenced by the interaction between the suspension and the support, as well as its roughness. The increase in moisture content with sucrose can be attributed to the fact that sucrose has a higher number of OH groups than the other sugars and, therefore, is more hydrophilic (Teixeira et al., 2007).

Collares, Finzer & Kieckbusch (2004) also performed detachment experiments consisting of drying suspensions of maltodextrin, gum Arabic, and sugar cane. The products were spread in the form of 0.10 mm films on glass plates and then dried in a hot air chamber, controlling the moment of the spontaneous detachment of the dry materials. The authors determined the samples' water content at the end of drying and used the temperature of the air chamber to compare the values with the empirically determined T<sub>g</sub>. The sugar cane's T<sub>g</sub>, due to its high concentration in sugars, was lower than the drying temperature. Therefore, the product was in a rubbery state and did not detach itself. Thus, the study concluded that spontaneous detachment is linked to the glass transition temperature. Although they did not carry out tests to measure the detachment force, the relationship with the composition and the physical state of the product was built. Similarly to this work, it was concluded that the detachment is influenced not only by the characteristics surface of the support material but also by the interfacial stresses between the solid support and the food solution. Further, they affirmed that the formulation and the drying process could be manipulated in such a way as to allow easier detachment, thus optimizing the drying processes.

As already mentioned, in at least one of the repetitions, the films broke when the texturometer probe removed the sample from Mylar<sup>®</sup>. This means that the films exhibited a *cohesive failure of the substrate*, when a fracture allows a layer of adhesive to remain adhered to the surface and attached to the probe (Ebnesajjad, 2014). This is a technological issue, as it

leaves material adhered to the drying surface. According to Kilcast and Roberts (1998), both product rheology and surface energy can contribute to cohesive failures, and it is possible to minimize the problem by changing the processing surface, the composition of the product, or the operational conditions. The effect of the surface tension on the stickiness of chocolates was shown by Keijbets et al. (2009); the quartz material, with the greatest difference in surface tension compared to the chocolate, had the strongest adhesion and presented cohesive failure, with the samples being separated from themselves and not from the probe.

In Figure 34, the averages of tensile strength and average load (adhesion force) were plotted together. The graphs show that the detachment forces using Mylar<sup>®</sup> have come closer to the films' tensile strengths, compared to Teflon<sup>®</sup>. Tensile strength is related to the mechanical properties of films and has a relation with cohesion; the higher the cohesion force between the structures (as starch molecules) within the film, the higher will be the tensile strength (Ahmad et al., 2015; Basiak, 2016). The smaller difference between the tensile strength values and the average detachment forces on the Mylar<sup>®</sup> support may explain why some of the samples reached the maximum tensile strength and broke (limit of cohesion) during the tests. Overall, the force required to detach the films from supports implies that adhesion was higher than cohesion. However, as affirmed as well by Adhikari et al. (2001), the adhesion of a film to a surface can be attributed to a combined effect of adhesive and cohesive forces, and the measure of detachment by the texturometer actually measures both forces, not being possible to completely differentiate them. Comparing the detachment forces over Teflon<sup>®</sup> for different samples, it is clear that the detachment measurements were lower than using the Mylar<sup>®</sup> support. Furthermore, the roughness R1 resulted in higher average values during the test, around 0.1 N, as also verified in the average results shown in Table 28. Observing the curves in Figure 34, one can admit that the average detachment forces on the original Teflon<sup>®</sup> and Teflon<sup>®</sup> with roughness R2 were very close to each other, with no statistical significances between these two supports (as seen in Table 28 as well).

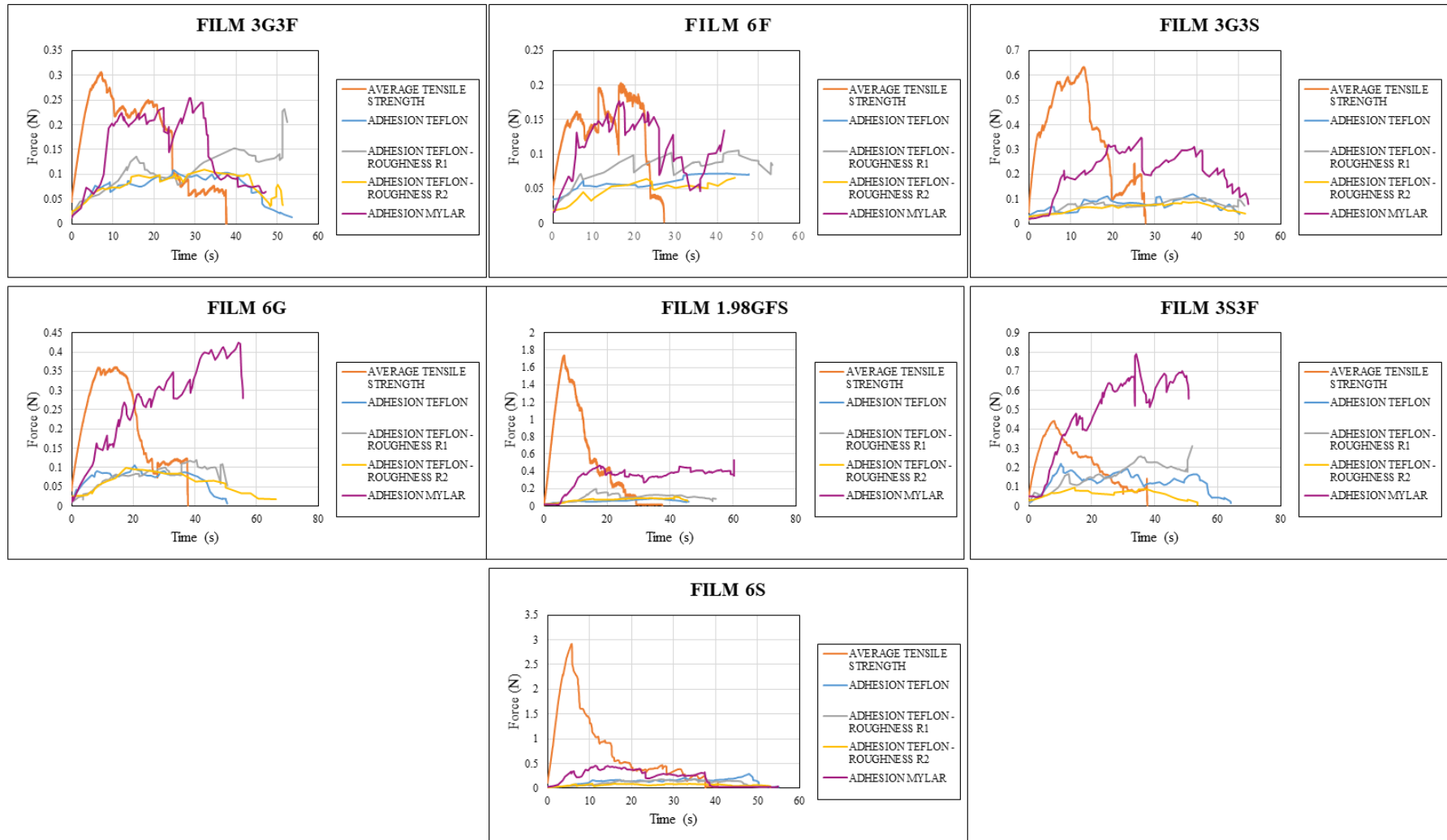


Figure 34 - Average tensile strength and adhesive forces of starch-based films.

Source: author.



#### 4.3.8.1. *Effect of temperature on the dry products detachment*

The detachment tests after cooling were performed over an aluminum plate covered with the original Teflon<sup>®</sup> support. The plate is a heat exchanger with water circulation in its interior for heating and cooling of the films after drying (Figure 16). The drying time for each sample was 40 min. Both films used in the tests presented the greatest value of tensile strength (6S and 1.98GSF), reported in Table 26, implying greater cohesion of these samples, contrary to the observed during the detachment tests, in which the sample breaks first.

Table 33 presents the maximum and the average maximum load (N) to detach the film samples from the original Teflon<sup>®</sup> right after drying and after cooling. Several cooling temperatures were tested. Table 34 shows the moisture content ( $\text{g g}^{-1}$ , d.b.) and the films' water activity right after drying.



Table 33 – Maximum and average load (N) for the detachment of Film 1.98 GSF and Film 6S from original Teflon® support, for different cooling temperatures.

Film Samples	Maximum load (N)							Average load (N)						
	98	88	80	65	55	45	35	98	88	80	65	55	45	35
1.98GSF	0.250 ± 0.029 <sup>bD</sup>	0.265 ± 0.022 <sup>aD</sup>	0.501 ± 0.138 <sup>bCD</sup>	0.615 ± 0.115 <sup>aBCD</sup>	0.876 ± 0.361 <sup>aABC</sup>	1.061 ± 0.089 <sup>aAB</sup>	1.341 ± 0.162 <sup>aA</sup>	0.174 ± 0.045 <sup>aCD</sup>	0.151 ± 0.007 <sup>aD</sup>	0.277 ± 0.108 <sup>aBCD</sup>	0.299 ± 0.034 <sup>aABCD</sup>	0.494 ± 0.237 <sup>aAB</sup>	0.624 ± 0.051 <sup>aA</sup>	0.500 ± 0.037 <sup>aABC</sup>
6S	0.374 ± 0.050 <sup>aB</sup>	0.394 ± 0.086 <sup>aB</sup>	0.798 ± 0.227 <sup>aB</sup>	0.563 ± 0.064 <sup>aB</sup>	0.963 ± 0.170 <sup>aB</sup>	1.183 ± 0.446 <sup>aAB</sup>	1.902 ± 0.847 <sup>aA</sup>	0.202 ± 0.032 <sup>aBC</sup>	0.181 ± 0.062 <sup>aC</sup>	0.413 ± 0.128 <sup>aABC</sup>	0.294 ± 0.015 <sup>aABC</sup>	0.533 ± 0.132 <sup>aA</sup>	0.475 ± 0.136 <sup>aAB</sup>	0.571 ± 0.066 <sup>aA</sup>

F: Fructose; G: Glucose; S: Sucrose.

Source: author.

Table 34 - Moisture content and water activity of Film 1.98 GSF and Film 6S produced on aluminum plate and using different cooling temperatures.

Film Samples	Moisture content (g g <sup>-1</sup> , d.b.)							a <sub>w</sub>						
	98	88	80	65	55	45	35	98	88	80	65	55	45	35
1.98GSF	0.188 ± 0.042 <sup>aA</sup>	0.174 ± 0.066 <sup>aA</sup>	0.159 ± 0.032 <sup>aA</sup>	0.126 ± 0.025 <sup>aA</sup>	0.159 ± 0.034 <sup>aA</sup>	0.184 ± 0.042 <sup>aA</sup>	0.159 ± 0.029 <sup>aA</sup>	0.578 ± 0.081 <sup>aA</sup>	0.606 ± 0.082 <sup>aA</sup>	0.592 ± 0.076 <sup>aA</sup>	0.526 ± 0.017 <sup>aA</sup>	0.528 ± 0.046 <sup>aA</sup>	0.598 ± 0.099 <sup>aA</sup>	0.583 ± 0.066 <sup>aA</sup>
6S	0.238 ± 0.043 <sup>aA</sup>	0.173 ± 0.021 <sup>aABC</sup>	0.148 ± 0.024 <sup>aC</sup>	0.156 ± 0.035 <sup>aC</sup>	0.121 ± 0.052 <sup>aC</sup>	0.240 ± 0.022 <sup>aAB</sup>	0.158 ± 0.023 <sup>aBC</sup>	0.692 ± 0.056 <sup>aA</sup>	0.659 ± 0.066 <sup>aA</sup>	0.603 ± 0.021 <sup>aA</sup>	0.597 ± 0.078 <sup>aA</sup>	0.586 ± 0.036 <sup>aA</sup>	0.715 ± 0.031 <sup>aA</sup>	0.665 ± 0.082 <sup>aA</sup>

F: Fructose; G: Glucose; S: Sucrose.

\* Means with different superscript capital letters on the line indicate that the values present a significant difference at a 95% confidence level by the Tukey test.

\*\* Means with different superscript lowercase letters in the column indicate that the values present a significant difference at a 95% confidence level by the Tukey test.

Source: author.

With the decrease in temperature, the product approaches its  $T_g$ , becoming more rigid and less rubbery, which in theory would facilitate its removal from the support (resulting in lower values of detachment force). However, the temperature reduction increased the film's adhesion to the support, which was also verified visually.

As occurred during the evaluation of the product's detachment over Mylar<sup>®</sup>, some of the samples of the Film 1.98 GSF that were cooled to 55 °C, 45 °C, or 35 °C broke during the analysis of the texturometer. This can happen because the films have firmly adhered to the support. Films 6S also broke when cooled down to 80 °C and below it. Therefore, the reported value in Table 33 was the maximum value obtained before the break. The higher temperature significantly affects sugar molecules, possibly explained by an onset of melting/dissolution with loss of crystallinity. The literature reports that the melting temperature for sucrose, for example, is 173 °C. However, variations in melting temperatures of organic crystals are well-known and acceptable because of amorphous residues, presence of water (solvent) at standard atmospheric surroundings, among other factors (Y. Roos, 1993a; Y. Roos et al., 2012). These changes in the sugar's structure may have promoted the increase in suspension's wettability, increasing its adhesion, and the decrease in tensile strength values compared to the results obtained at room temperature.

Indeed, other authors reported the same behavior when cooling temperatures were applied before detachment tests. Gent and Schultz (1972) performed detachment measurements of a copolymer of butadiene and styrene from Mylar<sup>®</sup> strips using temperatures of about 5°C. The authors reported that the adhesion forces were greater, mainly due to the decrease in the segmental mobility of the adhesive molecules at low temperature. As stated by Padday (1968), as the temperature increases above the  $T_g$ , the vibrational and translational energies of the monolayer adhered to the solid-liquid interface increase; as consequence, the van der Waals' force of attraction decreases. This means that the liquid suspension occupies a larger area of the surface, being "separated" from the first layer of the surface material, and that is why adhesion may decrease.

In general, changes in the cooling temperatures generated more fragile and easily breakable films. When water at 35 °C circulated inside the equipment to cool the Film 1.98 GSF, the sample was firmly attached to the support and was removed in the form of flakes, after scraping the surface with a spatula. For the Film 6S, temperatures of 35 °C, 45 °C, 55 °C, and 65 °C also led to flakes.

For film 1.98 GSF, the highest detachment forces without a break were obtained with cooling water at 65 °C. Compared to the film taken from the system at 98 °C, cooling increased

the adhesion force by 2.46 times. The statistical analysis revealed that the adhesion forces were mostly influenced by the cooling temperatures, presenting significant differences, that is, greater adhesion, when lower temperatures were applied (under 65 °C). For sample 6S, the highest adhesion forces without a break were obtained after cooling down the system to 88 °C, but the adhesion force remained practically the same as the one obtained at 98 °C. Furthermore, the use of different cooling temperatures promoted higher adhesion forces but did not promote significant statistical differences, except when flakes were formed (at 35 °C and 45 °C).

Regarding the sugar composition, the samples 1.98 GSF and 6S presented statistically significant differences in adhesion force only when temperatures of 98 °C and 80 °C were employed. However, the Film 6S broke during removal at 80 °C, so the greatest detachment force is related to the peak before the break.

Similar to the detachment results using the system with water circulation (Figure 15), the values of moisture content and water activity for Films 1.98 GSF and 6S were close and presented no statistically significant difference between them.

The average loads of adhesion, along with a description of the type of product observed after cooling, are represented in Figure 35 and Figure 36, for Film 1.98 GSF and Film 6S, respectively. Figure 37 displays the products obtained for both samples at each temperature. It is possible to observe the formation of flakes when the cooling temperature of 35 °C is used, for both samples tested. The Film 6S was removed as flakes at temperatures of 45, 55 and 65 °C as well, while the Film 1.98 GSF was taken as a film at a temperature of 45 °C and above.

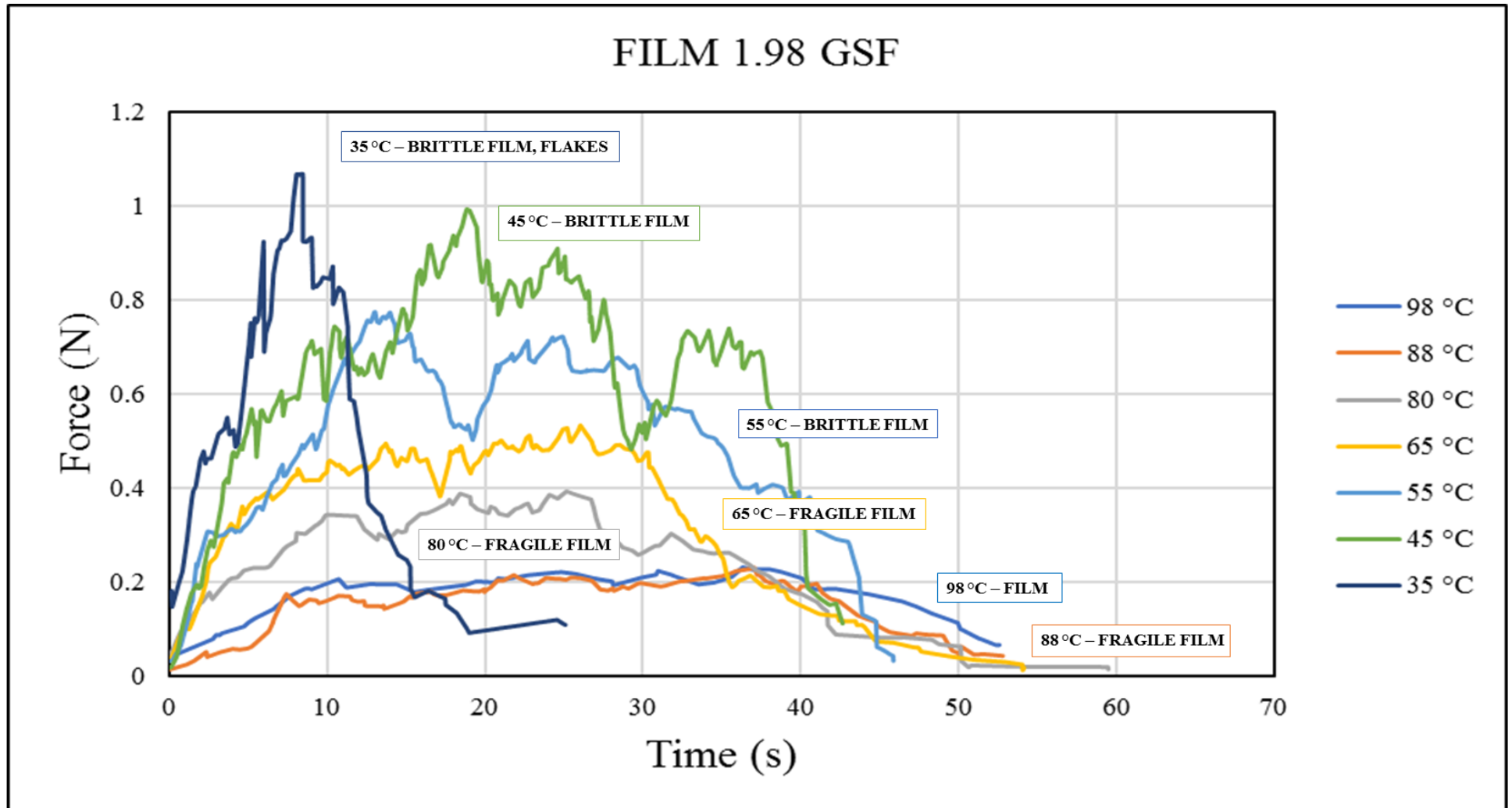


Figure 35 - Average load to detach Film 1.98 GSF when subjected to cooling temperatures; description of the type of product obtained.

Source: author.

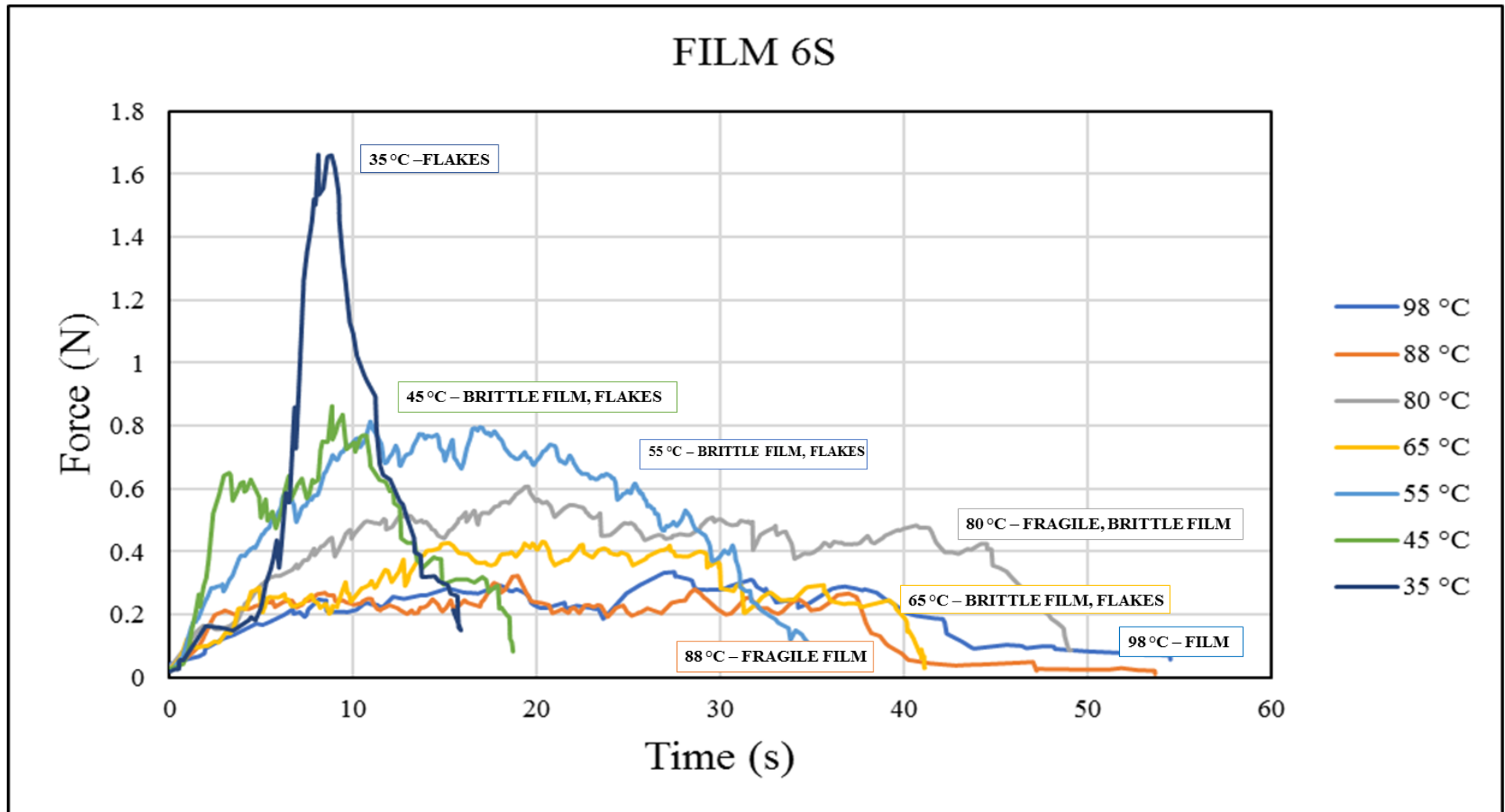


Figure 36 - Average load to detach Film 6S when subjected to cooling temperatures; description of the type of product obtained.

Source: author.



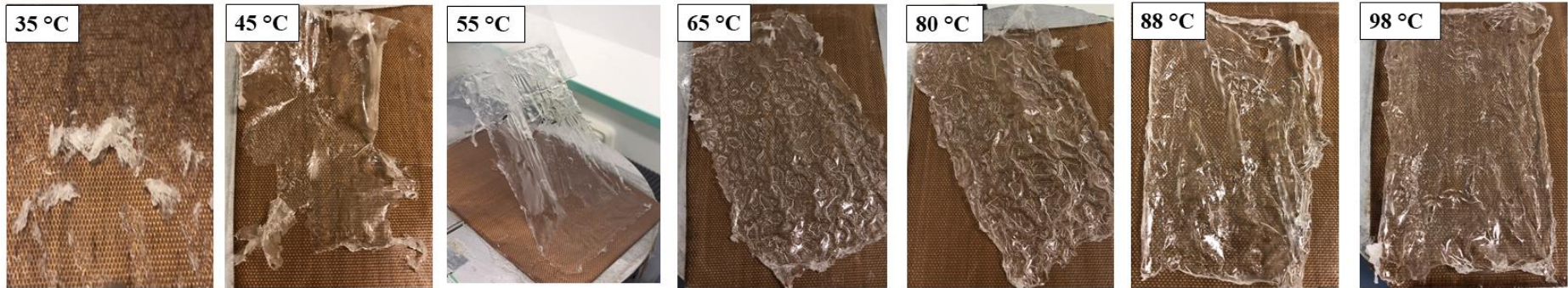
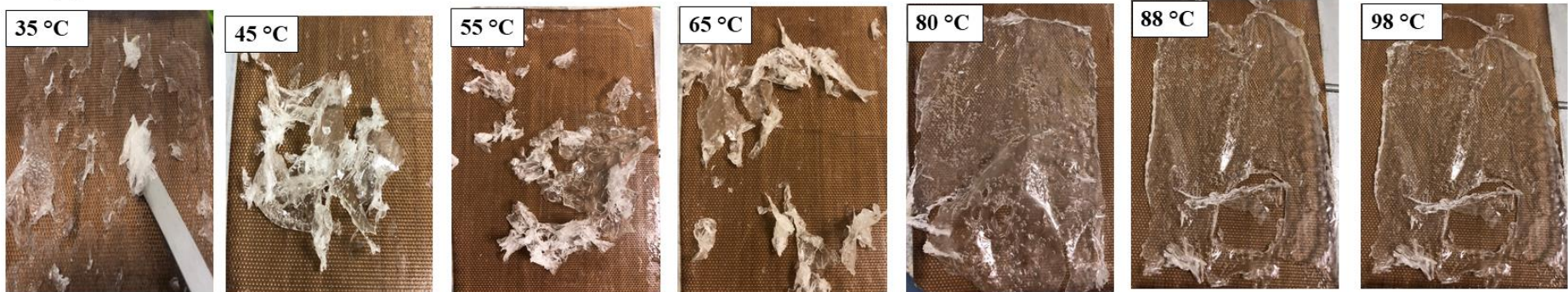
**(a) Film 1.98 GSF****(b) Film 6S**

Figure 37 - Dehydrated starch-based films obtained at several cooling temperatures.

Source: author.

#### 4.3.8.2. Effect of relative humidity (RH) on the dry products detachment

The influence of the conditioning RH in the removal of the Films 1.98 GSF and 6F from the original Teflon<sup>®</sup> was investigated. Samples dried over the support were placed in desiccators with saturated saline solutions corresponding to the desired RH (33%, 44%, 54%, 68%, and 84%) and kept at 20 °C for 30 days, to ensure that the equilibrium moisture content was reached. Then, the films were removed from the Teflon<sup>®</sup> strips, visually observing their adhesion (to assess whether they would be closer to the glassy or rubbery state), in addition to measuring their moisture content (Figure 38).

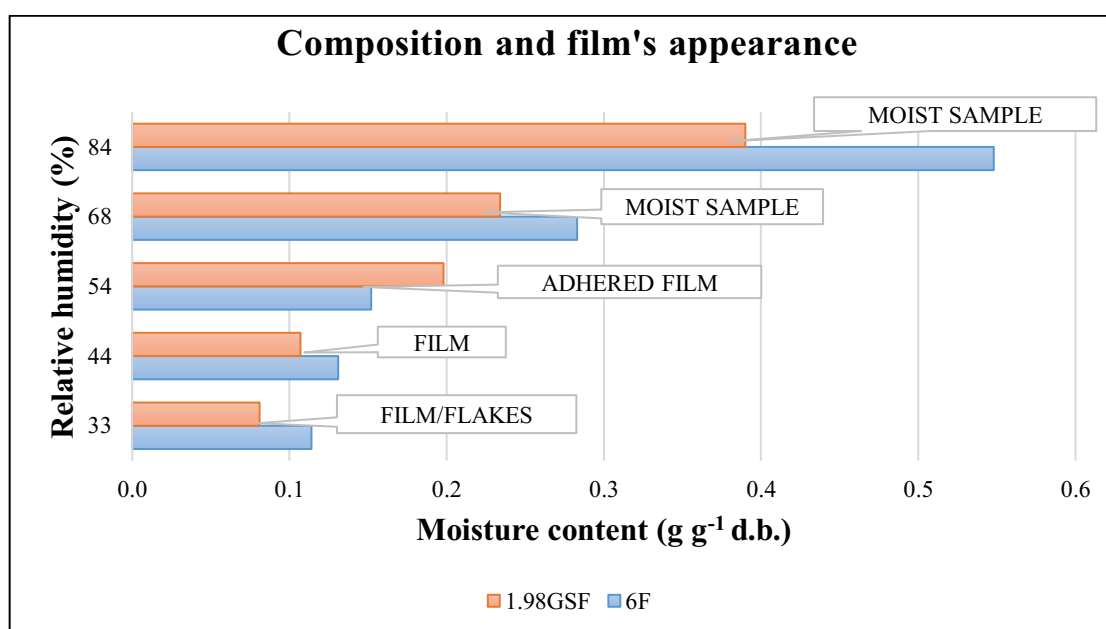


Figure 38 - Moisture content of the Films 1.98 GSF and 6F stored at a relative humidity of 33%, 44%, 54%, 68%, and 84%, concerning its appearance.

Source: author.

It was observed that, regardless of the sugar's composition, all the samples could be removed from the support. The films stored at 33% were visually "drier" and with some parts strongly adhered to the support, making it difficult to remove with the spatula and being obtained as flakes. At 44% and 54% RH, the samples could be removed from the support in the form of films. It was noticed that at 54% RH the films adhered slightly more to the Teflon<sup>®</sup> surface and the spatula was necessary only for the initial detachment.

The presence of water vapor in the ambient can form a liquid film by capillary condensation at the contact interface, contributing to the total force of adhesion (Ranade, 1987). Also, moisture may soften materials, (particles and surface) increasing the contact area and

consequently the adhesion force (Ibrahim et al., 2000; Iida et al., 1992). However, at a relative humidity of 68% and 84%, the samples had a "moist" appearance, being removed as pieces of a rubbery material, besides being sticky. Therefore, the increase of the RH above 33% increased adhesion to the Teflon<sup>®</sup> progressively until the point where the material "slides" off the support due to the amount of absorbed water. Stickiness of the films themselves, assessed by touch, was greater when RH was increased, in the same way as described for powder products (Downton et al., 1982; Papadakis & Bahu, 1992).

When exposed to a critical relative humidity of the surrounding air, crystalline materials do not absorb significant quantities of water. Amorphous structures, otherwise, absorb higher amounts of moisture, which decreases their glass transition temperature. The viscosity of the amorphous structure decreases with increasing difference between process temperature and glass transition temperature, as well as with increasing relative humidity, intensifying adhesion (Dopfer et al., 2013). The water surface tension and the interaction of water with the solid matrix are the main cause of stickiness in low moisture foods. Hence, any increase in the RH is associated with the possibility of an increased amount of water being adsorbed to the surface or absorbed into the product's bulk, causing stickiness or caking of the material. Among the factors that can induce adhesion (fats, low molecular weight sugars, organic acids, etc.), the temperature, viscosity, and RH have the greatest contribution (Adhikari et al., 2001).

The influence of relative humidity and the presence of sugar in the adhesion phenomenon was also attested by Valenzuela and Aguilera (2015). They reported that when 5% glucose was added and the apple leathers were stored at 44% RH, the adhesion force between two samples was maximum (1.35 N). According to these authors, the addition of glucose and the increase in relative humidity were the factors that most affected adhesion, compared to the leathers' surface rugosity and the compression time.

#### **4.3.9. Visual analysis**

Figure 39 shows the values given to the evaluation parameters of the films.



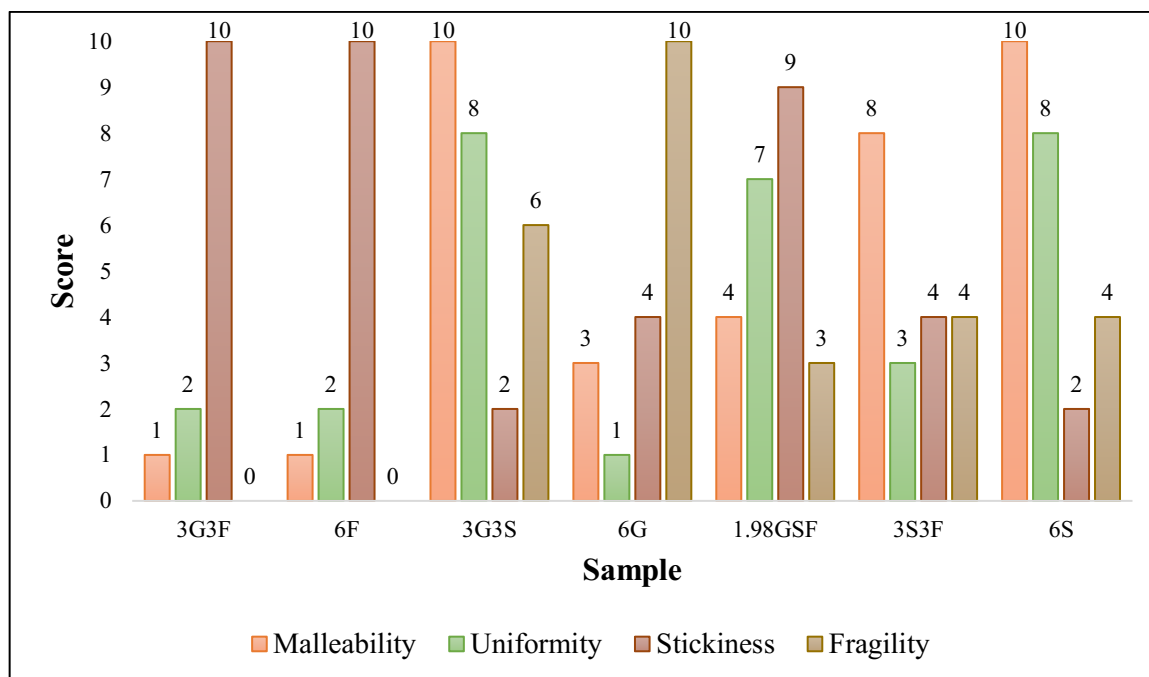


Figure 39 - Parameters of qualitative analysis of the starch-based films.

Source: author.

The films were evaluated right after their production in CTD with electrical resistances (Figure 17). The material consisting only of 4% starch did not form a film after drying, being removed in the form of flakes (as can be seen in Figure 41). Therefore, this sample was not evaluated in the qualitative analysis. Starch films prepared without plasticizers are difficult to handle, being fragile and brittle. Conversely, at higher plasticizer concentrations, they are soft, sticky, and hard to remove from the casting surface (De Moraes et al., 2013; Lagos et al., 2015). Plasticizers reduce internal hydrogen bonds, increasing intermolecular spacing and permeability while decreasing the starch films' brittleness (Laohakunjit & Noomhorm, 2004).

Films containing sucrose (3G3S, 3S3F, and 6S) presented the highest malleability and lower stickiness, with the exception of the film containing the mixture of glucose, sucrose, and fructose (Film 1.98 GSF). The malleability parameter represents the ease of handling. The malleable behavior of hydrophilic films could be related to the structural modifications of the starch network in the presence of plasticizers. The film matrix becomes less dense, and the movements of the polymer chains are facilitated (Mali et al., 2005). In general, films containing low molar mass sugars, with low Tg values, may also be responsible for a good malleability of films, which is an advantage for better handling or folding the product, as well as a potential use in food packaging applications (Azeredo et al., 2009; Valenzuela & Aguilera, 2015).

The subjective analysis agrees with the results of the Tg values, shown in Table 24, and the mechanical tests (Table 26), in which the films with sucrose in the composition showed a higher Tg and tensile strength, meaning that these samples were less sticky and more resistant to breakage. The film with fructose (Film 6F) showed great stickiness, which can be explained by the lower Tg of this sample.

Films containing glucose and fructose (Film 3G3F, Film 6F, and Film 6G) displayed lower uniformity than other films, presenting torn down regions and small bubbles. Also, Film 6G was fragile and displayed a white, opaque surface, particularly when stored at 44% RH (Figure 40). This appearance at the surface of plasticized edible films has been referred to as “blooming” (Aulton et al., 1981) and “blushing” (Sakellariou et al., 1986). According to Aulton, Abdul-Razzak & Hogan (1981), this phenomenon is associated with solubility, and it occurs when the plasticizer concentration exceeds its limit in the polymer, causing phase separation and physically “excluding” the added plasticizer of the system. The plasticizer may appear as spots on the film's surface, leading to weaker regions and easy rupture at low applied stress.

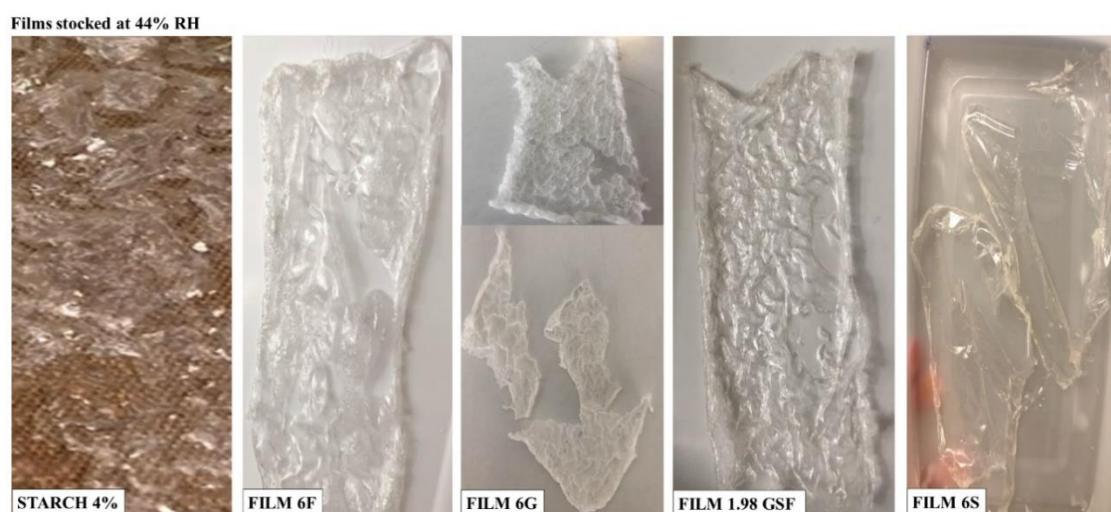


Figure 40 - Appearance of the starch-based films stored at 44% RH.

Source: author.

Figure 41 exhibits the visual appearance of the films produced on each of the supports used.



Figure 41 - Starch-based films formed over (a) Teflon<sup>®</sup>; (b) Teflon<sup>®</sup> R1; (c) Teflon<sup>®</sup> R2 and (d) Mylar<sup>®</sup>.

Source: author.

Evaluating the films formed on each support, shown in Figure 41, it is noticed that when the Teflon<sup>®</sup> roughness was increased, small bubbles appeared or became more noticeable in the film. In the adhesion topic (item 2.7), air pockets' phenomenon was explained, in which air could be trapped in the asperities of the surface of rigid materials due to roughness, causing adhesion to increase. The same thing is possible with microbubbles in the product. Microbubbles are pockets of trapped air inside the food material, at a direct contact point between the food and the surface, instead of imprisoned in grooves of the surface. These small bubbles also create suction effects that can increase adhesion, but on a smaller scale. If microbubbles are present in foods capable of stretching, such as chewing gum or bread dough, there is a greater adhesion to the contact surface. This creates long fibrils rather than the material being removed as a whole mass (Papaioannou et al., 2014). In this case, the food will continue to elongate as the external force continues to pull the food away from the surface until the force exceeds the cohesion force in the thinning fibrils or the adhesion force at the surface, leading to fracture of the product (Gay, 2002).

## 5. CONCLUSION

In the food industry, changes to the drying process to reduce adhesion are not widespread, since processes are created thinking about quality, performance and energy efficiency. Alterations on the surface of equipment are not usual since the materials selected are based primarily on their functionality in the process, as heat exchange or ease of cleaning. The consideration of surface tension and roughness is not common (Noren et al., 2019). Contrarily, the composition of a food material is more easily modified, by adding hydrocolloids or decreasing the concentration of compounds such as low molar sugars. However, the tendency to use hydrophobic materials with low surface energy increases, coupled with the control of the viscosity and temperature of the food to be processed.

By evaluating the addition of carrier agents to a strawberry pulp, it was possible to confirm that these hydrocolloids helped to postpone materials change from brittle to the rubbery or sticky state. Therefore, their presence is relevant to reduce the adhesion of samples on the Teflon<sup>®</sup> belt, promoting the complete removal of the dry material.

Dry films resulted from starch-based suspensions present low T<sub>g</sub>, due to the presence of low molar mass sugars. It indicates that during processing, all films were above their glass transition and that the adhesion phenomenon was likely to occur, as the samples were in a rubbery state.

The water sorption isotherms made clear the hygroscopic character of the films containing sugar in the composition. All samples with sugars had low tensile strengths, but sucrose produced a more resistant film.

The results obtained for the detachment of the starch-based films showed that, as predicted by the hypotheses of the present work, the composition of sugars affects the adhesion of the dry material to the support. Sucrose is related to the increase in adhesion to the Teflon<sup>®</sup> support (with its original roughness). The experiments using Teflon<sup>®</sup> R1 (with higher roughness) also evidenced that when roughness is increased, the presence of fructose significantly impacts on adhesion, along with sucrose. The solution's temperature must also be considered, as it influences the solution's wettability, which may increase adhesion. The wettability of the starch-based suspensions was determined at room temperature through contact angles, and the suspension containing only sucrose (6S) showed less wettability in the original Teflon<sup>®</sup> support, which indicates a lower adhesion on this material. However, during the drying process, in which the suspension temperature was increased, the wettability of that suspension was probably increased, increasing the adhesion. With the decrease in the system's

temperature after drying, the adhesion forces increased until the lowest temperature tested (35 °C), in which the films were strongly and completely adhered to the Teflon<sup>®</sup> support, being removed as flakes. The film's sugar composition affected this analysis due to the difference in the adhesion force and in the products obtained at each cooling temperature, when using the sample with three sugars (Film 1.98 GSF) or the sample with sucrose only (Film 6S).

The study's initial hypothesis that adhesion depends on the product's glass transition temperature is proven to be right. Although it is not the main factor of influence, as all the samples were above the T<sub>g</sub>, some of them adhered more to the solid material, depending on the sugar's composition and roughness of the support. The assumption that the moisture content plays a role in the formation of films or flakes was also verified through the films' storage at chosen relative humidity. Indeed, at a relative humidity of 33%, the samples were removed in the form of flakes. Intermediate relative humidity (44% to 54%) made it easier to remove the dry material as a whole film, with an initial detachment with a spatula. High relative humidity (68% and 84%) facilitated the samples removal since the products were highly humid, even though they were remarkably sticky.

Strawberry leathers stocked at 33% RH displayed low glass transition temperature, meaning that strawberry samples were in a rubbery state when they were removed from the continuous CTD process. Still, it was possible to completely detach the leathers, although the carrier agents helped to prevent the scraping of the Teflon<sup>®</sup>.

Therefore, it is possible to conclude that the best conditions to decrease adhesion and to remove whole films are the use of new Teflon<sup>®</sup> supports (thereby limiting greater adhesion to greater sucrose content), removal of the product at the drying temperature (in this study, 98 °C) and without cooling. Products rich in sucrose and fructose tend to be more adhesive, demanding equipment surfaces with low surface energy and roughness. Moreover, it is possible to add carrier agents to products with high concentrations of these sugars.

Although the hypotheses foreseen at the beginning of the present work have been evaluated, the study of adhesion during drying is still a subject surrounded by many unknowns. Some suggestions for future studies include the addition of fibers to the model suspensions, to assess the behavior of stronger films during the removal from the supports. In addition, some other interesting parameters to study are the drying of suspensions with greater spreading thicknesses, and to develop a methodology without variation of the detachment angle, thus allowing the determination of an adhesion force which is directly comparable to other food adhesion studies.

## REFERENCES

- Abonyi, B. I., Feng, H., Tang, J., Edwards, C. G., Chew, B. P., Mattinson, D. S., & Fellman, J. K. (2002). Quality retention in strawberry and carrot purees dried with Refractance Window (TM) system. *Journal of Food Science*, *67*(3), 1051–1056. <https://doi.org/10.1111/j.1365-2621.2002.tb09452.x>
- Abonyi, B. I., Tang, J., & Edwards, C. G. (1999). *Evaluation of Energy Efficiency and Quality Retention for the Refractance Window TM Drying System* (pp. 1–38).
- Abu-Jdayil, B., Mohameed, H. A., & Eassa, A. (2004). Rheology of wheat starch-milk-sugar systems: Effect of starch concentration, sugar type and concentration, and milk fat content. *Journal of Food Engineering*, *64*(2), 207–212. <https://doi.org/10.1016/j.jfoodeng.2003.09.034>
- Abul-Fadl, M. M., & Ghanem, T. H. (2011). Effect of Refractance-window (RW) drying method on quality criteria of produced tomato powder as compared to the convection drying method. *World Applied Sciences Journal*, *15*(7), 953–965.
- Adak, N., Heybeli, N., & Ertekin, C. (2017). Infrared drying of strawberry. *Food Chemistry*, *219*, 109–116. <https://doi.org/10.1016/j.foodchem.2016.09.103>
- Adhikari, B., Howes, T., Bhandari, B. R., & Truong, V. (2001). Stickiness in foods: a review of mechanisms and test methods. *International Journal of Food Properties*, *4*(1), 1–33. <https://doi.org/10.1081/JFP-100002186>
- Adhikari, B., Howes, T., Bhandari, B. R., & Truong, V. (2003). In situ characterization of stickiness of sugar-rich foods using a linear actuator driven stickiness testing device. *Journal of Food Engineering*, *58*(1), 11–22. [https://doi.org/10.1016/S0260-8774\(02\)00328-X](https://doi.org/10.1016/S0260-8774(02)00328-X)
- Adhikari, B., Howes, T., Shrestha, A., & Bhandari, B. R. (2007). Effect of surface tension and viscosity on the surface stickiness of carbohydrate and protein solutions. *Journal of Food Engineering*, *79*, 1136–1143. <https://doi.org/10.1016/j.jfoodeng.2006.04.002>
- AFNOR. (1995). *NF P94-050. Sols : Reconnaissance et Essais – Détermination de la teneur en eau pondérale des matériaux – Méthode par étuvage*.
- Aguilera, J. M., Chiralt, A., & Fito, P. (2003). Food dehydration and product structure. *Trends in Food Science and Technology*, *14*(10), 432–437. [https://doi.org/10.1016/S0924-2244\(03\)00122-5](https://doi.org/10.1016/S0924-2244(03)00122-5)
- Ahmad, M., Hani, N. M., Nirmal, N. P., Fazial, F. F., Mohtar, N. F., & Romli, S. R. (2015). Optical and thermo-mechanical properties of composite films based on fish gelatin/rice flour fabricated by casting technique. *Progress in Organic Coatings*, *84*, 115–127. <https://doi.org/10.1016/j.porgcoat.2015.02.016>



- Aichayawanich, S., Nopharatana, M., Nopharatana, A., & Songkasiri, W. (2011). Agglomeration mechanisms of cassava starch during pneumatic conveying drying. *Carbohydrate Polymers*, *84*(1), 292–298. <https://doi.org/10.1016/j.carbpol.2010.11.036>
- Alhamdan, A. M., & Hassan, B. H. (1999). Water sorption isotherms of date pastes as influenced by date cultivar and storage temperature. *Journal of Food Engineering*, *39*(3), 301–306. [https://doi.org/10.1016/S0260-8774\(98\)00170-8](https://doi.org/10.1016/S0260-8774(98)00170-8)
- Ali, A., De'Ath, D., Gibson, D., Parkin, J., Alam, Z., Ward, G., & Wilson, D. I. (2015). Development of a 'millimanipulation' device to study the removal of soft solid fouling layers from solid substrates and its application to cooked lard deposits. *Food and Bioprocess Processing*, *93*, 256–268. <https://doi.org/10.1016/j.fbp.2014.09.001>
- Anglès, M. N., & Dufresne, A. (2000). Plasticized Starch/Tunicin Whiskers Nanocomposites. 1. Structural Analysis. *Macromolecules*, *33*, 8344–8353.
- AOAC. (2012). *Official methods of analysis of AOAC International*. (19th ed., Issue 543/L357). AOAC international.
- Araya-Farias, M., & Ratti, C. (2009). Dehydration of Foods: General Concepts. In C. Ratti (Ed.), *Advances in food dehydration* (p. 488). CRC Press.
- Arvanitoyannis, I., Psomiadou, E., Nakayama, A., Aibab, S., & Yamamoto, N. (1997). Edible films made from gelatin, soluble starch and polyols, Part 3. *Food Chemistry*, *60*(4), 593–604.
- ASTM. (2001). Peel Resistance of Adhesives (T-Peel Test) D 1876 - 01. In *Annual Book of ASTM Standards* (Vol. 03, pp. 4–6). <https://doi.org/10.1520/D6862-11.adherends>
- ASTM. (2002). D 882 - 02: "Standard Test Method for Tensile Properties of Thin Plastic Sheeting". In *Annual Book of ASTM Standards* (Vol. 14, pp. 1–10). ASTM International.
- Aulton, M. E., Abdul-Razzak, M. H., & Hogan, J. E. (1981). The mechanical properties of hydroxypropylmethylcellulose films derived from aqueous systems part 1: The influence of plasticisers. *Drug Development and Industrial Pharmacy*, *7*(6), 649–668. <https://doi.org/10.3109/03639048109055689>
- Azeredo, H. M. C., Mattoso, L. H. C., Wood, D., Williams, T. G., Avena-Bustillos, R. J., & McHugh, T. H. (2009). Nanocomposite edible films from mango puree reinforced with cellulose nanofibers. *Journal of Food Science*, *74*(5). <https://doi.org/10.1111/j.1750-3841.2009.01186.x>
- Barbosa-Cánovas, G. V., Fontana Jr., A. J., Schmidt, S. J., & Labuza, T. P. (2007). *Water Activity in Foods: Fundamentals and Applications* (G. V. Barbosa-Cánovas, A. J. Fontana Jr., S. J. Schmidt, & T. P. Labuza (eds.)). Blackwell Publishing.
- Barbosa-Cánovas, G. V., Kokini, J. L., & Ma, L. (1996). The rheology of semiliquid foods. *Advances in Food and Nutrition Research*, *39*.

- Barbosa-Cánovas, G V, & Juliano, P. (2004). Adaptation of Classical Processes to New Technical Developments and Quality Requirements. *Journal of Food Science*, 69(5), E240–E250.
- Basiak, E. (2016). *Étude des caractéristiques physico-chimiques et fonctionnelles d'enrobages et de films à base d'amidon*. Université de Bourgogne.
- Basiak, E., Lenart, A., & Debeaufort, F. (2017). Effect of starch type on the physico-chemical properties of edible films. *International Journal of Biological Macromolecules*, 98, 348–356. <https://doi.org/10.1016/j.ijbiomac.2017.01.122>
- BeMiller, J. N., & Huber, K. C. (2008). Carbohydrates. In S. Damodaran, K. L. Parkin, & O. R. Fennema (Eds.), *Fennema's Food Chemistry* (4th ed., pp. 83–154). CRC Press.
- Ben-Zion, O., & Nussinovitch, A. (2002). Testing the rolling tack of pressure-sensitive adhesive materials. Part II: Effect of adherend surface roughness. *Journal of Adhesion Science and Technology*, 16(5), 599–619. <https://doi.org/10.1163/156856102760070394>
- Berthier, J. (2013). Theory of Wetting. In *Micro-Drops and Digital Microfluidics* (pp. 7–73). <https://doi.org/10.1016/b978-1-4557-2550-2.00002-x>
- Bhandari, B., & Howes, T. (1999). Implication of glass transition for the drying and stability of dried foods. *Journal of Food Engineering*, 40(1–2), 71–79. [https://doi.org/10.1016/S0260-8774\(99\)00039-4](https://doi.org/10.1016/S0260-8774(99)00039-4)
- Bhandari, B., & Howes, T. (2005). Relating the Stickiness Property of Foods Undergoing Drying and Dried Products to their Surface Energetics. *Drying Technology*, 23, 781–797. <https://doi.org/10.1081/DRT-200054194>
- Bhandari, B. R. (2007). Stickiness and Caking in Food Preservation. In M. Rahman (Ed.), *Handbook of Food Preservation* (pp. 387–401). CRC Press.
- Bhandari, B. R., Datta, N., & Howes, T. (1997). Problems Associated With Spray Drying Of Sugar-Rice Foods. *Drying Technology: An International Journal*, 15(2), 671–684.
- Bobé, U., Hofmann, J., Sommer, K., Beck, U., & Reiners, G. (2007). Adhesion - where cleaning starts. *Trends in Food Science & Technology*, 18, S36–S39. <https://doi.org/10.1016/j.tifs.2006.10.019>
- Bormashenko, E., Whyman, G., & Pogreb, R. (2009). What can we learn from the vibration of drops deposited on rough surfaces? Wetting transitions occurring on rough surfaces. In K. L. Mittal (Ed.), *Contact Angle, Wettability and Adhesion* (Vol. 6, pp. 33–52). VSP. <https://doi.org/10.1021/ba-1964-0043>
- Bosc, V., Ferrari, I., & Michon, C. (2008). Adhesion to solid surfaces of gels of iota-carrageenan alone or in mixture with casein. *Colloids and Surfaces A: Physicochemical and Engineering Aspects*, 331(1–2), 2–7. <https://doi.org/10.1016/j.colsurfa.2008.05.037>



- Bourne, M. (2002). *Food Texture and Viscosity: Concept and Measurement*. Academic Press.
- Brecht, J. K., Ritenour, M. A., Haard, N. F., & Chism, G. W. (2008). Postharvest Physiology of Edible Plants Tissues. In S. Damodaran, K. L. Parkin, & O. R. Fennema (Eds.), *Fennema's Food Chemistry* (4th ed., pp. 976–1046). CRC Press.
- Brennan, J. G. (1994). Food Dehydration. *Food Dehydration*, 72–76. <https://doi.org/10.1016/B978-1-85573-360-2/50018-X>
- Brunauer, S., Deming, L. S., Deming, W. E., & Teller, E. (1940). On a Theory of the van der Waals Adsorption of Gases. *Journal of the American Chemical Society*, 62(7), 1723–1732. <https://doi.org/10.1021/ja01864a025>
- Buffa, M., Trujillo, A. J., & Guamis, B. (2001). Rennet coagulation properties of raw, pasteurised and high pressure-treated goat milk. *Milchwissenschaft*, 56(5), 243–246.
- Cano-Chauca, M., Stringheta, P. C., Ramos, A. M., & Cal-Vidal, J. (2005). Effect of the carriers on the microstructure of mango powder obtained by spray drying and its functional characterization. *Innovative Food Science and Emerging Technologies*, 6(4), 420–428. <https://doi.org/10.1016/j.ifset.2005.05.003>
- Canteri, M. H. G., Moreno, L., Wosiacki, G., & De Scheer, A. P. (2012). Pectina: da Matéria-Prima ao Produto Final. *Polimeros*, 22(2), 149–157. <https://doi.org/10.1590/S0104-14282012005000024>
- Caparino, O. A., Sablani, S. S., Tang, J., Syamaladevi, R. M., & Nindo, C. I. (2013). Water Sorption, Glass Transition, and Microstructures of Refractance Window- and Freeze-Dried Mango (Philippine “Carabao” Var.) Powder. *Drying Technology*, 31(16), 1969–1978. <https://doi.org/10.1080/07373937.2013.805143>
- Caparino, O. A., Tang, J., Nindo, C. I., Sablani, S. S., Powers, J. R., & Fellman, J. K. (2012). Effect of drying methods on the physical properties and microstructures of mango (Philippine “Carabao” var.) powder. *Journal of Food Engineering*, 111(1), 135–148. <https://doi.org/10.1016/j.jfoodeng.2012.01.010>
- Castoldi, M., Zotarelli, M. F., Durigon, A., Carciofi, B. A. M., & Laurindo, J. B. (2015). Production of Tomato Powder by Refractance Window Drying. *Drying Technology*, 33(12), 1463–1473. <https://doi.org/10.1080/07373937.2014.989327>
- Chaléat, C., Halley, P. J., & Truss, R. W. (2014). Mechanical Properties of Starch-Based Plastics. In *Starch Polymers: From Genetic Engineering to Green Applications* (pp. 187–209). Elsevier B.V. <https://doi.org/10.1016/B978-0-444-53730-0.00023-3>
- Chambi, H., & Grosso, C. (2006). Edible films produced with gelatin and casein cross-linked with transglutaminase. *Food Research International*, 39(4), 458–466.

<https://doi.org/10.1016/j.foodres.2005.09.009>

- Chang, Y. P., Cheah, P. B., & Seow, C. C. (2000). Plasticizing-antiplasticizing effects of water on physical properties of tapioca starch films in the glassy state. *Journal of Food Science*, *65*(3), 445–451. <https://doi.org/10.1111/j.1365-2621.2000.tb16025.x>
- Chiumarelli, M., & Hubinger, M. D. (2014). Evaluation of edible films and coatings formulated with cassava starch, glycerol, carnauba wax and stearic acid. *Food Hydrocolloids*, *38*, 20–27. <https://doi.org/10.1016/j.foodhyd.2013.11.013>
- Collares, F. P., Finzer, J. R. D., & Kieckbusch, T. G. (2004). Glass transition control of the detachment of food pastes dried over glass plates. *Journal of Food Engineering*, *61*(2), 261–267. [https://doi.org/10.1016/S0260-8774\(03\)00098-0](https://doi.org/10.1016/S0260-8774(03)00098-0)
- Collares, F.P., Kieckbusch, T. G., & Finzer, J. R. D. (2002). Revisão : A Transição Vítrea em Produtos Alimentícios. *Brazilian Journal of Food Technology*, *5*, 117–130.
- Collares, Fernanda Paula. (2001). *Desprendimento de filmes de pastas alimenticias durante a secagem sobre superficies de solidos e sua relação com a transição vitrea*. UNICAMP.
- Copeland, L., Blazek, J., Salman, H., & Tang, M. C. (2009). Form and functionality of starch. *Food Hydrocolloids*, *23*(6), 1527–1534. <https://doi.org/10.1016/j.foodhyd.2008.09.016>
- Cordenunsi, B. R., Genovese, M. I., Oliveira Do Nascimento, J. R., Aymoto Hassimoto, N. M., José Dos Santos, R., & Lajolo, F. M. (2005). Effects of temperature on the chemical composition and antioxidant activity of three strawberry cultivars. *Food Chemistry*, *91*(1), 113–121. <https://doi.org/10.1016/j.foodchem.2004.05.054>
- Cuq, B., Gontard, N., Cuq, J. L., & Guilbert, S. (1996). Rheological model for the mechanical properties of myofibrillar protein-based films. *Journal of Agricultural and Food Chemistry*, *44*(4), 1116–1122. <https://doi.org/10.1021/jf950389n>
- Cuq, B., Gontard, N., Cuq, J. L., & Guilbert, S. (1997). Selected Functional Properties of Fish Myofibrillar Protein-Based Films As Affected by Hydrophilic Plasticizers. *Journal of Agricultural and Food Chemistry*, *45*(3), 622–626. <https://doi.org/10.1021/jf960352i>
- da Silva Simão, R. (2018). *Produção e caracterização de snacks de manga em forma de filmes, obtidos por cast-tape drying*.
- da Silva Simão, R., de Moraes, J. O., de Souza, P. G., Mattar Carciofi, B. A., & Laurindo, J. B. (2019). Production of mango leathers by cast-tape drying: Product characteristics and sensory evaluation. *LWT - Food Science and Technology*, *99*(May 2018), 445–452. <https://doi.org/10.1016/j.lwt.2018.10.013>
- Dann, J. R. (1970). Forces involved in the adhesive process. I. Critical surface tensions of polymeric solids as determined with polar liquids. *Journal of Colloid And Interface Science*, *32*(2), 302–

320. [https://doi.org/10.1016/0021-9797\(70\)90054-8](https://doi.org/10.1016/0021-9797(70)90054-8)
- de Bruijn, J., & Bórquez, R. (2014). Quality retention in strawberries dried by emerging dehydration methods. *Food Research International*, 63, 42–48. <https://doi.org/10.1016/j.foodres.2014.03.029>
- De Moraes, J. O., Scheibe, A. S., Sereno, A., & Laurindo, J. B. (2013). Scale-up of the production of cassava starch-based films using tape-casting. *Journal of Food Engineering*, 119(4), 800–808. <https://doi.org/10.1016/j.jfoodeng.2013.07.009>
- de Souza, P. G. (2015). *Produção e caracterização de açaí (Euterpe oleracea Mart.) desidratado em pó por cast-tape drying*. Universidade Federal de Santa Catarina.
- Domínguez, J. M. (2011). Drying. *Comprehensive Biotechnology*, 727–735. <https://doi.org/10.1016/B978-0-08-088504-9.00129-X>
- Dopfer, D., Palzer, S., Heinrich, S., Fries, L., Antonyuk, S., Haider, C., & Salman, A. D. (2013). Adhesion mechanisms between water soluble particles. *Powder Technology*, 238, 35–49. <https://doi.org/10.1016/j.powtec.2012.06.029>
- Dorrer, C., & Rühle, J. (2009). Some thoughts on superhydrophobic wetting. *Soft Matter*, 5(1), 51–61. <https://doi.org/10.1039/b811945g>
- Downton, G. E., Flores-luna, J. L., & King, C. J. (1982). Mechanism of Stickiness in Hygroscopic , Amorphous Powders. *Industrial & Engineering Chemistry Fundamentals*, 21(4), 447–451.
- Durigon, A., de Souza, P. G., Carciofi, B. A. M., & Laurindo, J. B. (2016). Cast-tape drying of tomato juice for the production of powdered tomato. *Food and Bioprocess Technology*, 100, 145–155. <https://doi.org/10.1016/j.fbp.2016.06.019>
- Durigon, A., Parisotto, E. I. B., Carciofi, B. A. M., & Laurindo, J. B. (2017). Heat transfer and drying kinetics of tomato pulp processed by cast-tape drying. *Drying Technology*, 39(37), 1–9. <https://doi.org/10.1080/07373937.2017.1304411>
- Ebnesajjad, S. (2011). Surface tension and its measurement. In *Handbook of Adhesives and Surface Preparation* (pp. 21–30). Elsevier Inc. <https://doi.org/10.1016/B978-1-4377-4461-3.10003-3>
- Ebnesajjad, S. (2014). Theories of Adhesion. In *Surface Treatment of Materials for Adhesive Bonding* (pp. 77–91). <https://doi.org/10.1016/B978-0-323-26435-8.00005-8>
- Extrand, C. W. (2009). Work of Wetting Associated with the Spreading of Sessile Drops. In K. L. Mittal (Ed.), *Contact Angle, Wettability and Adhesion* (pp. 81–93). CRC Press.
- FAO. (2013). Pectins. In S. O. Idowu, N. Capaldi, L. Zu, & A. Das Gupta (Eds.), *Compendium of Food Additive Specifications*, 52 (Vol. 9). Springer Berlin Heidelberg. <https://doi.org/10.1007/978-3-642-28036-8>
- FAO. (2017). *FAO Crop Database*. Food and Agriculture Organization. <http://www.faostat.fao.org>

- Fazaeli, M., Emam-Djomeh, Z., Kalbasi Ashtari, A., & Omid, M. (2012). Effect of spray drying conditions and feed composition on the physical properties of black mulberry juice powder. *Food and Bioproducts Processing*, 90(4), 667–675. <https://doi.org/10.1016/j.fbp.2012.04.006>
- Fellows, P. J. (2000). *Food processing technology, Principles and practice* (2nd ed.). Woodhead Publishing Limited and CRC Press LLC. <https://doi.org/10.1201/9780203485248>
- Femenia, A., Lefebvre, A. C., Thebaudin, J. Y., Robertson, J. A., & Bourgeois, C. M. (1997). Physical and sensory properties of model foods supplemented with cauliflower fiber. *Journal of Food Science*, 62(4), 635–639. <https://doi.org/10.1111/j.1365-2621.1997.tb15426.x>
- Ferry, J. D., & Myers, H. S. (1961). Viscoelastic Properties of Polymers. In *Journal of The Electrochemical Society* (Vol. 108). <https://doi.org/10.1149/1.2428174>
- Figueroa, Y., Guevara, M., Pérez, A., Cova, A., Sandoval, A. J., & Müller, A. J. (2016). Effect of sugar addition on glass transition temperatures of cassava starch with low to intermediate moisture contents. *Carbohydrate Polymers*, 146, 231–237. <https://doi.org/10.1016/j.carbpol.2016.03.054>
- Fletcher, P. D. I., & Nicholls, R. J. (2000). Contact angles of surfactant solutions in oil solvents on low energy solid surfaces. *Physical Chemistry Chemical Physics*, 2(3), 361–365. <https://doi.org/10.1039/a908926h>
- Fox, T. G., & Flory, P. J. (1950). Second-order transition temperatures and related properties of polystyrene. I. Influence of molecular weight. *Journal of Applied Physics*, 21(6), 581–591. <https://doi.org/10.1063/1.1699711>
- Frabetti, A. C. C., Durigon, A., & Laurindo, J. B. (2018). Effect of process variables on the drying of guava pulp by cast-tape drying. *LWT - Food Science and Technology*, 96, 620–626. <https://doi.org/10.1016/j.lwt.2018.06.021>
- Funke, U., Bergthaller, W., & Lindhauer, M. G. (1998). Processing and characterization of biodegradable products based on starch. *Polymer Degradation and Stability*, 59(1–3), 293–296. [https://doi.org/10.1016/S0141-3910\(97\)00163-8](https://doi.org/10.1016/S0141-3910(97)00163-8)
- Gao, W., Liu, P., Li, X., Qiu, L., Hou, H., & Cui, B. (2019). The co-plasticization effects of glycerol and small molecular sugars on starch-based nanocomposite films prepared by extrusion blowing. *International Journal of Biological Macromolecules*, 133, 1175–1181. <https://doi.org/10.1016/j.ijbiomac.2019.04.193>
- García, L., Cova, A., Sandoval, A. J., Müller, A. J., & Carrasquel, L. M. (2012). Glass transition temperatures of cassava starch-whey protein concentrate systems at low and intermediate water content. *Carbohydrate Polymers*, 87(2), 1375–1382. <https://doi.org/10.1016/j.carbpol.2011.09.035>

- Gardini, D., Deluca, M., Nagliati, M., & Galassi, C. (2010). Flow properties of PLZTN aqueous suspensions for tape casting. *Ceramics International*, 36(5), 1687–1696. <https://doi.org/10.1016/j.ceramint.2010.03.011>
- Gava, A. J., da Silva, C. A. B., & Frias, J. R. G. (2009). *Tecnologia de alimentos*. NBL.
- Gay, C. (2002). Stickiness - Some fundamentals of adhesion. *Integrative and Comparative Biology*, 42(6), 1123–1126. <https://doi.org/10.1093/icb/42.6.1123>
- Geankoplis, C. J. (1998). *Transport Processes and Unit Operations* (3rd ed.). Prentice-Hall International, Inc.
- Genin, N., & René, F. (1995). Analyse du rôle de la transition vitreuse dans les procédés de conservation agro-alimentaires. *Journal of Food Engineering*, 26(4), 391–408. [https://doi.org/10.1016/0260-8774\(94\)00059-I](https://doi.org/10.1016/0260-8774(94)00059-I)
- Gent, A. N., & Schultz, J. (1972). Effect of Wetting Liquids on the Strength of Adhesion of Viscoelastic Materials. *The Journal of Adhesion*, 3(4), 281–294. <https://doi.org/10.1080/00218467208072199>
- Ghanbarzadeh, B., & Almasi, H. (2011). Physical properties of edible emulsified films based on carboxymethyl cellulose and oleic acid. *International Journal of Biological Macromolecules*, 48(1), 44–49. <https://doi.org/10.1016/j.ijbiomac.2010.09.014>
- Ghanbarzadeh, B., Almasi, H., & Entezami, A. A. (2010). Physical properties of edible modified starch/carboxymethyl cellulose films. *Innovative Food Science and Emerging Technologies*, 11(4), 697–702. <https://doi.org/10.1016/j.ifset.2010.06.001>
- Gibson, M., Newsham, P., Gibson, M., & Newsham, P. (2018). Rheology. *Food Science and the Culinary Arts*, 89–103. <https://doi.org/10.1016/B978-0-12-811816-0.00007-5>
- Gontard, N. (1991). *Films et enrobages comestibles : étude et amélioration des propriétés filmogènes du gluten*. CIRAD-CEEMAT.
- Good, R. J. (1992). Contact angle, wetting and adhesion. *J. Adhesion Sci. Technol.*, 6(12), 1269–1302.
- Goula, A. M., Karapantsios, T. D., Achilias, D. S., & Adamopoulos, K. G. (2008). Water sorption isotherms and glass transition temperature of spray dried tomato pulp. *Journal of Food Engineering*, 85(1), 73–83. <https://doi.org/10.1016/j.jfoodeng.2007.07.015>
- Grajales-Lagunes, A., Rivera-Bautista, C., Loredo-García, I. O., González-García, R., González-Chávez, M. M., Schmidt, S. J., & Ruiz-Cabrera, M. A. (2018). Using model food systems to develop mathematical models for construction of state diagrams of fruit products. *Journal of Food Engineering*, 230, 72–81. <https://doi.org/10.1016/j.jfoodeng.2018.02.025>
- Guan, F., & Seib, P. A. (1994). Instrumental probe and method to measure stickiness of cooked

- spaghetti and noodles. *Cereal Chemistry*, 71(4), 330–337.
- Guilleminet, J., Bistac, S., & Schultz, J. (2002). Relationship between polymer viscoelastic properties and adhesive behaviour. *International Journal of Adhesion and Adhesives*, 22(1), 1–5. [https://doi.org/10.1016/S0143-7496\(01\)00027-6](https://doi.org/10.1016/S0143-7496(01)00027-6)
- Gutiérrez, T. J., Tapia, M. S., Pérez, E., & Famá, L. (2015). Structural and mechanical properties of edible films made from native and modified cush-cush yam and cassava starch. *Food Hydrocolloids*, 45, 211–217. <https://doi.org/10.1016/j.foodhyd.2014.11.017>
- Hammami, C., & René, F. (1997). Determination of freeze-drying process variables for strawberries. *Journal of Food Engineering*, 32(2), 133–154. [https://doi.org/10.1016/S0260-8774\(97\)00023-X](https://doi.org/10.1016/S0260-8774(97)00023-X)
- Harper, W. J. (2009). Model food systems and protein functionality. In *Milk Proteins: From Expressions to Food* (pp. 409–428). Elsevier Inc. <https://doi.org/10.1016/B978-0-12-374039-7.00014-3>
- Hoseney, R. C., & Smewing, J. (1999). Instrumental measurement of stickiness of doughs and other foods. *Journal of Texture Studies*, 30, 123–136.
- Hubinger, M., Menegalli, F. C., Aguerre, R. J., & Suarez, C. (1992). Water Vapor Adsorption Isotherms of Guava, Mango and Pineapple. *Journal of Food Science*, 57(6), 1405–1407. <https://doi.org/10.1111/j.1365-2621.1992.tb06869.x>
- Ibrahim, T. H., Burk, T. R., Etzler, F. M., & Neuman, R. D. (2000). Direct adhesion measurements of pharmaceutical particles to gelatin capsule surfaces. *Journal of Adhesion Science and Technology*, 14(10), 1225–1242. <https://doi.org/10.1201/b12164-42>
- Iida, K., Otsuka, A., Danjo, K., & Sunada, H. (1992). Measurement of Adhesive Force between Particles and Polymer Films. *Chemical Pharmaceutical Bulletin*, 40(1), 189–192.
- Incropera, F. P., Lavine, A. S., Bergman, T. L., & DeWitt, D. P. (2007). *Fundamentals of heat and mass transfer*. Wiley.
- Jayasundera, M., Adhikari, B., Adhikari, R., & Aldred, P. (2011). The effects of proteins and low molecular weight surfactants on spray drying of model sugar-rich foods: Powder production and characterisation. *Journal of Food Engineering*, 104(2), 259–271. <https://doi.org/10.1016/j.jfoodeng.2010.12.017>
- Johari, G. P., Hallbrucker, A., & Mayer, E. (1987). The glass–liquid transition of hyperquenched water. *Nature*, 330(6148), 552–553.
- Jones, J. K. (1995). Strawberry. In J. Smartt & N. W. Simmonds (Eds.), *Evolution of crop plants* (Longman, pp. 412–417).
- Karbowiak, T., Debeaufort, F., & Voilley, A. (2006). Importance of Surface Tension



- Characterization for Food , Pharmaceutical and Packaging Products : A Review. *Critical Reviews in Food Science and Nutrition*, 46(5), 391–407. <https://doi.org/10.1080/10408390591000884>
- Karim, A. M., Rothstein, J. P., & Kavehpour, H. P. (2018). Experimental study of dynamic contact angles on rough hydrophobic surfaces. *Journal of Colloid and Interface Science*, 513, 658–665. <https://doi.org/10.1016/j.jcis.2017.11.075>
- Kaur, G., Saha, S., Kumari, K., & Datta, A. K. (2017). Mango pulp drying by refractance window method. *Agricultural Engineering International*, 19(4).
- Keijbets, E. L., Chen, J., Dickinson, E., & Vieira, J. (2009). Surface energy investigation of chocolate adhesion to solid mould materials. *Journal of Food Engineering*, 92(2), 217–225. <https://doi.org/10.1016/j.jfoodeng.2008.11.008>
- Kilburn, D., Claude, J., Schweizer, T., Alam, A., & Ubbink, J. (2005). Carbohydrate polymers in amorphous states: An integrated thermodynamic and nanostructural investigation. *Biomacromolecules*, 6(2), 864–879. <https://doi.org/10.1021/bm049355r>
- Kilcast, D., & Roberts, C. (1998). Perception and measurement of stickiness in sugar-rich foods. *Journal of Texture Studies*, 29(1), 81–100. <https://doi.org/10.1111/j.1745-4603.1998.tb00155.x>
- Kinloch, A. J. (1987). Interfacial contact. In *Adhesion and Adhesives, Science and Technology* (pp. 18–51). Springer Netherlands. <https://doi.org/10.1007/978-94-015-7764-9>
- Kothekar, S. C., Ware, A. M., Waghmare, J. T., & Momin, S. A. (2007). Comparative analysis of the properties of Tween-20, Tween-60, Tween-80, Arlacel-60, and Arlacel-80. *Journal of Dispersion Science and Technology*, 28(3), 477–484. <https://doi.org/10.1080/01932690601108045>
- Krevelen, D. W. van, & Nijenhuis, K. te. (2009). Properties of Polymers. In *Endeavour* (4th ed.). Elsevier B.V. [https://doi.org/10.1016/0160-9327\(92\)90023-I](https://doi.org/10.1016/0160-9327(92)90023-I)
- Kumagai, H., MacNaughtan, W., Farhat, I. A., & Mitchell, J. R. (2002). The influence of carrageenan on molecular mobility in low moisture amorphous sugars. *Carbohydrate Polymers*, 48(4), 341–349. [https://doi.org/10.1016/S0144-8617\(01\)00269-7](https://doi.org/10.1016/S0144-8617(01)00269-7)
- Labuza, T. P. (1980). The effect of water activity on reaction kinetics of food deterioration. *Food Technology*, 34(59), 36–41.
- Lagos, J. B., Vicentini, N. M., Dos Santos, R. M. C., Bittante, A. M. Q. B., & Sobral, P. J. A. (2015). Mechanical properties of cassava starch films as affected by different plasticizers and different relative humidity conditions. *International Journal of Food Studies*, 4(1), 116–125. <https://doi.org/10.7455/ijfs/4.1.2015.a10>
- Lam, C. N. C., Wu, R., Li, D., Hair, M. L., & Neumann, A. W. (2002). Study of the advancing and

- receding contact angles: liquid sorption as a cause of contact angle hysteresis. *Advances in Colloid and Interface Science*, 96, 169–191. [https://doi.org/10.1016/S0001-8686\(01\)00080-X](https://doi.org/10.1016/S0001-8686(01)00080-X)
- Laohakunjit, N., & Noomhorm, A. (2004). Effect of plasticizers on mechanical and barrier properties of rice starch film. *Starch/Staerke*, 56(8), 348–356. <https://doi.org/10.1002/star.200300249>
- Liu, X., Wang, L., Qiao, Y., Sun, X., Ma, S., Cheng, X., Qi, W., Huang, W., & Li, Y. (2018). Adhesion of liquid food to packaging surfaces : Mechanisms , test methods, influencing factors and anti-adhesion methods. *Journal of Food Engineering*, 228, 102–117. <https://doi.org/10.1016/j.jfoodeng.2018.02.002>
- Loibl, F., Schmidt, M. C., Auer-Seidl, A., Kirchner, C., Holtz, C., Müller, K., Stramm, C., & Langowski, H.-C. (2012). The Emptying Behaviour of Highly Viscous Liquids . Part II : Development of Test Methods and Evaluation of Untreated and Coated Films. *Journal of Adhesion Science and Technology*, 26, 2469–2503. <https://doi.org/10.1163/156856111X610117>
- Lorentz, H., Rogers, R., & Jones, L. (2007). The impact of lipid on contact angle wettability. *Optometry and Vision Science*, 84(10), 946–953. <https://doi.org/10.1097/OPX.0b013e318157a6c1>
- Lorevice, M. V., De Moura, M. R., Aouada, F. A., & Mattoso, L. H. C. (2012). Development of novel guava puree films containing chitosan nanoparticles. *Journal of Nanoscience and Nanotechnology*, 12(3), 2711–2717. <https://doi.org/10.1166/jnn.2012.5716>
- Lourdin, D., Coignard, L., Bizot, H., & Colonna, P. (1997). Influence of equilibrium relative humidity and plasticizer concentration on the water content and glass transition of starch materials. *Polymer*, 38(21), 5401–5406. [https://doi.org/10.1016/S0032-3861\(97\)00082-7](https://doi.org/10.1016/S0032-3861(97)00082-7)
- Lund, D. (1984). Influence of time , temperature , moisture , ingredients , and processing conditions on starch gelatinization. *CRC Critical Reviews in Food Science and Nutrition*, 20(4), 249–273. <https://doi.org/10.1080/10408398409527391>
- Maceiras, R., Álvarez, E., & Cancela, M. A. (2007). Rheological properties of fruit purees: Effect of cooking. *Journal of Food Engineering*, 80(3), 763–769. <https://doi.org/10.1016/j.jfoodeng.2006.06.028>
- Madrigal, L., Sandoval, A. J., & Müller, A. J. (2011). Effects of corn oil on glass transition temperatures of cassava starch. *Carbohydrate Polymers*, 85(4), 875–884. <https://doi.org/10.1016/j.carbpol.2011.04.013>
- Mali, S., Sakanaka, L. S., Yamashita, F., & Grossmann, M. V. E. (2005). Water sorption and mechanical properties of cassava starch films and their relation to plasticizing effect. *Carbohydrate Polymers*, 60(3), 283–289. <https://doi.org/10.1016/j.carbpol.2005.01.003>



- Marcilla, A., & Beltrán, M. (2012). Mechanisms of Plasticizers action. *Handbook of Plasticizers*, 119–133. <https://doi.org/10.1016/b978-1-895198-50-8.50007-2>
- Maritza, A. M., Sabah, M., Anaberta, C. M., Montejano-Gaitán, J. G., & Allaf, K. (2012). Comparative study of various drying processes at physical and chemical properties of strawberries (Fragariavarcamarosa). *Procedia Engineering*, 42(August), 267–282. <https://doi.org/10.1016/j.proeng.2012.07.418>
- Mazza, G. (1982). Moisture sorption isotherms of potato slices. *International Journal of Food Science & Technology*, 17(1), 47–54. <https://doi.org/10.1111/j.1365-2621.1982.tb00158.x>
- McGuire, J. (2005). Surface Properties. In M. A. Rao, S. S. H. Rizvi, & A. K. Datta (Eds.), *Engineering Properties of Foods* (Third Edit, pp. 679–701). CRC Press.
- McHugh, T. H., & Senesi, E. (2000). Apple Wraps: A Novel Method to Improve the Quality and Extend the Shelf Life of Fresh-cut Apples. *Journal of Food Science*, 65(3), 480–485. <https://doi.org/10.1111/j.1365-2621.2000.tb16032.x>
- McMinn, W. A. M., & Magee, T. R. A. (1997). Moisture sorption characteristics of starch materials. *Drying Technology*, 15(5), 1527–1551. <https://doi.org/10.1080/07373939708917306>
- Méndez-Lagunas, L., Rodríguez-Ramírez, J., Cruz-Gracida, M., Sandoval-Torres, S., & Barriada-Bernal, G. (2017). Convective drying kinetics of strawberry (*Fragaria ananassa*): Effects on antioxidant activity, anthocyanins and total phenolic content. *Food Chemistry*, 230, 174–181. <https://doi.org/10.1016/j.foodchem.2017.03.010>
- Michalski, M. C., Desobry, S., Babak, V., & Hardy, J. (1999). Adhesion of food emulsions to packaging and equipment surfaces. *Colloids and Surfaces A: Physicochemical and Engineering Aspects*, 149, 107–121. [https://doi.org/10.1016/S0927-7757\(98\)00299-4](https://doi.org/10.1016/S0927-7757(98)00299-4)
- Miller, J. D., Veeramasoneni, S., Drelich, J., Yalamanchili, M. R., & Yamauchi, G. (1996). Effect of roughness as determined by atomic force microscopy on the wetting properties of PTFE thin films. *Polymer Engineering and Science*, 36(14), 1849–1855. <https://doi.org/10.1002/pen.10580>
- Momany, F. A., & Willett, J. L. (2002). Molecular dynamics calculations on amylose fragments. I. Glass transition temperatures of maltodecaose at 1, 5, 10, and 15.8% hydration. *Biopolymers*, 63(2), 99–110. <https://doi.org/10.1002/bip.10014>
- Moraes, J. O. (2013). *Produção e caracterização de filmes de amido-glicerol-fibras de celulose elaborados por tape-casting*. Universidade Federal de Santa Catarina.
- Moraga, G., Martínez-Navarrete, N., & Chiralt, A. (2004). Water sorption isotherms and glass transition in strawberries: Influence of pretreatment. *Journal of Food Engineering*, 62(4), 315–321. [https://doi.org/10.1016/S0260-8774\(03\)00245-0](https://doi.org/10.1016/S0260-8774(03)00245-0)

- Morris, B. A. (2017). Adhesion. In *The Science and Technology of Flexible Packaging* (pp. 351–400). <https://doi.org/10.1016/c2013-0-00506-3>
- Mosquera, L. H., Moraga, G., & Martínez-Navarrete, N. (2012). Critical water activity and critical water content of freeze-dried strawberry powder as affected by maltodextrin and arabic gum. *Food Research International*, *47*(2), 201–206. <https://doi.org/10.1016/j.foodres.2011.05.019>
- Müller, C. M. O., Laurindo, J. B., & Yamashita, F. (2009). Effect of cellulose fibers on the crystallinity and mechanical properties of starch-based films at different relative humidity values. *Carbohydrate Polymers*, *77*(2), 293–299. <https://doi.org/10.1016/j.carbpol.2008.12.030>
- Muzaffar, K., Nayik, G. A., & Kumar, P. (2015). Stickiness Problem Associated with Spray Drying of Sugar and Acid Rich Foods: A Mini Review. *Journal of Nutrition & Food Sciences*, *S12*(003), 10–13. <https://doi.org/10.4172/2155-9600.s12-003>
- Naqash, F., Masoodi, F. A., Rather, S. A., Wani, S. M., & Gani, A. (2017). Emerging concepts in the nutraceutical and functional properties of pectin—A Review. *Carbohydrate Polymers*, *168*, 227–239. <https://doi.org/10.1016/j.carbpol.2017.03.058>
- Nemzer, B., Vargas, L., Xia, X., Sintara, M., & Feng, H. (2018). Phytochemical and physical properties of blueberries, tart cherries, strawberries, and cranberries as affected by different drying methods. *Food Chemistry*, *262*(January), 242–250. <https://doi.org/10.1016/j.foodchem.2018.04.047>
- Nguyen, T. K., Khalloufi, S., Mondor, M., & Ratti, C. (2020). Moisture profile analysis of food models undergoing glass transition during air-drying. *Journal of Food Engineering*, *281*(November 2019), 109995. <https://doi.org/10.1016/j.jfoodeng.2020.109995>
- Nguyen Vu, H. P., & Lumdubwong, N. (2016). Starch behaviors and mechanical properties of starch blend films with different plasticizers. *Carbohydrate Polymers*, *154*, 112–120. <https://doi.org/10.1016/j.carbpol.2016.08.034>
- Nicholls, R. J., Appelqvist, I. A. M., Davies, A. P., Ingman, S. J., & Lillford, P. J. (1995). Glass transitions and the fracture behaviour of gluten and starches within the glassy state. *Journal of Cereal Science*, *21*(1), 25–36. [https://doi.org/10.1016/S0733-5210\(95\)80005-0](https://doi.org/10.1016/S0733-5210(95)80005-0)
- Nindo, C. I., Powers, J. R., & Tang, J. (2007). Influence of Refractance Window evaporation on quality of juices from small fruits. *LWT - Food Science and Technology*, *40*(6), 1000–1007. <https://doi.org/10.1016/j.lwt.2006.07.006>
- Nindo, C. I., & Tang, J. (2007). Refractance window dehydration technology: A novel contact drying method. *Drying Technology*, *25*(1), 37–48. <https://doi.org/10.1080/07373930601152673>
- Nindo, C. I., Tang, J., Powers, J. R., & Takhar, P. S. (2007). Rheological properties of blueberry puree for processing applications. *LWT - Food Science and Technology*, *40*(2), 292–299.

<https://doi.org/10.1016/j.lwt.2005.10.003>

- Noren, N. E., Scanlon, M. G., & Arntfield, S. D. (2019). Differentiating between tackiness and stickiness and their induction in foods. *Trends in Food Science and Technology*, 88(September 2018), 290–301. <https://doi.org/10.1016/j.tifs.2019.03.014>
- Novotná, P., Landfeld, A., Kýhos, K., Houška, M., & Strohal, J. (2018). Use of helical ribbon mixer for measurement of rheological properties of fruit pulps. *Czech Journal of Food Sciences*, 19(No. 4), 148–153. <https://doi.org/10.17221/6599-cjfs>
- Nussinovitch, A. (2017). Adhesion: definition and nomenclature. In *Adhesion in Foods* (pp. 1–16). Wiley-Blackwell. <https://doi.org/10.1002/9781118851579>
- Odrizola-Serrano, I., Soliva-Fortuny, R., & Martín-Belloso, O. (2010). Changes in bioactive composition of fresh-cut strawberries stored under superatmospheric oxygen, low-oxygen or passive atmospheres. *Journal of Food Composition and Analysis*, 23(1), 37–43. <https://doi.org/10.1016/j.jfca.2009.07.007>
- Okos, M. R., Campanella, O., Narsimhan, G., Singh, R. K., & Weitnauer, A. C. (2007). Food Dehydration. In D. R. Heldman & D. B. Lund (Eds.), *Handbook of Food Engineering* (2nd ed., p. 1023). CRC Press. <https://doi.org/10.1201/9781420014372>
- Olympus Corporation. (2019). *Roughness (3D) parameter*. [https://www.olympus-ims.com/en/knowledge/metrology/roughness/3d\\_parameter/](https://www.olympus-ims.com/en/knowledge/metrology/roughness/3d_parameter/)
- Oroian, M., Ropciuc, S., Amariei, S., & Gutt, G. (2015). Correlations between density, viscosity, surface tension and ultrasonic velocity of different mono- and di-saccharides. *Journal of Molecular Liquids*, 207, 145–151. <https://doi.org/10.1016/j.molliq.2015.03.033>
- Ortiz-Jerez, M. J., Gulati, T., Datta, A. K., & Ochoa-Martínez, C. I. (2015). Quantitative understanding of Refractance Window<sup>TM</sup> drying. *Food and Bioproducts Processing*, 95, 237–253. <https://doi.org/10.1016/j.fbp.2015.05.010>
- Ortiz-Jerez, M. J., & Ochoa-Martínez, C. I. (2015). Heat Transfer Mechanisms in Conductive Hydro-Drying of Pumpkin (*Cucurbita maxima*) Pieces. *Drying Technology*, 33(8), 965–972. <https://doi.org/10.1080/07373937.2015.1009538>
- Otoni, C. G., Avena-Bustillos, R. J., Azeredo, H. M. C., Lorevice, M. V., Moura, M. R., Mattoso, L. H. C., & McHugh, T. H. (2017). Recent Advances on Edible Films Based on Fruits and Vegetables—A Review. *Comprehensive Reviews in Food Science and Food Safety*, 00, 1–19. <https://doi.org/10.1111/1541-4337.12281>
- Padday, J. F. (1968). Effect of temperature on the wettability of low-energy surfaces. *Journal of Colloid And Interface Science*, 28(3–4), 557–564. [https://doi.org/10.1016/0021-9797\(68\)90089-1](https://doi.org/10.1016/0021-9797(68)90089-1)

- Papadakis, S. E., & Bahu, R. E. (1992). The sticky issues of drying. *Drying Technology*, *10*(4), 817–837. <https://doi.org/10.1080/07373939208916484>
- Papaioannou, J., Giannousakis, A., Dimakopoulos, Y., & Tsamopoulos, J. (2014). Bubble deformation and growth inside viscoelastic filaments undergoing very large extensions. *Industrial and Engineering Chemistry Research*, *53*(18), 7548–7569. <https://doi.org/10.1021/ie403311n>
- Park, S. Il, & Zhao, Y. (2006). Development and characterization of edible films from cranberry pomace extracts. *Journal of Food Science*, *71*(2). <https://doi.org/10.1111/j.1365-2621.2006.tb08902.x>
- Passerone, A., Valenza, F., & Muolo, M. L. (2013). Wetting at high temperature. In M. Ferrari, L. Liggieri, & R. Miller (Eds.), *Drops and bubbles in contact with solid surfaces* (pp. 300–322). CRC Press.
- Perdomo, J., Cova, A., Sandoval, A. J., García, L., Laredo, E., & Müller, A. J. (2009). Glass transition temperatures and water sorption isotherms of cassava starch. *Carbohydrate Polymers*, *76*(2), 305–313. <https://doi.org/10.1016/j.carbpol.2008.10.023>
- Peressini, D., Bravin, B., Lapasin, R., Rizzotti, C., & Sensidoni, A. (2003). Starch-methylcellulose based edible films: Rheological properties of film-forming dispersions. *Journal of Food Engineering*, *59*(1), 25–32. [https://doi.org/10.1016/S0260-8774\(02\)00426-0](https://doi.org/10.1016/S0260-8774(02)00426-0)
- Pérez, A., Sandoval, A. J., Cova, A., & Müller, A. J. (2014). Glass transitions and physical aging of cassava starch - Corn oil blends. *Carbohydrate Polymers*, *105*(1), 244–252. <https://doi.org/10.1016/j.carbpol.2014.01.032>
- Pizzi, A., & Mittal, K. L. (2003). *Handbook of Adhesive Technology* (Second Edi). Marcel Dekker.
- Pocius, A. V. (1986). Fundamentals of Structural Adhesive Bonding. In S. R. Hartshorn (Ed.), *Structural Adhesives, Chemistry and Technology* (pp. 1–68). Plenum Press. <https://doi.org/10.4139/sfj.40.1171>
- Pocius, A. V. (2012a). Introduction. In *Adhesion and Adhesives Technology - An Introduction* (pp. 1–15). Hanser Gardner Publications, Inc.
- Pocius, A. V. (2012b). Mechanical Tests of Adhesive Bond Performance. In *Adhesion and Adhesives Technology - An Introduction* (pp. 47–83). Hanser Gardner Publications, Inc.
- Quéré, D. (2008). Wetting and Roughness. *Annual Review of Materials Research*, *38*(1), 71–99. <https://doi.org/10.1146/annurev.matsci.38.060407.132434>
- Quirijns, E. J., Van Boxtel, A. J. B., Van Loon, W. K. P., & Van Straten, G. (2005). Sorption isotherms, GAB parameters and isosteric heat of sorption. *Journal of the Science of Food and Agriculture*, *85*(11), 1805–1814. <https://doi.org/10.1002/jsfa.2140>

- Rahman, M. S. (2006). State diagram of foods: Its potential use in food processing and product stability. *Trends in Food Science and Technology*, 17(3), 129–141. <https://doi.org/10.1016/j.tifs.2005.09.009>
- Ramiasa, M., Ralston, J., Fetzer, R., & Sedev, R. (2014). The influence of topography on dynamic wetting. *Advances in Colloid and Interface Science*, 206, 275–293. <https://doi.org/10.1016/j.cis.2013.04.005>
- Ranade, M. B. (1987). Adhesion and removal of fine particles on surfaces. *Aerosol Science and Technology*, 7(2), 161–176. <https://doi.org/10.1080/02786828708959155>
- Rao, M. A. (1977). Rheology of liquid foods - a review. *Journal of Texture Studies*, 8(2), 135–168. <https://doi.org/10.1111/j.1745-4603.1977.tb01173.x>
- Rao, M. A. (2007a). Rheological behavior of processed fluid and semisolid foods. In Gustavo Barbosa-Cánovas (Ed.), *Rheology of Fluid and Semisolid Foods: Principles and Applications* (Second, pp. 223–261). Springer.
- Rao, M. A. (2007b). Role of rheological behavior in sensory assessment of foods and swallowing. In Gustavo Barbosa-Cánovas (Ed.), *Rheology of Fluid and Semisolid Foods: Principles and Applications* (Second, pp. 403–417). Springer.
- Ratti, C. (2009). Novel Food Dryers and Future Perspectives. In C. Ratti (Ed.), *Advances in food dehydration* (pp. 447–458). CRC Press.
- Ratti, C., & Mujumdar, A. (2006). Infrared Drying. *Handbook of Industrial Drying, Third Edition, May 2015*. <https://doi.org/10.1201/9781420017618.ch18>
- Rha, C. (1975). Thermal Properties of Food Materials. In C. Rha (Ed.), *Theory, Determination and Control of Physical Properties of Food Materials* (pp. 311–355). D. Reidel Publishing Company.
- Rizvi, S. S. H. (2014). Thermodynamic properties of foods in dehydration. In *Engineering Properties of Foods, Fourth Edition* (pp. 359–435). <https://doi.org/10.1201/b16897>
- Roos, Y. (1993a). Melting and glass transitions of low molecular weight carbohydrates. *Carbohydrate Research*, 238(C), 39–48. [https://doi.org/10.1016/0008-6215\(93\)87004-C](https://doi.org/10.1016/0008-6215(93)87004-C)
- Roos, Y. (1993b). Water activity and physical state effects on amorphous food stability. *Journal of Food Processing and Preservation*, 16(6), 433–447. <https://doi.org/10.1111/j.1745-4549.1993.tb00221.x>
- Roos, Y. (2010). Glass Transition Temperature and Its Relevance in Food Processing. *Annual Review of Food Science and Technology*, 1(1), 469–496. <https://doi.org/10.1146/annurev.food.102308.124139>
- Roos, Y., Franks, F., Karel, M., Labuza, T., Levine, H., Mathlouthi, M., Reid, D., Shalaev, E., &

- Slade, L. (2012). Comment on the melting and decomposition of sugars. *Journal of Agricultural and Food Chemistry*, 60(41), 10359–10362. <https://doi.org/10.1021/jf3002526>
- Roos, Y. H. (1987). Effect of Moisture on the Thermal Behavior of Strawberries Studied using Differential Scanning Calorimetry. *Journal of Food Science*, 52(1), 146–149. <https://doi.org/10.1111/j.1365-2621.1987.tb13992.x>
- Roos, Y., & Karel, M. (1991a). Phase transitions of mixtures of amorphous polysaccharides and sugars. *Biotechnology Progress*, 7(1), 49–53. <https://doi.org/10.1021/bp00007a008>
- Roos, Y., & Karel, M. (1991b). Plasticizing Effect of Water on Thermal Behavior and Crystallization of Amorphous Food Models. *Journal of Food Science*, 56(1), 38–43.
- Roos, Y., Karel, M., & Kokini, J. (1996). Glass Transitions in low moisture and frozen foods: effects on shelf life and quality. *Food Technology*, November, 95–108.
- Ruiz-Cabrera, M. A., Rivera-Bautista, C., Grajales-Lagunes, A., González-García, R., & Schmidt, S. J. (2016). State diagrams for mixtures of low molecular weight carbohydrates. *Journal of Food Engineering*, 171, 185–193. <https://doi.org/10.1016/j.jfoodeng.2015.10.038>
- Saavedra-Leos, M. Z., Grajales-Lagunes, A., González-García, R., Toxqui-Terán, A., Pérez-García, S. A., Abud-Archila, M. A., & Ruiz-Cabrera, M. A. (2012). Glass Transition Study in Model Food Systems Prepared with Mixtures of Fructose, Glucose, and Sucrose. *Journal of Food Science*, 77(5). <https://doi.org/10.1111/j.1750-3841.2012.02678.x>
- Sabarez, H. T. (2015). Modelling of drying processes for food materials. In *Modeling Food Processing Operations*. Elsevier Ltd. <https://doi.org/10.1016/B978-1-78242-284-6.00004-0>
- Saha, D., & Bhattacharya, S. (2010). Hydrocolloids as thickening and gelling agents in food: A critical review. *Journal of Food Science and Technology*, 47(6), 587–597. <https://doi.org/10.1007/s13197-010-0162-6>
- Saikhwan, P., Geddert, T., Augustin, W., Scholl, S., Paterson, W. R., & Wilson, D. I. (2006). Effect of surface treatment on cleaning of a model food soil. *Surface and Coatings Technology*, 201, 943–951. <https://doi.org/10.1016/j.surfcoat.2006.01.021>
- Sajjan, S. U., & Rao, M. R. R. (1987). Effect of hydrocolloids on the rheological properties of wheat starch. *Carbohydrate Polymers*, 7(5), 395–402. [https://doi.org/10.1016/0144-8617\(87\)90005-1](https://doi.org/10.1016/0144-8617(87)90005-1)
- Sakellariou, P., Rowe, R. C., & White, E. F. T. (1986). An evaluation of the interaction and plasticizing efficiency of the polyethylene glycols in ethyl cellulose and hydroxypropyl methylcellulose films using the torsional braid pendulum. *International Journal of Pharmaceutics*, 31(1), 55–64. [https://doi.org/https://doi.org/10.1016/0378-5173\(86\)90212-7](https://doi.org/https://doi.org/10.1016/0378-5173(86)90212-7)
- Sánchez-Moreno, C., De Pascual-Teresa, S., De Ancos, B., & Cano, M. P. (2012). Nutritional



- Quality of Fruits. In N. K. Sinha, J. S. Sidhu, J. Barta, J. S. B. Wu, & M. P. Cano (Eds.), *Handbook of Fruits and Fruit Processing* (2nd ed., pp. 133–151). Wiley-Blackwell. <https://doi.org/10.1002/9781118865606.ch6>
- Saravacos, G. D., & Stinchfield, R. M. (1965). Effect of Temperature and Pressure on the Sorption of Water Vapor by Freeze-Dried Food Materials. *Journal of Food Science*, *30*(5), 779–786.
- Sears, J. K., & Darby, J. R. (1982). *The Technology of Plasticizers*. John Wiley and Sons Ltd.
- Shah, B. N., & Schall, C. A. (2006). Measurement and modeling of the glass transition temperatures of multi-component solutions. *Thermochimica Acta*, *443*(1), 78–86. <https://doi.org/10.1016/j.tca.2006.01.003>
- Sharma, M., Kristo, E., Corredig, M., & Duizer, L. (2017). Effect of hydrocolloid type on texture of pureed carrots: Rheological and sensory measures. *Food Hydrocolloids*, *63*, 478–487. <https://doi.org/10.1016/j.foodhyd.2016.09.040>
- Sharma, S. K., Zaydouri, A., Roudaut, G., & Duplâtre, G. (2011). Effect of water on glass transition in starch/sucrose matrices investigated through positron annihilation lifetime spectroscopy: A new approach. *Physical Chemistry Chemical Physics*, *13*(43), 19338–19344. <https://doi.org/10.1039/c1cp21243e>
- Singh, A., Geveke, D. J., & Yadav, M. P. (2017). Improvement of rheological, thermal and functional properties of tapioca starch by using gum arabic. *LWT - Food Science and Technology*, *80*, 155–162. <https://doi.org/10.1016/j.lwt.2016.07.059>
- Singh, P. (2007). Heating and Cooling Processes for Foods. In D. Heldman & D. Lund (Eds.), *Handbook of Food Engineering* (2nd ed., p. 1023). CRC Press.
- Sothornvit, R., & Krochta, J. M. (2001). Plasticizer effect on mechanical properties of  $\beta$ -lactoglobulin films. *Journal of Food Engineering*, *50*(3), 149–155. [https://doi.org/10.1016/S0260-8774\(00\)00237-5](https://doi.org/10.1016/S0260-8774(00)00237-5)
- Teixeira, E. M., Da Róz, A. L., Carvalho, A. J. F., & Curvelo, A. A. S. (2007). The effect of glycerol/sugar/water and sugar/water mixtures on the plasticization of thermoplastic cassava starch. *Carbohydrate Polymers*, *69*(4), 619–624. <https://doi.org/10.1016/j.carbpol.2007.01.022>
- Telis, V. R. N., & Martínez-Navarrete, N. (2009). Collapse and color changes in grapefruit juice powder as affected by water activity, glass transition, and addition of carbohydrate polymers. *Food Biophysics*, *4*(2), 83–93. <https://doi.org/10.1007/s11483-009-9104-0>
- Telis, V. R. N., & Sobral, P. J. A. (2001). Glass Transitions and State Diagram for Freeze-dried Pineapple. *LWT - Food Science and Technology*, *34*(4), 199–205. <https://doi.org/10.1006/fstl.2000.0685>
- Telis, V. R. N., & Sobral, P. J. A. (2002). Glass transitions for freeze-dried and air-dried tomato.

*Food Research International*, 35(5), 435–443. [https://doi.org/10.1016/S0963-9969\(01\)00138-7](https://doi.org/10.1016/S0963-9969(01)00138-7)

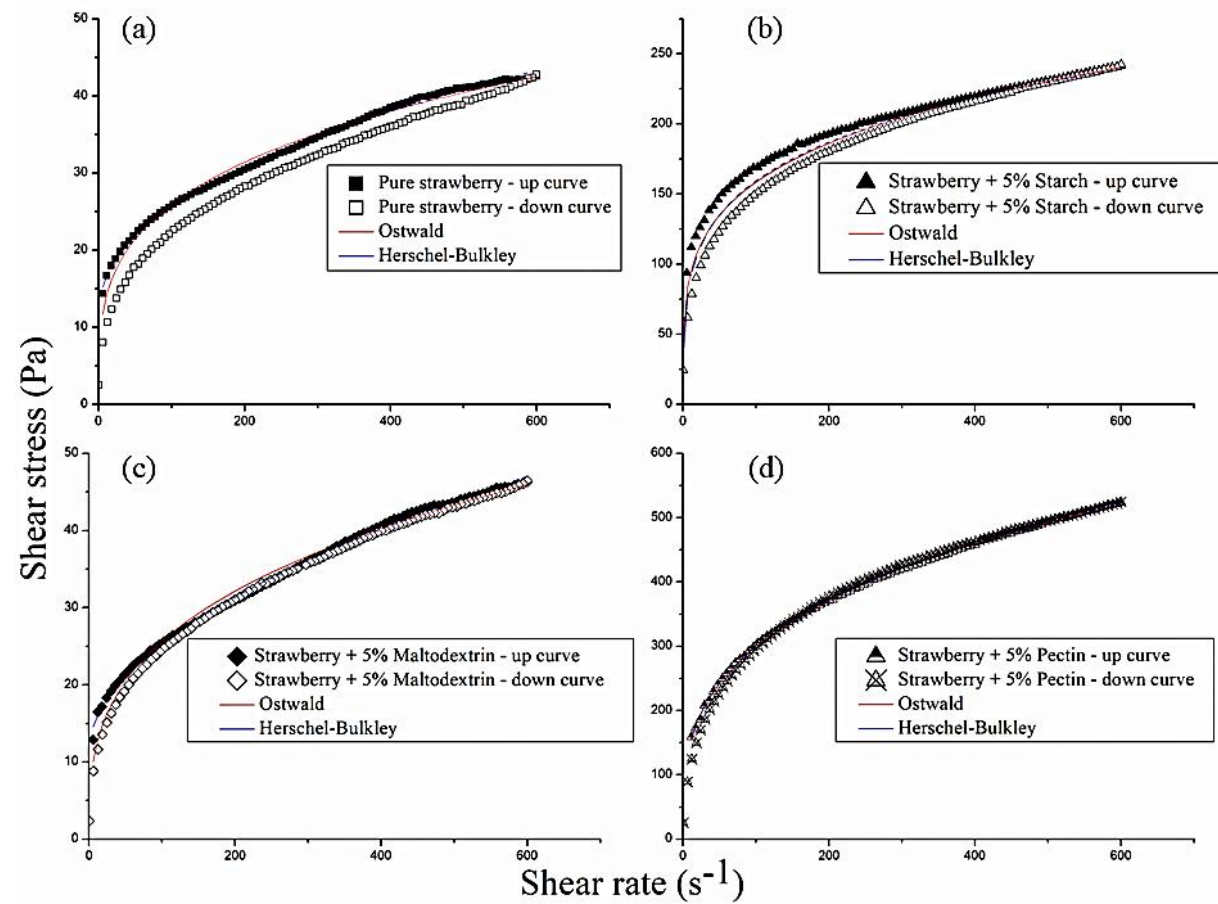
- Tonon, R. V., Baroni, A. F., Brabet, C., Gibert, O., Pallet, D., & Hubinger, M. D. (2009). Water sorption and glass transition temperature of spray dried açai (*Euterpe oleracea* Mart.) juice. *Journal of Food Engineering*, 94(3–4), 215–221. <https://doi.org/10.1016/j.jfoodeng.2009.03.009>
- Tontul, I., & Topuz, A. (2017). Effects of different drying methods on the physicochemical properties of pomegranate leather (pestil). *LWT - Food Science and Technology*, 80, 294–303. <https://doi.org/10.1016/j.lwt.2017.02.035>
- Torreggiani, D., Forni, E., Guercilena, I., Maestrelli, A., Bertolo, G., Archer, G. P., Kennedy, C. J., Bone, S., Blond, G., Contreras-Lopez, E., & Champion, D. (1999). Modification of glass transition temperature through carbohydrates additions: Effect upon colour and anthocyanin pigment stability in frozen strawberry juices. *Food Research International*, 32(6), 441–446. [https://doi.org/10.1016/S0963-9969\(99\)00106-4](https://doi.org/10.1016/S0963-9969(99)00106-4)
- Torres, F. G., Troncoso, O. P., Torres, C., Díaz, D. A., & Amaya, E. (2011). Biodegradability and mechanical properties of starch films from Andean crops. *International Journal of Biological Macromolecules*, 48(4), 603–606. <https://doi.org/10.1016/j.ijbiomac.2011.01.026>
- Travalini, A. P., Lamsal, B., Magalhães, W. L. E., & Demiate, I. M. (2019). Cassava starch films reinforced with lignocellulose nanofibers from cassava bagasse. *International Journal of Biological Macromolecules*, 139, 1151–1161. <https://doi.org/10.1016/j.ijbiomac.2019.08.115>
- Tsami, E., Krokida, M. K., & Drouzas, A. E. (1998). Effect of drying method on the sorption characteristics of model fruit powders. *Journal of Food Engineering*, 38(4), 381–392. [https://doi.org/10.1016/S0260-8774\(98\)00130-7](https://doi.org/10.1016/S0260-8774(98)00130-7)
- Tzeng, G. S., Chen, H. J., Wang, Y. Y., & Wan, C. C. (1997). The effects of roughening on teflon surfaces. *Surface and Coatings Technology*, 89(1–2), 108–113. [https://doi.org/10.1016/S0257-8972\(96\)02916-7](https://doi.org/10.1016/S0257-8972(96)02916-7)
- USDA. (2015). *Agricultural Research Service, Nutrient Data Laboratory*. USDA National Nutrient Database for Standard Reference, Release 28. <https://ndb.nal.usda.gov/ndb/nutrients/>
- Valenzuela, C., & Aguilera, J. M. (2015). Effects of different factors on stickiness of apple leathers. *Journal of Food Engineering*, 149, 51–60. <https://doi.org/10.1016/j.jfoodeng.2014.09.029>
- Valli, J. (1986). A review of adhesion test methods for thin hard coatings. *Journal of Vacuum Science & Technology A: Vacuum, Surfaces, and Films*, 4(6), 3007–3014. <https://doi.org/10.1116/1.573616>
- Vaughan, J. G., & Geissler, C. A. (1997). *The New Oxford Book of Food Plants* (O. University (ed.)).



- Vega-Mercado, H., Góngora-Nieto, M., & Barbosa-Cánovas, G. V. (2001). Advances in dehydration of foods. *Journal of Food Engineering*, 49(4), 271–289. [https://doi.org/10.1016/S0260-8774\(00\)00224-7](https://doi.org/10.1016/S0260-8774(00)00224-7)
- Wang, X., Sun, X., Liu, H., Li, M., & Ma, Z. (2011). Barrier and mechanical properties of carrot puree films. *Food and Bioprocess Processing*, 89(2), 149–156. <https://doi.org/10.1016/j.fbp.2010.03.012>
- Wang, Y., & Truong, T. (2017). Glass Transition and Crystallization in Foods. In *Non-Equilibrium States and Glass Transitions in Foods: Processing Effects and Product-Specific Implications* (pp. 153–172). Elsevier Ltd. <https://doi.org/10.1016/B978-0-08-100309-1.00007-9>
- Wani, A. A., Singh, P., Shah, M. A., Schweiggert-Weisz, U., Gul, K., & Wani, I. A. (2012). Rice Starch Diversity: Effects on Structural, Morphological, Thermal, and Physicochemical Properties-A Review. *Comprehensive Reviews in Food Science and Food Safety*, 11(5), 417–436. <https://doi.org/10.1111/j.1541-4337.2012.00193.x>
- Williams, M. L., Landel, R. F., & Ferry, J. D. (1955). The Temperature Dependence of Relaxation Mechanisms in Amorphous Polymers and Other Glass-forming Liquids. *Journal of the American Chemical Society*, 77(14), 3701–3707. <https://doi.org/10.1021/ja01619a008>
- Williams, P. A., & Phillips, G. O. (2009). Introduction to food hydrocolloids. In G. O. Phillips & P. A. Williams (Eds.), *Handbook of Hydrocolloids (second Edition)* (Second, pp. 1–22). CRC Press.
- Yeow, Y. L., Perona, P., & Leong, Y. K. (2002). A reliable method of extracting the rheological properties of fruit purees from flow loop data. *Journal of Food Science*, 67(4), 1407–1411. <https://doi.org/10.1111/j.1365-2621.2002.tb10298.x>
- Zabetakis, I., & Holden, M. A. (1997). Strawberry Flavour: Analysis and Biosynthesis. *Journal of the Science of Food and Agriculture*, 74(4), 421–434. [https://doi.org/10.1002/\(SICI\)1097-0010\(199708\)74:4<421::AID-JSFA817>3.0.CO;2-6](https://doi.org/10.1002/(SICI)1097-0010(199708)74:4<421::AID-JSFA817>3.0.CO;2-6)
- Zhang, X., Tong, Q., Zhu, W., & Ren, F. (2013). Pasting, rheological properties and gelatinization kinetics of tapioca starch with sucrose or glucose. *Journal of Food Engineering*, 114(2), 255–261. <https://doi.org/10.1016/j.jfoodeng.2012.08.002>
- Zhou, D. N., Zhang, B., Chen, B., & Chen, H. Q. (2017). Effects of oligosaccharides on pasting, thermal and rheological properties of sweet potato starch. *Food Chemistry*, 230, 516–523. <https://doi.org/10.1016/j.foodchem.2017.03.088>
- Zisman, W. A. (1964). Relation of the Equilibrium Contact Angle to Liquid and Solid Constitution. In *Advances in Chemistry* (pp. 1–51). American Chemical Society. <https://doi.org/10.1021/ba-1964-0043.ch001>

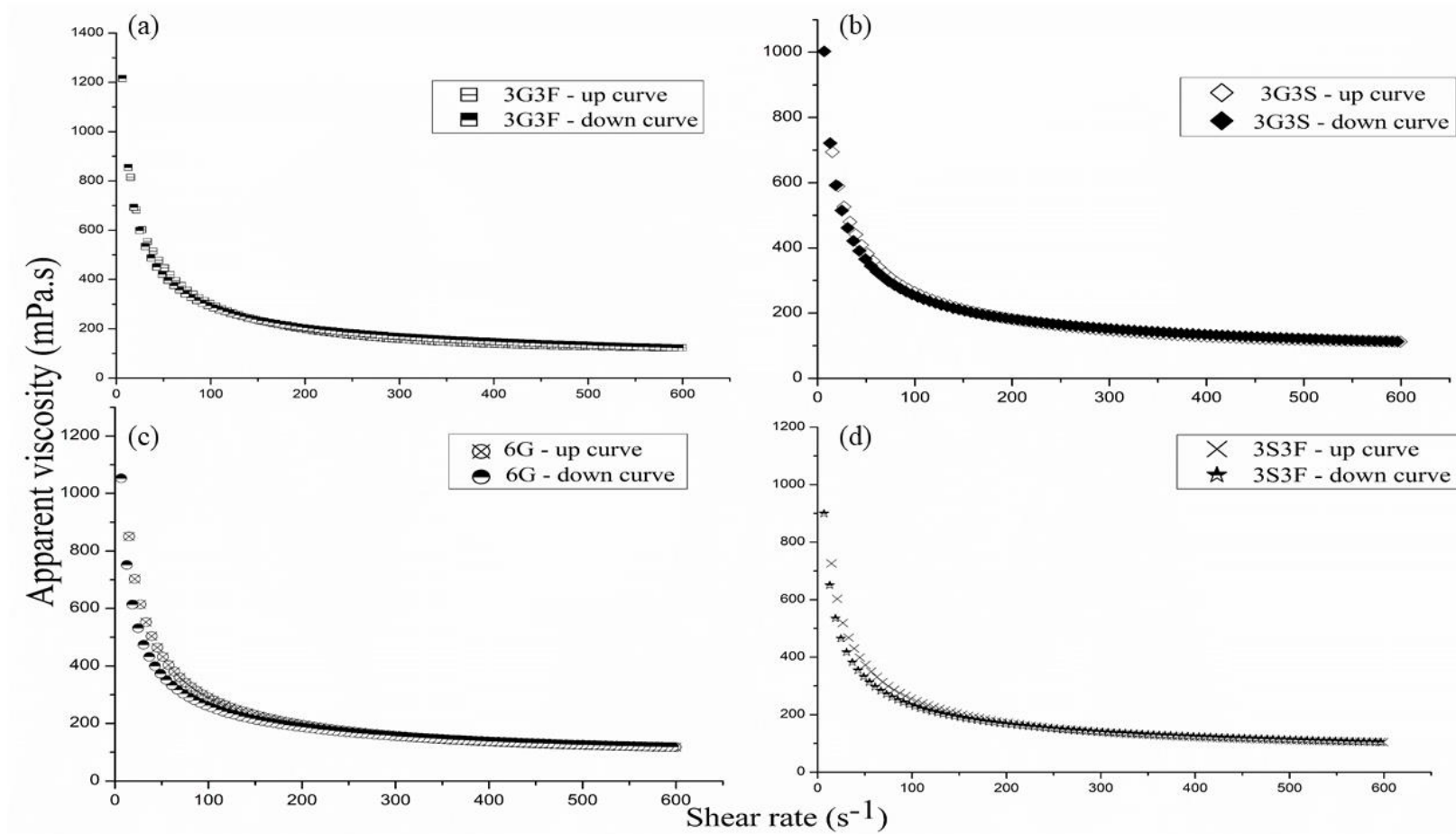
- Zotarelli, M. F., Carciofi, B. A. M., & Laurindo, J. B. (2015). Effect of process variables on the drying rate of mango pulp by Refractance Window. *Food Research International*, *69*, 410–417. <https://doi.org/10.1016/j.foodres.2015.01.013>
- Zotarelli, M. F., da Silva, V. M., Durigon, A., Hubinger, M. D., & Laurindo, J. B. (2017). Production of mango powder by spray drying and cast-tape drying. *Powder Technology*, *305*, 447–454. <https://doi.org/10.1016/j.powtec.2016.10.027>

## APPENDIX A



Appendix A 1 - Shear stresses versus shear rates of strawberry suspensions: (a) Pure strawberry; (b) Strawberry + 5% starch; (c) Strawberry + 5% maltodextrin; (d) Strawberry + 5% pectin.

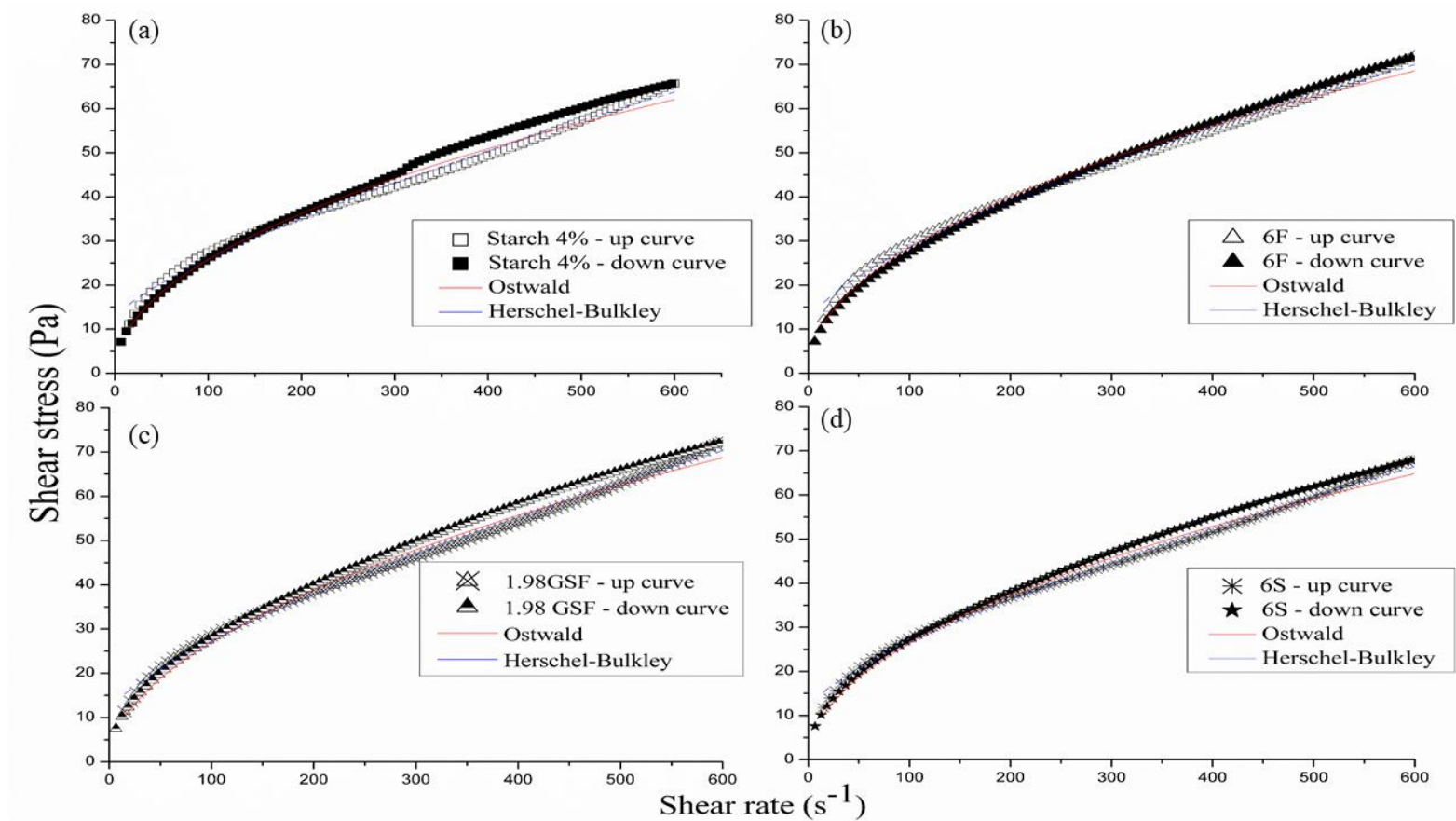
Source: author.



Appendix A 2 - Viscosity curves of starch formulations: (a) Suspension 3G3F (3 g of glucose + 3 g of fructose / 100 g suspension); (b) Suspension 3G3S (3 g glucose + 3 g sucrose / 100 g suspension); (c) Suspension 6G (6 g glucose / 100 g suspension); (d) Suspension 3S3F (3 g sucrose + 3 g fructose / 100 g suspension).

F: Fructose; G: Glucose; S: Sucrose.

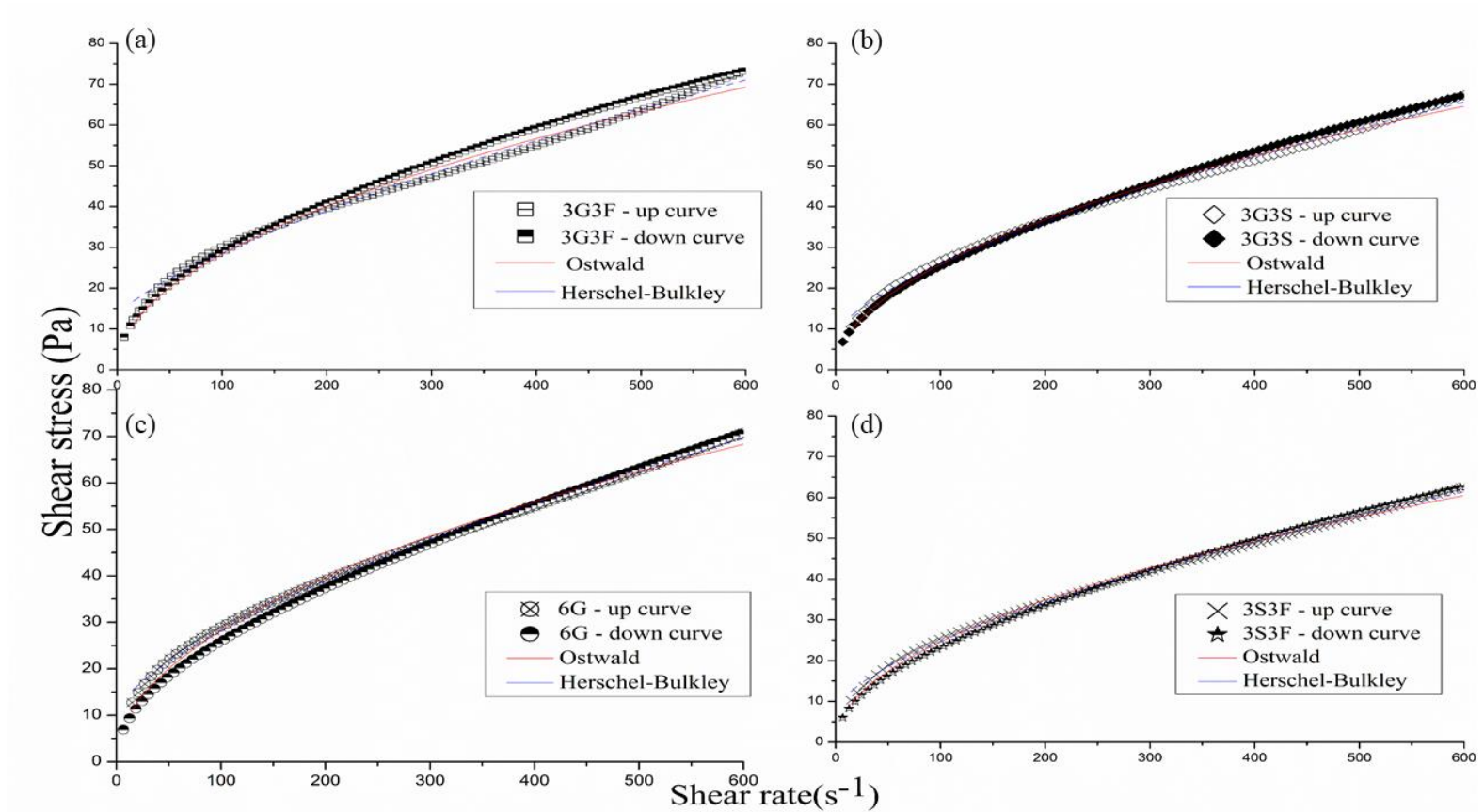
Source: author.



Appendix A 3 - Shear stresses versus shear rates of starch formulations: (a) Suspension of cassava starch 4%; (b) Suspension 6F (6 g fructose / 100 g suspension); (c) Suspension 1.98 GSF (1.98 g glucose + 1.98 g sucrose + 1.98g g fructose / 100 g suspension); (d) Suspension 6S (6 g sucrose / 100 g suspension).

F: Fructose; G: Glucose; S: Sucrose.

Source: author.



Appendix A 4 - Shear stresses versus shear rates of starch formulations: (a) Suspension 3G3F (3 g glucose + 3 g fructose / 100 g suspension); (b) Suspension 3G3S (3 g glucose + 3 g sucrose / 100 g suspension); (c) Suspension 6G (6 g glucose / 100 g suspension); (d) Suspension 3S3F (3 g sucrose + 3 g fructose / 100 g suspension).

F: Fructose; G: Glucose; S: Sucrose.

Source: author.

Appendix A 5 - Shear stresses ( $\sigma$ ) and viscosity values ( $\eta$ ) calculated for shear rates of 11 s<sup>-1</sup>, 23 s<sup>-1</sup> and 101 s<sup>-1</sup>.

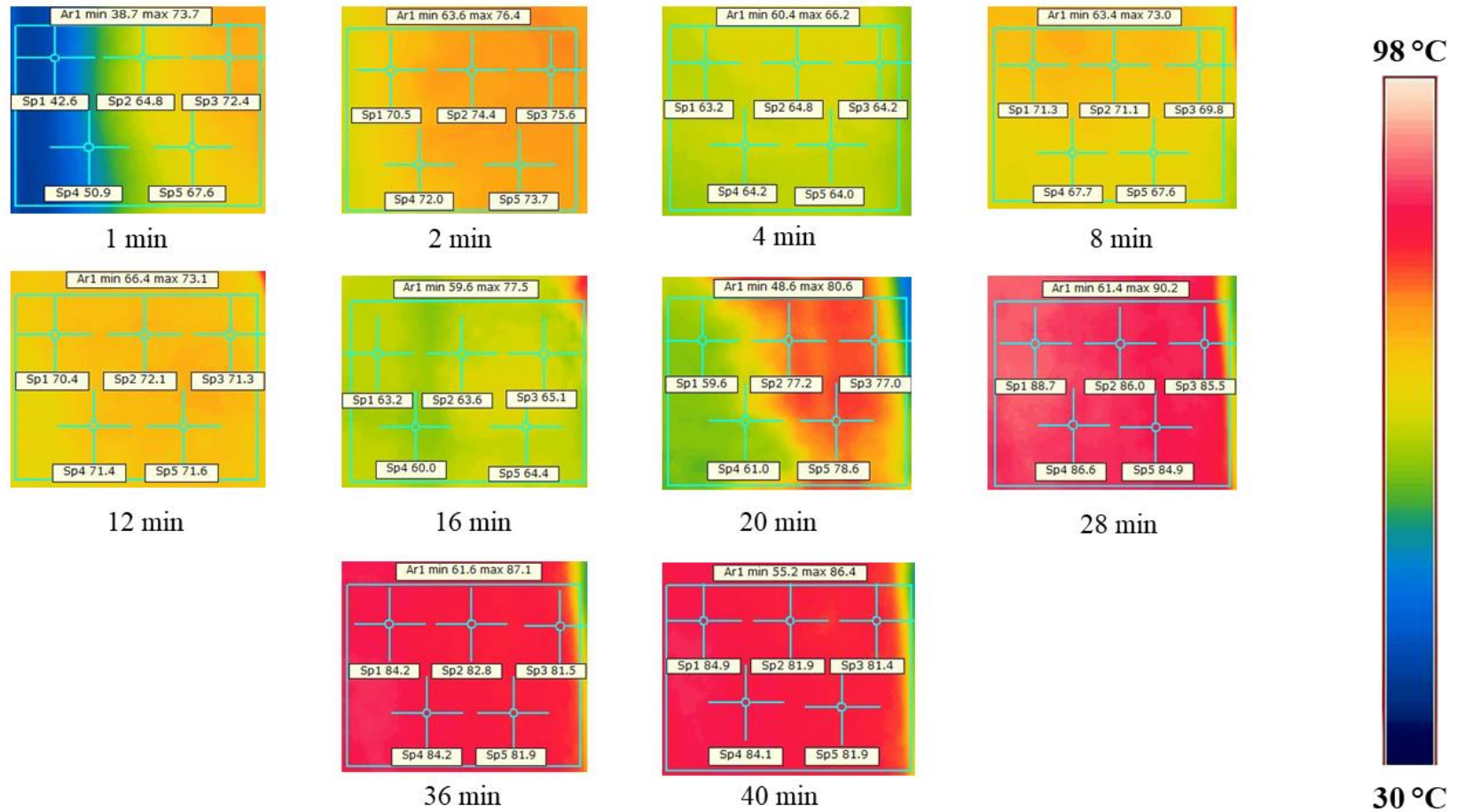
Samples	Shear stress ( $\sigma$ )	Viscosity ( $\eta$ )	Shear stress ( $\sigma$ )	Viscosity ( $\eta$ )	Shear stress ( $\sigma$ )	Viscosity ( $\eta$ )
	Shear rate ( $\dot{\gamma}$ )		Shear rate ( $\dot{\gamma}$ )		Shear rate ( $\dot{\gamma}$ )	
	11 s <sup>-1</sup>		23 s <sup>-1</sup>		101 s <sup>-1</sup>	
Starch 4%	9.49 ± 1.51 <sup>a</sup>	0.86 ± 0.15 <sup>a</sup>	14.18 ± 1.59 <sup>a</sup>	0.61 ± 0.07 <sup>a</sup>	27.57 ± 4.54 <sup>a</sup>	0.27 ± 0.05 <sup>a</sup>
3G3F	10.40 ± 1.04 <sup>a</sup>	0.94 ± 0.11 <sup>a</sup>	15.02 ± 1.79 <sup>a</sup>	0.65 ± 0.08 <sup>a</sup>	30.29 ± 2.26 <sup>a</sup>	0.30 ± 0.02 <sup>a</sup>
6F	10.48 ± 1.07 <sup>a</sup>	0.95 ± 0.10 <sup>a</sup>	15.46 ± 1.38 <sup>a</sup>	0.67 ± 0.06 <sup>a</sup>	29.91 ± 1.73 <sup>a</sup>	0.29 ± 0.02 <sup>a</sup>
3G3S	8.90 ± 0.26 <sup>a</sup>	0.80 ± 0.03 <sup>a</sup>	13.22 ± 0.57 <sup>a</sup>	0.57 ± 0.03 <sup>a</sup>	26.83 ± 2.43 <sup>a</sup>	0.26 ± 0.03 <sup>a</sup>
6G	10.93 ± 1.06 <sup>a</sup>	0.99 ± 0.11 <sup>a</sup>	15.48 ± 1.77 <sup>a</sup>	0.67 ± 0.08 <sup>a</sup>	29.14 ± 3.21 <sup>a</sup>	0.29 ± 0.03 <sup>a</sup>
1.98GSF	9.56 ± 0.21 <sup>a</sup>	0.86 ± 0.02 <sup>a</sup>	14.27 ± 0.78 <sup>a</sup>	0.62 ± 0.04 <sup>a</sup>	28.69 ± 2.23 <sup>a</sup>	0.28 ± 0.02 <sup>a</sup>
3S3F	8.72 ± 0.55 <sup>a</sup>	0.83 ± 0.06 <sup>a</sup>	12.59 ± 0.22 <sup>a</sup>	0.56 ± 0.01 <sup>a</sup>	25.50 ± 2.04 <sup>a</sup>	0.25 ± 0.02 <sup>a</sup>
6S	9.99 ± 0.56 <sup>a</sup>	0.92 ± 0.03 <sup>a</sup>	14.31 ± 1.72 <sup>a</sup>	0.62 ± 0.07 <sup>a</sup>	27.75 ± 4.02 <sup>a</sup>	0.27 ± 0.04 <sup>a</sup>

F: Fructose; G: Glucose; S: Sucrose.

Source: author.



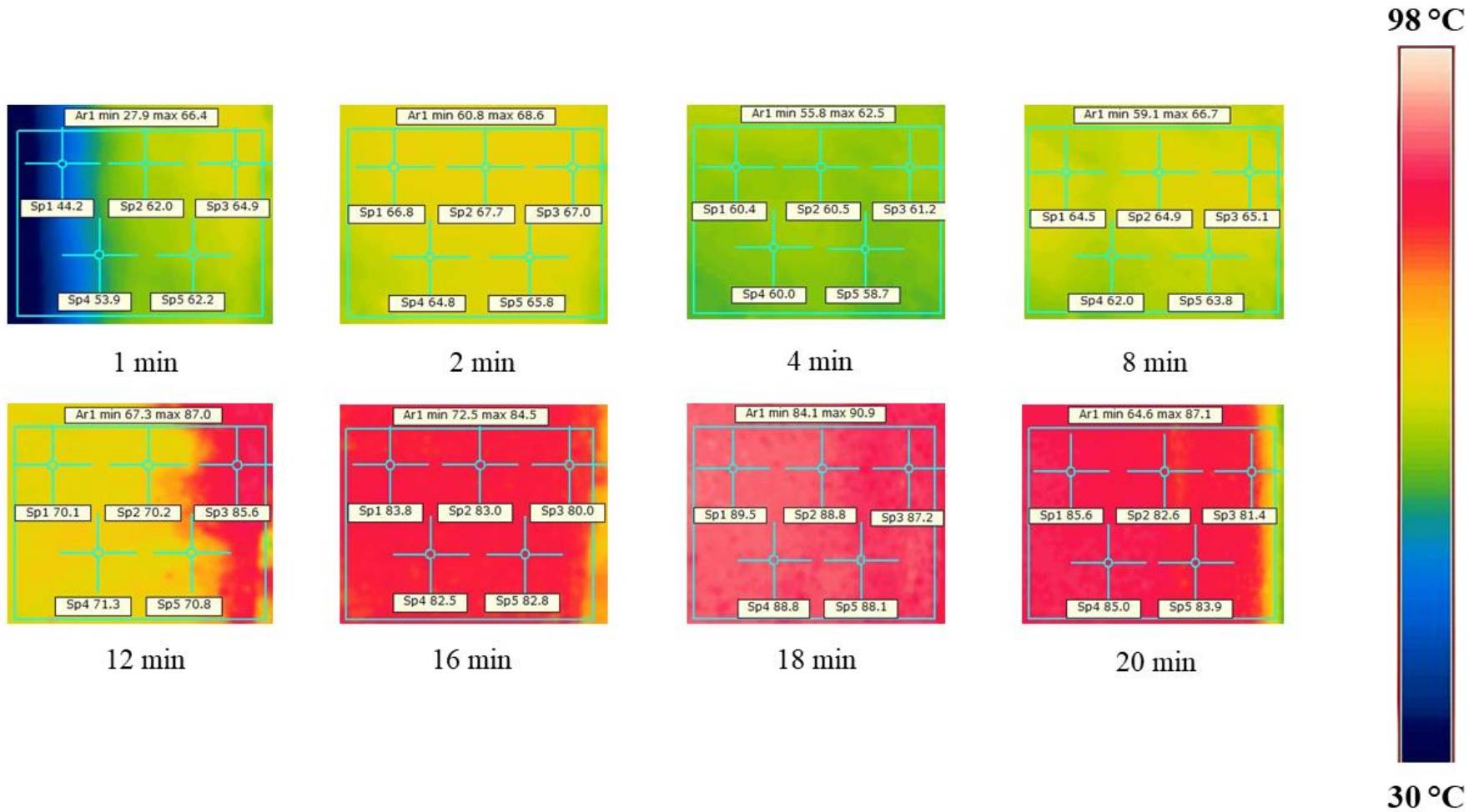
## APPENDIX B



Appendix B 1 - Thermographs of the drying of the strawberry suspension with the addition of maltodextrin in continuous CTD.

Source: author.





Appendix B 2 - Thermographs of the drying of the strawberry suspension with the addition of pectin in continuous CTD.

Source: author.